Investigation of Glacial Retreat, Terrace Abandonment, and Catchment-wide Denudation Rates in the Vakhsh Catchment, Tajikistan

Dissertation

der Mathematisch-Naturwissenschaftlichen Fakultät

der Eberhard Karls Universität Tübingen

zur Erlangung des Grades eines

Doktors der Naturwissenschaften

(Dr. rer. nat.)

vorgelegt von

Elena Grin

aus Schytomyr/Ukraine

Tübingen

2019

Gedruckt mit Genehmigung der Mathematisch-Naturwissenschaftlichen Fakultät der Eberhard Karls Universität Tübingen.

Tag der mündlichen Qualifikation:	25.10. 2019
Dekan:	Prof. Dr. Wolfgang Rosenstiel
1. Berichterstatter:	Prof. Todd A. Ehlers
2. Berichterstatter:	Prof. Ronny Schönberg

Ich erkläre hiermit, dass ich die zur Promotion eingereichte Arbeit mit dem Titel „**Investigation of Glacial Retreat, Terrace Abandonment, and Catchment-wide Denudation Rates in the Vakhsh Catchment, Tajikistan**“ selbstständig verfasst, nur die angegebenen Quellen und Hilfsmittel benutzt und wörtlich oder inhaltlich übernommene Stellen (alternativ: Zitate) als solche gekennzeichnet habe. Ich erkläre, dass die Richtlinien zur Sicherung guter wissenschaftlicher Praxis der Universität Tübingen (Beschluss des Senats vom 25.05.2000) beachtet wurden. Ich versichere an Eides statt, dass diese Angaben wahr sind und, dass ich nichts verschwiegen habe.

Tubingen, den 18.02.2020

Ort, Datum | Unterschrift

Abstract

The development of the Vakhsh catchment is linked to the tectonic development of the Pamir during the India-Asia collision. The northward motion of the Pamir block relative to Eurasia, as well as its uplift and shortening, confined the Vakhsh River system between the western Tian Shan and the Pamir along the Pamir Thrust System deformation zone (PTS). The northern Pamir overthrusts the western Tian Shan and the Alai Valley experiences shortening along the PTS. At the present, the Vakhsh catchment drains two orogens along a thrust system and provides an opportunity for understanding denudation associated with plate convergence.

During the Quaternary, the Vakhsh River catchment experienced changes in climatic conditions such as Quaternary glaciation and the Holocene thermal optimum, which caused fluctuations in sediment supply and water discharge. This study investigates the timing of glaciation, terrace formation as well as modern and paleo-denudation rates in the context of the tectonic and paleo-climatic conditions of the region.

Glacial deposits, such as moraines, are archives that record advance and retreat cycles driven by climate change. Collecting spatial and temporal data about glaciations is essential for the reconstruction of both, the regional and global timing of ice ages and climate change. The investigation of glacial extent and timing in the Vakhsh River catchment was addressed by studying the glacial deposits near the former terminus of the Fedchenko Glacier. The Fedchenko Glacier is particularly important for understanding the glacial chronology in Central Asia, because it is the longest (~72 km) glacier outside the Polar Regions and the timing of its advance and retreat may be representative for the climate evolution of the Westerly-dominated Central Asia region.

The present-day climate is dominated by the Mid-Latitude Westerlies and supplies the region with 400 – 1,000 mm annual precipitation. The present-day mean annual temperatures range between -6.7 and 12 ˚C. *Inter alia*, the interaction between precipitation and temperature induces flooding and increases mass movement events during snow melt. To understand and

quantify the temporal and spatial influence of climate and tectonics on the evolution of mountain belts and the fluvial systems within is of a major importance for human existence in this challenging environment.

To target the timing and possible causes for fluctuations in sediment supply, I investigated a flight of fluvial terraces along the main trunk. The incision into the investigated terraces started at Holocene times ~ 3 ka ago and was accompanied by high incision rates of 4 – 29 mm/yr. The paleo-denudation rates associated with the terraces range between 1.75 ± 0.41 mm/yr and 2.01 ± 0.36 mm/yr. The modern denudation rates cover the same magnitude (1.28 ± 0.16 – 1.94 ± 0.26 mm/yr) along the main trunk. The investigation of the tributaries yielded the greatest variation in modern denudation rates in the western Tian Shan tributaries (0.18 ± 0.02 mm/yr to 2.05 ± 0.27 mm/yr). The Alai Valley displays an intermediate signal of 1.14 ± 0.14 mm/yr and the northern Pamir tributaries display rates (1.78 ± 0.23 mm/yr and 1.63 ± 0.21 mm/yr) at the higher end of the spectrum. Additionally $^{26}Al/^{10}Be$ ratios were used to test, whenever the tributaries are prone to store or mix fresh sediment with shielded material. The results indicate no immediate storage or mixing ($^{26}Al/^{10}Be$ ratios: 6.0 ± 1.0 to 7.6 ± 1.2), except for one western Tian Shan catchment ($^{26}Al/^{10}Be$ ratio: 5.2 ± 0.5).

Zusammenfassung

Der geologische Werdegang des Pamir während der Indien-Eurasien-Kollision beeinflusste maßgeblich die Entwicklung des Einzugsgebiets des Flusses Vakhsh. Die nordwärts gerichtete Verschiebung des Pamirblocks relativ zu Eurasien, dessen Hebung und Verkürzung, positionierten den Vakhsh zwischen dem westlichen Tian Shan und dem nördlichen Pamir entlang der Deformationszone des PTS (Pamir Thrust System), an der sich der nördliche Pamir über den westlichen Teil des Tian Shan schiebt. Gegenwärtig repräsentiert der Fluss Vakhsh ein aktives Beispiel eines Flusses, der zwischen zwei Gebirgszügen gefangen, entlang einer Deformationszone entwässert. Dieser Umstand bietet die Gelegenheit, die Denudation beider Gebirgszüge im Zusammenhang mit der intrakontinentalen Deformationszone zu untersuchen. Ferner umschließt das über 39 000 km^2 große Einzugsgebiet des Vakhsh mehrere Landschaftsformen, wie die beiden Gebirgszüge westlicher Tian Shan und nördlicher Pamir, aber auch das Alai-Tal und die Tadschikische Depression. Im Quartär unterlag das Einzugsgebiet des Vakhsh mehreren Klimaschwankungen. Sowohl das Quartäre Eiszeitalter als auch das Holozäne Optimum verursachten Fluktuationen in Sedimentzufuhr und Abflussvolumen.

Die Ziele der vorliegenden Arbeit sind die Bestimmung a) des Zeitpunktes des Gletschervorstoßes während des Quartärs, b) des Beginns der Inzision in die Terrassenablagerungen entlang des Hauptstroms und c) der zeitlichen und räumlichen Evolution der Denudationsraten im Kontext des tektonischen Umfelds und der Klimageschichte der Region. Glaziale Ablagerungen, wie etwa Moränen, können herangezogen werden, um klimatisch bedingte Vergletscherungszyklen zu datieren. Die Rekonstruktion von Vergletscherungszyklen auf einer regionalen Skala und deren Korrelation mit globalen Daten ist unabdingbar für das Verständnis der Klimageschichte. Um den Zeitpunkt und die Ausdehnung der letzten großen Vergletscherung im Einzugsgebiet des Vakhsh zu bestimmen, wurden Proben von glazialen Ablagerungen in der Umgebung des ehemaligen Terminus des Fedchenko Gletschers entnommen. Dieser Gletscher nimmt insofern eine wichtige Rolle

ein, dass er aufgrund seiner Ausdehnung (~72 km) der längste Gletscher außerhalb der Polarregion ist. Die Chronologie seines Rückzugs könnte exemplarisch sein für das in der Westwindzone gelegene Zentralasien.

Die Westwinde versorgen das Einzugsgebiet des Vakhsh mit 400 – 1.000 mm Niederschlag pro Jahr. Die gegenwärtigen Temperaturen erreichen monatliche Durchschnittswerte von -6,7 ˚C bis 12˚C. Das Zusammenspiel zwischen Niederschlag und Temperatur resultiert in gehäuft auftretenden Hangrutschungen und Flutereignissen während der Schneeschmelze. Das Verstehen und Quantifizieren der Konsequenzen von Klima und Tektonik auf die Entstehung von Flusssystemen in Gebirgen ist von großer Wichtigkeit für die menschliche Existenz unter solch herausfordernden Bedingungen. Um mögliche Ursachen und das Timing von Sedimenteintragsfluktuationen zu ergründen, wurde eine Terrassensequenz entlang des Hauptflusses untersucht. Das Einschneiden in die Terrassensedimente begann währen des Holozäns, vor etwa 3 ka und ging mit hohen Einschneidungsraten einher (4 - 29 mm/Jahr). Die mit der Terrassensequenz assoziierten Palaeo-Denudationsraten liegen zwischen 1,75 ± 0,41 mm/Jahr und 2,01 ± 0,36 mm/Jahr. Die modernen Denudationsraten entlang des Haupstroms liegen mit 1,28 ± 0,16 – 1,94 ± 0,26 mm/Jahr in derselben Größenordnung. Die Untersuchung der Zuflüsse zeigt, dass die größte Variation in den Denudationsraten bei den Zuflüssen im Tian Shan liegt (0,18 ± 0,02 mm/Jahr bis 2,05 ± 0,27 mm/Jahr). Das Alai-Tal nimmt mit 1,14 ± 0,14 mm/Jahr eine intermediäre Stellung ein und die Zuflüsse des nördlichen Pamir weisen Denudationsraten von 1,78 ± 0,23 mm/Jahr und 1,63 ± 0,21 mm/Jahr auf. Zusätzlich wurden $^{26}Al/^{10}Be$ Verhältnisse gemessen, um eventuell vorhandene Abschirmung und Ablagerung der Flusssedimente nachvollziehen zu können. Die Resultate weisen keine solchen Signale auf (6,0 ± 1,0 bis 7,6 ± 1,2), außer im Falle eines Zuflusses aus dem Tian Shan (5,2 ± 0,5).

Table of Contents

I Acknowledgments

First of all, I would like to thank Prof. Todd A. Ehlers, Prof. Ronny Schönberg, and Dr. Mirjam Schaller, for the guidance, patience, and encouragement they provided during this project. I am also very grateful to my family, who always supported me.

I would also like to thank all, who were involved in the process of sample processing and data acquisition: The German Federal Ministry of Education and Research funded this study in the CAME project bundle TIPTIMON. Our Tajik co-workers Djamilla Baidulloeva and Boy Mahmat smoothed our way in Tajikistan. David Grabowski and Christian Rexroth assisted in the field. Dorothea Muehlbayer-Renner and Matthias Loose helped with the sample preparation. I am grateful to Vasila Sulaymanova, and Dr. Konstanze Stübner for the companionship during the field seasons. I thank the team at the CologneAMS and Sabine Flaiz, for all the measurements they did in the course of this project. I am very grateful to Dagmar Kost, who always kept the lab running smoothly. I thank Prof. Lothar Ratschbacher for sharing his profound knowledge about Tajikistan and for the constructive comments on my first paper. I thank Dr. Byron Adams for his patience in explaining to me the pitfalls of k_{sn} analysis.

I am especially grateful, that I had the opportunity to be part of a research group, which consists of enthusiastic scientists and good friends. Thank you for advice and fun times Solmaz Mohadjer, Sebastian Mutz, Matthias Nettesheim, and especially Sarah Falkowski, who always kept an open ear for me. I thank also Sumeyya Eroglu and Susann Zilkenat for the moral support. Many thanks go to Silke Malmsheimer, who spent countless hours with Katharina.

Finally, my eternal thanks go to my beloved husband Iwan, who always had my back. I could not have done this without you.

II Publication of Data

Chapter 3 (^{10}Be Surface-Exposure Age Dating of the Last Glacial Maximum in the Northern Pamir (Tajikistan)) is already published as (Grin et al., 2016). Chapter 4 (Holocene denudation rates and terrace ages of the Vakhsh River, Tajikistan) and Chapter 5 (Spatial Distribution of Cosmogenic ^{10}Be Derived Denudation Rates between the Western Tian Shan and Northern Pamir, Tajikistan) are published as (Grin et al., 2018). The introduction chapter (1) consists of both introduction chapters of the previously named publications.

III List of Figures

IV List of Tables

V Abbreviations

07KNSTD	2007 K. Nishiizumi Standard
a	year
AMS	Accelerator Mass Spectrometer
a.s.l	above sea level
ESR	Electron Spin Resonance
GeV	Giga electron Volt
GPS	Global Positioning System
ICP-MS	Inductively coupled plasma-mass spectrometry
OES	Optical Emission Spectrometry
ka	thousand years
k_{sn}	normalized river steepness index
LGM	Last Glacial Maximum
LM	lateral moraine
MeV	Mega electron Volt
Myr	million years
mm/yr	millimeter per year
MIS	Marine Isotope Stage
OSL	Optically Stimulated Luminescence
PTS	Pamir Thrust System
RM	recessional moraine
s. d.	standard deviation
SLHL	Sea Level High Latitude
SWHTS	Semi-arid Western Himalayan-Tibet Stage
TCN	Terrestrial Cosmogenic Nuclides
TRMM	Tropical Radar Moisture Measurements
vs.	versus
VTS	Vakhsh Thrust System
yr	year

1 INTRODUCTION

Almost all landscapes, no matter how different they may be from each other, have one feature in common: they are drained by river networks. Rivers experience and record the same conditions as the landscapes they drain. This makes them a powerful tool to investigate the spatial and temporal changes landscapes experience with changes in climate conditions and tectonic activity. Despite the awareness of regional scale tectonic and geodynamic processes in the Pamir and western Tian Shan, limited information is available concerning the denudational response to the processes in the Vakhsh River catchment. This chapter gives an introduction into the tectonic and geodynamic setting, and the climate records of the Pamir and Western Tian Shan region.

1.1 GEOLOGIC SETTING

This section covers the tectonic setting and gives a short introduction into the lithologies found in the Vakhsh River catchment to illustrate the main driving influences on the Vakhsh River catchment.

1.1.1 TECTONIC SETTING

The India-Eurasia collision results in the northward motion of the Pamir orogen relative to Eurasia and in a convergence between the Northern Pamir and Western Tian Shan (e.g., Burtman and Molnar, 1993; Pavlis et al., 1997; Mechie et al., 2012; Schneider et al., 2013; Kufner et al., 2018; Figure 1). The eastern part of the Pamir orogen continues to move northward and causes uplift and shortening of Northern Pamir and Alai Valley. The Northern Pamir region accommodates 10 - 15 mm/yr shortening, about one third of the total convergence between India and Asia (Coutand et al., 2002; Sippl et al. 2008; Zubovich et al., 2010; Ischuk et al. 2013;). This amount of shortening results in crustal thickening, internal deformation, uplift, and northward motion of the Pamir towards the Western Tian Shan (Figure 1). The western part of the Pamir orogen rotates anti-clockwise and extrudes westward into the Tajik Basin (Schurr et al. 2014; Kufner et al. 2018). As a response, this area

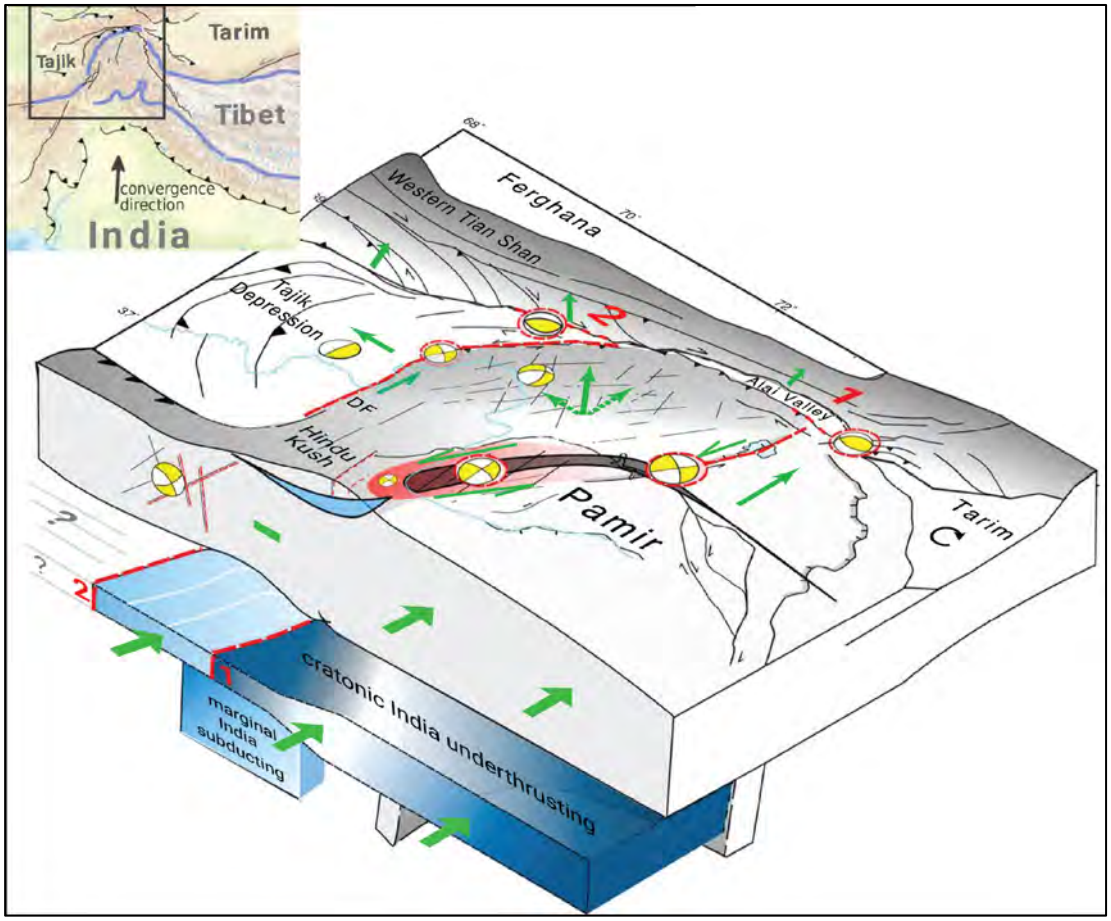

Figure 1: Tectonic situation of the Pamir and its surroundings. Yellow focal mechanisms show the dominant crustal deformation directions. Green arrows indicate main crustal movement direction. Red dashed lines and red numbers refer to the subcrustal bodies associated with the Indian subduction beneath Eurasia (after Kufner et al. 2018).

exhibits the most frequent seismicity in the region (Kulikova, 2016; Kufner et al. 2018). Associated with this displacement of the Pamir is the Pamir Thrust System (PTS) and further to the west the Vakhsh Thrust System (VTS; e.g., Schurr et al., 2014), which are located between the Northern Pamir and the Western Tian Shan (Figure 2). Earthquakes occur on active faults at the borders of the basin. The basin, once situated between the two orogens, is today divided into the Tajik Depression and the Tarim Basin. In the east the Alai Valley is a part of the former corridor between the two basins. Among the Tajik Depression and the Alai Valley the two orogens are only separated by the Vakhsh River trunk (Burtman and Molnar, 1993; Burtman, 2000; Coutand et al., 2002; Amidon and Hynek, 2010; Figure 1). At subcrustal levels, two slabs were identified (Kufner et al. 2018 and references therein). The north-dipping Indian lithosphere can be traced under the Hindu Kush today. The convergence of the Pamir towards Western Tian Shan

resulted in a south-dipping intracontinental subduction zone (Figure 1; Pavlis et al. 1997; Sippl et al. 2013; Shurr et al. 2014; Kufner et al. 2018). At the present, the Vakhsh River (Figure 1) is the single active river system draining between two orogens along an intracontinental subduction zone (Pavlis et al., 1997).

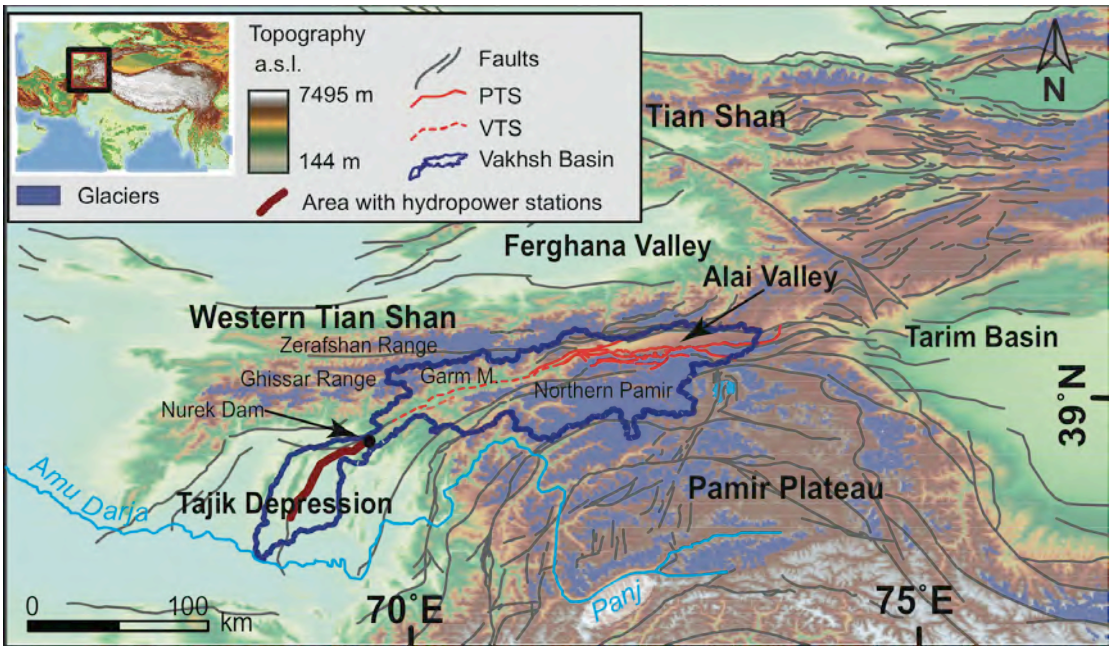

Figure 2: Overview map of the investigated area with present-day glacier extent (Randolph Glacier Inventory 5.0). Fault and thrust distribution is based on (Mohadjer et al., 2016, 2017). PTS: Pamir Thrust System, VTS: Vakhsh Thrust System, which is part of the PTS. The area with hydropower stations is highlighted in dark red along the main trunk starting at the Nurek Dam site.

1.2 GEOMORPHOLOGY OF THE VAKHSH CATCHMENT

The main river channel of the westward draining Vakhsh River is situated along the VTS (Figure 2). We divide the Vakhsh River catchment (~39,000 km^2) into four different sub-regions for our analysis based on their tectonic and topographic position (Figure 2). The Alai Valley, the Western Tian Shan, and the Northern Pamir are the focus of this study. After passing numerous levee systems, the Vahksh River drains part of the loess-filled Tajik Depression before it joins the Panj River to form the Amu Darya River (Figure 2). This section introduces the main geomorphic characteristics of the various landscapes encompassed by the Vakhsh catchment (Table 1) and summarizes the known exhumation and denudation rates in this region. In order to be able to compare the Vakhsh tributaries more easily with one another, the Strahler Order (STO; Strahler, 1957) is used. The Strahler Order

ranks a stream one level higher as soon as at least two streams of the same rank drain into a mutual trunk.

1.2.1 ALAI VALLEY

In the northeastern part of the Vakhsh River catchment, the Kyzylsu River drains the Alai Valley. The Kyzylsu catchment has a mean elevation of 3,505 m, is a Strahler Order 6 river, and has a catchment area of 8,329 km^2 (Figure 3A; Table 1). This catchment displays low hillslope angles (0 – 20˚) along the Kyzylsu main channel and its main tributaries (STO 5 and 4) due to abundant Quaternary alluvium (Figure 3B, C).

1.2.2 WESTERN TIAN SHAN

In the northern part of the Vakhsh River catchment, the Sarbog (1,758 km^2), Yarkhuch (1,124 km^2), and Tandykul (1,293 km^2; Figure 3A; Table 1) tributaries drain the Western Tian Shan. These tributaries are all STO 5, and have mean elevations of 2,950 – 3,731 m, and maximum elevations >5,000 m. Small valley glaciers exist today above ~3,300 m in the Western Tian Shan in the headwaters of these catchments.

1.2.3 NORTHERN PAMIR

The Northern Pamir part of the Vakhsh River catchment is separated from the Tian Shan region by the PTS (e.g. Hamburger et al., 1992; Burtman and Molnar, 1993; Pavlis et al. 1997; Coutand et al., 2002; Schurr et al., 2014). The two major rivers in this region are STO 6 and include the Muksu River (6,673 km^2) in the east, and the Obkhimghou River (6,544 km^2) in the west. These catchments have mean elevations between 3,382 – 4,500 m, and maximum elevations above 7,000 m. Numerous valley glaciers dominate the landscape above ~3,500 m (Figure 3A). The Muksu River catchment is the most heavily glaciated catchment in the Vakhsh River catchment (presently 34 % of the Muksu River catchment area; Table 1) and contains the high altitude Fedshenko Glacier, the longest glacier outside the Polar Regions (Figure 3A).

1.2.4 LITHOLOGIES IN THE VAKHSH CATCHMENT

The lithologies exposed in the Vakhsh River catchment are diverse (Figure 3B; Table 1). The Western Tian Shan is dominated by crystalline

bodies, but also comprises a variety of Carboniferous, Devonian, and Silurian sedimentary and metasedimentary rocks (e.g., red sandstone, limestone with quartz lenses, schist, quartzite). The rivers in the Northern Pamir drain across various Cretaceous to Permian lithologies (e.g., red sandstone, sandy clay, conglomerates), whereas the Alai Valley is filled with Neogene and Quaternary fluvial and glacial sediments (Leith, 1985; Vlasov et al., 1991; Figure 3B).

1.2.5 DEFORMATION AND EXHUMATION RATES

Previous studies have documented deformation of the region across different time scales. GPS measurements along the Western Tian Shan and in the Pamir indicate present-day shortening of 10 – 15 mm/yr, mostly accommodated by the Northern Pamir (Sippl et al., 2008; Ischuk et al., 2013). Over longer (million year) time scales, exhumation rates from various regions of the Pamir have also been determined from $^{40}Ar/^{39}Ar$ thermochronometry on white mica (Carrapa et al., 2014). From this, the average Cenozoic exhumation rates are estimated at 0.2 - 0.4 mm/yr for the northeastern Pamir and 0.5 – 1.0 mm/yr for the Central Pamir (Carrapa et al., 2014). The exhumation rates for the northwestern Pamir are expected to be higher than in the northeastern part, because the northwestern Pamir is an orographic precipitation barrier (Carrapa et al., 2014; Pohl et al., 2015a; Pohl et al., 2015b). In the Western Tian Shan, exhumation rates based on apatite fission track and apatite (U-Th)/He analysis, are ~0.5 mm/yr over the last ~10 Myr (Käßner et al., 2016). Exhumation rates along the Ghissar Range are 0.2 – 0.3 mm/yr and 0.2 – 1.0 mm/yr in the Garm Massif (Käßner et al., 2016).

1.2.6 CATCHMENT-WIDE DENUDATION RATES

In situ-produced cosmogenic nuclides in river sediment are commonly used to show relationships between rock uplift and catchment-wide denudation rates (e.g., Wittmann et al., 2007). Catchment-wide denudation rates from cosmogenic nuclides along the Panj River, the main river draining the Southern and Central Pamir, range between 0.54 mm/yr and 1.45 mm/yr (Fuchs et al., 2015). In contrast, on the Pamir Plateau the catchment-wide denudation rates are as low as 0.05 – 0.16 mm/yr (Fuchs et al., 2015).

Table 1: Catchment-related geomorphic parameters.

Location ID	Sample ID	Latitude	Longitude	Drainage area total	Drainage area non-glaciated	Glaciated area	Mean elevation	Local relief 5 km radius	Average hillslope	Average k_{sn}
		°N	°E	km²	km²	%	m (±1σ)	m (±1σ)	° (±1σ)	(±1σ)
Vakhsh main trunk										
V1	mod7001	38.74477	69.83218	29670	25497	14	3559 ± 987	1914 ± 676	23 ± 14	210 ± 228
V2	mod7003	38.86478	69.97709	29040	24868	14	3538 ± 970	1926 ± 684	23 ± 14	208 ± 223
V3	mod7002	38.85148	69.97854	29018	24846	14	3538 ± 969	1912 ± 680	23 ± 14	208 ± 223
V4	mod7005	39.01980	70.37091	19508	16366	16	3711 ± 948	1875 ± 780	24 ± 14	192 ± 192
V5	mod7006	39.16610	71.08647	16888	13860	18	3859 ± 886	1842 ± 823	24 ± 14	192 ± 200
V6	mod7007	39.19270	71.20881	15539	12666	18	3904 ± 886	1829 ± 851	23 ± 14	188 ± 201
V7	mod6005	39.26691	71.37693	15253	12387	19	3924 ± 876	1835 ± 859	23 ± 15	186 ± 201
Locations resampled one year later along main trunk										
V1b	13 mod 7001	38.74475	69.83133	29670	25497	14	3559 ± 987	1914 ± 676	23 ± 13.9	210 ± 228
V4b	13 mod 7005	39.02029	70.37051	19508	16366	16	3711 ± 948	1875 ± 780	24 ± 14.3	192 ± 192
Western Tian Shan										
Obi Garm Tributary										
TS1	mod4001	38.71578	69.78272	285	285	0	2029 ± 390	2212 ± 558	21 ± 10.7	165 ± 146
Sarbog Tributary										
TS2	mod4012	39.01307	70.14259	292	283	3	2975 ± 728	2077 ± 329	30 ± 10.3	222 ± 139
TS3	mod4011	39.13641	70.19878	1296	1198	8	3266 ± 635	2222 ± 420	30 ± 11.6	238 ± 178
TS4	mod5001	39.03497	70.18875	1758	1656	6	3090 ± 712	2203 ± 285	30 ± 11.4	212 ± 164
Yarkutch Tributary										
TS5	mod4007	39.31721	70.63815	112	105	7	3340 ± 442	1900 ± 216	30 ± 10.8	261 ± 71
Tandykul Tributary										
TS6	mod4002	39.42830	71.22105	178	130	27	3731 ± 555	2435 ± 461	30 ± 14.5	254 ± 95
TS7	mod4003	39.42527	71.22238	201	163	19	3747 ± 499	2060 ± 279	31 ± 13.9	257 ± 199
TS8	mod5004	39.29603	71.22601	631	536	15	3478 ± 625	1796 ± 279	31 ± 13.2	254 ± 173
TS9	mod5003	39.29609	71.23148	526	468	11	3532 ± 569	2164 ± 360	26 ± 12.6	235 ± 122
TS10	mod6002	39.24385	71.22711	1293	1139	12	3391 ± 675	1987 ± 361	29 ± 13.1	256 ± 191
Alai Valley										
Kyzylsu River										
A1	mod6003	39.30426	71.43349	8328	7720	7	3505 ± 662	1545 ± 956	19 ± 13.4	120 ± 81
Northern Pamir										
Obkhimghou River										
P1	mod6001	38.85989	70.10363	6544	5627	14	3382 ± 883	2011 ± 413	25 ± 12.8	287 ± 341
Muksu River										
P2	mod6004	39.17273	71.55499	6674	4416	34	4500 ± 759	2212 ± 558	29 ± 14.2	380 ± 321

Table 2: Lithologies assigned to the epoches used in the geologic map according to Vlasov et al. 1991.

Epoch	Lithologies
Quaternary	pebbles, sand, boulders, blocks
Neogene	sandstone, siltstone, conglomerate, clay,
Paleogene	sandstone, clay, limestone, marl, gypsum
Cretaceous	red sandstone, sandish clay, marl, limestone
Jurrassic	sandstone, conglomerates, siltstones, layers with coal, gypsum
Triassic	conglomerates
Permian	conglomerates, sandstone with interlayers of felsic effusiva, tuff
Carboniferous	conglomerates, sandstones, siltstone, shist, limestones
Devonian	coal layers, limestone, limestone with quartzite lenses
Silurian	sandstone, shist, quartzites
Ordovician	limestone, siltstone, shist, conglomerate
Crystalline rocks	granites, granodiorites

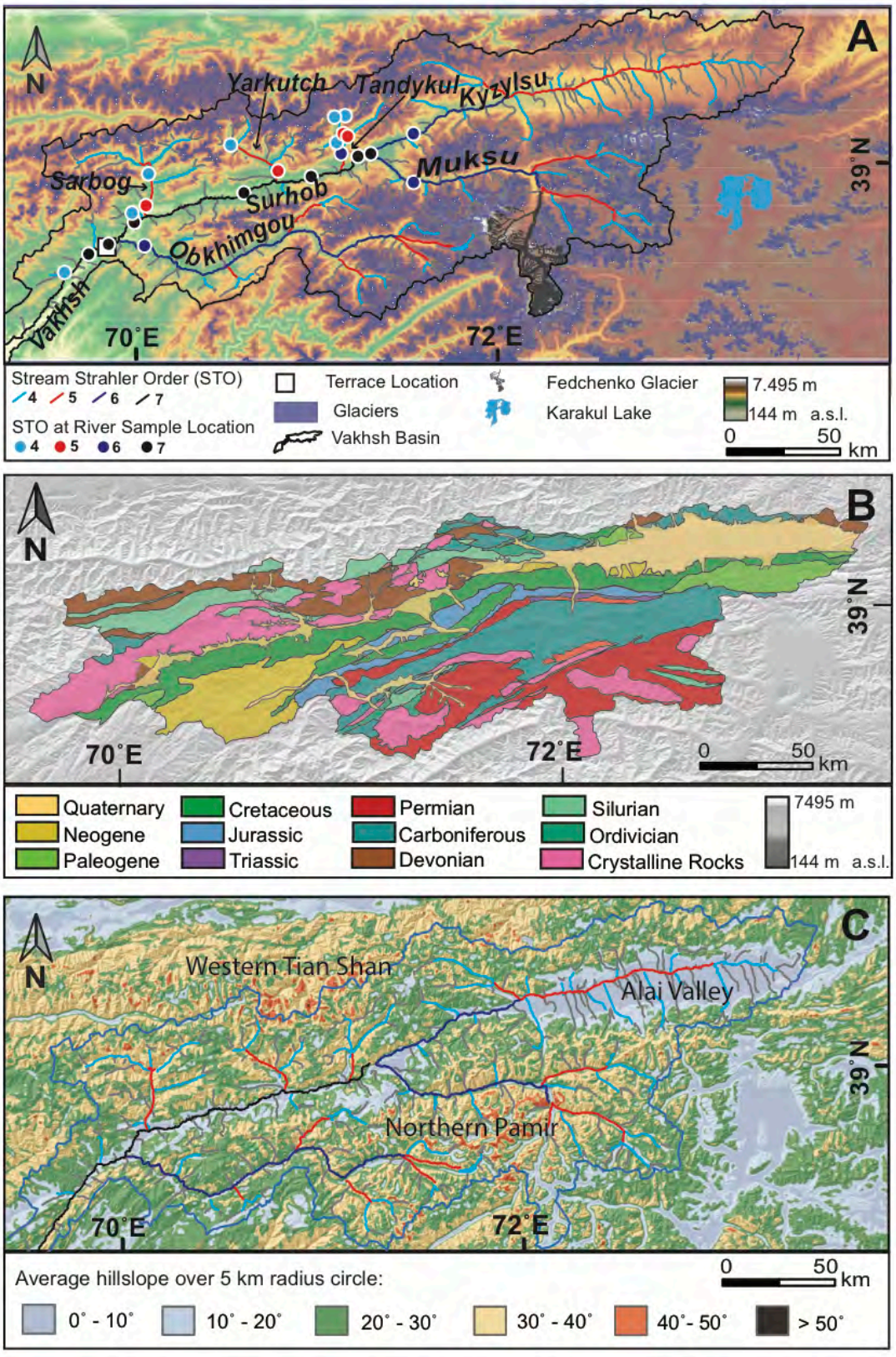

Figure 3: A) Location of the sampling sites in the Vakhsh River catchment. The square indicates the location of the terrace set and the circles show the area of sample locations for modern catchment-wide denudation rate samples. B) Geologic map simplified after Vlasov et al. (1991). C) Slope map of the investigated area based on 30 m DEM (http://gdex.cr.usgs.gov/gdex/ [2015]).

1.3 CLIMATE SETTING

A landscape is not only shaped by tectonic activity. The second important factor is climate. While changes in tectonic activity are thought to cover several million years, climate cycles occur on a millennial time-scale already. In combination, the amount of precipitation and range of temperature control the physical, chemical, and biological processes and thus ultimately regulate the generated volume, the transport, and the timing of sediment flux in a landscape (Allen, 2008; Whipple, 2009). In this section, insight is given into existing glacial records of the Tian Shan and Pamir and the climatic changes the region has experienced until the present day.

1.3.1 PALEO-CLIMATE

Previous studies (locations shown in Figure 4) highlighted that glaciations in the Western Tian Shan occurred during MIS (Marine Isotope Stage) 2, 4, and MIS 5 (Koppes et al., 2008; Narama et al., 2009; Zech, 2012). In the Pamir, glaciation has been identified during MIS 1, 2, 4, 5, 7, and MIS 9 (Abramowski et al., 2006; Seong et al., 2009; Röhringer et al., 2012; Zech et al., 2005a, 2013). The tentative late MIS 3 – early MIS 4 glaciation signal at the Pamir Plateau, identified by Abramowski et al. (2006), was recalculated by Dortch et al. (2013) to MIS 4. The Mid Latitude Westerlies dominate the climate in the Tian Shan and the Pamir (Figure 5A). The Indian Summer Monsoon controls the Himalayan climate. Dortch et al. (2013) suggested that these differences in prevailing winds and moisture transport have been a long-lasting phenomenon and resulted in asynchronous glaciations in the Himalaya, Tian Shan, and Pamir. For example, the monsoon triggered glaciations during MIS 2 and MIS 5 (Dortch et al., 2013) have been reported from the Tian Shan or the Pamir. In contrast, remnants from the MIS 3 or MIS 6 glaciations were not found in Tian Shan or in Pamir. Koppes et al. (2008) argued that the MIS 5 glaciation in the eastern Tian Shan could have been sourced by moisture from the large intramontane lakes in this region rather the Indian Summer Monsoon. A MIS 5 glaciation identified in the southern Pamir and eastern Tian Shan was interpreted by Röhringer et al. (2012) and Dortch et al. (2013) in the southern Pamir as evidence that the Indian Summer Monsoon moisture reached up to the south of the Pamir

Plateau. The Muztaghata region (Figure 4) of the eastern (Chinese) Pamir has been influenced partly by the Monsoon and partly by the Westerlies, which results in a more extensive glaciation history than in other parts of the Pamir (Seong et al., 2009). The lack of older glaciations in the Northern Pamir and Western Tian Shan could be the result of a lack in age constraints on preserved moraines (e.g. Zech, 2012), or they may not have existed at this location due to climate differences.

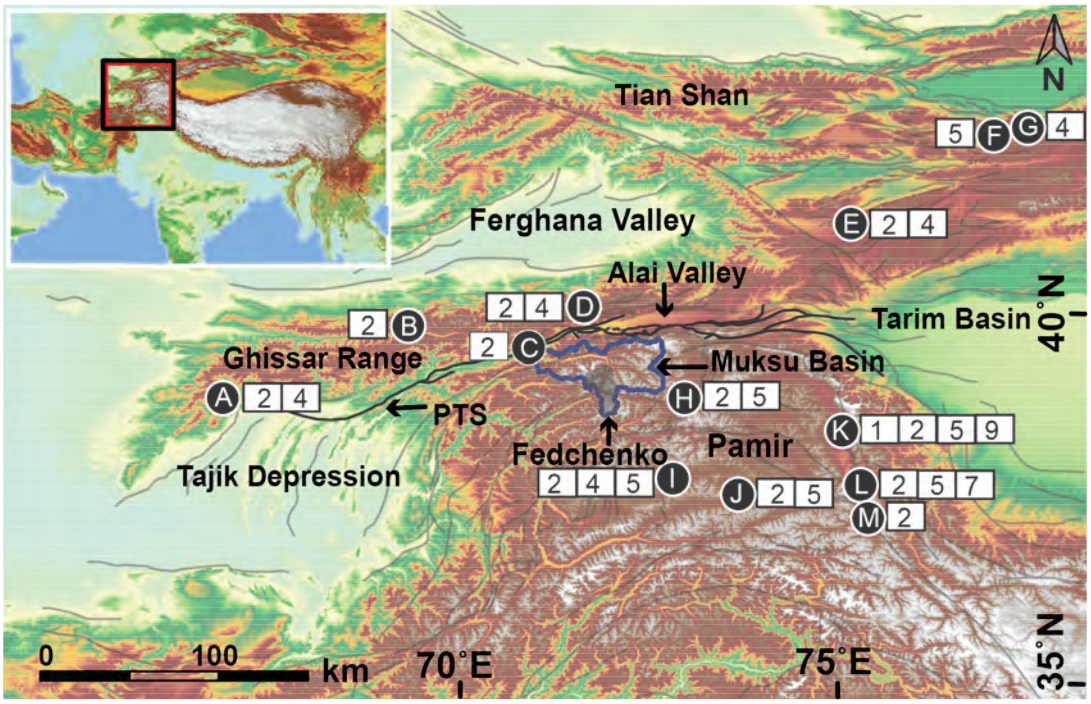

Figure 4: Location of the study area. The heavily glaciated Muksu catchment is located in the northern Pamir (see Figure 2). Overview of the regional glaciations, given as the MIS stages, is shown in white boxes (after Dortch et al., 2013). Letters refer to published data: A) Ghissar (Zech et al., 2013), B) Aksu (Abramovski et al., 2006), C) Muksu (this study), D) Koksu (Abramovski et al., 2006), E) Kitsh-Kurumdu (Zech et al. 2012), F) Ata Bash and G) Gulbel (Koppes et al., 2008), H) Ailuitek and Gurumdi (Abramovski et al., 2006), I) Yashikul and Bogoshir (Zech et al., 2005a, Abramovski et al., 2006; Röhringer et al., 2012), J) Alichur and Uchkol (Abramovski et al. 2006), K) Muztaghata (Seong et al., 2009), L) Kuzigun (Owen et al., 2012), M) Tashkurgan (Xu et al., 2013).

The MIS 2 glacial extent was observed to be smaller in both the Tian Shan and the Pamir than older glaciations due to a southward shift in the Siberian atmospheric high-pressure cell (Siberian high; Aizen et al., 2001; Weiers, 1995). The strength of the Westerlies is mainly dependent on the position of the Siberian high (Aizen et al. 2001a), because it can block humid western air masses and thus cause aridity in Central Asia. Svendsen et al. (2004) argued that during the last glaciation period, the Fennoscandian ice sheet could have functioned as an additional precipitation trap, which resulted

in less precipitation carried by the Westerlies. Overall, the Westerlies are thought to have been drier and colder during the LGM than today (e.g. Röhringer et al., 2012). Previous paleo-climate studies in the Northern Pamir identified a Holocene thermal optimum with increased humidity at 8.0 to 4.0 ka (Nikonov et al., 1989). A warmer and drier period than present-day was identified in the Western Tian Shan around 3.5 to 2.0 ka (Nikonov et al., 1981). Traces of a Little Ice Age event have been suggested for the Pamir but were not studied in detail. The sparse and inconsistent data on previous glaciations in this region require additional studies; in particular, studies are needed that constrain the timing of glaciation in the Northern Pamir.

1.3.2 PRESENT-DAY CLIMATE

The Mid Latitude Westerlies (Figure 5A), dependent on the position of the Siberian atmospheric high-pressure cell (Aizen et al. 2001) are the dominant climatic influence in the Western Tian Shan and Northern Pamir (Burtman and Molnar, 1993; Benn and Owen, 1998; Fuchs et al., 2014). Precipitation decreases from west to east. Present-day temperatures and precipitation are highly seasonal (Figure 5B–D; Table 3). Mean annual temperatures range between –6.7 and 12.2 °C. The majority of the mean annual precipitation (81 to 1161 mm) occurs between February and May.

Table 3: Mean annual precipitation and temperature data derived from local weather stations during 1960 - 1990.

ID in Fig.3	Location Name	Longitude	Latitude	Elevation in m	Precipitation in mm	available data in %	Temperature in ˚C	available data in %
1	Faizabad[1]	69.32	38.55	1215	844	100	-	0
2	Bustonabad	69.63	38.67	1983	775	93.6 - 100	8.0	93.5 - 100
3	Komsomolabad	69.98	38.87	1259	881	93.6 - 100	-	0
4	Garm	69.95	39	1316	743	100	11.3	93.5 - 100
5	Dehavz[1]	70.2	39.45	2561	300	100	4.6	96.8 - 100
6	Hovaling[1]	69.95	38.35	1468	999	93.6	12.2	96.8 - 100
7	Tavildara	70.48	38.7	1616	908	96.8 - 100	9.5	90.3 - 100
8	Harurabad[1]	70.7	38.63	3347	675	93.6 - 96.8	-0.8	96.8 - 100
9	Lyairun	70.9	38.9	2008	918	96.8	7.8	87.1 - 93.5
10	Daraut-Kurgan	72.18	39.55	2470	302	100	3.2	83.9 - 96.8
11	Altynmazar	72.22	39.18	2782	162	100	-	0
12	Fedchenko Glacier	72.22	38.83	4169	1161	100	-6.7	90.3 - 100
13	Sarytash	73.25	39.73	3153	370	100	-2.1	93.5 - 96.8
14	Karakul[1]	73.56	39.01	3935	81	100	-3.5	93.5 - 100

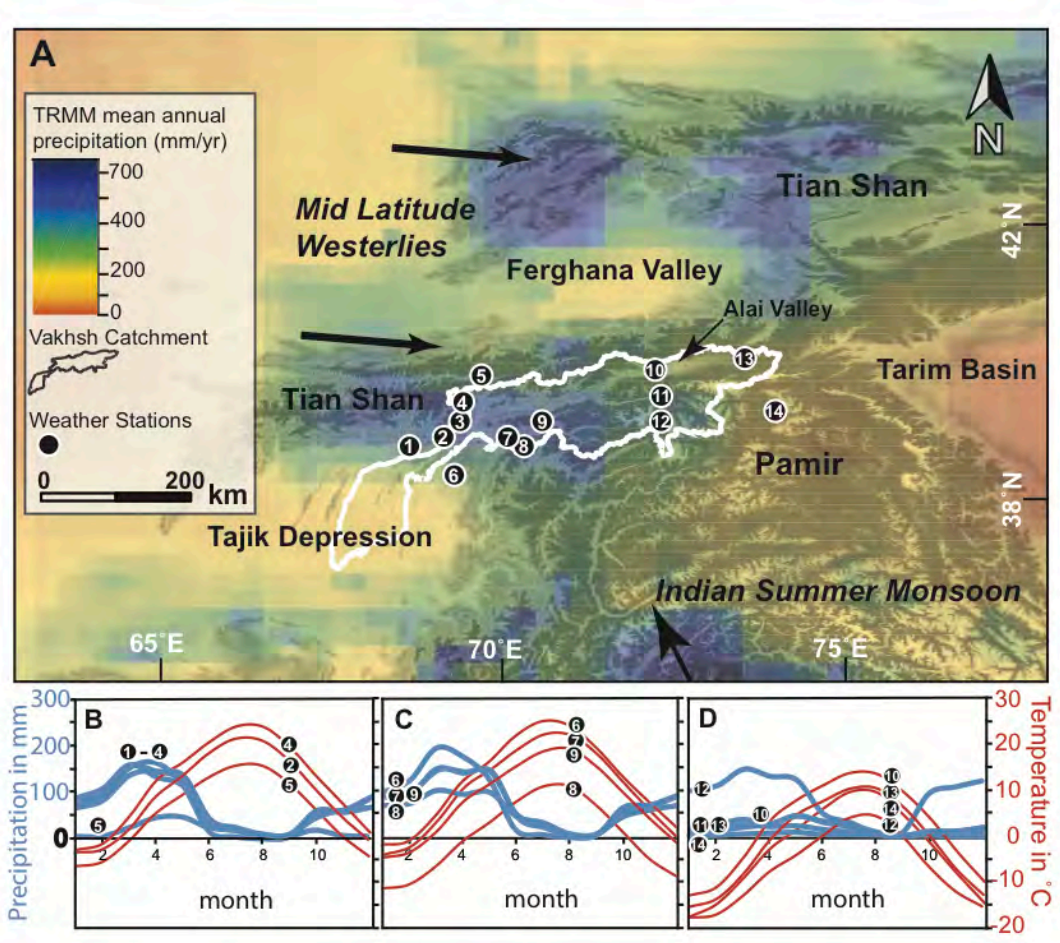

Figure 5: A) Precipitation map derived from the Tropical Rainfall Measurement Mission (TRMM) data set (Huffman et al., 2007) displaying the spatial distribution of the mean annual precipitation (years: 1998 to 2015) across the Pamir and the Western Tian Shan. Subplots B to D show the time series of precipitation and temperature curves calculated based on Soviet weather stations from 1960 to 1990. Stations are located in (1) Faizabad, (2) Bustonabad, (3) Komsomolabad, (4) Garm, (5) Dehavz, (6) Hovaling, (7) Tavildara, (8) Harurabad, (9) Lyairun, (10) Dataut-Kurgan, (11) Altyn-Mazar, (12) Fedchenko Glacier, (13) Sarytash, and (14) Karakul. Further data derived from the weather stations is shown in Table 3.

During this time, snowmelt produces additional discharge that increases the sediment transport capacity of rivers. The average annual discharge at the Nurek Dam site is 645 m^3/s with a maximum flood discharge of 3,900 m^3/s and a minimum of 120 – 200 m^3/s (Dam Safety Assessment, 2000).

1.4 AIM AND STRUCTURE OF THE STUDY

It is unknown if spatial and temporal gradients in denudation rates exist in the Vakhsh River catchment and what their relationship to fault activity in the Tian Shan and Northern Pamir, or regional climate gradients might be. In the

following, I state the hypotheses and how I planned to test them. Afterwards I introduce the structure of the thesis.

1.4.1 HYPOTHESIS AND SCIENTIFIC QUESTIONS

To determine, to what scale tectonics and climate shape the landscape in the Vakhsh River catchment, the spatial distribution of modern denudation rates across the catchment is analyzed. I expect that if denudation rates are mainly dictated by tectonics, they decrease westwards as soon as the tributaries in the Western Tian Shan are out of range from the Pamirs convergence towards the Tian Shan. Conversely, the influence from climate follows the opposite trend and decreases towards the east to correlate with decreasing annual precipitation.

Furthermore, to investigate the influence of climate cycles in this region, I study the glacial deposits of the ~72 km long Fedchenko Glacier. This glacier should be large enough to have lived through several glacial cycles and to tell their tale. From this, I not only hope to extend the records of glaciation history in this region, but also want to test, if the timing of deposition of the vast and well-preserved terrace sets along the Vakhsh main trunk correlates with the last glacial retreat.

1.4.2 METHODS USED IN THIS WORK

This study draws on the broad application possibilities of terrestrial cosmogenic nuclides (TCN). I study the vast Vakhsh River catchment by using one single TCN (^{10}Be). The variability of catchment–wide denudation rates on a millennial scale is tested by the measurement of present-day and paleo-denudation rates. Resampling locations during the second field season tests the potential seasonal variation in denudation rates. The sampling approach is motivated by the need to understand if lateral gradients in fault activity, or climate could contribute to any observed gradients in millennial time-scale denudation. I focus on differences in denudation rates between neighboring landscapes Alai Valley, Western Tian Shan, and Northern Pamir. The Tajik Depression was excluded from this study, because this region hosts several dams with reservoirs along the Vakhsh main trunk, which complicates the investigation of this area with TCN. This newly generated data can be

compared with published thermochronology data to draw conclusions about the long-term (several million years) history of landscape denudation.

Additionally depth profiles were taken from a set of fluvial terraces (one terrace was also sampled for a burial isochron age), an alluvial fan, and a lateral moraine to estimate their ages and erosion rates since their surface abandonment and onset of incision or exposure, respectively. To investigate possible sediment storage, I additionally measured the TCN ^{26}Al in several samples, which can be extracted from the same quartz grains as the ^{10}Be.

I compared catchment characteristics (e.g., hillslope, local relief, and the normalized river steepness index $k_{sn,}$) with denudation rates to identify when rivers change between transport-limited and detachment-limited conditions and to investigate any possible uplift patterns recorded in the river profiles.

Samples for moraine boulder exposure ages were taken from a recessional and five lateral moraines in the Fedchenko glacier hosting tributary to be able to identify the timing of potentially several glacial retreats and a possible correlation with the onset of terrace deposition along the main trunk. The Fedchenko Glacier is particularly important for understanding the glacial chronology in Central Asia, because it is the largest (~72 km) glacier outside the Polar Regions and the timing of its advance and retreat may be characteristic for the climate evolution of the Westerly-dominated Central Asia region. Glacial deposits, such as moraines, are archives that record advance and retreat cycles driven by climate change. Collecting spatial and temporal data about glaciations is essential for the reconstruction of both the regional and global timing of ice ages and climate change (e.g. Gillespie and Molnar, 1995; Thackray et al., 2008; Clark et al., 2009; Hughes et al., 2013).

1.4.3 STRUCTURE OF THE THESIS

This thesis is divided in 6 Chapters. The first chapter is an introduction into the geologic setting and the known climate history of the study area. The second chapter deals with the methodological background of the cosmogenic nuclides and the topographic analyses performed during this study.

In the chapters 3, 4, and 5 the data is preceded by a short overview of the sample collection and a detailed outline of the prerequisites for the

specific application types of TCN. Chapter 3 presents the ^{10}Be surface-exposure age dating of the glacial deposits from the Fedchenko Galcier. Chapter 4 displays the Holocene denudation rates and terrace ages of the Vakhsh River main trunk. Chapter 5 shows spatial distribution of cosmogenic ^{10}Be derived denudation rates between the Western Tian Shan and Northern Pamir. Chapter 6 summarizes the findings of this study and reflects on the follow-through of the scientific questions and aims of the study.

2 Background to Methods used

2.1 TERRESTRIAL COSMOGENIC NUCLIDES

In 1912 Viktor F. Hess was the first to discover the existence of terrestrial cosmogenic nuclides (TCN). However, widespread geological application of TCN had to wait until the upcoming use of Accelerator Mass Spectrometers (AMS) in the 1980's. Subsequently the TCN became widely spread in geosciences, filling the gap of absolute dating methods between the >1 ka and several Ma and thus allowing to address a large set of geomorphic questions (Ivy-Ochs and Kober, 2007). This introduction focuses only on radioactive TCN as applied during this study and does not discuss the characteristics of stable TCN (e.g. ^{3}He, ^{21}Ne; Ivy-Ochs and Schaller, 2009 and references therein).

The origin of TCN lies outside the solar system. So-called galactic rays are particles, which were accelerated during a supernova. These particles are mostly protons (87%), alpha-particles (12%), and carbon (~1%). Supernovae are thought to happen every 50 years in our galaxy (Diehl et al., 2006) and the mean cosmic ray flux is considered to be stable over the last 10 Ma (Leya et al., 2001). The energy of the galactic particles ranges between 100 MeV and 10 GeV. Nuclei and electrons with energies of ~1-100 MeV accelerated by solar winds in our solar system contribute ~1 % to the flux (Masarik and Beer, 2009; Reedy, 2013). However, the interaction between solar modulation and the Earth's magnetic field results in deflection of cosmic rays particles. Particles perpendicular to the magnetic fields with rigidities less than 0.6 GeV reach Earth's atmosphere, whereas the parallel traveling ones are deflected unless they have enough energy to exceed the influence of electric fields (<10 GeV). This results in TCN production being lowest at the equator and highest at the poles. The production of TCN arises from the interaction of secondary cosmic particles (neutrons and muons, mostly) with Earth surface material. Cosmic particles entering the Earth's atmosphere (primary cosmic rays) induce a cascade of spallation in the atmosphere, because their energies are far greater than atomic nuclei binding energies of 7 – 9 MeV. During spallation, protons and neutrons are ejected from the target nuclei.

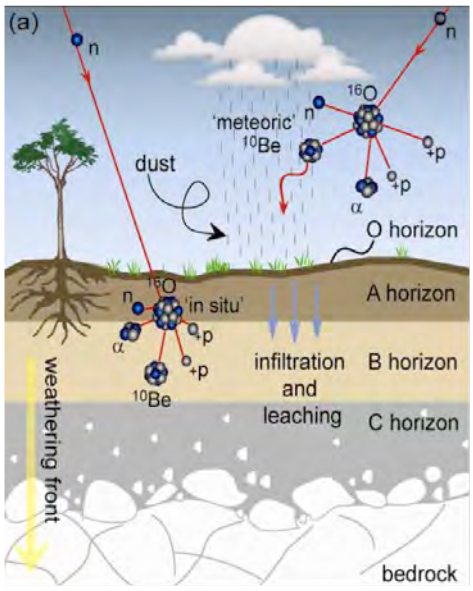

Figure 6: Possible interactions between secondary cosmic particles and elements in the atmosphere and earth, shown on the example of oxygen as target element (Willenbring and von Blanckenburg 2010).

The ejected neutrons and protons maintain the direction of the incoming cosmic particle. The result is a lighter isotope, which in case of ^{10}Be and ^{26}Al does not have any naturally occurring counterparts on Earth (Dunai, 2001). After the contact of a target nucleus with a primary cosmic ray particle (Figure 6; Willenbring and von Blanckenburg, 2010), the spallation cascade is driven mostly by neutrons (secondary cosmic rays), which carry a significant fraction of the incoming primarily cosmic ray particle energy.

The neutron energy spectrum is altitude-dependent. The secondary neutrons concentration decreases nearly exponentially with the atmospheric depth (Lal, 1991). Additionally, the interaction between primary cosmic rays and the atoms in the atmosphere also produces short-lived mesons, which decay into muons. Muons are elementary particles similar to electrons but with a 200-fold greater mass (Dunai, 2010) Muons dominate the production rate beneath the rock surface, whereas the spallation products control the rock surface production rate. Negative (stopped) muon capture occurs in ~2% of all reactions in case of ^{10}Be and ^{26}Al. Fast muons produce neutrons due to occurring *Bremsstrahlung* and thus cause spallation reactions (Groom et al., 2001)

The attenuation path length is the depth, where the cosmic ray flux decreases by a factor of 1/e. After 5 path lengths only 1% of the surface flux remains (Gosse and Phillips, 2001) The attenuation path length (neutrons: 150 g cm^{-2}; muons ~1,510 g cm^{-2} (Braucher et al., 2013) depends on the geomagnetic latitude, altitude, penetrated material, the particle's energy, and the inclination angle. The concentration of measured TCN in rocks depends in the first place, on the location parameters, such as geographic location (latitude), altitude, topographic shielding by the surroundings, and self-shielding induced by geometry. Depending on the application of TCN,

additional constraints must be accounted for as will be explained in detail in the methods sections of chapters 3 - 5.

2.1.1 ^{10}BE PRODUCTION

The main *in-situ* production of ^{10}Be occurs by spallation of heavier target-elements, e.g. O and Si. Therefore quartz is the preferred target mineral. Due to this target minerals widespread abundance, a large set of rocks is easily accessible by TCN-based applications. The abundance of oxygen in the atmosphere also gives rise to the meteoric ^{10}Be component, which is ~10^3 times higher than the terrestrial and needs to be separated from the sample material via additional chemical treatment.

Fast and stopped muon reactions contribute ~4% of the ^{10}Be production at sea level high latitude (SLHL). Several scaling schemes were proposed for the production rate calculation throughout the years (e.g. Lal 1991, Stone 2000, Dunai 2001). The scaling scheme proposed by Dunai (2001), on which all calculations in this study are based, utilizes a production rate of 4.43 +- 0.5 atoms/$g_{(qtz)}$$yr^{-1}$ SLHL. The used half-live for ^{10}Be is 1.387 ± 0.016 Myr (Chmeleff et al., 2010; Korschinek et al., 2010).

2.1.2 ^{26}AL PRODUCTION

^{10}Be is the most commonly used nuclide, either alone or paired with ^{14}C or ^{26}Al as presented during this study. The naturally occurring ^{27}Al is a very common trace element in minerals, thus the natural aluminum concentration must be determined before ^{26}Al can be measured. This way is ensured, that all natural ^{27}Al was successfully removed during leaching procedures. ^{26}Al is produced by spallation of ^{27}Al and Si. Fast and stopped muons account for ~4.5% of the production rate at SLHL in quartz. The half-life of ^{26}Al is 708 ± 17 ka (Nishiizumi, 2004). While ^{26}Al can be used on its own, it is often paired with ^{10}Be to investigate possible sediment storage along a river or an erosion rate for an exposed surface (Lal, 1991).

2.2 TOPOGRAPHIC ANALYSIS

2.2.1 CATCHMENT AREA ISOLATION

The calculation of topographic parameters is based on a digital elevation model (DEM), which was provided by the NASA Shuttle Radar Topographic Mission (SRTM). The DEM tiles have a resolution of 3 arc sec (90 m at the equator) and a size of 5 x 5 degrees per tile (http://www.cgiar-csi.org; Reuter et al., 2007). Each pixel in a DEM tile contains information about its elevation and the pixels at the corners provide additionally the coordinates of the DEM. The DEM files were prepared with ArcGIS for topographic parameters and river channel steepness calculation or MatLab for catchment-wide denudation rate calculations. The preparation included mosaic several DEM tiles into one seamless DEM, which contains the entire region of interest. The DEM is reprojected into Universal Transverse Mercator (UTM; WGS84 datum). The ArcGIS tool 'Fill' interpolates the data in all small gaps, which might have been caused by water bodies, heavy shadow, or insufficient textural detail, which occurs in mountainous regions and deserts. Usually, large gaps, which cannot be filled with interpolation, are filled by the provider of the satellite data by constructing a reference grid based on other available datasets, which then are merged with the satellite image. The identification of the fluvial network is calculated by the tool 'flow direction', which calculates the spatial orientation of each pixel relative to its surrounding eight neighbors and records the direction water would take on its surface. The tool 'flow accumulation' connects the data gained from the 'flow direction' calculation to fluvial networks. To extract the needed fluvial network area, a pixel in the fluvial network is selected as the outlet point, from which the area of the catchment is calculated upstream until the watershed pixels are identified. This watershed polygon can be used to clip the DEM to needed catchment size for further topographic analyses, which are only performed for the region of interest (in this case the upper Vakhsh catchment area).

2.2.2 CATCHMENT-WIDE DENUDATION RATE CALCULATION

The *in-situ* ^{10}Be production rate of a specific location is dependent on the geolocation, elevation, hillslope angle (self-shielding), the shielding

caused by its environment (e.g. topographic shielding by a nearby mountain wall, shielding by a water body, glacier, dense vegetation, or anthropogenic structures), and the abundance of the target mineral. The MatLab script modified after Chronos and s16 prepares the DEM as described in section 2.2.1. All DEM pixels, which are part of a glacier surface or an area where the lithology does not contain the target mineral, were excluded from the calculations. For this purpose, polygons from the Randolph Glacier Inventory 5.0 for Central Asia (https://www.glims.org/RGI/rgi50_dl.html; Pfeffer et al., 2014) and manually created and georeferenced polygons from the digitalized geological map (Vlasov et al. 1991) were used to identify the excluded pixels. The ^{10}Be production rate was then calculated for each of the remaining pixel and then incorporated into the denudation rate calculation. The pixel-wise calculated denudation rate was averaged to produce the catchment-wide denudation rate.

2.2.3 MORAINE BOULDER SHIELDING

In case of the moraine boulders, the self-shielding as well as the topographic shielding were recorded manually in the field. The topographic shielding was recorded each 60°. The self-shielding was avoided by sampling the topmost surface. A possible tilt of the sampled boulder surface was recorded and included into calculations.

2.2.4 ELEVATION, RELIEF, AND HILLSLOPE ANGLE

For the topographic parameters calculations the DEM was prepared as described in section 2.2.1. The hillslope angle is determined with the ArcGIS tool ‘slope’, which calculates the slope angle for each pixel by incorporating its eight neighbors into the calculation. Elevation information can be directly derived from the pixel information. The relief is calculated via a 5-km-radius moving window.

2.2.5 RIVER STEEPNESS ANALYSIS

River networks experience the same boundary conditions (climate, lithology, tectonics) as the landscape they drain (Howard et al., 1994; Whipple, 2004). As a result, they adapt their network and channel layout and shape the landscape according to the change in the boundary conditions.

Analyses of river networks give us insight in the temporal and spatial extent of these landscape-shaping conditions (e.g. Roe et al., 2002; Duvall, 2004; Wobus et al., 2006; Whittaker et al., 2007). One way to observe and identify the impact of climate, lithology, and tectonics on a landscape is to analyze the river channel steepness.

River channel steepness analyses were originally developed on the simplified system of bedrock rivers, which had to be in steady-state with their environment (Wobus et al., 2006). The form of steady-state river profiles was first described by Hack in 1957 and more precisely so by Flint's law (Flint, 1974):

$$S = k_s A^{-\theta} \quad (1)$$

where the local channel gradient (S) and the upstream drainage area (A) are described by a power-law relationship. The channel steepness index (k_s) is the local channel steepness and the concavity index (θ) describes the concavity of the river profile. The steady-state is thought to be achieved, when the river profile is fully adjusted to the conditions imposed on it by climate, tectonics and lithology, where small-scale fluctuations in climate and tectonics cannot be picked up by the response time of the fluvial system (~> 100 ka; Whipple et al., (2013)) and thus do not disturb the steady-state. In detail, that includes rivers with sediment-starved conditions (transport-capacity > sediment load), which can directly erode the in-place bedrock on a regular basis (e.g. Willett, 1999; Whipple, 2004). This way, the boundary conditions are directly imprinted into the river channel. In the case, where the river channel is covered by alluvium, the information about any change in the boundary conditions might be lost by a seasonal redistribution in the alluvium cover. In reality, an entire catchment composed of bedrock streams is very rare. However, most of the fluvial systems partially fulfill the steady-state or bedrock type prerequisites. Most of the streams (~80 %) contributing to a large catchment (>50 km^2) are bedrock rivers (Whipple, 2004). These bedrock rivers drain into a main stream, which is often filled with colluvium. The bedrock of sediment-filled channels can still be eroded seasonally on a regular basis (e.g. during snowmelt, monsoon, etc.), provided the transport capacity is high enough to lift the sediment load in the river channel.

To be able to analyze river profiles based on Flint's law, one should keep in mind, that the geometry and behavior of river source areas (streams with drainage areas less than 5 km^2; e.g. Stock and Dietrich, (2006)), or glaciated river heads cannot be described by the equation above. They are removed from the analyses. Further, the DEM used for channel analyses may introduce considerable amount of noise, by e.g. recorded landslides or simply by inaccuracy in the DEM (e.g. Wobus et al., 2006). And last, even steady-state river profiles may be segmented, where each segment has its unique k_s and θ values.

So how are different river networks compared, if even individual segments of a river profile can differ greatly from each other? The answer lies in the channel concavity. The index θ varies from 0.3 to 1.2 (e.g. Whipple and Tucker, 2002; Whipple, 2004) and was found to vary independently from tectonics, lithology, or climate conditions the analyzed streams experienced. But even smallest variations in θ influence greatly k_s, which is the index of choice to extract information about climate, lithology and tectonics in the end. To be able to gather the data about the boundary conditions without θ interfering, the concavity index is set to a reference concavity (0.45; (Whipple, 2004)), which leads to a normalized k_{sn} (Wobus et al., 2006):

$$S = k_{sn} A^{-\theta_{ref}} \tag{2}$$

and gives way to comparison between river profile segments as well as between entire river networks. There are two ways to treat the k_{sn} data. The first is to compare the k_{sn} values of a stream to values of other catchment parameters, such as measured erosion rates, relief, etc. These parameters were found to have a correlation with the normalized steepness index, if the catchment is in (nearly) steady state (e.g. Safran et al., 2005; Ouimet et al., 2009; DiBiase et al., 2010; Cyr et al., 2010).

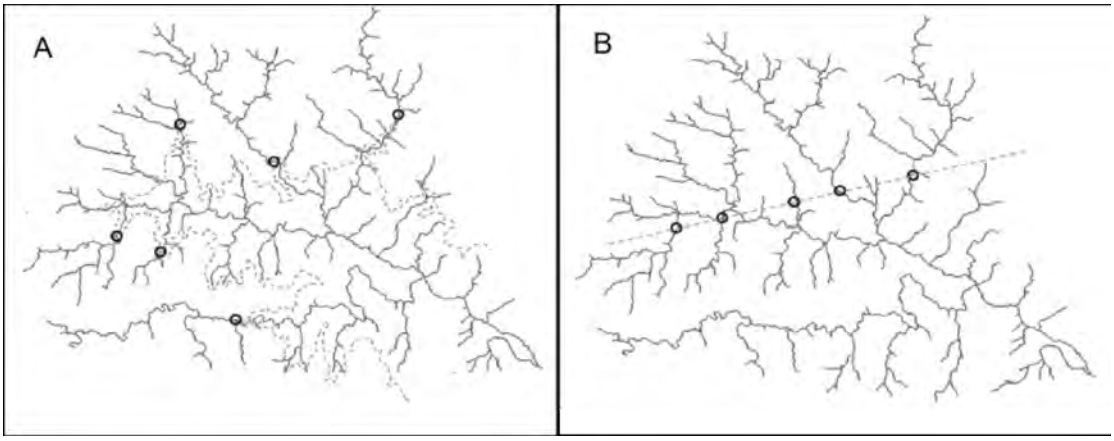

Figure 7: Example of different patterns in knickpoint distribution. A: knickpoint distribution records uplift in the catchment. Knickpoints travel upstream into the tributaries and can be found roughly at the same elevation. B: knickpoint distribution along a fault. Knickpoint distribution follows the sptial layout of the knickpoint causing feature. Modified after Wobus et al. 2006.

The second way to process the k_{sn}, is to create longitudinal river profiles and map the values of k_{sn}. Changes in river steepness are referred to as knickpoints (e.g. Schoenbohm et al., 2004; Crosby and Whipple, 2006; Berlin and Anderson, 2007). Knickpoints migrate along the stream and its tributaries or stay locked in place. There are also two different kinds of knickpoints (Haviv et al., 2006). The vertical-step knickpoint is a discrete step in the river profile. It presents itself often as a waterfall. The steepness index of the upstream area is the same as downstream of the waterfall. This type occurs for example in response to base-level drop at the outlet. The upstream propagating vertical-step knickpoint simply adjusts the channel to the new base level. The second type is the slope-break knickpoint, where the knickpoint separates two channel segments with different steepness indices (Wobus et al., 2006). This second type records a change in boundary conditions, such as climate, or tectonics and has a rather transient nature. The migration of both types of knickpoints is dependent on the lithology, channel width, involved erosion processes, etc. (e.g. Crosby and Whipple, 2006; Bishop, 2007; Goldrick and Bishop, 2007). Both types can occur in steady-state and in transient river networks and the presence of one type does not exclude the other. Everything that has an impact on the erosion of a bedrock channel (e.g. faults, change in rock resistance, differences in uplift rates) causes the formation of knickpoints. A close field survey of the river

channel and its surroundings helps to identify the cause of the knickpoint formation. After the identification of locally induced knickpoints (such as by faults, changes in lithology, landslides, etc.) the uplift history recording knickpoint patterns can be identified (Figure 7).

Author	Author position	Scientific ideas %	Data generation %	Analyses & interpretation	Paper writing %
Elena Grin	PhD Student	50	80	60	60
Todd Ehlers	Professor	30	0	10	15
Mirjam Schaller	Postdoc	10	10	20	15
Vasila Sulaymonova	PhD Student	0	10	5	0
Lothar Ratschbacher	Professor	5	0	5	5
Richard Gloaguen	Professor	5	0	0	5
Title of paper:	^{10}Be Surface-Exposure Age Dating of the Last Glacial Maximum in the Northern Pamir (Tajikistan)				
Status in publication process:	published				
Reference:	Grin, E., Ehlers, T.A., Schaller, M., Sulaymonova, V., Ratschbacher, L., Gloaguen, R., 2016. ^{10}Be Surface-Exposure Age Dating of the Last Glacial Maximum in the Northern Pamir (Tajikistan). Quat. Geochronol. doi:10.1016/j.quageo.2016.03.007				

3 10Be Surface-Exposure Age Dating of the Last Glacial Maximum in the Northern Pamir (Tajikistan)

3.1 Sample Collection

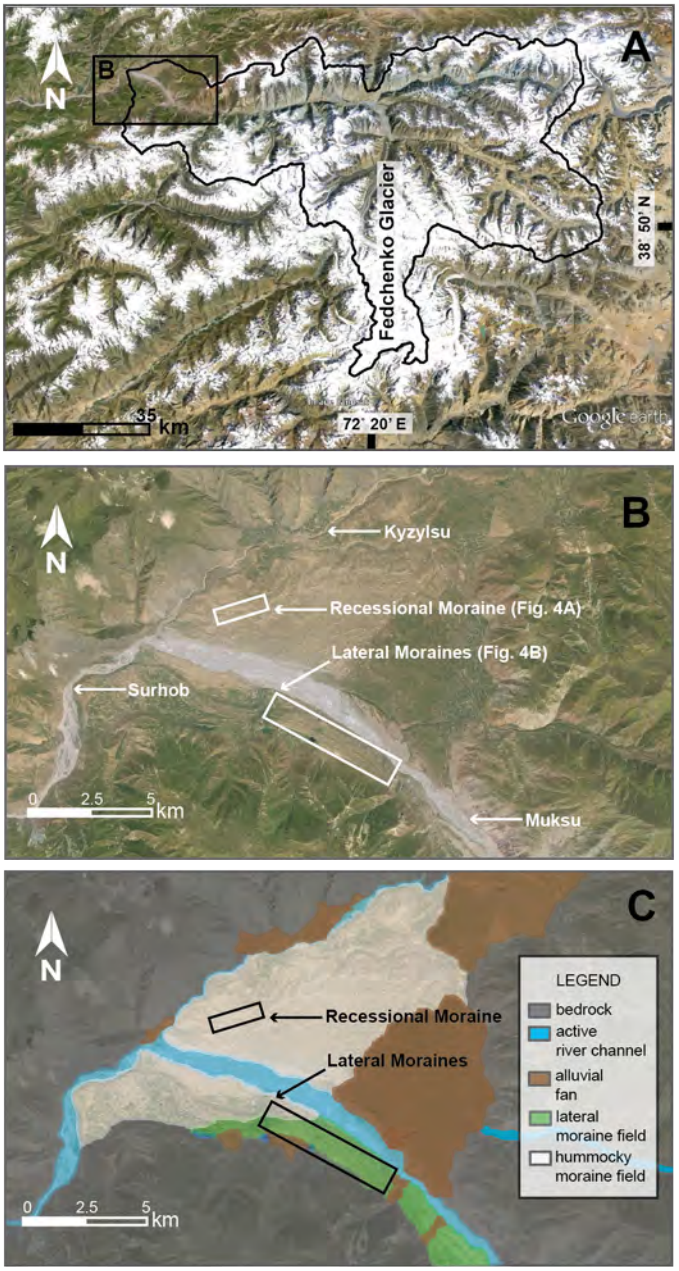

Figure 8: A) Google Earth image showing the glaciated Muksu catchment. B) Sampling areas comprising recessional and lateral moraines in the lower Muksu catchment. C) Interpretation of the geomorphologic features in the sampling area.

In the lowermost Muksu valley (Figure 8A), we investigated a field of hummocky moraines at an altitude of ~2,060 m as well as a suite of lateral moraines at ~2,280 m (Figure 8B,C). The recessional moraine stretches over two kilometers along the formerly glaciated valley on the hummocky moraine field (Figure 8A). The lateral moraines are located ~5 km upstream from the recessional moraine on the southwestern valley side (Figure 8B,C). We sampled 20 boulders from the furthest downstream, best-preserved, recessional moraine. This moraine could also represent the terminal moraine during the last glacial advance, but this

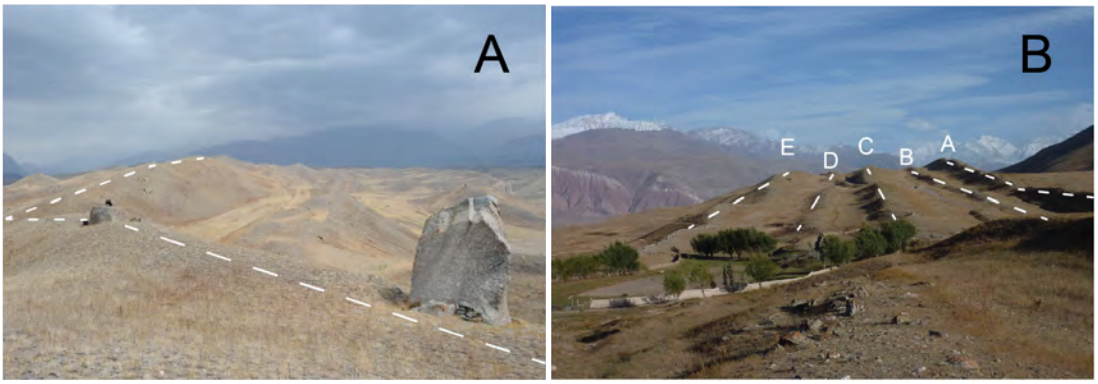

Figure 9: A) Recessional moraine on the hummocky moraine field. Boulder in the front is ~4 m high. B) Lateral moraines with A being farthest and E closest to the active river channel.

was not clearly discernible in the field. We did not sample other moraine remnants, as land use or post-depositional fluvial reworking affected them. From the rounded crests of five lateral moraines, we sampled 41 boulders (Figure 9B; Appendix Table 1). The range of boulder heights from the recessional moraine is 5.0–0.5 m (mean 1.16 m without the largest two boulders) and 1.5–0.5 m (mean 0.93 m) for the lateral moraines (Table 4; Appendix Table 2). We removed rock chips from the uppermost ~2.5 cm of the top surface of the boulders for analysis. Measurements for topographic shielding correction were taken every 60 degrees. Putkonen and Swanson (2003) suggested that a minimum of three samples from a ~10 m high, ~20 ka old moraine crest is sufficient for an age determination. However, we collected additional samples to obtain a robust age determination for the smaller moraine crests. The sampled lateral moraines show some post-depositional degradation from erosion and/or anthropogenic (grazing) use; the exact amount of degradation is unknown. Rodent burrows locally indicate bioturbation of the moraine material underlying the boulders. We sampled a ~2 m deep depth profile on one lateral moraine crest to obtain an estimate of the magnitude of moraine degradation, but it yielded insufficient quartz for ^{10}Be measurement.

Out of the 20 samples collected from the recessional moraine, 16 yielded enough quartz to allow cosmogenic ^{10}Be dating; 31 out of 41 samples of the lateral moraine set were amenable for dating (Table 4; Appendix Table 3 and 14). Quartz preparation (Appendix Tables 6 -12) and Be

separation with ion-exchange chromatography followed the procedure described by von Blanckenburg (2005).

3.2 METHODS

Exposure age dating with cosmogenic nuclides is mostly based on spallation reactions in a target mineral, which is exposed or close (1-3 cm) to the surface of interest. Further observations, e.g. self-shielding through a complex shape of the specimen or post-depositional tilting, and topological shielding by the surroundings must be recorded on site. Although most of the secondary neutron flux is coming in perpendicular, in case of old surfaces, the particle flux from other angles plays an increasing role. Dating moraine boulders also may include surfaces, which were previously exposed and thus have an unknown component of inherited TCN. This issue is often resolved by sampling a series of boulders, which helps to identify outliers. This tactic is also used to minimize the risk of tilted samples. More often than not, the rock surfaces also experience erosion during exposure, which must be accounted for.

The boulder-exposure ages were calculated with the CRONUS-Earth online calculator (v. 2.2; Balco et al., 2008; Appendix Tables 14 - 16), using blank-corrected data (Appendix Table 4) and the beryllium-isotope standard for ^{10}Be measurements defined by Nishiizumi et al. (2007) (07KNSTD). We employed both the Dunai (2001) and Lal (1991) (as modified by Stone (2000) scaling factors for the exposure-age calculations (Table 4). The ages calculated from the Dunai (2001) scaling are slightly older than the ones calculated after Stone (2000) and Lal (1991). For better comparison with the published data from the region, we used the exposure ages calculated after Stone (2000).

We evaluated the impact of erosion on the ages by comparing no erosion minimum exposure ages with ages calculated using an erosion rate of 0.03 cm/yr for the maximum exposure age. The effect of erosion on exposure ages was explored to provide an estimate of the uncertainty in the exposure ages, in the event moraine and boulder erosion occurred. The incorporation of erosion results in 4 % higher ages. However, erosion is affecting different rock

types differently, and individual boulders of the same lithology randomly (Röhringer et al., 2012). An additional factor that could influence the exposure ages is snow cover. For our study area (and many previous studies in the region), no reliable snow-cover data exist. Therefore, all exposure ages are uncorrected for snow shielding and considered minimum ages. Other studies in similar regions of Central Asia also report ages without a snow-shielding correction (e.g. Kong et al., 2009; Owen et al., 2012; Xu et al., 2013; Lifton et al., 2014).

To determine the exposure ages of moraines, different approaches have been used (Zech et al., 2005b; Owen, 2009; Dortch et al., 2013; Kelly et al., 2013). Herein, the exposure ages were calculated using Kernel probability density plots of the complete exposure-age sample population. We used the internal error to identify outliers in the populations of ages, employing Greg Balco's online available Matlab script named 'camelplot' (http://depts.washington.edu/cosmolab/pubs/gb_pubs/camelplot.m [09/2015]). For sample populations where a cluster of ages can be identified (as in our recessional moraine sample population discussed below), the outliers can be discarded based on the kernel plots and the mean of the remaining population can be interpreted as the moraine age (e.g. Dortch et al., 2013). If the age population shows a tendency towards too young ages, e.g. due to post-depositional shielding or erosion, as we infer for our lateral moraine data (see below), the oldest age of a population can be considered as the one closest to the moraine-formation age (Putkonen and Swanson, 2003; Zech et al., 2005b; Applegate et al., 2010).

Putkonen and Swanson (2003) showed that it is impossible to completely exclude boulders affected by post-depositional processes from an age calculation, but the calculation of the normalized age from a population of ages can assist in understanding the depositional age. The normalized boulder age range is calculated using the difference between the maximum and minimum ages from a single moraine population, divided by the maximum age; values may range from 0 to 1. Putkonen and Swanson (2003) suggested that a population of non-affected boulders yields a normalized age range of 0.12 (12 %), which represents the random systematic errors of the calculated

exposure ages. The conditions of having boulders unaffected by inheritance or post-depositional shielding are rarely met. Given this, Putkonen and Swanson (2003) found that the mean normalized age range is 38 % and can form the basis for interpreting exposure ages. In this study, we used the normalized age approach together with the kernel probability density plots to examine whether the mean age or the oldest population age better represents the moraine data.

3.3 RESULTS

3.3.1 RECESSIONAL MORAINE EXPOSURE AGES

The recessional moraine is the only one with a well-preserved arcuate ridge morphology (Figure 9A); it extends over two kilometers.

We avoided sampling the few incised parts of the moraine and collected all samples from its crest. There are no better-preserved moraines further down valley from this location, so it is the best indicator of the maximum extent of the ice in the valley at the time of glaciation. Figure 10 shows the age distribution found on all investigated moraines. The kernel probability density analysis (Figure 11A) of all exposure ages shows two peaks (11.7 ± 0.5 and 17.5 ± 1.5 ka) and The outliers (11.3 ± 1.0, 11.5 ± 1.1, 11.6 ± 1.1, 12.4 ± 1.2, 14 ± 1.3, 25.6 ± 2.3, 28.7 ± 2.6, 35.6 ± 3.2 ka) comprise both too young and too old ages relative to the mean age of 17.5 ± 1.5 ka. Figure 10 shows that this mean, calculated without the identified outliers, is in good agreement with the three largest boulders (samples ER 10: 17.4 ± 1.6 ka, ER 15: 17.3 ± 1.6 ka, and ER 8: 17.0 ± 1.6 ka). We consider the mean age of 17.5 ± 1.5 ka the best minimum estimate for the depositional age of the recessional moraine. The 16 ^{10}Be exposure ages range from 11.3 ± 1.0 to 35.6 ± 3.3 ka (Table 4, Figure 10) with a normalized age range of 0.68.

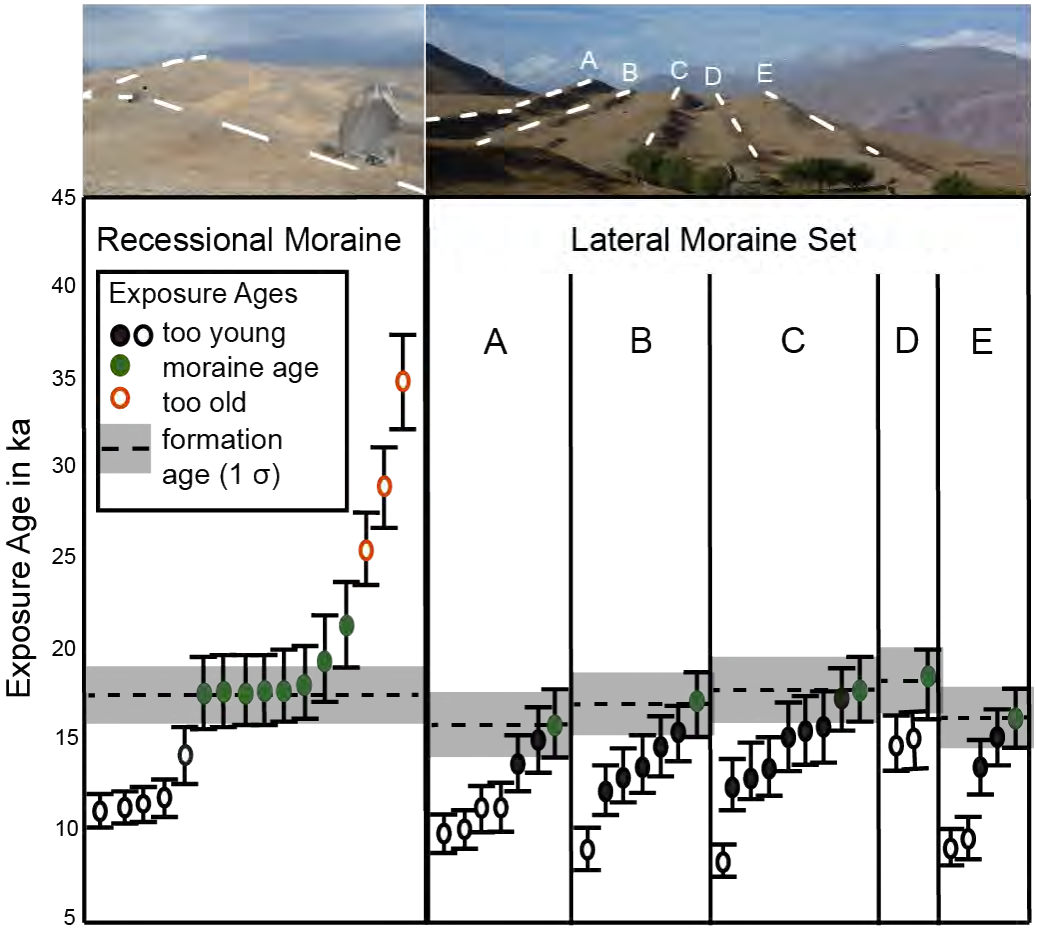

Figure 10: ^{10}Be exposure-age distributions in individual moraines. Boulder exposure ages are shown with one-sigma error bars. Outliers according to Kernel probability plots are indicated with empty symbols.

Table 4: Cosmogenic ^{10}Be surface exposure ages for recessional moraine and lateral moraines were calculated with CHRONUS-Earth Online Calculator (v.2.2.; Balco et al. 2008) using a rock density of 2.4 g/cm^3, 07KNSTD ^{10}Be standard. No correction for snow shielding was applied. Altitudes were determined with a handheld GPS with an accuracy of ± 5m.

Sample ID	Longitude	Latitude	Altitude in m	Boulder Height in cm	Chip Thickness in cm	Shielding Factor at sample site	Boulder Lithology
Recessional Moraine							
ER001	39.28185	71.42316	2068	180	3.0	0.99	Granodiorite
ER002	39.28128	71.42244	2072	70	2.5	0.99	Granodiorite
ER003	39.28107	71.42232	2078	110	2.0	0.99	Granodiorite
ER004	39.28098	71.42111	2068	140	2.5	0.99	Granodiorite
ER006	39.28064	71.41969	2075	50	2.0	0.99	Granodiorite
ER008	39.28021	71.41484	2059	220	2.5	0.99	Granodiorite
ER009	39.28021	71.41484	2059	140	2.5	0.99	Granodiorite
ER010	39.28001	71.41446	2062	500	2.5	0.99	Granodiorite
ER011	39.28207	71.42548	2078	90	2.0	0.99	Granodiorite
ER013	39.28186	71.42601	2078	100	2.0	0.99	Granodiorite
ER014	39.28164	71.42662	2082	150	2.5	0.99	Granodiorite
ER015	39.28188	71.42793	2090	400	2.0	0.99	Granodiorite
ER016	39.28175	71.42785	2090	100	2.5	0.99	Quartz vein
ER017	39.28307	71.42754	2069	100	2.5	0.99	Granodiorite
ER019	39.28304	71.42702	2077	100	2.5	0.99	Granodiorite
ER020	39.28411	71.42448	2060	100	1.5	0.99	Red Sst Congl.[5]
Lateral Moraines							
LMA002	39.23157	71.45891	2258	110	2.5	0.99	Granodiorite
LMA003	39.23128	71.45942	2258	110	2.5	0.99	Granodiorite
LMA004	39.23128	71.45942	2258	80	2.0	0.99	Granodiorite
LMA005	39.23098	71.46027	2264	80	2.5	0.99	Granodiorite
LMA008	39.23011	71.46222	2276	70	2.0	0.99	Granodiorite
LMA009	39.22859	71.46568	2315	150	2.0	0.99	Granodiorite
LMA010	39.22761	71.46804	2337	60	2.0	0.99	Granodiorite
LMB001	39.23146	71.46003	2262	90	2.5	0.99	Granodiorite
LMB002	39.22726	71.47054	2313	60	1.5	0.99	Red Sst Congl.[5]
LMB004	39.22653	71.47211	2315	90	2.5	0.99	Granodiorite
LMB005	39.23091	71.46139	2266	50	2.5	0.99	Granodiorite
LMB006	39.22257	71.47916	2316	110	2.5	0.99	Granodiorite
LMB007	39.22294	71.47839	2316	80	2.0	0.99	Granodiorite
LMB008	39.22361	71.47729	2318	120	1.5	0.99	Red Sst Congl.[5]
LMC001	39.22558	71.47550	2303	100	2.5	0.99	Granodiorite
LMC002	39.22879	71.46790	2311	80	2.5	0.99	Quartz vein
LMC003	39.23003	71.46506	2293	120	2.5	0.99	Quartz vein
LMC004	39.23003	71.46506	2293	120	2.5	0.99	Granodiorite
LMC005	39.2309	71.46325	2285	70	2.5	0.99	Granodiorite
LMC006	39.23096	71.46301	2279	110	3.0	0.99	Granodiorite
LMC008	39.23105	71.46276	2278	90	2.0	0.99	Red Sst Congl.[5]
LMC009	39.23118	71.46252	2278	50	2.5	0.99	Granodiorite
LMC010	39.23162	71.46124	2271	110	1.5	0.99	Red Sst Congl.[5]
LMD001	39.23211	71.46103	2251	130	2.0	0.99	Granodiorite
LMD002	39.23184	71.46165	2255	90	3.0	0.99	Granodiorite
LMD003	39.23448	71.45472	2241	50	2.5	0.99	Granodiorite
LME003	39.22499	71.47882	2281	130	1.5	0.99	Quartz veign
LME005	39.22637	71.47633	2288	110	1.5	0.99	Red Sst Congl.[5]
LME007	39.2282	71.47279	2305	110	1.5	0.99	Quartz vein
LME010	39.23125	71.46468	2285	80	3.0	0.99	Granodiorite
LME012	39.23259	71.46098	2255	80	3.0	0.99	Granodiorite

^{10}Be conc. in atoms/g	Lal(1991) & Stone(2000) Min. Exposure Age[1] in ka	Stone/Dunai[2]	Lal(1991) & Stone(2000) Max. Exposure Age[3] in ka	no Erosion / Erosion[4]	Sample ID
					Recessional Moraine
5.20E+05 ± 1.77E+04	25.6 ± 2.3	0.97	27.3 ± 2.7	0.94	ER001
3.40E+05 ± 1.15E+04	17.0 ± 1.6	0.95	17.7 ± 1.7	0.96	ER002
2.31E+05 ± 9.21E+03	11.6 ± 1.1	0.91	12.0 ± 1.2	0.97	ER003
7.40E+05 ± 2.45E+04	35.6 ± 3.3	0.98	38.6 ± 3.9	0.91	ER004
2.28E+05 ± 7.63E+03	11.5 ± 1.1	0.91	11.9 ± 1.1	0.97	ER006
3.37E+05 ± 1.17E+04	17.0 ± 1.6	0.94	17.7 ± 1.7	0.96	ER008
3.38E+05 ± 1.16E+04	17.1 ± 1.6	0.94	17.8 ± 1.7	0.96	ER009
3.47E+05 ± 1.23E+04	17.4 ± 1.6	0.95	18.2 ± 1.8	0.96	ER010
2.79E+05 ± 9.46E+03	14.0 ± 1.3	0.93	14.5 ± 1.4	0.97	ER011
3.42E+05 ± 1.15E+04	17.0 ± 1.6	0.95	17.6 ± 1.7	0.96	ER013
3.98E+05 ± 1.30E+04	19.7 ± 1.8	0.95	20.7 ± 2.0	0.95	ER014
3.50E+05 ± 1.28E+04	17.3 ± 1.6	0.95	18.0 ± 1.7	0.96	ER015
2.27E+05 ± 7.55E+03	11.3 ± 1.0	0.91	11.6 ± 1.1	0.97	ER016
5.87E+05 ± 1.92E+04	28.7 ± 2.6	0.97	30.8 ± 3.0	0.93	ER017
4.25E+05 ± 1.53E+04	21.0 ± 1.9	0.96	22.1 ± 2.2	0.95	ER019
2.45E+05 ± 9.40E+03	12.4 ± 1.2	0.92	12.7 ± 1.2	0.98	ER020
					Lateral Moraines
2.84E+05 ± 1.09E+04	12.7 ± 1.2	0.93	13.1 ± 1.3	0.97	LMA002
3.24E+05 ± 1.58E+04	14.4 ± 1.4	0.94	15.0 ± 1.5	0.96	LMA003
2.01E+05 ± 7.03E+03	9.0 ± 0.8	0.89	9.2 ± 0.9	0.98	LMA004
3.38E+05 ± 1.14E+04	15.0 ± 1.4	0.94	15.5 ± 1.5	0.96	LMA005
2.28E+05 ± 7.63E+03	10.1 ± 0.9	0.91	10.3 ± 1.0	0.97	LMA008
2.40E+05 ± 1.05E+04	10.3 ± 1.0	0.91	10.6 ± 1.0	0.97	LMA009
2.08E+05 ± 8.28E+03	8.8 ± 0.8	0.89	9.0 ± 0.9	0.98	LMA010
3.27E+05 ± 1.26E+04	14.5 ± 1.4	0.94	15.1 ± 1.5	0.96	LMB001
1.84E+05 ± 1.54E+04	7.9 ± 0.9	0.88	8.0 ± 1.0	0.98	LMB002
2.79E+05 ± 1.03E+04	12.0 ± 1.1	0.92	12.4 ± 1.2	0.97	LMB004
3.07E+05 ± 1.07E+04	13.6 ± 1.3	0.93	14.1 ± 1.3	0.97	LMB005
3.80E+05 ± 1.54E+04	16.2 ± 1.5	0.95	16.9 ± 1.7	0.96	LMB006
2.94E+05 ± 1.34E+04	12.6 ± 1.2	0.93	13.0 ± 1.3	0.97	LMB007
2.61E+05 ± 1.08E+04	11.1 ± 1.1	0.92	11.4 ± 1.1	0.98	LMB008
3.38E+05 ± 1.95E+04	14.6 ± 1.5	0.94	15.2 ± 1.6	0.96	LMC001
3.54E+05 ± 1.90E+04	15.2 ± 1.5	0.95	15.7 ± 1.6	0.96	LMC002
3.46E+05 ± 1.33E+04	15.0 ± 1.4	0.94	15.6 ± 1.5	0.96	LMC003
3.97E+05 ± 1.48E+04	17.1 ± 1.6	0.95	17.9 ± 1.7	0.96	LMC004
2.61E+05 ± 1.01E+04	11.5 ± 1.1	0.92	11.8 ± 1.1	0.97	LMC005
3.87E+05 ± 1.57E+04	16.9 ± 1.6	0.95	17.6 ± 1.7	0.96	LMC006
1.67E+05 ± 6.89E+03	7.3 ± 0.7	0.87	7.4 ± 0.7	0.99	LMC008
2.77E+05 ± 1.06E+04	12.2 ± 1.1	0.92	12.6 ± 1.2	0.97	LMC009
2.92E+05 ± 1.19E+04	12.9 ± 1.2	0.93	13.2 ± 1.3	0.97	LMC010
3.24E+05 ± 1.10E+04	14.5 ± 1.3	0.94	15.0 ± 1.4	0.96	LMD001
4.12E+05 ± 1.57E+04	18.2 ± 1.7	0.96	19.0 ± 1.9	0.96	LMD002
3.44E+05 ± 1.40E+04	15.4 ± 1.5	0.94	16.0 ± 1.6	0.96	LMD003
1.80E+05 ± 7.67E+03	7.9 ± 0.7	0.88	8.0 ± 0.8	0.98	LME003
3.49E+05 ± 1.34E+04	15.1 ± 1.4	0.94	15.6 ± 1.5	0.97	LME005
1.97E+05 ± 9.82E+03	8.5 ± 0.8	0.89	8.6 ± 0.9	0.98	LME007
2.84E+05 ± 9.22E+03	12.5 ± 1.1	0.93	12.9 ± 1.2	0.97	LME010
3.17E+05 ± 1.18E+04	14.2 ± 1.3	0.94	14.7 ± 1.4	0.97	LME012

(1) Exposure age calculated with no erosion.
(2) Difference in exposure ages calculated with Stone (2000) and Dunai (2001) calibration sets.
(3) Maximum exposure age data was calculated with an estimanted erosion of 0.3 cm/kyr.
(4) Difference in exposure ages calculated without erosion and with 0.3 cm/kyr erosion.
(5) Red Sandstone Conglomerate.

3.3.2 LATERAL MORAINE EXPOSURE AGE

The five lateral moraines (LMA-LME) have distinct but well-rounded crests (Figure 11B). We sampled all five moraines individually to assess the time interval over which this glaciation occurred. The overall age range is 7.3 ± 0.9 to 18.2 ± 1.7 ka (Table 4, Figure 11B). Lateral moraine A (7 samples) yielded ages from 8.8 ± 1.4 to 15.0 ± 1.4 ka. Ages from moraine B (7 samples) range from 7.9 ± 0.9 to 16.2 ± 1.5 ka, those of moraine C (9 samples) from 7.3 ± 0.9 to 17.1 ± 1.6 ka. Moraine D (3 samples) ages cover 14.5 ± 1.3 to 18.2 ± 1.7 ka, and lateral moraine E (5 samples) yielded ages from 7.9 ± 0.7 to 15.1 ± 1.4 ka (Figure 12). In general, all lateral moraines have a similar range of ages but do not show distinct age clusters, as is the case for the recessional moraine (Figure 11 and Figure 12). Therefore, we refrain from interpreting the overall mean age (12.8 ± 3.2 ka) as their formation age. As shown in Figure 10, we interpret only the oldest ages of the individual moraine age populations as the formation ages. Moraine A, located closest to the valley flank and highest up, yielded the youngest exposure age (15.0 ± 1.4 ka) within the moraine set. Moraines B (16.2 ± 1.5 ka), C (17.1 ± 1.6 ka), and D (18.2 ± 1.7 ka)

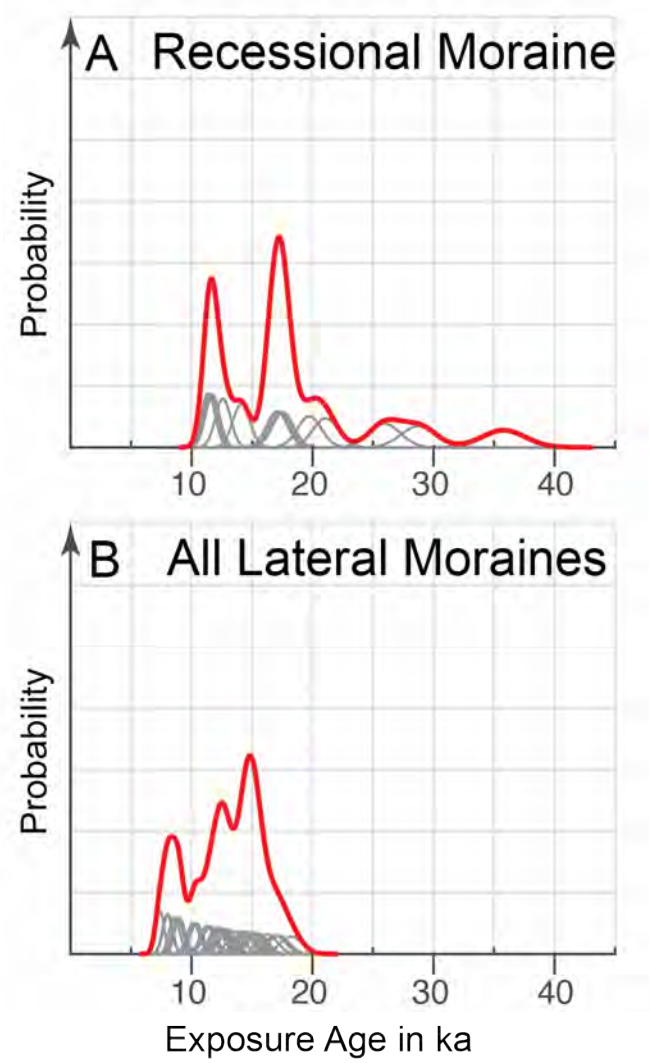

Figure 11: Plots for the A) recessional moraine exposure-age distribution and B) for all lateral moraine exposure-age populations. Thin grey lines are Gaussian curves for individual ages and red lines are the kernel probability plots for the recessional and all lateral moraine age populations.

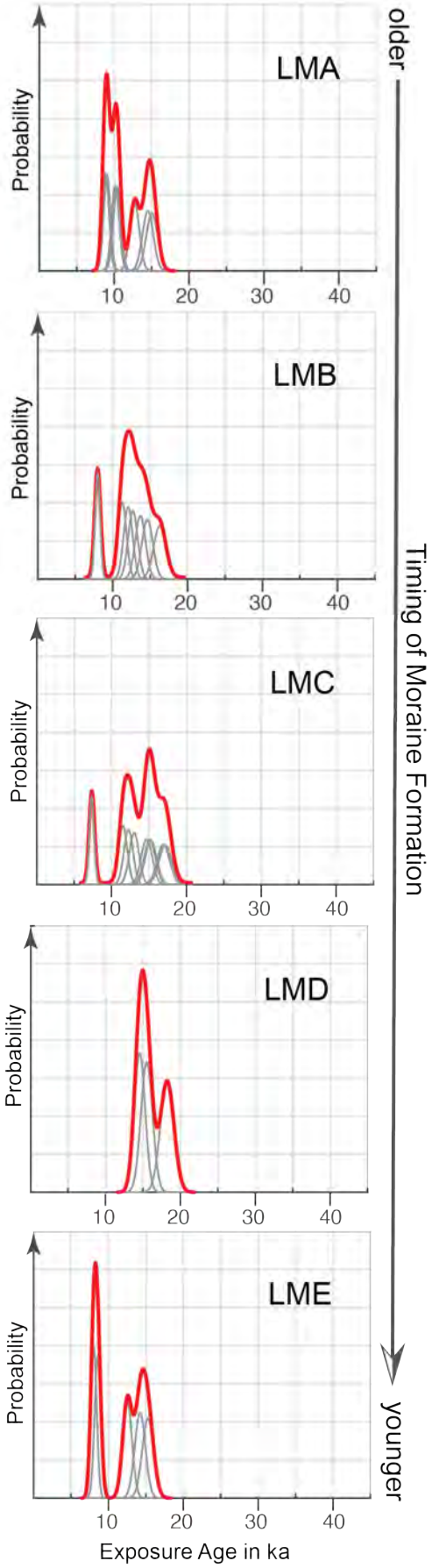

progressively increase in age. The lowest, thus last deposited moraine E (15.1 ± 1.4 ka) yielded the same exposure age as the highest, thus earliest deposited moraine A. The analysis of the lateral moraine ages using the kernel probability density plots (Figure 12) indicates a few outliers that are too young but no outliers that are too old (Figure 10, open symbols).

3.3.3 COMPARISON OF EXPOSURE AGES AND BOULDER HEIGHTS AND LITHOLOGY

Among others, factors that affect individual boulder exposure ages are: 1) Inheritance due to pre-depositional irradiation; 2) post-depositional shielding due to, for example, sediment cover after glacial retreat; 3) post-depositional reorientation of unstable boulders; 4) moraine degradation that results in a combination of items 2) and 3); 5) post-depositional shielding by snow, depending on the height and the geometry of the boulder; and 6) boulder weathering and erosion that depends on climate and rock type. Granodiorite comprises 75% of the boulder samples. The age distribution along the crests appeared to be random (Figure 13).

Figure 12: Kernel probability density plots for each lateral moraine (LM) exposure-age population. Grey lines represent Gaussian curves of individual ages with uncertainties. red lines represent the kernel probability plot for each lateral moraine age population.

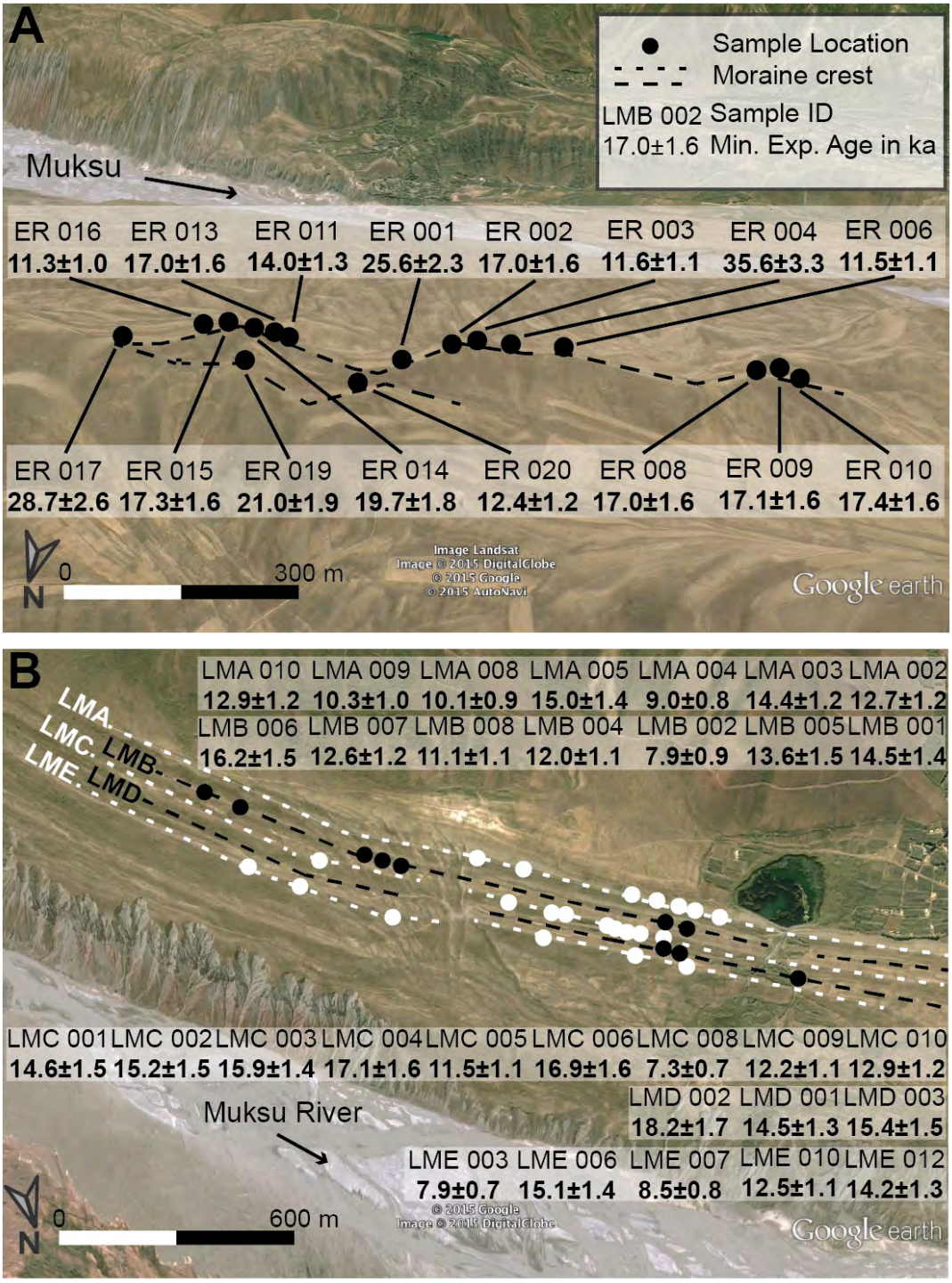

Figure 13: Boulder exposure age distributions along the locations on the A) recessional and B) lateral moraines.

Figure 14 indicates that boulders smaller than ~1 m height tend to underestimate the depositional age, regardless of their lithology. Boulders larger than ~1 m are prone to both underestimation and overestimation of the depositional age, although we observed overestimation only in our granodiorite samples. Only boulders over 2 m height reliably reproduce the

depositional age (Figure 14). The ages of the quartz veins and red sandstone are consistently younger than the exposure age of the lateral moraines (Figure 14; Table 4). The lateral moraine boulders tend to underestimate the moraine formation age regardless of the boulder height and lithology. We interpret this observation to be primarily caused by lateral moraine degradation.

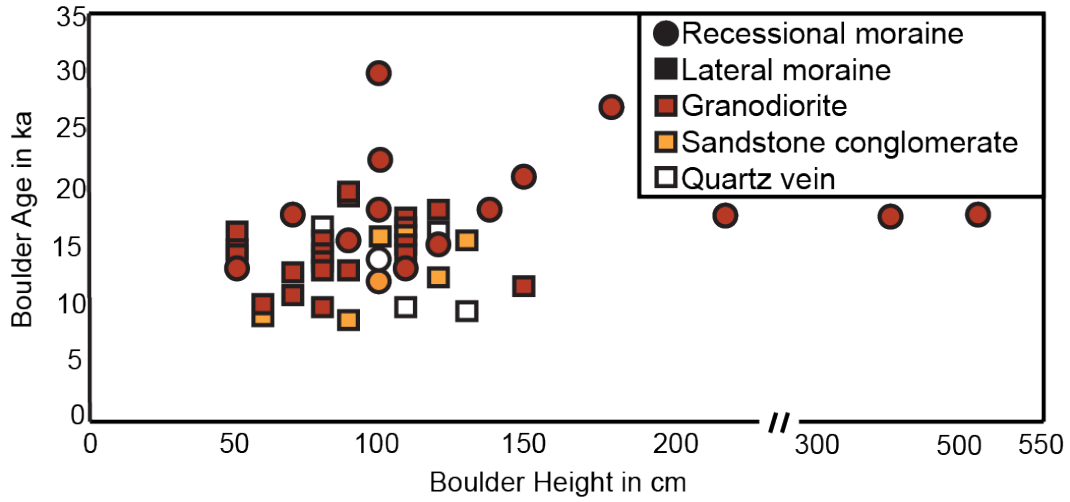

Figure 14: Boulder-age dependence on boulder height and lithology. No correlation between boulder age and boulder height could be observed for the granodiorite boulders. The quartz vein and the red sandstone conglomerate samples tend to underestimate the likely exposure age.

3.4 DISCUSSION

In the following, we first discuss our new results and then compare them with the exposure-age results from other publications.

3.4.1 SYNTHESIS OF RESULTS

Figure 11 shows the kernel probability density plots of the ages of the recessional moraine, highlighting the two exposure-age peaks at 17.5 ± 1.5 and 11.7 ± 0.5 ka. We interpret the older peak as the time of glacial retreat from the LGM. We refrain to interpret the younger peak as a second glacial stage. Instead, the random spatial distribution of the younger ages along the recessional moraine crest likely represents a signal of moraine degradation. Four of the lateral moraines, except moraine D, also display a younger degradation signal (A: 8.9 ± 0.8 ka, B: 7.9 ± 0.9 ka, C: 7.3 ± 0.7 ka, E: 8.2 ± 0.8 ka) in addition to the LGM signal. It is unlikely that a younger glaciation

would randomly affect boulders on all moraine crests without overprinting the LGM signal systematically or completely.

We found no anomalously older peaks for the lateral moraines, suggesting that pre-depositional irradiation is not a problem for these samples. Figure 12 shows, that the individual lateral moraines, in contrast to the recessional moraine, display a range of exposure ages without distinct clusters. We interpret the oldest lateral moraine ages to be closest to the moraine-formation age. Post-depositional degradation of the lateral moraines is indicated by the apparent inversion of their relative age estimates, whereby the individual lateral moraine exposure ages are younger towards the valley flank. Moraine degradation results in an underestimation of their formation age. The variation in the oldest ages of the lateral moraines may indicate that some of these moraines are older than the recessional moraine. We suggest all studied moraines formed at slightly different times (perhaps within the uncertainties of the method) and the subsequent moraine degradation has obviated information on the individual lateral moraine ages.

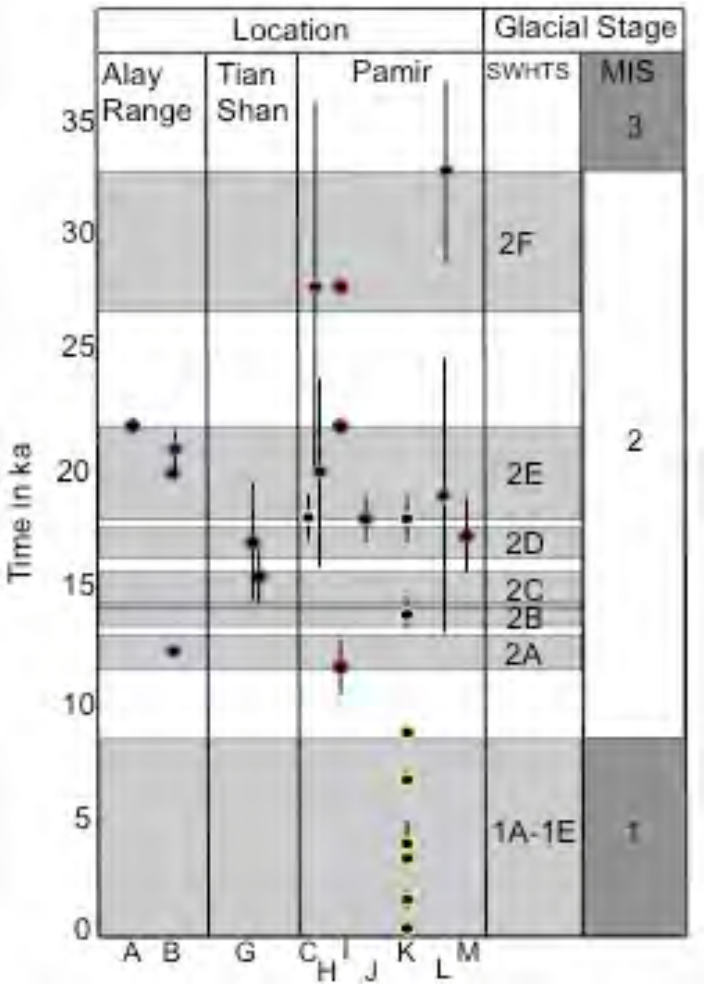

Figure 15: Published cosmogenic ^{10}Be moraine exposure-age data from the Ghissar-Alai Range, Tian Shan, and Pamir after Dortch et al. (2013) for the last 40 ka. Location numbers at the bottom of the Figure refer to Figure 1, where the spatial distribution of the regional glacial stages (SWHTS) is shown.

The lateral moraines likely formed between 15.0 ± 1.4 and 18.2 ± 1.7 ka, and the recessional moraine at 17.5 ± 1.5 ka. These dates suggest that

the two moraine types are representing the same signal of glaciation, which correlates with the LGM in the Pamir and Tian Shan (Abramowski et al., 2006; Seong et al., 2009; Zech, 2012; Dortch et al., 2013; Zech et al., 2013).

3.4.2 COMPARISON WITH PREVIOUS STUDIES

In this study, the mean age of the recessional moraine (17.5 ± 1.5 ka) and the oldest age from the lateral moraines (18.2 ± 1.7 ka) yielded a maximum age of the most recent glaciation at 18.2 ± 1.7 ka. This local glacial stage corresponds to the regional Semi-arid Western Himalayan-Tibet Stage (SWTHS) 2E of Dortch et al. (2013) (Figure 15). This stage correlates with MIS 2 and the LGM. Thus, the predominant precipitation source for the glaciers in the northern Pamir was likely the Westerlies (Aizen, 2011; Dortch et al., 2013; Lambrecht et al., 2014). Comparison of our data with published data from the Tian Shan and the Pamir suggests that the glaciation during MIS 2 prevailed longer in the Pamir region (SWTHS 2F–2A) in contrast to the later glaciation onset in the western Tian Shan (SWTHS 2E - 2A; Figure 15). In comparison with other studies, the Fedchenko glacier system does not have a record of glacial stages other than MIS 2. The reasons could be: (1) previous glacial advances in this region did not extend to elevations as low as 2,300 m a.s.l. or the youngest glaciation (17.5 ± 1.5 ka) removed evidence of them, (2) fluvial erosion by the Muksu River removed evidence of previous glaciations, or less likely (3) previous glaciations never occurred in this catchment.

3.5 CONCLUSION

We present ^{10}Be boulder exposure ages from recessional and lateral moraines preserved in the Muksu catchment of the northern Pamir. These moraines stem from a large glacier within the present-day Fedchenko glacier catchment. Field observations and our new ages imply the following:

(1) The last glacial retreat in the lower Muksu catchment occurred at 17.5 ± 1.5 ka (exposure age of the recessional moraine) and therefore can be correlated with the regional glacial stage SWHTS 2E (Dortch et al., 2013), which links to MIS 2 and the LGM. We derived the recessional moraine age from the mean exposure ages after discarding outlier ages that are too young

due to moraine degradation and too old due to inheritance based on kernel probability-density plots.

(2) The lateral moraine ages were influenced by post-depositional moraine degradation, which resulted in a secondary age cluster at <10 ka. Consequently, we interpret the oldest ages as the minimum exposure ages. The differences in the formation ages of the individual lateral moraines are smaller than the estimated exposure-age uncertainty. Therefore, combined with the observed moraine degradation, it is difficult to constrain the formation ages of the individual lateral moraines with ^{10}Be exposure age dating.

(3) The lateral moraines and the recessional moraine likely formed during the same event and experienced degradation over approximately the same time. The tectonically and fluvially active setting of the Muksu River catchment likely destroyed remnants of older and/or younger glacial stages at the investigated sites. The combined results from the recessional and lateral moraines suggest a LGM age of the glaciation in the Muksu catchment. The LGM glaciation is also recorded on the Pamir Plateau and in the Tian Shan.

Author	Author position	Scientific ideas %	Data generation %	Analyses & interpretation %	Paper writing %
Elena Grin	PhD Student	50	75	55	55
Mirjam Schaller	Postdoc	20	20	20	20
Todd Ehlers	Professor	30	5	25	25
Title of paper:	Spatial distribution of cosmogenic 10Be derived denudation rates between the Western Tian Shan and Northern Pamir, Tajikistan				
Status in publication process:	published (direct.com/science/article/pii/S0169555X18303027)				
Reference:	Grin, E., Schaller, M., Ehlers, T.A., 2018. Spatial distribution of cosmogenic ^{10}Be derived denudation rates between the Western Tian Shan and Northern Pamir, Tajikistan. Geomorphology 321, 1–15. doi: 10.1016/j.geomorph.2018.08.007				

4 Holocene denudation rates and terrace ages of the Vakhsh River, Tajikistan

4.1 Field work and setting

Thick alluvial sediment infill, deposited by the river and by alluvial fans, can be traced in the lower investigated section of the Vakhsh River (Figure 16A). The investigated terrace site is located upstream of a sediment-filled canyon along the main trunk and displays a sequence of unpaired fluvial fill terraces (Figure 16B, C). We investigated the set of eight fluvial fill terraces on the southern (Pamir side) riverbank (Figure 16D). The terrace set is intertwined with an alluvial fan. The abandoned alluvial fan surface corresponds to the height of the topmost identified fill terrace (T8, Figure 17). We observed that the alluvial fan material partly overlays the terrace set as shown in Figure 17, which indicates that the alluvial fan was still active after incision into the terrace material had already started. The river subsequently incised terraces into alluvial and fluvial deposits. At present, the alluvial fan is episodically incised by a seasonal surge stream, which drains directly into the Vakhsh. Three of the fluvial terraces (T1, T3, and T5) and the highest surface of the alluvial fan (AF) were sampled for cosmogenic depth profile dating (Figure 17). Each depth profile consists of 5 samples, taken at a depth of 0.5 m, 1.0 m, 1.5 m, 2.0 m, and 3.0 m. The sampling at each horizon was conducted over a 10 cm depth interval. Terrace T1 is situated at 1,153 m above sea level (a.s.l.) and 19 m above the active river channel, which is at 1,134 m a.s.l. Terrace T3 is located 34 m above the active river channel (1,168 m a.s.l.) and the uppermost sampled terrace T5 positioned 54 m above the active river channel (1,188 m a.s.l.). The depth profiles for the youngest terrace T1 and the alluvial fan depth profile (AF) were excavated (Appendix Table 1).

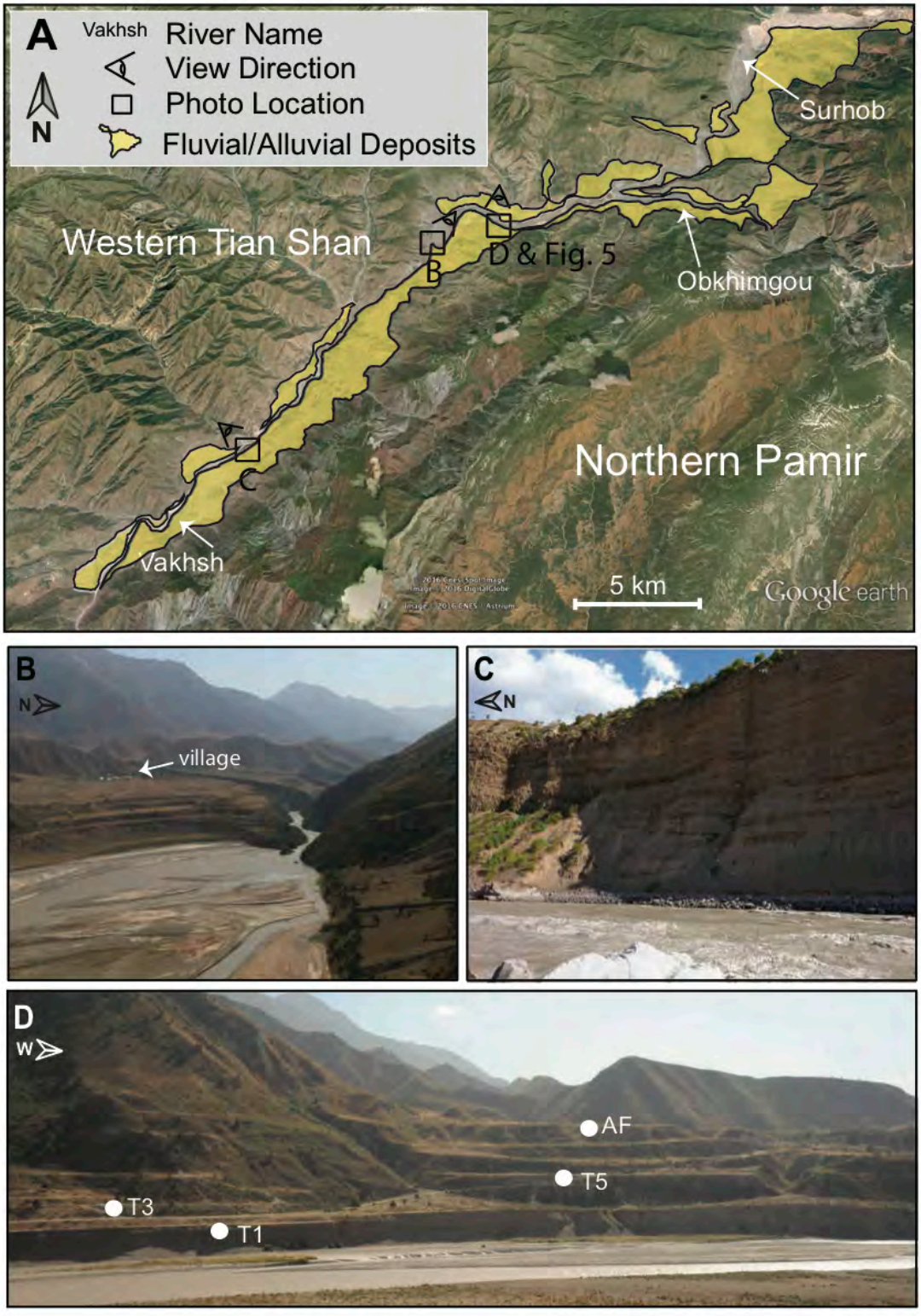

Figure 16: A) Extent of the valley infill with sediments transported by rivers and alluvial fans. B) Starting point of the incised sediment canyon just downstream of the investigated terrace site depicting the braided character of the riverbed. C) The sediment canyon at the sampling location of 12mod7001 featuring the thickness of the valley infill. For scale: on top are small (3-5 m high) trees. D) Field photo showing the sampling site of the terrace set. Dots indicate the position of the sampled depth profiles. T1, T3, and T5 are the terrace depth profile locations. For scale: T1 is 19 m above the modern river channel. AF is the alluvial fan profile location.

The other two terrace depth profiles T3 and T5 were acquired from road cuts that were excavated ~1 - 2 m laterally to acquire fresh material before sampling (Figure 17 and Figure 18). Terraces from higher locations were too steep to access (T8) or had highly disturbed and reworked surfaces that did not make them suitable for sampling. Because secondary cosmic particles interact with atomic nuclei, the density of the penetrated material must be known. For this purpose, one bulk density sample was taken from the depth profile of the alluvial fan at a depth of 2 m (~1.8 g/cm^3). The fluvial terrace density (~2.6 g/cm^3) is based on the lithologies of the boulders. Each terrace depth profile sample was composed of ~5 kg of material that was sieved in the field to the 4 mm size fraction. The quartz purification took place at the University of Tübingen (Appendix Tables 3 and 6 - 12)

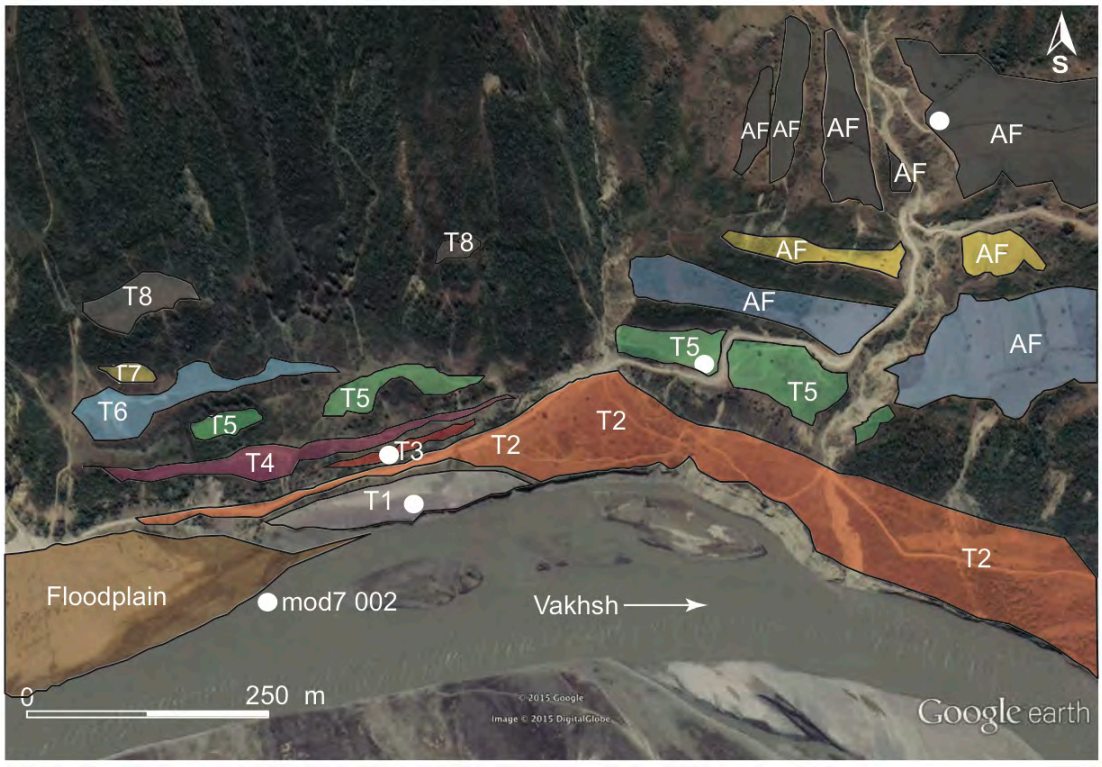

Figure 17: Google Earth image showing the distribution of terraces (T1 – T8) and the alluvial fan (AF) partly overlaying the terrace set. Recent small alluvial fans, which stem from seasonal surge streams, are visible along the terrace set. Sampling locations of the depth profiles are indicated as white dots.

4.2 METHODS

4.2.1 TERRACE EXPOSURE AGE CALCULATION

The exposure age calculations from cosmogenic depth profiles were based on the Bayesian Monte Carlo approach in the Matlab age calculator

program of Hidy et al. (2010). This calculator yields a best-fit exposure age for the terraces, the amount of the inherited ^{10}Be concentration, and the post-depositional terrace surface denudation rate.

The ^{10}Be production rate decreases exponentially with depth. The deepest sample at 3.0 m is only affected by muonic ^{10}Be production and is considered almost completely shielded from ^{10}Be production at the sampling site. The curve fitted through all measured ^{10}Be concentrations of each depth profile reveals the deviation of the ^{10}Be concentration produced after deposition and the inherited ^{10}Be concentration in the shielded sample (Appendix Table 18). The inherited ^{10}Be concentration is produced during denudation in the sediment source area. A paleo-denudation rate can thus be calculated from the inherited ^{10}Be amount based on the calculations used for modern catchment-wide denudation rates.

The Hidy et al. (2010) calculator generates results as relative probability density functions, which are constructed from the age results of all solutions generated from a Monte Carlo

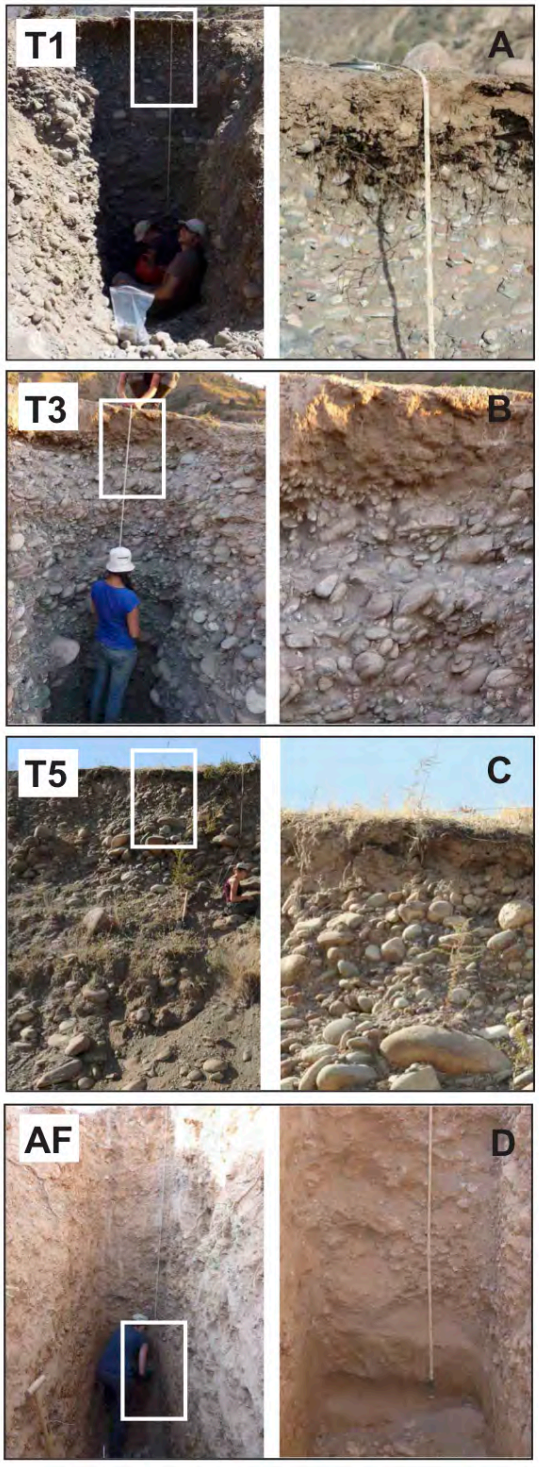

Figure 18: Photos from the field displaying the depth profile characteristics. Photos on the left show the entire depth profile and the photos on the right display close-up pictures from the first meter (A, B, C). The close-up pictures show the varying extents of alluvial material deposited by the river during the incision of each terrace. A clear difference can be seen between the material of the fluvial terraces (A, B, C) and the alluvial fan (D). The close-up of the last meter of the depth profile AF (D) shows a clayish matrix with angular non-oriented pebble-sized clasts.

simulation (Mercader et al., 2012). The site-specific input data consist of production rate, bulk density of the terrace material, and shielding by topography and snow cover. Due to the lack of snow cover data the estimated snow cover (1 m over three months) is a maximum cover and the terrace exposure ages can be considered to be the maximum exposure ages. A snow density of 0.3 g/cm^3 (Onuchin and Burenina, 1996) was incorporated into the calculation (Gosse and Phillips, 2001), yielding a shielding factor of 0.95. The calculator allows the user to specify whenever the ^{10}Be concentrations (Appendix Table 3 and 4) of one depth profile should be included in the Monte Carlo simulation with one, two, or more sigma uncertainty.

Further constraints can be used to focus the Monte Carlo Simulation on a range of geologically plausible results to reduce runtimes. The first run of each depth profile with 10,000 iterations was used to constrain a window for most plausible results, which are terrace denudation threshold terrace denudation rate, amount of ^{10}Be inheritance, and terrace exposure age. The constrained window then was subsequently used for a Monte Carlo Simulation with one million iterations.

4.2.2 TERRACE INCISION RATE CALCULATION

The terrace incision rates were calculated by dividing the difference in the elevation between the terrace and the active river channel by the exposure age of the terrace. All sample elevation measurements were taken with a handheld GPS with a barometer and have an uncertainty of ±5 m determined from repeated measurements. To reflect the uncertainty of the calculated terrace exposure ages in the incision rate calculation, we used terrace exposure age and elevation data that lie within the two-sigma uncertainty. Thus, the incision rate is presented as a range of values that accounts for the previous uncertainties in terrace age and elevation. Assuming a uniform rate during terrace incision, one may also use the calculated incision rate to estimate the timing of the onset of terrace incision by dividing the elevation difference between the highest terrace (T8) and river channel by the uniform incision rate.

4.2.3 PALEO-DENUDATION RATE CALCULATION

Paleo-denudation rates are determined from the lowest and thus most shielded sample of each depth profile. The ^{10}Be concentration in the shielded sample is mainly inherited. The inherited ^{10}Be concentration, which is stored in fluvial fill terraces (e.g. Schaller et al., 2002), represents the denudation signal from the landscape during terrace formation. In order to calculate a cosmogenic nuclide-derived catchment-wide denudation rate, the ^{10}Be concentration, the catchment-wide nuclide production rate, the depth dependence, and the decay constant need to be known (Dunai, 2000) . The sea level high latitudes ^{10}Be production rate of 4.5 atoms/(g*yr) was used as published by (Balco et al., 2008). The catchment-wide production rate was determined from digital elevation models (DEM) with a resolution of 90 m (http://www.cgiar-csi.org; Reuter et al., 2007). The ^{10}Be production rate of each pixel is determined for its elevation and latitude as well as the surrounding topographic shielding. The denudation rate calculations were corrected for glacial cover based on the Randolph Glacier Inventory 5.0 for Central Asia (https://www.glims.org/RGI/rgi50_dl.html; Pfeffer et al., 2014). The exact distribution of non-quartz lithologies was not traceable across the entire catchment. We infer from geological maps (Vlasov et al., 1991) and personal observations during field work, that quartz-bearing lithologies dominate the Vakhsh catchment, thus no correction for locally restricted non-quartz lithologies was applied. The calculation was done using the same scaling scheme (Dunai, 2000) as for the terrace exposure age calculation. However, the muon production for the denudation rate calculation is based on Balco et al., (2013) whereas the age calculation of Hidy et al., (2010) is based on (Heisinger et al., 2002a, 2002b). This results in small differences between a) muonic sea level high latitude production rates, and b) the depth dependence of muon production rates. Nonetheless, the differences in the muon calculation are not visible within the error. It is more important to use the same production-rate scaling scheme than the same muonic production rate.

4.3 RESULTS

4.3.1 OBSERVED TERRACE SEDIMENT CONTENT AND INTERNAL STRUCTURE

All investigated fluvial fill terraces display similar clast lithologies, sedimentary structures, and degree of roundness of the material. The terraces are cobble- to boulder-supported fill terraces with 1 – 3 cm thick sand layers between well-rounded 20 – 40 cm sized boulders (Figure 18A-C). The boulders consist mostly of granodiorite and sandstone. All sampled terraces displayed imbricated and well-rounded cobbles (<10 cm) in the upper 10 – 30 cm, which in turn is covered by a fine sand-clay horizon. The thickness of the oriented cobble horizon and the fine sand – clay alluvium horizon varies from terrace to terrace from 10 – 30 cm. Plants and insects on all terraces cause possible bioturbation with roots reaching into the oriented cobble layer. Anthropogenic agricultural land use during summer and pastureland use during autumn may have a significant influence on the mixing of the near-surface fine-grained horizon of the investigated terraces. The fluvial terrace deposits are partly overlain by an abandoned alluvial fan, as can be seen in Figure 17. The alluvial fan catchment area encompasses ~4 km^2 and the catchment is comprised of red sandstone with limestone layers. The alluvial fan sampling location is situated at 144 m above the active river channel at an altitude of 1,278 m a.s.l. at the highest abandoned surface of the alluvial fan. The alluvial fan consists of a mix of sand to clay-sized material (overlain by a ~10 cm thick soil horizon supported by roots (Figure 18D). Layers as thin as 10 cm with 3 – 5 cm large angular limestone pebbles were found in the alluvial fan.

4.3.2 TERRACE EXPOSURE AGES AND INCISION RATES

Results from the analysis of depth profile samples collected in the fluvial terraces and the alluvial fan are listed in Table 5. Measured terrace ^{10}Be concentrations range from 17.7 ±1.5 to 31.3 ±2.1*10^3 atoms/$g_{(qtz).}$ Terrace T5 displays an exponential decrease with depth in nuclide concentration, but this is not evident for terrace T1 or T3. The uppermost samples in terraces T1 and T3 show lower nuclide concentration than the samples below. This observation could indicate that the surface layer from

which the uppermost sample is collected is disturbed (e.g., by biotic and human activity; e.g., Lal and Chen, 2005; Schaller et al., 2009) and/or external material (e.g., alluvial or wind-blown sediment) is deposited after terrace exposure over the terrace material. Therefore, the uppermost samples in T1 and T3 were excluded from exposure age calculation. In addition, the lowermost sample of terrace T3 is also excluded as this nuclide concentration is the highest in the depth profile and suggests either a measurement or sample processing error. The model results for the terrace exposure ages, nuclide inheritance, and surface denudation are shown with an uncertainty of ±2 σ from the Bayesian analysis (Figure 19; Table 6). Four out of five samples from T1 (Figure 19A) reveal a Bayesian most probable terrace exposure age of $3.6^{+2.3}_{-1.9}$ ka with a post-depositional terrace surface denudation rate of 76^{+88}_{-72} mm/kyr. The calculated average incision rate based on T1 ranges from 4 – 7 mm/yr. Based on the three samples from terrace T3 (Figure 19B), the calculated terrace exposure age is $2.6^{+3.0}_{-2.1}$ ka. The calculated terrace surface denudation rate is 78^{+188}_{-73} mm/kyr. The estimated average incision rate for T3 is 5 – 28 mm/yr. The five samples from terrace T5 (Figure 19C) provided a terrace exposure age of $2.9^{+1.5}_{-1.5}$ ka. The calculated terrace surface denudation rate is 100^{+45}_{-96} mm/kyr. The calculated average incision rate is 7 – 29 mm/yr (Table 6). The AF depth profile measurements cannot be used for further calculations, because the ^{10}Be concentrations do not decrease with depth.

Table 5: Location and ^{10}Be concentration of depth profile samples.

Sample ID[1]	Latitude °N	Longitude °E	Elevation m a.s.l.	Sampling depth cm	Quartz dissolved g	^{9}Be[2] mg	^{10}Be/^{9}Be ratio	^{10}Be/^{9}Be 1σ error !	^{10}Be conc.[3] 10^3atoms/$g_{(qtz)}$ (± 1σ)
T1									
a	38.84832	69.97050	1153	*50 ± 5*	33.617	0.3326	3.75E-14	13.35	*23.5 ± 3.4*
b				**100 ± 5**	26.206	0.3333	3.28E-14	6.57	**26.2 ± 2.0**
c				**150 ± 5**	24.681	0.3261	2.71E-14	5.63	**22.2 ± 1.6**
d				**200 ± 5**	28.002	0.3256	2.48E-14	6.4	**17.7 ± 1.5**
e				**300 ± 5**	40.88	0.3268	3.54E-14	5.03	**17.9 ± 1.1**
T3									
a	38.84755	69.97125	1168	*50 ± 5*	17.036	0.3260	1.96E-14	7.39	*22.6 ± 2.3*
b				**100 ± 5**	35.91	0.3271	4.44E-14	6.11	**25.8 ± 1.8**
c				**150 ± 5**	26.55	0.3264	3.21E-14	6.93	**24.8 ± 2.0**
d				**200 ± 5**	36.48	0.3264	3.51E-14	7.13	**19.8 ± 1.6**
e				*300 ± 5*	57.011	0.3290	8.06E-14	11.5	*30.3 ± 3.6*
T5									
a	38.84645	69.96555	1188	**50 ± 5**	26.93	0.3257	4.07E-14	6.03	**31.3 ± 2.1**
b				**100 ± 5**	26.83	0.3255	3.15E-14	6.77	**23.9 ± 1.9**
c				**150 ± 5**	26.9	0.3255	2.69E-14	8.38	**20.2 ± 2.0**
d				**200 ± 5**	41.83	0.3263	3.65E-14	6.46	**18.0 ± 1.3**
e				**300 ± 5**	48.18	0.3254	4.46E-14	5.85	**19.2 ± 1.3**
AF									
a	38.84336	69.96070	1275	50 ± 5	16.725	0.3262	4.15E-14	15.63	*51.5 ± 8.6*
b				*100 ± 5*	29.393	0.3286	1.96E-14	6.18	**13.2 ± 1.2**
c				*150 ± 5*	25.163	0.3258	3.30E-14	57.81	*26.8 ± 16.5*
d				*200 ± 5*	35.907	0.3303	1.27E-14	7.66	**6.6 ± 0.9**
e				*300 ± 5*	39.491	0.3290	2.17E-15	17.94	*0.1 ± 0.6*

[1] Values in bold were incorporated in depth profile calculations whereas values displayed in italic are excluded from calculations

[2] ~0.8 ml of carrier solution with a concentration of 372.5 mg/l (GFZ Potsdam carrier)

[3] Blank corrected ^{10}Be concentration. A total of 12 blanks were processed with an average ^{10}Be/^{9}Be ratio of 1.60 ± 0.88^{-15}.

Table 6: Depth profile results with calculated paleo-denudation rates and incision rates.

Location ID	Latitude	Longitude	Elevation above river	Terrace surface abandonment age	Terrace surface denudation [1]	Inheritance	Paleo denudation rate [2]	Incision rate [3]
	°N	°E	m	ka (±2σ)	mm/ky (±2σ)	10^3 atoms/$g_{(qtz)}$ (±2σ)	mm/yr (±2σ)	mm/yr
T1	38.84832	69.97050	19 ± 5	3.6 +2.3/-1.9	76 +88/-72	16.3 +2.2/-2.5	2.01 +0.36/-0.39	4 - 7
T3	38.84748	69.97122	34 ± 5	2.6 +3.0/-2.1	78 +188/-73	19.0 +3.8/-5.2	1.75 +0.41/-0.54	5 - 28
T5	38.84636	69.96547	54 ± 5	2.9 +1.5/-1.5	100 +45/-96	16.4 +3.2/-2.4	2.00 +0.37/-0.37	7 -29

[1] For readability the terrace surface denudation rates are given in mm/ky.

[2] Paleo-denudation rate is based on the ^{10}Be inheritance component.

[3] Incision rate is calculated using the terrace surface elevation above river bed divided by the terrace surface abandonment age.

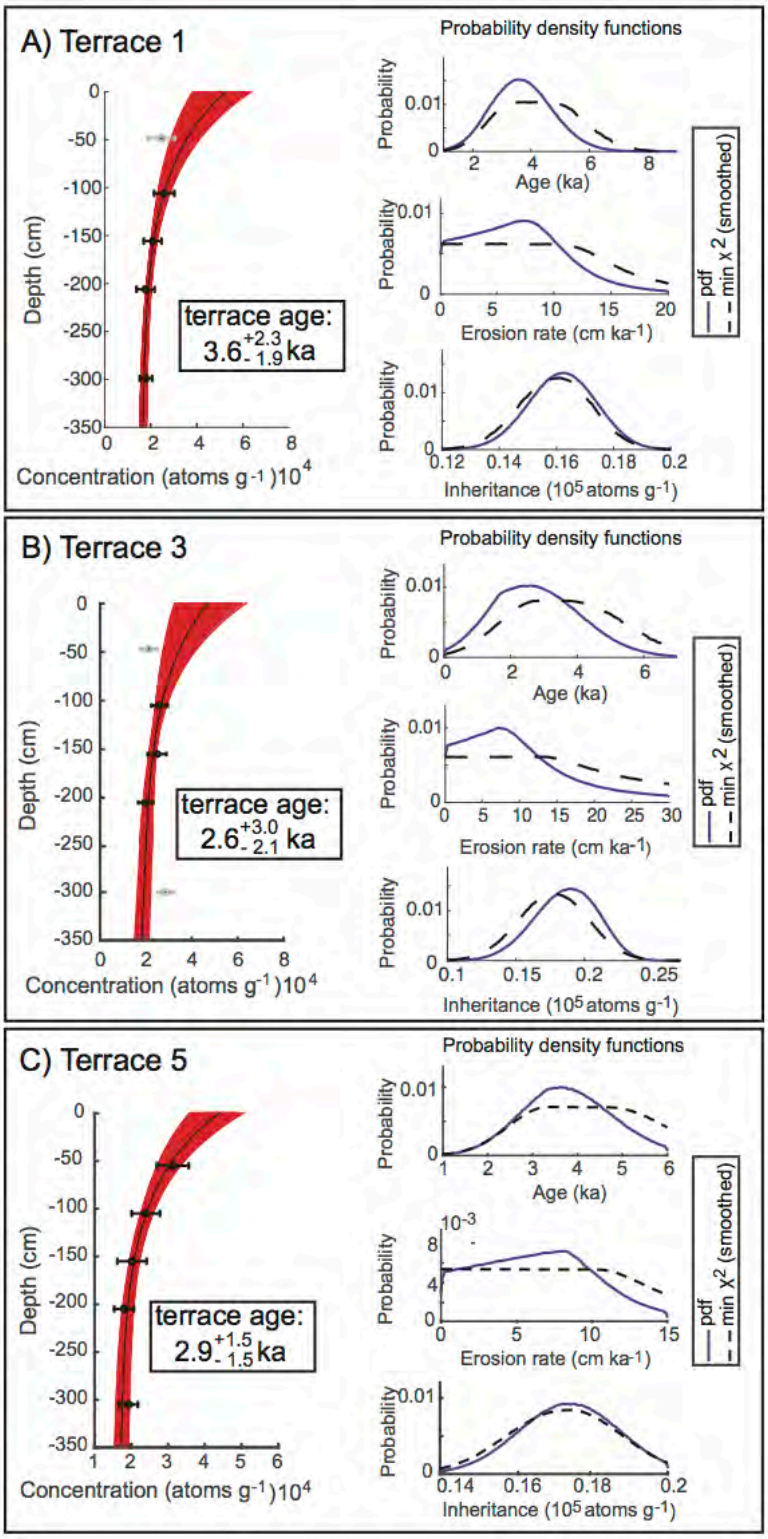

Figure 19: A-C) Results from depth profile calculations based on Hidy et al. (2010). Measured ^{10}Be concentrations were incorporated with two-sigma uncertainties. Grey dots represent measurements, which were not incorporated into the calculation. Age results are shown in Bayesian two-sigma deviations. Probability density functions are shown for predicted age, terrace surface denudation, and the inheritance component. The black line indicates the best fit; the red area displays the range of possible fits from one million runs.

4.3.3 PALEO-DENUDATION RATES

Calculation of paleo-denudation rates is based on the inherited ^{10}Be nuclide concentration derived from depth profile dating of T1, T3, and T5 (Table 6). The inherited ^{10}Be concentrations (and 2 s.d. uncertainty) range between $16.3 \begin{smallmatrix} + 2.2 \\ - 2.5 \end{smallmatrix} \times 10^3$ atoms/$g_{(qtz)}$ and $19.0 \begin{smallmatrix} + 3.8 \\ - 5.2 \end{smallmatrix} \times 10^3$ atoms/$g_{(qtz)}$. The paleo-denudation rates based on the nuclide inheritance calculated for T1, T3, and T5 are 2.01 ± 0.39 mm/yr, 1.75 ± 0.54 mm/yr, and 2.00 ± 0.37 mm/yr, respectively.

4.4 DISCUSSION

The three terrace exposure ages of T1, T3, and T5 are $3.6^{+2.3}_{-1.9}$ ka, $2.6 \begin{smallmatrix} + 3.0 \\ - 2.1 \end{smallmatrix}$ ka, and $2.9^{+1.5}_{-1.5}$ ka, respectively. These terrace exposure ages indicate when the terrace step was exposed and shortly later abandoned. Despite expectations that terrace T1 should reveal the youngest and T5 the oldest ages, we note that all exposure ages are within the standard deviation. These findings indicate fast incision over the last ~3 ka. However, as all five analyzed samples were included into the exposure age calculation of T5, this age is considered as the most reliable one for further considerations. Using the age and elevation above the modern river channel for terrace T5 an incision rate of 7 to 29 mm/yr was calculated. This range of incision rates for T5 can be used to extrapolate a range of minimum terrace formation ages of 3.8 and 15.7 ka for the entire 110 m high terrace set (up to terrace T8 where samples were not available). This estimated age range is also in agreement with the minimum terrace formation age of 5.9 ± 1.0 ka based on OSL dating from a terrace on the opposite river bank at 21 m elevation above the modern river channel (Fuchs et al., 2014).

We cannot determine from available observations the cause of terrace formation and incision in the Vakhsh River catchment but discuss a possible explanation in the following. The observed similar grain sizes below each terrace surface and the absence of paleo-soil horizons, that would suggest prolonged exposure and a hiatus in terrace formation, might indicate that the entire terrace sequence was deposited in one cycle. However, we note that

evidence for landslide damming of the Vakhsh river as a mechanism for infilling before terrace formation was not observed along the river. For example, no large landslide deposits preserved along the valley walls, or laminated sediments from lake sedimentation behind a landslide dam were visible along the Vakhsh valley.

Holocene changes in local to regional climate are an alternative explanation for the cause of valley infilling and subsequent incision. Changes in paleo-precipitation rates would influence the sediment carrying capacity of the river and lead to fluctuations in aggradation and incision. The reportedly wetter conditions during the Holocene thermal optimum (~ 8 - 4 ka ago) might have introduced more hillslope material to the river and surpassed its transport capacity, resulting in aggradation of the terrace sequence (e.g., Scherler et al., 2015). Incision into the deposited material most likely started during drier and warmer period than present-day from 3.5 to 2.0 ka ago. The drier conditions might have resulted in more stable hillslopes. Additionally, warmer conditions might have improved the river discharge by increased glacial melting. However, this type of terrace formation would more likely need several cycles of aggradation and incision and induce more variability to the grain size distribution in the terrace profiles than observed.

The paleo-denudation rate of 2.0 ± 0.37 mm/yr at ~3 ka derived from T5 is within error of modern catchment-wide denudation rates (section 5.3.2). Due to the restricted time resolution in terrace exposure ages, no change of paleo-denudation rates over time can be investigated. However, the similarity of modern and paleo-denudation rates may indicate no drastic and resolvable erosional changes in the Vakhsh River catchment over the last ~3 ka due to climatic changes suggested during this time period.

4.5 SUMMARY AND CONCLUSIONS

Cosmogenic depth profiles were analyzed from three fill terraces in the Vakhsh main trunk.

(1) The terrace exposure ages of the fill terraces indicate terrace surface exposure at ~3 ka. Based on this age and a terrace incision rate

range of 7 – 29 mm/yr, the terrace formation happened between 3.8 and 15.7 ka ago.

(2) Paleo-denudation rates based on the cosmogenic depth profiles in the fill terraces indicate values of ~2.0 mm/yr at the time of terrace deposition. These rates are comparable to modern denudation rates.

(3) The similar grain size distribution and no present soil horizons in the investigated terrace sequence suggest, that the terraces were deposited in one cycle.

(4) The wetter conditions during Holocene thermal optimum (~ 8 – 4 ka ago) may be responsible for aggradation of the terrace sequence, which most likely was incised during the drier climate period 3.5 – 2.0 ka ago.

Author	Author position	Scientific ideas %	Data generation %	Analyses & interpretation %	Paper writing %
Elena Grin	PhD Student	80	90	80	75
Mirjam Schaller	Postdoc	10	5	10	10
Todd Ehlers	Professor	10	5	10	15
Title of paper:	Spatial distribution of cosmogenic 10Be derived denudation rates between the Western Tian Shan and Northern Pamir, Tajikistan				
Status in publication process:	published (direct.com/science/article/pii/S0169555X18303027)				
Reference:	Grin, E., Schaller, M., Ehlers, T.A., 2018. Spatial distribution of cosmogenic ^{10}Be derived denudation rates between the Western Tian Shan and Northern Pamir, Tajikistan. Geomorphology 321, 1–15. doi: 10.1016/j.geomorph.2018.08.007				

5 Spatial Distribution of Cosmogenic ^{10}Be Derived Denudation Rates Between the Western Tian Shan and Northern Pamir, Tajikistan

5.1 Sample Collection and Processing

Our focus in sample collection was on the upper part of the Vakhsh River catchment (~29,700 km^2) to avoid the influence of hydropower stations present in the Tajik Depression (Figure 2). The investigated area extends from the confluence of the Kyzylsu and Muksu Rivers to the margin of the Nurek Dam area (Figure 2). For simplicity, the term 'Vakhsh River' will be used hereafter to address the investigated stretch of ~140 km along the main river. No distinction between the Surhob and Vakhsh Rivers will be made (Figure 3A). A total of 22 sand samples were collected (Appendix Table 1). Seven sand samples were collected at regular intervals from the active river channel along the Vakhsh River above the Nurek Dam just below the confluence of the Muksu and Kyzylsu Rivers (V1 to V7; Table 1; Figure 3A, black dots). The river channel is often braided and bordered with fluvial and alluvial deposits. Sample V1 was taken where the Vakhsh River enters a sediment-filled valley. Sand sample V2 was taken further upstream from the active river channel in the vicinity of the sampled terraces (see section 4.1). One year later, two locations (V1 and V4) along the main trunk were resampled to evaluate the consistency of results with the previous year's sampling. An additional 13 samples were collected from rivers that join the Vakhsh River (Figure 3A, Table 1). These 13 samples include 3 samples from the Kyzylsu, Muksu, and the Obkhimghou Rivers that were sampled upstream of their confluence with the Vakhsh River to quantify denudation rates in the Alai Valley and Northern Pamir, and 10 samples from 4 rivers draining the Western Tian Shan (Figure 3A, Table 1). For all modern river samples, 5 to >10 kg sand and pebble-sized (<1cm) material was collected along a 20-100 m stretch of the active river channel.

5.2 METHODS

5.2.1 DETERMINATION OF GEOMORPHIC PARAMETERS

Geomorphic parameters (Table 1), such as mean elevation, local relief, average hillslope angle, and normalized steepness index (k_{sn}), were determined for comparison to catchment-wide denudation rates. Geomorphic parameters presented in this study are based on a 30 m ASTER-DEM (http://gdex.cr.usgs.gov/gdex/[Aug/2016]) analyzed with ArcGIS and TopoToolbox 2 (Schwanghart and Scherler, 2014). The catchment-averaged mean elevation was calculated by averaging the altitude information from all pixels included in a catchment. Local relief was calculated in TopoToolbox 2 (Schwanghart and Scherler, 2014) using a moving window with 5 km radius on the DEM. A hillslope map was generated in ArcGIS v 10.1 using a moving window with 5 km radius (Figure 3C). Finally, the catchment-averaged k_{sn} values were calculated on the fluvial portions of each catchment, without inclusion of glaciated riverheads. The normalization of k_s (k_{sn}) was done by setting the reference concavity to 0.45 (Whipple, 2004). This way, all analyzed river profiles can be compared with each other

The normalized steepness index (k_{sn}) calculations were performed with the stream profiler tool (Crosby and Whipple, 2006; Kirby and Whipple, 2012). Values of k_{sn} provide insight on the presence of knickpoints in detachment-limited bedrock rivers (Kirby and Whipple 2012). The knickpoints can be located in areas where the river is adjusting to external changes (e.g., base level changes due to fault activity; Whittaker, 2012). These features result in a change in river steepness such that the k_{sn} value above the knickpoint differs from the value below. In case of uniform regional uplift or basin level change the knickpoints in a trunk stream and tributaries are located at the same altitude range throughout the affected region (e.g., Snyder et al., 2000; Kirby and Whipple, 2012). Alternatively, non-tectonically induced knickpoints can be caused by local factors such as transitions between hillslope- vs. fluvial-dominated stream sections in the source area, glacial incision vs. fluvial incision, or lithological variations. (e.g., Duvall, 2004; Pritchard et al., 2009; Whipple et al., 2013; Adams and Ehlers, 2017). These types of knickpoints do not necessarily occur at the same elevation within a catchment.

5.2.2 MODERN DENUDATION RATE CALCULATION

The modern and paleo-denudation rates are calculated from *in situ*-produced ^{10}Be concentrations (Appendix Table 3 - 12, and 17) in quartz from modern river channel sediment or fluvial terraces (e.g. Schaller et al., 2002; von Blanckenburg, 2005). The nuclide concentration measured in a sample is inversely proportional to the denudation rate. Calculation of denudation rates from measured cosmogenic nuclide concentrations requires knowledge of the catchment-wide production rates for spallogenic and muonic nuclide production, the nucleonic and muonic attenuation lengths, the nuclide half-life, and the density of sample material.

Catchment-wide production rates were calculated using a 90 m SRTM-DEM (http://srtm.csi.cgiar.org) of the Vakhsh River catchment. The catchment-wide production rate is extracted from this DEM following the approach of Glotzbach et al., (2013). Our scaling from Sea Level High Latitude (SLHL) production rates to sample locations (Appendix Table 1) is based on Dunai (2000). The individual production rates were also corrected for topographic shielding. The spallogenic and muonic SLHL production rates used for ^{10}Be are 4.90 ± 0.56 (Balco et al. 2008) and 0.028 ± 0.004 atoms/(g*yr), respectively (Braucher et al., 2013). The attenuation lengths of 160 and 4656 g/cm^2 are used for spallogenic and muonic production (Braucher et al. 2013). The half-life used for calculation is 1.387 ± 0.016 Myr (Chmeleff et al., 2010; Korschinek et al., 2010) whereas the material density is 2.7 g/cm^3.

Furthermore, two additional factors were accounted for in the calculation of the production rates before determining denudation rates. These are glacier cover and quartz-content in eroded lithologies. In the case of glaciated valleys, the production rate for topography under the glacier was excluded from the denudation rate calculation. Lithologies without any quartz were also excluded from the production rate calculation. Geological maps (Vlasov et al., 1991) and observations during fieldwork were used to determine that quartz-bearing lithologies dominate the Vakhsh catchment. Exceptions to this come from various Devonian lithologies (e.g., coal layers, limestone, limestone with quartzite lenses) in the Western Tian Shan, which were excluded from the production rate calculations.

5.2.3 ^{26}AL/^{10}BE RATIO

The sediment must have short residence time in the river systems (Anderson et al., 1996). Any deposition can result in additional exposure and/or shielding, which can be resolved using at least two TCN systems, e.g. ^{10}Be and ^{26}Al. Particularly the ^{26}Al/^{27}Al ratios (Appendix Table 5) are used to investigate any burial in the system. Material from existing terraces may contribute a partially irradiated signal to the denudation rate. Additionally, the mixing from tributaries may be insufficient and the denudation rates may over- or underrepresent whole areas in the catchment.

The estimated ^{26}Al/^{10}Be ratio (Appendix Table 13) indicates whenever the sediment is transported without any interim sedimentation and burial throughout the catchment. Ratios below the range of 6.5 - 7.2 indicate burial and storage during transport, which is traceable due to different decay times and production rates of the used nuclides (Goethals et al., 2009; Chmeleff et al., 2010; Korschinek et al., 2010; Wittmann et al., 2011), The relatively high errors for ^{26}Al/^{10}Be ratios are a known problem (Wittmann et al. 2007), which mainly results from the measurement of natural ^{27}Al, the measurement of the cosmogenic nuclide ratios, and the subsequent propagation of errors. Nonetheless, the ratios are useful to show the tendency towards possible burial and reworking of buried material.

5.2.4 PRESENT-DAY CLIMATE DATA

Two different data sets were used to represent the present-day climate in the investigated region: (A) The Tropical Radar Moisture Measurements (TRMM) data was used to generate the precipitation map and the spatial distribution of annual precipitation (Huffman et al., 2007). The map shown in Figure 5A spans the years 1998 – 2014. Measurements of 14 local Soviet weather stations distributed in the catchment (9 stations) and close-by (5 stations) were used to generate the temperature and precipitation curves in Figure 5B-D (Williams and Konovalov, 2008; Appendix Table 19 and 20). The time span used encompasses the years 1960 – 1990 (Table 7). Three stations did not yield enough data to calculate temperature curves (Faizabad, Komsomolabad, and Altynmazar). For precipitation, the monthly data was averaged for each month over 31 years. The temperature data is given in

monthly maximum and minimum temperature. Both values were used to yield a mean monthly temperature. The amount of missing months is indicated by the completeness of data in percent (Appendix Table 19 and 20).

Table 7: Mean annual precipitation and temperature data derived from local weather stations during 1960 - 1990.

ID in Fig.3	Location Name	Longitude °N	Latitude °E	Elevation m	Precipitation mm	Available data[1] %	Temperature ˚C	Available data[1] %
1	Faizabad[2,3]	69.32	38.55	1215	844	100	-	0
2	Bustonabad	69.63	38.67	1983	775	93.6 - 100	8.0	93.5 - 100
3	Komsomolabad[3]	69.98	38.87	1259	881	93.6 - 100	-	0
4	Garm	69.95	39	1316	743	100	11.3	93.5 - 100
5	Dehavz[2]	70.2	39.45	2561	300	100	4.6	96.8 - 100
6	Hovaling[2]	69.95	38.35	1468	999	93.6	12.2	96.8 - 100
7	Tavildara	70.48	38.7	1616	908	96.8 - 100	9.5	90.3 - 100
8	Harurabad[2]	70.7	38.63	3347	675	93.6 - 96.8	-0.8	96.8 - 100
9	Lyairun	70.9	38.9	2008	918	96.8	7.8	87.1 - 93.5
10	Daraut-Kurgan	72.18	39.55	2470	302	100	3.2	83.9 - 96.8
11	Altynmazar[3]	72.22	39.18	2782	162	100	-	0
12	Fedchenko Glacier	72.22	38.83	4169	1161	100	-6.7	90.3 - 100
13	Sarytash	73.25	39.73	3153	370	100	-2.1	93.5 - 96.8
14	Karakul[2]	73.56	39.01	3935	81	100	-3.5	93.5 - 100

(1) Precipitation and temperature data in % demonstrate the availability of recorded monthly data during the years 1960 - 1990 (Williams and Konovalov, 2008).
(2) Weather stations located in the vicinity of the Vakhsh River catchment.
(3) No record of sufficient monthly temperature data.

5.3 RESULTS

5.3.1 GEOMORPHIC PARAMETERS

The elevation, relief, and hillslope angle of each catchment investigated is provided in Table 1. The main trunk of the Vakhsh River has a local (5 km radius) relief of ~2,000 m, and the mean elevation decreases from 3,924 m to 3,559 m along the investigated area. The average hillslope angle is ~23˚. The Western Tian Shan tributaries display a steady increase in catchment average elevation from west to east (2,029 m to 3,391 m), while the relief and the average hillslope angle are similar within one sigma standard deviation of the mean (Table 1). The Alai Valley has a high mean catchment elevation of 3,505 m. However, abundant alluvial infill in the valley results in the lowest local relief (1,545 ± 956 m) and mean slope (19˚) of the studied catchments. The Muksu River in the Northern Pamir contains the highest catchment average elevation (4,500 m) while the relief and slope are similar to the Western Tian Shan tributaries (Table 1). The Obkhimghou River displays topographic parameters similar to the Western Tian Shan tributaries.

In general, low k_{sn} values (<100) are found throughout the catchment of the Vakhsh River. However more locally, many locations along the river

profiles are characterized by high k_{sn} values which exceed >400 (Figure 20 and Figure 21). The combination of the Central Asia Fault Database (Mohadjer et al., 2016, 2017) and the calculated k_{sn} values shows that many prominent regions with high k_{sn} values are closely related to the presence of faults crossing the rivers. However, in some cases high k_{sn} values are related to major changes in lithology. The longitudinal profiles further depict convex sections in the profiles, which correlate with lithological boundaries (Figure 20 and Figure 21). The relationships described above are presented in more detail for individual river segments in the following paragraphs. Longitudinal river profiles of the Vakhsh tributaries do not display a steady-state concave geometry. Tributary profiles in the Western Tian Shan contain numerous knick-zones with high k_{sn} values (arrows in Figure 20A, C, and E; see also Figure 22) that often coincide with variations in lithology along the profile (arrows in Figure 20C, D, and F). The sediment-filled Alai Valley tributary (Kyzylsu River, Figure 21 and Figure 22) contains a convex longitudinal river profile and low (~50-150) k_{sn} values. The Muksu and Obkhimghou River profiles exhibit high k_{sn} (>400) values where the river crosses the PTS.

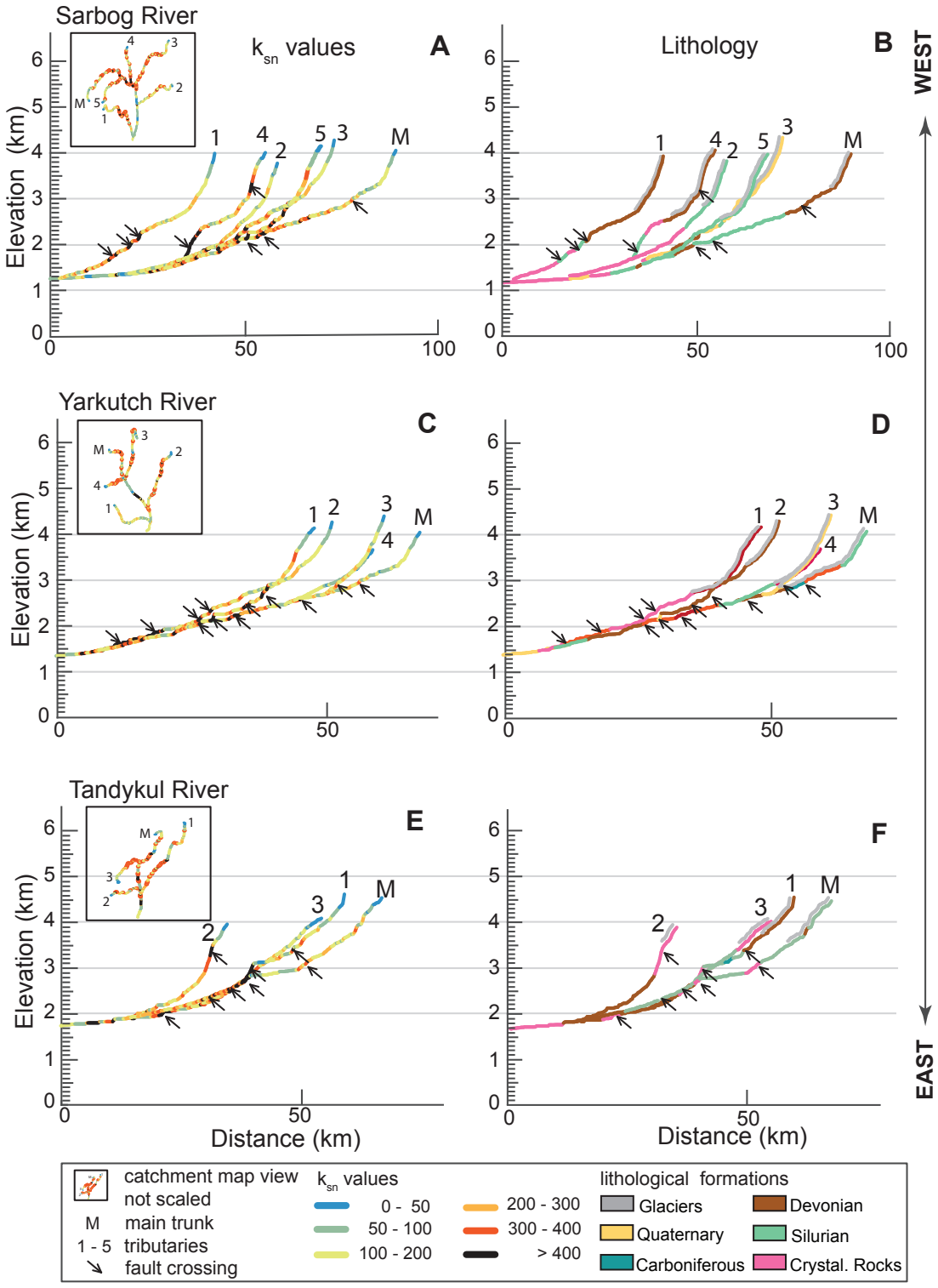

Figure 20: Longitudinal river profiles of the main Western Tian Shan tributaries, A, C, E display the k_{sn} values with faults crossing the riverbeds (Mohadjer et al., 2016, 2017). B, D, F show the boundaries of lithological formations as published by Vlasov et al. (1991).

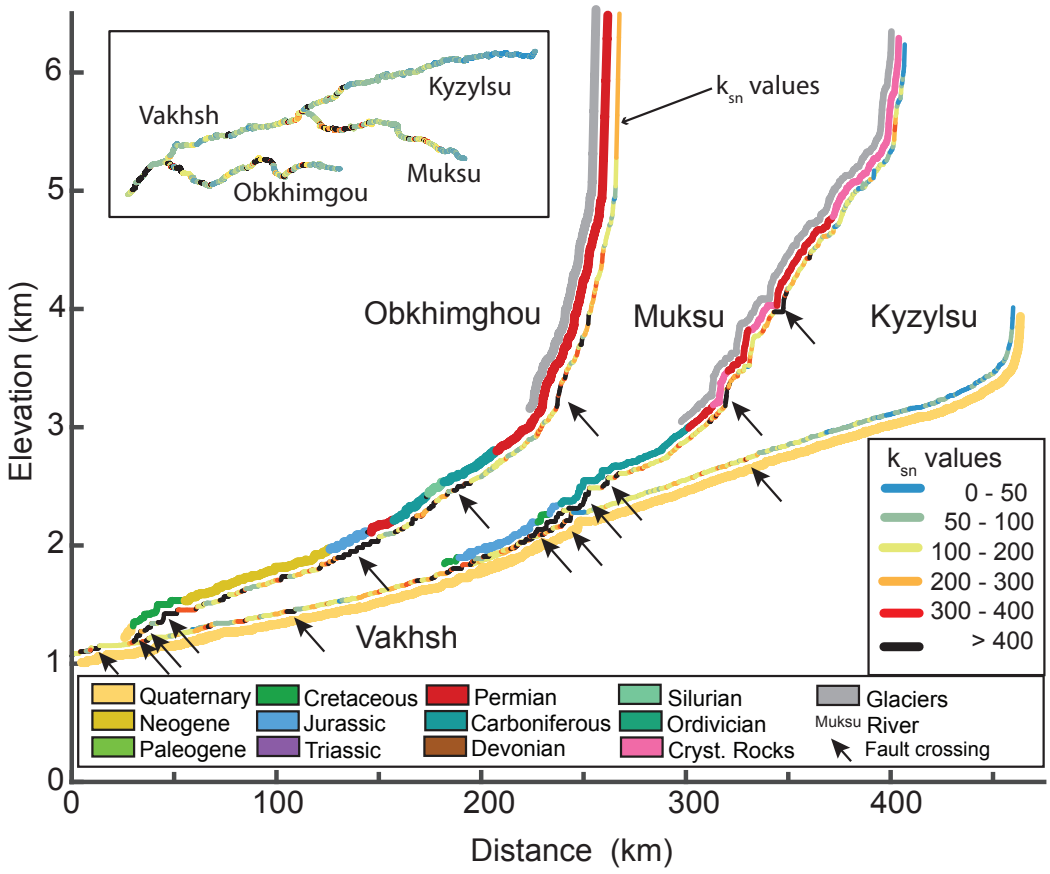

Figure 21: Longitudinal river profiles of the Northern Pamir rivers Obkhimghou and Muksu Rivers, as well as the Kyzylsu River, which drains the Alai Valley. The river profiles are overlain with k_{sn}, lithological formation boundaries (Vlasov et al. 1991), and fault locations crossing the riverbeds (Mohadjer et al., 2016, 2017).

5.3.2 CATCHMENT-WIDE DENUDATION RATES

Seven sand-sized samples from the active main river channel were analyzed for ^{10}Be nuclide concentrations to calculate catchment-wide denudation rates (Table 8 and Figure 23; Samples V1-V7). Nuclide concentrations range from 16.9 ± 1.3 to 25.0 ± 1.6 × 10^3 atoms/$g_{(qtz)}$. The lowest nuclide concentration is reported from sample V2 where the terrace deposits are located. The eastern-most sample (V7) located below the confluence of the Kyzylsu and Muksu Rivers has a calculated denudation rate of 1.62 ± 0.22 mm/yr. Generally, the modern denudation rates along the Vakhsh River overlap within one-sigma error. Nevertheless, a slight decrease in denudation rates from east to west (V7 to V1) is observed. At the terrace location (V2) the modern river denudation rate is 1.94 ± 0.26 mm/yr. Two locations (V1b and V4b; Figure 23A) were resampled one year later.

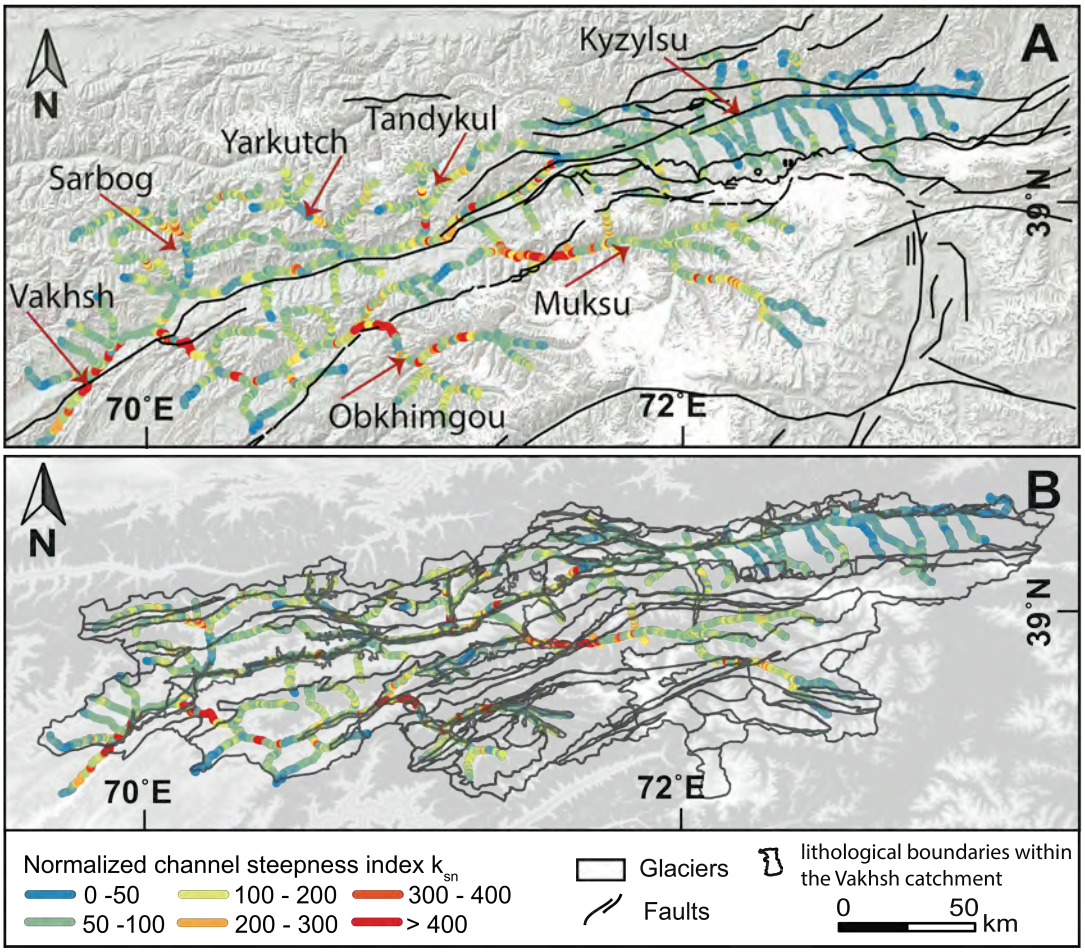

Figure 22: A) Fault locations and k_{sn} values in map view. The streams with a length of > 10 km are considered to be rivers. This way we avoid the influence of non-fluvial behavior of glaciers and small springs. B) Stratigraphic boundaries simplified after Figure 3 in the main text for an overlay with the k_{sn} map of the Vakhsh River catchment. For simplicity, the stratigraphic boundaries will be referred to as lithological boundaries in the text.

Results at each location yield denudation rates, which are within error the same (V1: 1.28 ± 0.16 mm/yr vs. V1b: 1.28 ± 0.15 mm/yr and V4: 1.50 ± 0.20 mm/yr vs. V4b: 1.52 ± 0.19 mm/yr). Samples from catchments draining the Western Tian Shan reveal nuclide concentrations ranging from 15.4 ± 1.1 to 85.0 ± 3.1 × 10^3 atoms/$g_{(qtz)}$ (Table 8; Figure 23B and C). The highest nuclide concentration stems from the western most sampled catchment, the Obi Garm Tributary (Sample TS1; Figure 23C). This concentration yields the lowest denudation rate of 0.18 ± 0.02 mm/yr. Moving from west to east in the Western Tian Shan, the Sarbog Tributary samples (TS2 to TS4) yielded ^{10}Be concentrations from 31.0 ± 1.5 × 10^3 – 38.6 ± 1.8 × 10^3 atoms/$g_{(qtz)}$, resulting in calculated denudation rates of 0.77 ± 0.09 – 1.00 ± 0.13 mm/yr (Figure 23B and C). Two samples from the Yarkutch catchment, which contains a coalmine, were not measurable due to

strong contamination of the sample material. Only sample TS5 taken from the Yarkutch upper reach, which is not influenced by any coal layers, yielded a denudation rate of 0.68 ± 0.08 mm/yr. The samples of the Tandykul Tributary (TS6 to TS10; Fig. 8B and C) revealed a wide range of ^{10}Be concentrations (15.4 ±1.1*10^3 – 70.2 ±2.6*10^3 atoms/g$_{(qtz)}$) and denudation rates from 0.83 ±0.10 (TS9) to 2.70 ± 0.36 mm/yr (TS8). The Kyzylsu River (AV1, Figure 23B) drains the Alai Valley and has a measured ^{10}Be concentration of 30.3 ± 1.6 × 10^3 atoms/g$_{(qtz)}$ and a calculated denudation rate of 1.14 ± 0.14 mm/yr (Figure 23B). The Northern Pamir rivers Obkhimghou (Sample P1) and Muksu (Sample P2) display lower concentrations than the Kyzylsu River (P1: 16.8 ± 1.0 × 10^3 atoms/g$_{(qtz)}$ and P2: 25.2 ±1 .5 × 10^3 atoms/g$_{(qtz)}$) and thus higher denudation rates (P1: 1.78 ± 0.23 mm/yr and P2: 1.63 ± 0.21 mm/yr) than the Kyzylsu River (Figure 23B).

In summary, the denudation rates for the main trunk of the Vakhsh River decrease from east to west. Overall such a decrease in denudation rates is also observed in the catchments in the Western Tian Shan. Rivers draining the Northern Pamir show comparable denudation rates as the eastern most samples collected in the Western Tian Shan. The river draining the Alai Valley displays lower denudation rates than many of its neighboring rivers (Figure 23B).

5.3.3 ^{26}AL/^{10}BE RATIOS IN MODERN RIVER SEDIMENTS

The ^{26}Al/^{10}Be ratios were measured from 10 samples (Table 9). The main trunk samples yield ^{26}Al/^{10}Be ratios between 6.0 ± 1.0 and 6.3 ± 1.2. The Northern Pamir rivers Obkhimghou (7.4 ± 1.2) and Muksu (7.6 ± 1.2) display the highest ^{26}Al/^{10}Be ratios in the Vakhsh River system. The Western Tian Shan catchment Sarbog (TS4) contains the lowest ^{26}Al/^{10}Be ratio of 5.2 ± 0.5. The measured ratios in the Tandykul catchment range between 6.6 ± 1.0 for the main trunk (TS10), 6.7 ± 1.2 for the western tributary (TS8), and 6.9 ± 0.6 for the eastern tributary (TS9). Overall, the ^{26}Al/^{10}Be ratios reported above do not suggest sediment storage and reworking (^{26}Al/^{10}Be ratio > 6.75; (Balco and Rovey, 2008). The one exception to this is the Sarbog Tributary (TS4; ratio 5.2 ± 0.5) indicating a slightly reduced ^{26}Al/^{10}Be ratio.

Table 8: ^{10}Be analytical information and catchment-wide denudation rates.

Location ID	Sample ID	Quartz dissolved g	^{9}Be[1] mg	^{10}Be/^{9}Be ratio	^{10}Be/^{9}Be 1σ error %	^{10}Be conc.[2] 10^3atoms/$g_{(qtz)}$ (± 1σ)	Shielding correction	Surface production rate[3] spallogenic	muonic	**Denudation rate[4] mm/yr (± 1σ)**	Apparent age a
Vakhsh main trunk											
V1	mod7001	35.26	0.3256	4.24E-14	5.55	24.96 ± 1.58	0.98	39.97	0.12	**1.28 ± 0.16**	469
V2	mod7003	42.98	0.3320	3.46E-14	6.61	16.89 ± 1.29	0.98	40.41	0.12	**1.94 ± 0.26**	309
V3	mod7002	46.38	0.3333	5.03E-14	4.93	23.22 ± 1.28	0.98	40.40	0.12	**1.40 ± 0.17**	429
V4	mod7005	34.96	0.3256	3.91E-14	5.69	23.12 ± 1.52	0.98	42.89	0.13	**1.50 ± 0.20**	400
V5	mod7006	26.99	0.3297	2.88E-14	6.90	21.95 ± 1.82	0.98	44.79	0.13	**1.67 ± 0.23**	359
V6	mod7007	36.31	0.3265	3.78E-14	6.70	21.55 ± 1.64	0.98	45.34	0.13	**1.72 ± 0.23**	349
V7	mod6005	54.69	0.3266	5.96E-14	7.19	23.01 ± 1.76	0.98	45.58	0.14	**1.62 ± 0.22**	370
Locations resampled one year later along main trunk											
V1b	13 mod 7001	39.01	0.3328	4.71E-14	5.13	25.78 ±1.49	0.98	39.97	0.12	**1.28 ± 0.15**	469
V4b	13 mod 7003	38.0644	0.3321	3.98E-14	5.27	22.09 ± 1.35	0.98	42.89	0.13	**1.52 ± 0.19**	400
Western Tian Shan											
Obi Garm Tributary											
TS1	mod4001	39.6698	0.3278	1.56E-13	3.58	84.95 ± 3.13	0.99	19.73	0.07	**0.18 ± 0.02**	3333
Sarbog Tributary											
TS2	mod4012	38.6635	0.3282	6.99E-14	4.27	38.57 ± 1.79	0.98	35.51	0.10	**0.77 ± 0.09**	779
TS3	mod4011	37.42	0.3275	5.49E-14	4.42	30.94 ± 1.54	0.97	38.86	0.11	**1.00 ± 0.13**	600
TS4	mod5001	40.75	0.3250	7.46E-14	4.53	38.72 ± 1.88	0.97	36.84	0.10	**0.74 ± 0.09**	811
Yarkutch Tributary											
TS5	mod4007					46.34 ± 2.07	0.98	41.00	0.11	**0.68 ± 0.08**	882
Tandykul Tributary											
TS6	mod4002	39.9474	0.3151	5.47E-14	4.59	27.78 ± 1.43	0.96	55.86	0.13	**1.57 ± 0.19**	531
TS7	mod4003	38.0402	0.3283	3.95E-14	4.94	21.64 ± 1.26	0.96	56.09	0.13	**1.90 ± 0.25**	316
TS8	mod5004	47.23	0.3305	3.49E-14	6.08	15.42 ± 1.10	0.96	49.27	0.12	**2.70 ± 0.36**	222
TS9	mod5003	46.44	0.3302	1.50E-13	3.64	70.21 ± 2.63	0.99	43.13	0.12	**0.83 ± 0.10**	723
TS10	mod6002	46.42	0.3303	4.20E-14	5.00	19.05 ± 1.11	0.97	39.69	0.11	**2.10 ± 0.27**	286
Alai Valley											
Kyzylsu River											
A1	mod6003	35.77	0.3311	5.09E-14	4.60	30.30 ± 1.57	0.99	43.85	0.12	**1.14 ± 0.14**	526
Northern Pamir											
Obkhimghou River											
P1	mod6001	46.52	0.3309	3.72E-14	4.96	16.76 ± 1.00	0.98	37.03	0.11	**1.78 ± 0.23**	337
Muksu River											
P2	mod6004	33.30	0.3310	3.98E-14	4.96	25.15 ± 1.47	0.97	48.40	0.16	**1.63 ± 0.21**	368

[1] ~0.8 ml of carrier solution with a concentration of 372.5 mg/l (GFZ Potsdam carrier)

[2] Blank corrected ^{10}Be concentration. A total of 12 blanks were processed with an average ^{10}Be/^{9}Be ratio of $1.60 \pm 0.88 \cdot 10^{-15}$.

[3] The average catchment-wide ^{10}Be production rates are based on Dunai (2000), Braucher et al. (2013), and the scaling method of Dunai (2000).

[4] The catchment-wide denudation rate calculations were performed with the modified MatLab script published by Glotzbach et al. (2013).

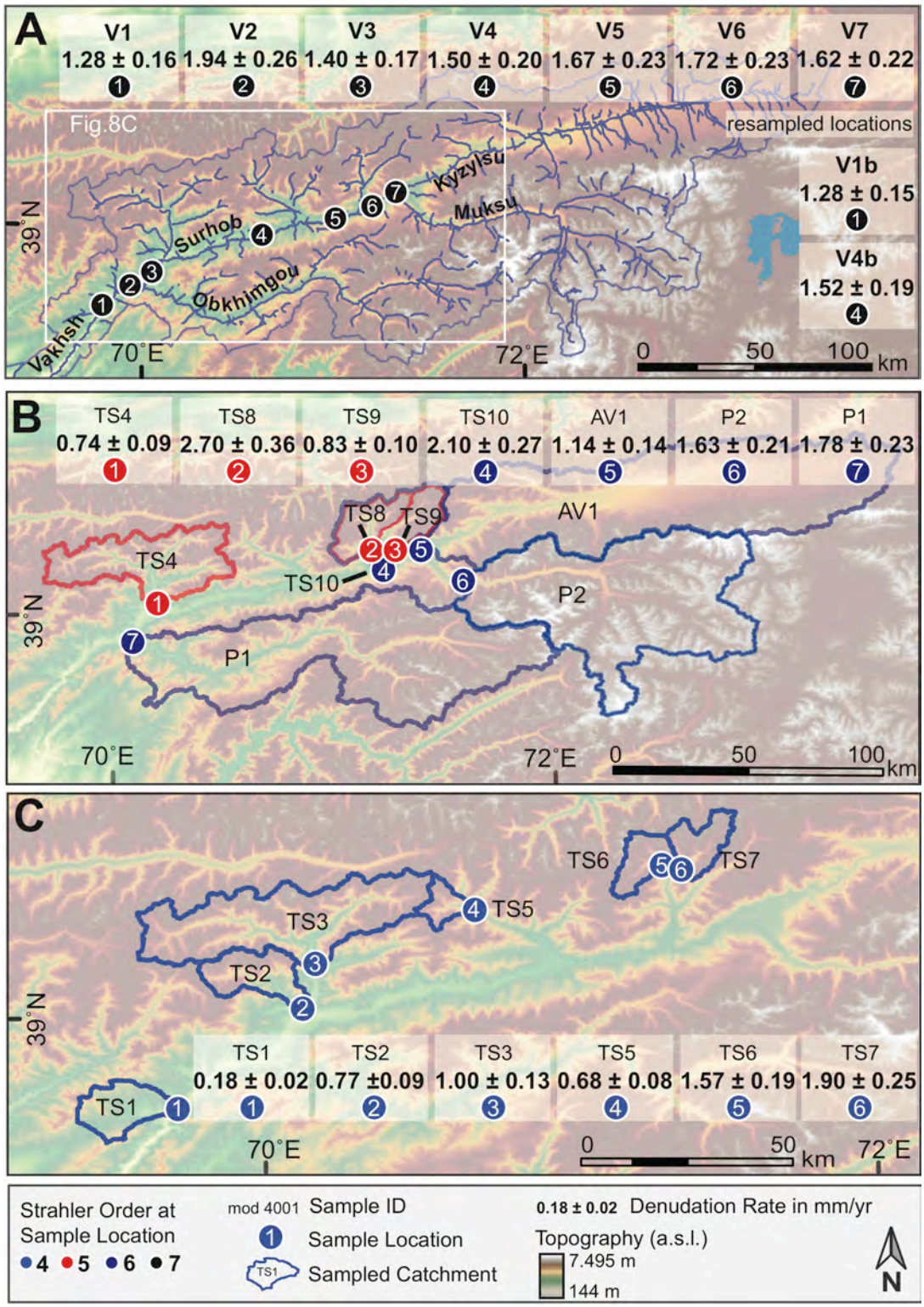

Figure 23: Modern catchment-wide denudation rates A) along the main trunk of the Vakhsh River with results for resampled locations, B) denudation rates from Strahler Order 5 and 6 tributaries, and C) denudation rates from Strahler Order 4 tributaries.

Table 9: $^{26}Al/^{10}Be$ ratios in modern river sediment.

Location ID	Sample ID	Latitude °N	Longitude °E	^{27}Al conc. ppm	^{26}Al conc. 10^3atoms/$g_{(qtz)}$ (± 1σ)	^{10}Be conc. 10^3atoms/$g_{(qtz)}$ (± 1σ)	$^{26}Al/^{10}Be$ ratio
Vakhsh main trunk							
V2	mod7003	38.86478	69.97709	137	107.1 ± 18.9	16.9 ± 1.3	6.3 ± 1.2
V4	mod7005	39.01980	70.37091	219	138.2 ± 22.2	23.1 ± 1.5	6.0 ± 1.0
V5	mod7006	39.16610	71.08647	170	102.4 ± 17.1	16.8 ± 1.5	6.1 ± 1.2
V7	mod6005	39.26691	71.37693	121	157.5 ± 17.6	23.0 ± 1.8	6.8 ± 0.9
Western Tian Shan							
Sarbog Tributary							
TS4	mod5001	39.03497	70.18875	79	201.7 ± 17.0	38.7 ± 1.9	5.2 ± 0.5
Tandykul Tributary							
TS8	mod5004	39.29603	71.22601	152	102.8 ± 17.0	15.4 ± 1.1	6.7 ± 1.2
TS8	mod5003	39.29609	71.23148	118	482.0 ± 40.0	70.2 ± 2.6	6.9 ± 0.6
TS10	mod6002	39.24385	71.22711	147	125.1 ± 17.8	19.1 ± 1.1	6.6 ± 1.0
Northern Pamir							
Obkhimghou River							
P1	mod6001	38.85989	70.10363	116	123.3 ± 16.5	16.8 ± 1.5	7.4 ± 1.2
Muksu River							
P2	mod6004	39.17273	71.55499	145	190.8 ± 27.9	25.1 ± 1.5	7.6 ± 1.2

5.4 DISCUSSION

5.4.1 SYNTHESIS OF CATCHMENT-WIDE DENUDATION RATES

Cosmogenic nuclide concentrations determined in river sediments of the Vakhsh River catchment indicate spatial variation in the denudation rates (Figure 23). General trends evident in the calculated denudation rates (Table 8; Figure 23) are: 1) increasing denudation rates from west to east in the main trunk of the Vakhsh River (Figure 23A); 2) increasing denudation rates in the Western Tian Shan tributaries from west to east (Figure 23B and C); 3) lower denudation rate in the Alai valley in comparison to neighboring catchments of the Tandykul tributary; and 4) similar denudation rates of the Northern Pamir rivers and the easternmost Western Tian Shan tributaries.

Catchment-wide denudation rates reported here for the Vakhsh River catchment range from 0.18 ± 0.02 to 2.70 ± 0.36 mm/yr. These rates integrate denudation over the last hundreds to thousand years and are in general agreement with denudation rates estimated from sediment accumulated upstream of the Nurek Dam over ~30 years. The mean annual sediment load of the river at the Nurek Dam site is ~76×10^6 m^3/yr (Dam Safety Assessment, (2000)) and the drainage area is ~30,000 km^2. Assuming a density for the sediment load (~2.0 g/cm^3) and eroded berdock (~2.6 g/cm^3),

the river load-based catchment-wide denudation rate is ~1.9 mm/yr. The cosmogenic and river load-derived catchment denudation rates are similar to the million-year time scale thermochronometer-derived apparent exhumation rates in the Vakhsh River area. For example, the average Cenozoic apparent exhumation rates in this region range between 0.5 – 1.0 mm/yr for the central Pamir (Carrapa et al., 2014). Exhumation rates in the Western Tian Shan over the last ~10 Myr suggest rates of ~0.2 – 1.0 mm/yr (Käßner et al., 2016). In the vicinity of sample TS1 (0.18 ± 0.02 mm/yr) in the Ghissar Range rates of 0.2 - 0.3 mm/yr are reported (Käßner et al., 2016). Thus, although the range of cosmogenic nuclide-derived denudation rates in the Vakhsh River catchment is large, denudation rates calculated over shorter (e.g., sediment load) or longer (thermochronometer) time scales lie within the range of rates suggested by our data. The consistency in denudation rates summarized here over a range of time scales is somewhat surprising given that fluctuations in climate over millennial to million year timescales is often attributed to causing temporal variations in denudation rates (e.g. Herman et al., 2013; Michel et al., 2018). However, as previously reported in other studies (e.g. Stock et al., 2009; Adams and Ehlers, 2018), tectonic gradients in rock uplift rate can set the regional scale tempo for denudation, upon which smaller scale, climate driven fluctuations in denudation are superimposed.

5.4.2 FACTORS INFLUENCING DENUDATION RATES

The highest variability in denudation rates is reported from the small catchments situated in the Western Tian Shan whereas the larger Vakhsh River main trunk, the Muksu, the Obkhimghou, and the Kyzylsu Rivers show less variability (Table 8, Figure 24). This observation of higher variability of denudation rates in smaller tributaries was also made by Matmon et al. (2003). The catchments described above are separated by active structures including the PTS (Figure 2). In the following, we discuss how different topographic, climate, and tectonic features of the region correspond to the reported denudation rates.

Figure 24 and Figure 25 show comparisons between different topographic metrics and denudation rates. In general, there is no clear relationship between catchment-wide denudation rate and topographic

characteristics such as upstream catchment area (Figure 24) and mean catchment elevation, local relief, hillslope angle, or catchment mean k_{sn} (Figure 25). In fact, the simplest interpretation of denudation rate and topographic metrics compared here is that the topographic metrics have little to no relationship with the reported denudation rates. In more detail, slight trends in the denudation rate with some topographic metrics can be inferred for the Western Tian Shan tributaries (circles, Figure 25). For example, the mean in the reported denudation rates and topographic metrics shows a slight increase as mean elevation, hillslope angle, and k_{sn} values increase. In the Western Tian Shan denudation rates increase with increasing slope (Figure 25C). The westernmost catchment in the Western Tian Shan contains the lowest denudation rate (Obi Garm: 0.18 ±0.02 mm/yr) with the lowest hillslope angle (21 °). The maximum reported hillslopes of 31 ° correspond to the highest denudation rates. Furthermore, denudation rates in the Western Tian Shan also increase with increasing k_{sn} to a maximum k_{sn} value of 250. However, the slight increase in denudation rates with topographic metrics in the Western Tian Shan is not visible when comparing denudation rates of the Western Tian Shan with local relief. The previous (weak) relationships between denudation rates and topographic metrics might only be visible for the Western Tian Shan because these catchments contain the largest range of denudation rates in the data set (e.g., from 0.18 ± 0.02 to 2.70 ± 0.36 mm/yr). However, these trends are not significant outside of the 1 s.d. level and cannot rigorously be interpreted.

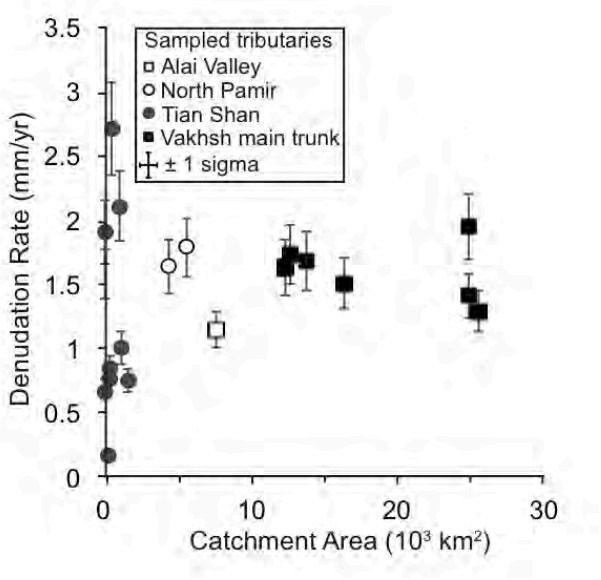

Figure 24: Cosmogenic denudation rates vs. upstream catchment area.

The described regional trends in denudation rates from the Western Tian Shan and Vakhsh River main trunk are not easily explainable via regional precipitation trends. In the Western Tian Shan denudation rates increase from west to east, but TRMM satellite and 30 years of meteorological station data from the region (Figure 5) show a decline in precipitation eastwards (Figure 26). Hence, the observed eastward increase in denudation rates is inversed to the regional precipitation rate trend.

Recent work (Mohadjer et al. 2016, 2017, and studies referenced therein) highlights the location of recent (Quaternary to present) tectonic activity in the region, which could be a contributing factor towards rock uplift. However, the effects of active faulting on denudation rates are only weakly evident in the average normalized steepness index values (k_{sn}) from the Western Tian Shan tributaries that range from 165 in the west to ~250 in the east. However, the described trend in k_{sn} does not have a clear correlation with denudation rates (Figure 25D) suggesting other, currently unrecognized, factors might also be at play. The lack of clear relationships between denudation rate and topographic and climatic measures means that regional

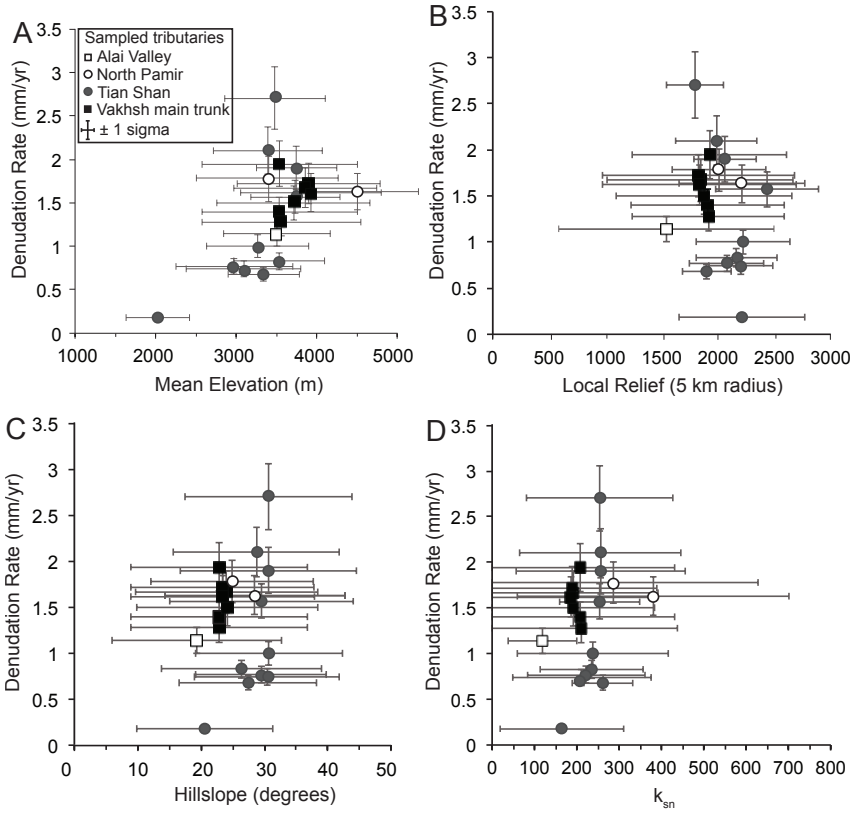

Figure 25: Cosmogenic denudation rates vs.: A) mean elevation; B) local relief; C) hillslope; and D) k_{sn} values.

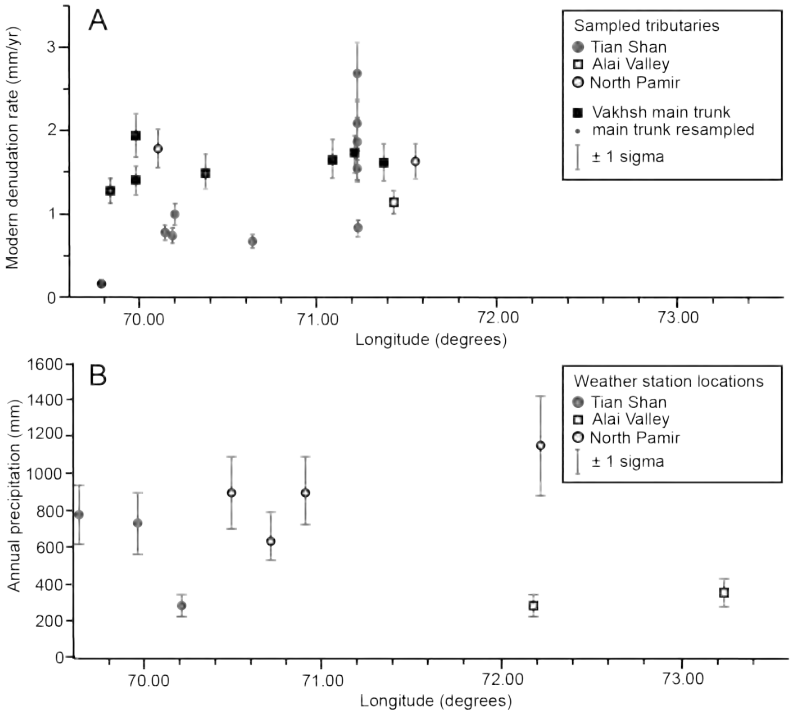

Figure 26: Denudation rates (A) and meteorological station precipitation rates (B) versus longitude for catchments samples presented in this study.

trends in denudation rates likely reflect small gradients in tectonic-driven rock uplift along the PTS faults. Denudation from rivers draining the Northern Pamir dominates the denudation rates measured in the Vakhsh River samples. A west to east increase in denudation rates as in the Western Tian Shan cannot be identified in the Northern Pamir due to the limited number of samples from this region. Only two data points from large catchments (>6,000 km^2) are available in the Northern Pamir whereas 10 data points from smaller catchments (<1,500 km^2) are available in the Western Tian Shan. The large catchments in the Northern Pamir have denudation rates that are comparable to the higher rates in the Western Tian Shan. In summary, a west to east increase in denudation rates is observed in the Western Tian Shan but it is not evident in the Northern Pamir. The previous difference and lateral gradients between the Western Tian Shan and Northern Pamir could indicate that either there is no west to east gradient in denudation rates present in the Northern Pamir, or the smaller number of samples available from the Northern Pamir is not sufficient to document it.

5.4.3 POTENTIAL FACTORS COMPLICATING THE INTERPRETED DENUDATION RATES

There are several surface process related factors in the study area that could influence the interpretation of catchment-wide denudation rates and are discussed here.

First, glacial ice and snow cover can influence the calculation of production rates. In this study, our approach was to exclude the present-day glacier covered portions of the catchment for calculation of production rates. Denudation rates in each catchment are high enough such that the corresponding apparent ages and integration time scale of the reported denudation rates are low (<1,000 yrs, Table 8). Given this, our calculation of denudation rates using production rates from the presently ice-free portions of catchments provides a reasonable estimate of late Holocene denudation rates without a strong glacial influence on denudation rates. Denudation rates from the neighboring Muksu and Obkhimghou catchments draining the Northern Pamir we report here are similar (1.63 ± 0.21 and 1.78 ± 0.23 mm/yr, respectively) but have different present-day ice cover (34% and 14%). The

consistency in denudation rates between these neighboring catchments draining the same tectonic unit suggests our correction of ice cover on production rates provides representative catchment-wide denudation rates for this tectonic unit. Another bias in the denudation rate calculation could arise from seasonal snow shielding. As higher elevations are covered longer with thicker snow packs this could influence production rates. Unfortunately, due to the remote nature of the Vakhsh River catchment, sufficient meteorological data does not exist in the catchments to correct for snow pack thickness effects on production rates.

Second, sediment storage and reworking into the modern river sediment can lead to an increase or decrease in the nuclide concentration and influence the calculated denudation rates. For example, the modern river sample V2 was collected at the terrace sequence location. Incorporation of the terrace sediment material into the river at this location could explain the low nuclide concentration measured in sample V2. Indeed, the calculated denudation rate at this location is ~0.5 mm/yr higher than in neighboring samples from up- or down-stream of sample V2. As another example, the Sarbog catchment sample TS4 displays a $^{26}Al/^{10}Be$ ratio of 5.2 ± 0.5 suggesting incorporation of buried and reworked material into the modern river channel (Table 9). However, all other reported $^{26}Al/^{10}Be$ ratios are near a value of 6.75, and therefore suggest that sediment burial and reworking of sediment into the modern channel is the exception rather the rule for the samples reported here.

Third, the quartz content of the diverse lithologies present in the catchment could influence the calculation of denudation rates. However, catchments with abundant quartz-poor lithologies (e.g., the Devonian age lithologies in the Tandykul tributaries) were excluded in the calculated production and denudation rates. Thus, the denudation rates reported here should be representative of the entire Vakhsh River catchment as quartz-rich lithologies are widespread elsewhere in the study area.

5.5 SUMMARY AND CONCLUSIONS

The Vakhsh River catchment drains along the Pamir Thrust System situated in the collision zone between the Northern Pamir and the

Western Tian Shan. This region was investigated to learn more about the response in denudation to rates where tectonic displacement and shortening are very high. The different analyses applied to the Vakhsh River catchments reveal the following:

(1) Denudation rates of tributaries to the Vakhsh River system are determined with cosmogenic nuclides in river sediment. The denudation rates range from 0.18 to 2.70 mm/yr. The small tributaries of the Western Tian Shan indicate an increase in denudation rates from west to east. Large tributaries draining the Northern Pamir reveal denudation rates of ~1.70 mm/yr, whereas the river draining the Alai Valley shows rates of ~1.10 mm/yr.

(2) Catchment-wide denudation rates from all samples show no clear relationship to topographic metrics such as elevation, local relief, hillslope angle, and normalized steepness index. However, the Western Tian Shan catchments show a weak relationship to the previous metrics.

(3) Catchment-wide denudation rates in the westernmost tributaries in the Western Tian Shan are of the same magnitude as thermochronometer-derived exhumation rates. This resemblance between exhumation and catchment-wide denudation rates despite different response times might indicate that this part of the Tian Shan is primarily prone to the influence of tectonics and does not reflect controls in denudation rates due to climate change or lateral gradients in modern precipitation rates.

6 Summary and Conclusion

The aim of this thesis is to explore the temporal and spatial response patterns of the Vakhsh catchment to climate and tectonics.

6.1 MORAINE BOULDER DATA

The first step was to establish the glaciation record in the Vakhsh catchment. I investigated the Fedchenko Glacier hosting tributary using cosmogenically derived boulder exposure ages. The Fedchenko Glacier is the largest glacier in the catchment, thus its glacial deposits are more easily accessible compared to the numerous small glaciers found in the Vakhsh catchment. Additionally, vastness and variety of the deposits suggested the possibility of the investigation of several glacial retreats. Results on boulder exposure from a recessional moraine showed, that the latest glacial retreat, which represents the local LGM signal at ~17.5 ka, is preserved in the lower part of the glaciated tributary. Older glacial deposits were obliterated or may be situated in less accessible higher parts of the tributary The boulder age distribution on the lateral moraines revealed, that the entire set belonged to one glacial retreat period around ~18 ka.

The age distribution of both moraine types was not similar. I interpreted the mean age on the recessional moraine as the timing of deposition, because it correlated with the most reliable boulders sampled. The age distribution showed clearly too young and too old outliers. The oldest samples were most likely exposed to irradiation during their transport on the glacier, whereas the too young boulders were subsequently uncovered or tilted during moraine degradation. The lateral moraines showed no outliers that were too old. I therefore interpreted the oldest age peak on lateral moraines at ~18ka as the timing of glacial retreat. The single lateral moraine ages are identical within the margin of error, which makes it impossible to estimate the time in between their individual deposition. A second peak in the lateral moraine age distribution at ~8 ka corresponds to the Holocene climate optimum and represents the degradation of the lateral moraines. To estimate the degree of moraine crest degradation, I sampled a depth profile on one lateral moraine.

Unfortunately, the individual samples did not yield enough quartz for reliable measurements.

6.2 TERRACE SET DATA

The second step was to investigate the possible correlations between the terrace set history, paleo-denudation and the existing paleo-climate records. The degradation of moraines during the wetter conditions of the Holocene thermal optimum (~8 – 4 ka) implies an increase in sediment introduction into the river. As a result, the transport capacity might have been surpassed along the downstream section of the main trunk, leading to aggradation of among others, the investigated ~100 m thick terrace set. The following drier and warmer period (~3.5 – 2.0 ka) induced the fast incision (~7 – 29 mm/yr) into the fluvial deposits and subsequent terrace surface abandonment ~3 ka ago. The sampled depth profiles revealed mixing in the upper 0.5 m of the profile, which can be explained by anthropogenic use as pasture and farm land. Otherwise the terrace surface erosion rate of ~1 cm/kyr indicates a reasonably stable terrace surface. This coincides also with our field observations of clearly traceable terrace outlines. The young age of the terrace set, the fast incision into the fluvial fill, and the non-incorporation of the uppermost samples into the calculations makes it difficult to resolve the individual timing of terrace surface abandonment with depth profiles. The depth profile of the alluvial fan, which is intertwined into the terrace set, did not yield enough reliable measurements. The causes are, that the alluvial fan is too young, the source area too small, and the erosion of the source area surface to deep to maintain a stable inherited nuclide concentration signal.

6.3 VAKHSH MAIN TRUNK DENUDATION RATES

To be able to investigate the temporal variations in denudation rates in the Vakhsh catchment, I took modern river samples along the main trunk and resampled two locations during the following field season to investigate the seasonal variation, which the catchment might experience. The results show, that the Vakhsh main trunk did not experience any changes in denudation on an annual timescale, which is concordant with the assumptions of the TCN application theory.

Further I calculated paleo-denudation rates based on the inherited cosmogenic nuclide concentrations in the terrace depth profiles. The paleo-denudation rate, which represents the signal ~3 ka ago, was slightly higher (~2 mm/yr), than the modern denudation rate (~1.3 mm/yr) measured in the lower section of the main trunk. The modern river denudation rate at the terrace site is identical with the paleo-denudation rate, which indicates the still ongoing incision into the deposited alluvial material at the site.

6.4 ACTIVE CHANNEL DENUDATION RATES

The third step was to compile the present-day climate records for the Vakhsh region and compare the spatial distribution of precipitation with measured modern river denudation rates. The compiled satellite records covered only 17 years, which is considered to be insufficient data (minimum 30 years needed to provide a climate signal). The compiled weather station data has a sufficient spatial and temporal coverage and supports the precipitation record provided by the TRMM satellite. The comparison of the spatial distribution of modern denudation rates with the compiled data showed an inverse trend between denudation rates and precipitation pattern in the Western Tian Shan tributaries. The absence of a positive relationship between denudation rates and precipitation pattern most likely reflects the influence of local to regional tectonic-driven influence along the PTS faults. No statement can be made about the spatial correlations between the precipitation patterns and the distribution of denudation rates in the Northern Pamir and the Alay Valley, because in total only three data points represent these regions.

6.5 TOPOGRAPHIC METRICS

The response of the Vakhsh catchment to tectonics and geology was investigated with topographic metrics e.g. catchment size, mean catchment elevation, hillslope angle, and k_{sn}. In summary, the topographic metrics show a weak (Western Tian Shan) to no correlation with the spatial distribution of the denudation rates. The catchment-size vs. denudation rates display the highest diversity in rates among the relatively small Western Tian Shan tributaries. This behavior might be based on local differences in fault activity

and uplift patterns and was also observed elsewhere. The Western Tian Shan denudation rate distribution correlates weakly positively with catchment mean elevation, hillslope angle, and average k_{sn}, but not with relief. The decrease in denudation rates from east to west is observed best in the Western Tian Shan (from 2.1 to 0.02 mm/yr) and appears more moderate along the main trunk. The decrease along the lower section of a main trunk is a commonly observed behavior. The PTS, which also runs along the Vakhsh main trunk, does not disturb the slight decrease of the denudation rates. The k_{sn} values depict reliably lithology boundaries and faults crossing the tributaries, but no uplift pattern could be observed in the Vakhsh catchment using the k_{sn} approach. The reasons for the lack of an uplift pattern could be, that the fault- and lithology-induced knickpoints at least partly overlay the uplift-induced knickpoints. The uplift might also produce a comparatively weaker signal than the faults and lithology boundaries and therefore disappear in the data noise.

The Northern Pamir denudation rates (~1.7 mm/yr) are lower than the rates in the eastern tributaries of the Western Tian Shan. The Alai Valley yields an even more moderate denudation rate (~1.1 mm/yr). Evidently, three data points are not sufficient data to be correlated reasonably with topographic metrics. However, the observation that the Northern Pamir unit drains at a uniform rate can be made. The Northern Pamir tributaries dictate also the denudation rate of the Vakhsh main trunk. The denudation rate measured in the Alai Valley reflects its rather shallow topography. To establish a more reliable spatial distribution of the Northern Pamir and the Alai Valley, a closer survey and higher sampling density in these areas is necessary.

Many possible influences on catchment-wide denudation rates, which have the potential to distort the denudation rate calculation, were evaluated carefully. For example, the present-day glaciation database served well for glacial cover calculation, since the denudation rates integrate only over several centuries. However, the glacial sediment intake into the fluvial system may vary from glacier to glacier, but at this point no data exists from the snout of any glacier in this region, nor a method to model such an estimate. The non-quartz bearing lithologies were closely monitored in the field. The observations were complemented with existing maps, where the tributaries

were not accessible. The $^{26}Al/^{10}Be$ ratios revealed no sediment storage along the main trunk or in the tributaries except a tendency for storage in one tributary in the west on the Western Tian Shan side. However, no estimate of the thickness, extent, and duration of snow cover can be made and incorporated in the calculation at this point. Additionally, the details of local fault activity are not well known to assess its impact on local denudation rate distribution. The available geologic maps describe the lithologies well, but show their extent only grouped in geologic periods, which results in insufficient data regarding the comparison between lithology boundaries and k_{sn} values. With a more detailed coverage of lithology boundaries across the riverbeds, potential uplift-induced knickpoints might be observed.

6.6 CONCLUSION

Do we see any influence of climate on landscape shaping in such a highly active tectonic setting as found in the Vakhsh catchment?

6.6.1 MODERN DENUDATION RATES

The arid Alai Valley displays the same magnitude of denudation as the Northern Pamir. Both landscapes experience internal shortening, introduced by the Pamir convergence towards the western Tian Shan. The slightly higher denudation rates in the Northern Pamir catchments however, might be induced by the mountainous character in contrast to the rather flat Alai Valley geomorphology. But also presence of a higher annual precipitation and the presence of extensive glacial cover in the Northern Pamir can be responsible for this effect. To resolve the underlying dynamics and their influences on the denudation rates, future studies might focus on the spatial and temporal discharge distribution and sediment load capacities in the Vakhsh tributaries. The western Tian Shan shows the greatest range in modern denudation rates, with the lowest in the west, which is consistent with the tectonic setting.

6.6.2 TERRACE DATA SET

The paleo-denudation data and the Holocene terrace deposition allow a glimpse on conditions 3 ka ago. Given the dimensions of the terraces encountered along the lower main trunk of the Vakhsh, I wanted to test the hypothesis, if their deposition was correlated with the glacial retreat after the

LGM (~18 ka). The surprisingly young ages of ~ 3 ka however call for another cause for deposition. During this study, I can only offer an observation of the overlapping timing of terrace deposition and the end of the Holocene thermal optimum (~ 8 – 4 ka ago), which then was followed by a more warmer and arid climate (from 3.5 to 2.0 ka ago). This change in climate conditions can cause terrace deposition. But this study does not yield enough data to confirm, that the magnitude of terrace material can be deposited during these conditions. Future studies may investigate composition and structure of several flights of terraces in more detail to deal with still unanswered questions: (a) Did the entire catchment contribute to the terrace material or did one landscape/tributary dominate? What are the reasons for a possible dominance? (b) What caused the onset of deposition and subsequent the incision? (c) Can the history of the terraces found in the tributaries be correlated to the ones along the main trunk?

6.6.3 GLACIAL DEPOSITS

There is no doubt, that the glacial deposits document climate conditions. Even after the deposition climate remains the primary influence of moraine degradation. However, a more detailed insight in the degradation process cannot be given in this study, because the attempt to date one lateral moraine and to estimate its surface erosion rate, failed due to low quartz content. In terms of establishing a glaciation record for the Vakhsh catchment, this study provides extensive data for the regional LGM signal, but no remnants of earlier glaciations were found in the lower part of the Fedchenko Glacier tributary.

6.6.4 COMPARISON WITH THERMOCHRONOLOGY DATA

At this point, it is impossible to correlate landscape history to climate cycles on several million years time-scales. Yet we can compare the denudation rates to existing thermochronology data, which represents the tectonic conditions. The data of this study and the published thermochronology data showed a somewhat unusual stability in denudation rates over million-years timescale.

This indicates tectonics as the main underlying force, with climate-induced small temporal variations in denudation rates.

7 References

Abramowski, U., Bergau, A., Seebach, D., Zech, R., Glaser, B., Sosin, P., Kubik, P.W., Zech, W., 2006. Pleistocene glaciations of Central Asia: results from 10Be surface exposure ages of erratic boulders from the Pamir (Tajikistan), and the Alay–Turkestan range (Kyrgyzstan). Quat. Sci. Rev. 25, 1080–1096. doi:10.1016/j.quascirev.2005.10.003

Adams, B.A., Ehlers, T.A., 2017. Deciphering topographic signals of glaciation and rock uplift in an active orogen: a case study from the Olympic Mountains, USA. Earth Surf. Process. Landforms 42, 1680–1692. doi:10.1002/esp.4120

Adams, B.A., Ehlers, T.A., 2018. Tectonic controls of Holocene erosion in a glaciated orogen. Earth Surf. Dyn. 6, 595–610. doi:10.5194/esurf-6-595-2018

Aizen, E.M., Aizen, V.B., Melack, J.M., Nakamura, T., Ohta, T., 2001. Precipitation and atmospheric circulation patterns at mid-latitudes of Asia. Int. J. Climatol. 21, 535–556. doi:10.1002/joc.626

Aizen, V.B., 2011. Pamir glaciers. Encycl. Snow, Ice Glaciers 2, 1987–1990.

Allen, P.A., 2008. From landscapes into geological history. Nature 451, 274–276. doi:10.1038/nature06586

Amidon, W.H., Hynek, S.A., 2010. Exhumational history of the north central Pamir. Tectonics 29, 1–13. doi:10.1029/2009TC002583

Anderson, R.S., Repka, J.L., Dick, G.S., 1996. Explicit treatment of inheritance in dating depositional surfaces using in situ 10Be and 26Al. Geology24,47.doi:10.1130/0091-7613(1996)024<0047:ETOIID>2.3.CO;2

Applegate, P.J., Urban, N.M., Laabs, B.J.C., Keller, K., Alley, R.B., 2010. Modeling the statistical distributions of cosmogenic exposure dates from moraines. Geosci. Model Dev. 3, 293–307. doi:10.5194/gmd-3-293-2010

Balco, G., Rovey, C.W., 2008. An isochron method for cosmogenic-nuclide dating of buried soils and sediments. Am. J. Sci. 308, 1083–1114. doi:10.2475/10.2008.02

Balco, G., Soreghan, G.S., Sweet, D.E., Marra, K.R., Bierman, P.R., 2013. Cosmogenic-nuclide burial ages for Pleistocene sedimentary fill in Unaweep Canyon, Colorado, USA. Quat. Geochronol. 18, 149–157. doi:10.1016/j.quageo.2013.02.002

Balco, G., Stone, J.O., Lifton, N.A., Dunai, T.J., 2008. A complete and easily accessible means of calculating surface exposure ages or erosion rates from 10Be and 26Al measurements. Quat. Geochronol. 3, 174–195. doi:10.1016/j.quageo.2007.12.001

Benn, D.I., Owen, L.A., 1998. The role of the Indian summer monsoon and the mid-latitude westerlies in Himalayan glaciation: review and speculative discussion. J. Geol. Soc. London. 155, 353–363. doi:10.1144/gsjgs.155.2.0353

Berlin, M.M., Anderson, R.S., 2007. Modeling of knickpoint retreat on the Roan Plateau, western Colorado. J. Geophys. Res. 112, F03S06. doi:10.1029/2006JF000553

Bishop, P., 2007. Long-term landscape evolution : linking tectonics and surface processes 365, 329–365. doi:10.1002/esp

Braucher, R., Bourlès, D., Merchel, S., Vidal Romani, J., Fernadez-Mosquera, D., Marti, K., Léanni, L., Chauvet, F., Arnold, M., Aumaître, G., Keddadouche, K., 2013. Determination of muon attenuation lengths in depth profiles from in situ produced cosmogenic nuclides. Nucl. Instruments Methods Phys. Res. Sect. B Beam Interact. with Mater. Atoms 294, 484–490. doi:10.1016/j.nimb.2012.05.023

Burtman, V., Molnar, P., 1993. Geological and Geophysical Evidence for Deep Subduction of continental crust beneath the Pamir. Geol. Soc. Am. Spec. Pap. doi:10.1130/SPE281-p1

Burtman, V.S., 2000. Cenozoic crustal shortening between the Pamir and Tien Shan and a reconstruction of the Pamir-Tien Shan transition zone for the Cretaceous and Palaeogene. Tectonophysics 319, 69–92. doi:10.1016/S0040-1951(00)00022-6

Carrapa, B., Mustapha, F.S., Cosca, M., Gehrels, G., Schoenbohm, L.M., Sobel, E.R., DeCelles, P.G., Russell, J., Goodman, P., 2014. Multisystem dating of modern river detritus from Tajikistan and China: Implications for crustal evolution and exhumation of the Pamir. Lithosphere 6, 443–455. doi:10.1130/L360.1

Chmeleff, J., von Blanckenburg, F., Kossert, K., Jakob, D., 2010. Determination of the Be-10 half-life by multicollector ICP-MS and liquid scintillation counting. Nucl. Instruments Methods Phys. Res. Sect. B-Beam Interact. with Mater. Atoms 268, 192–199. doi:10.1016/j.nimb.2009.09.012

Clark, P.U., Dyke, A.S., Shakun, J.D., Carlson, A.E., Clark, J., Wohlfarth, B., Mitrovica, J.X., Hostetler, S.W., McCabe, A.M., 2009. The Last Glacial Maximum. Science 325, 710–714. doi:10.1126/science.1172873

Coutand, I., 2002. Late Cenozoic tectonic development of the intramontane Alai Valley, (Pamir-Tien Shan region, central Asia): An example of intracontinental deformation due to the Indo-Eurasia collision. Tectonics. doi:10.1029/2002TC001358

Crosby, B.T., Whipple, K.X., 2006. Knickpoint initiation and distribution within fluvial networks: 236 waterfalls in the Waipaoa River, North Island, New Zealand. Geomorphology 82, 16–38. doi:http://dx.doi.org/10.1016/j.geomorph.2005.08.023

Crosby, B.T., Whipple, K.X., 2006. Knickpoint initiation and distribution within fluvial networks: 236 waterfalls in the Waipaoa River, North Island, New Zealand. Geomorphology 82, 16–38. doi:10.1016/j.geomorph.2005.08.023

Cyr, A.J., Granger, D.E., Olivetti, V., Molin, P., 2010. Quantifying rock uplift rates using channel steepness and cosmogenic nuclide–determined erosion rates: Examples from northern and southern Italy. Lithosphere 2, 188–198. doi:10.1130/L96.1

Dam Safity Assessment, 2000. Aral Sea Basin Program Water & Environmental Managment Project, Component C: Dam Safety and Reservoir Managment, Nurek Dam Safety Assessment Report.

DiBiase, R.A., Whipple, K.X., Heimsath, A.M., Ouimet, W.B., 2010. Landscape form and millennial erosion rates in the San Gabriel Mountains, CA. Earth Planet. Sci. Lett. 289, 134–144. doi:10.1016/j.epsl.2009.10.036

Diehl, R., Halloin, H., Kretschmer, K., Lichti, G.G., Schönfelder, V., Strong,

A.W., von Kienlin, A., Wang, W., Jean, P., Knödlseder, J., Roques, J.-P., Weidenspointner, G., Schanne, S., Hartmann, D.H., Winkler, C., Wunderer, C., 2006. Radioactive 26Al from massive stars in the Galaxy. Nature 439, 45–47. doi:10.1038/nature04364

Dortch, J.M., Owen, L.A., Caffee, M.W., 2013. Timing and climatic drivers for glaciation across semi-arid western Himalayan-Tibetan orogen. Quat. Sci. Rev. 78, 188–208. doi:10.1016/j.quascirev.2013.07.025

Dunai, T.J., 2000. Scaling factors for production rates of in situ produced cosmogenic nuclides: a critical reevaluation. Earth Planet. Sci. Lett. 176, 157–169. doi:10.1016/S0012-821X(99)00310-6

Dunai, T.J., 2001. Influence of secular variation of the geomagnetic field on production rates of in situ produced cosmogenic nuclides. Earth Planet. Sci. Lett. 193, 197–212. doi:10.1016/S0012-821X(01)00503-9

Dunai, T.J., 2010. Cosmogenic Nuclides: Principles, Concepts and Applications in the Earth Surface Sciences. Cambridge University Press, Cambridge, p. 198.

Duvall, A., 2004. Tectonic and lithologic controls on bedrock channel profiles and processes in coastal California. J. Geophys. Res. 109, F03002. doi:10.1029/2003JF000086

Flint, J.J., 1974. Stream gradient as a function of order, magnitude, and discharge. Water Resour. Res. 10, 969–973. doi:10.1029/WR010i005p00969

Fuchs, M.C., Gloaguen, R., Krbetschek, M., Szulc, A., 2014. Rates of river incision across the main tectonic units of the Pamir identified using optically stimulated luminescence dating of fluvial terraces. Geomorphology 216, 79–92. doi:10.1016/j.geomorph.2014.03.027

Fuchs, M.C., Gloaguen, R., Merchel, S., Pohl, E., Sulaymonova, V.A., Andermann, C., Rugel, G., 2015. Millennial erosion rates across the Pamir based on 10Be concentrations in fluvial sediments: dominance of topographic over climatic factors. Earth Surf. Dyn. Discuss. 3, 83–128. doi:10.5194/esurfd-3-83-2015

Gillespie, A., Molnar, P., 1995. Asynchronous maximum advances of mountain and continental glaciers. Rev. Geophys. doi:10.1029/95RG00995

Glotzbach, C., Paape, A., Baade, J., Reinwarth, B., Rowntree, K., Miller, J., 2016. Cenozoic landscape evolution of the Kruger National Park as derived from cosmogenic nuclide analyses. Terra Nova, 28: 316– 322. doi.org/10.1111/ter.12223

Goethals, M.M., Hetzel, R., Niedermann, S., Wittmann, H., Fenton, C.R., Kubik, P.W., Christl, M., von Blanckenburg, F., 2009. An improved experimental determination of cosmogenic 10Be/21Ne and 26Al/21Ne production ratios in quartz. Earth Planet. Sci. Lett. 284, 187–198. doi:10.1016/j.epsl.2009.04.027

Goldrick, G., Bishop, P., 2007. Regional analysis of bedrock stream long profiles: evaluation of Hack's SL form, and formulation and assessment of an alternative (the DS form). Earth Surf. Process. Landforms 32, 649–671. doi:10.1002/esp.1413

Gosse, J.C., Phillips, F.M., 2001. Terrestrial in situ cosmogenic nuclides: theory and application. Quat. Sci. Rev. 20, 1475–1560. doi:10.1016/S0277-3791(00)00171-2

Grin, E., Ehlers, T.A., Schaller, M., Sulaymonova, V., Ratschbacher, L., Gloaguen, R., 2016. 10Be Surface-Exposure Age Dating of the Last Glacial Maximum in the Northern Pamir (Tajikistan). Quat. Geochronol. doi:10.1016/j.quageo.2016.03.007

Grin, E., Schaller, M., Ehlers, T.A., 2018. Spatial distribution of cosmogenic 10Be derived denudation rates between the Western Tian Shan and Northern Pamir, Tajikistan. Geomorphology 321, 1–15. doi:10.1016/j.geomorph.2018.08.007

Groom, D.E., Mokhov, N.V., Striganov, S.I., 2001. Muon stopping power and range tables 10 MeV–100 TeV. At. Data Nucl. Data Tables 78, 183–356. doi:10.1006/adnd.2001.0861

Hamburger, M.W., Sarewitz, D.R., Pavlis, T.L., Popandopulo, G.A., 1992. Structural and seismic evidence for intracontinental subduction in the Peter the First Range, central Asia. Geol. Soc. Am. Bull. doi:10.1130/0016-7606(1992)104<0397:SASEFI>2.3.CO;2

Haviv, I., Enzel, Y., Whipple, K.X., Zilberman, E., Stone, J., Matmon, A., Fifield, L.K., 2006. Amplified erosion above waterfalls and oversteepened bedrock reaches. J. Geophys. Res. 111, F04004. doi:10.1029/2006JF000461

Heisinger, B., Lal, D., Jull, A.J.T., Kubik, P., Ivy-Ochs, S., Knie, K., Nolte, E., 2002a. Production of selected cosmogenic radionuclides by muons: 2. Capture of negative muons. Earth Planet. Sci. Lett. 357–369.

Heisinger, B., Lal, D., Jull, A.J.T., Kubik, P., Ivy-Ochs, S., Neumaier, S., Knie, K., Lazarev, V., Nolte, E., 2002b. Production of selected cosmogenic radionuclides by muons 1. Fast muons. Earth Planet. Sci. Lett. 345–355.

Herman, F., Seward, D., Valla, P.G., Carter, A., Kohn, B., Willett, S.D., Ehlers, T.A., 2013. Worldwide acceleration of mountain erosion under a cooling climate. Nature 504, 423–426. doi:10.1038/nature12877

Hidy, A.J., Gosse, J.C., Pederson, J.L., Mattern, J.P., Finkel, R.C., 2010. A geologically constrained Monte Carlo approach to modeling exposure ages from profiles of cosmogenic nuclides: An example from Lees Ferry, Arizona. Geochemistry Geophys. Geosystems 11, Q0AA10. doi:10.1029/2010GC003084

Howard, A.D., Dietrich, W.E., Seidl, M.A., 1994. Modeling fluvial erosion on regional to continental scales. J. Geophys. Res. Solid Earth 99, 13971–13986. doi:10.1029/94JB00744

Huffman, G.J., Bolvin, D.T., Nelkin, E.J., Wolff, D.B., Adler, R.F., Gu, G., Hong, Y., Bowman, K.P., Stocker, E.F., 2007. The TRMM Multisatellite Precipitation Analysis (TMPA): Quasi-Global, Multiyear, Combined-Sensor Precipitation Estimates at Fine Scales. J. Hydrometeorol. doi:10.1175/JHM560.1

Hughes, P.D., Gibbard, P.L., Ehlers, J., 2013. Timing of glaciation during the last glacial cycle: evaluating the concept of a global 'Last Glacial Maximum' (LGM). Earth-Science Rev. 125, 171–198. doi:10.1016/j.earscirev.2013.07.003

Ischuk, A., Bendick, R., Rybin, A., Molnar, P., Khan, S.F., Kuzikov, S., Mohadjer, S., Saydullaev, U., Ilyasova, Z., Schelochkov, G., Zubovich, A. V., 2013. Kinematics of the pamir and hindu kush regions from gps geodesy. J. Geophys. Res. Solid Earth 118, 2408–2416. doi:10.1002/jgrb.50185

Ivy-Ochs, S., and Kober, F. 2007. Cosmogenic nuclide dating; exposure geochronology. In Encyclopedia of Quaternary science. Edited by S.A. Elias. Elsevier, Amsterdam, Netherlands. pp. 436-445.

Ivy-Ochs, S., Schaller, M., 2009. Examining Processes and Rates of Landscape Change with Cosmogenic Radionuclides, in: Radioactivity in the Environment. pp. 231–294. doi:10.1016/S1569-4860(09)01606-4

Käßner, A., Ratschbacher, L., Jonckheere, R., Enkelmann, E., Khan, J., Sonntag, B.-L., Gloaguen, R., Gadoev, M., Oimahmadov, I., 2016. Cenozoic intracontinental deformation and exhumation at the northwestern tip of the India-Asia collision-southwestern Tian Shan, Tajikistan, and Kyrgyzstan. Tectonics 35, 2171–2194. doi:10.1002/2015TC003897

Kelly, M.A, Lowell, T. V., Applegate, P.J., Phillips, F.M., Schaefer, J.M., Smith, C. a., Kim, H., Leonard, K.C., Hudson, A.M., 2013. A locally calibrated, late glacial 10Be production rate from a low-latitude, high-altitude site in the Peruvian Andes. Quat. Geochronol. 1–16. doi:10.1016/j.quageo.2013.10.007

Kirby, E., Whipple, K.X., 2012. Expression of active tectonics in erosional landscapes. J. Struct. Geol. 44, 54–75. doi:10.1016/j.jsg.2012.07.009

Kong, P., Fink, D., Na, C., Huang, F., 2009. Late Quaternary glaciation of the Tianshan, Central Asia, using cosmogenic 10Be surface exposure dating. Quat. Res. 72, 229–233. doi:10.1016/j.yqres.2009.06.002

Koppes, M., Gillespie, A.R., Burke, R.M., Thompson, S.C., Stone, J., 2008. Late Quaternary glaciation in the Kyrgyz Tien Shan. Quat. Sci. Rev. 27, 846–866. doi:10.1016/j.quascirev.2008.01.009

Korschinek, G., Bergmaier, A., Faestermann, T., Gerstmann, U.C., Knie, K., Rugel, G., Wallner, A., Dillmann, I., Dollinger, G., von Gostomski, C.L., Kossert, K., Maiti, M., Poutivtsev, M., Remmert, a., 2010. A new value for the half-life of 10Be by Heavy-Ion Elastic Recoil Detection and liquid scintillation counting. Nucl. Instruments Methods Phys. Res. Sect. B Beam Interact. with Mater. Atoms 268, 187–191. doi:10.1016/j.nimb.2009.09.020

Kufner, S.-K., Schurr, B., Ratschbacher, L., Murodkulov, S., Abdulhameed, S., Ischuk, A., Metzger, S., Kakar, N., 2018. Seismotectonics of the Tajik Basin and Surrounding Mountain Ranges. Tectonics 37, 2404–2424. doi:10.1029/2017TC004812

Kulikova, G., 2016. Source parameters of the major historical earthquakes in the Tien-Shan region from the late 19th to the early 20th century. Doctoral thesis (164 pp.). Germany: University of Potsdam.

Lal, D., 1991. Cosmic ray labeling of erosion surfaces: in situ nuclide production rates and erosion models. Earth Planet. Sci. Lett. 104, 424–439. doi:10.1016/0012-821X(91)90220-C

Lal, D., Chen, J., 2005. Cosmic ray labeling of erosion surfaces II: Special cases of exposure histories of boulders, soils and beach terraces. Earth Planet. Sci. Lett. 236, 797–813. doi:10.1016/j.epsl.2005.05.025

Lambrecht, A., Mayer, C., Aizen, V., Floricioiu, D., Surazakov, A., 2014. The evolution of Fedchenko glacier in the Pamir, Tajikistan, during the past eight decades. J. Glaciol. 60, 233–244. doi:10.3189/2014JoG13J110

Leith, W., 1985. A mid-Mesozoic extension across Central Asia? Nature 313, 567–570. doi:10.1038/313567a0

Leya, I., Neumann, S., Wieler, R., Michel, R., 2001. The production of cosmogenic nuclides by galactic cosmic-ray particles for 2π exposure geometries. Meteorit. Planet. Sci. 36, 1547–1561. doi:10.1111/j.1945-5100.2001.tb01845.x

Lifton, N., Beel, C., Clas, H., Kassab, C., Rogozhina, I., Heermance, R. V., Oskin, M., Burbank, D., Blomdin, R., Gribenski, N., Caffee, M., Goehring, B.M., Heyman, J., Ivanov, M., Li, Y., Li, Y., Petrakov, D., Usubaliev, R., Codilean, A.T., Chen, Y., Harbor, J., Stroeven, A.P., 2014. Constraints on the late Quaternary glacial history of the Inylchek and Sary-Dzaz valleys from in situ cosmogenic 10 Be and 26 Al , eastern Kyrgyz Tian Shan. Quat. Sci. Rev. 101. doi:10.1016/j.quascirev.2014.06.032

Masarik, J., Beer, J., 2009. An updated simulation of particle fluxes and cosmogenic nuclide production in the Earth's atmosphere. J. Geophys. Res. 114, D11103. doi:10.1029/2008JD010557

Matmon, A., Bierman, P.R., Larsen, J., Southworth, S., Pavich, M., Caffee, M., 2003. Temporally and spatially uniform rates of erosion in the southern Appalachian Great Smoky Mountains. Geology 31, 155. doi:10.1130/0091-7613(2003)031<0155:TASURO>2.0.CO;2

Mechie, J., Yuan, X., Schurr, B., Schneider, F., Sippl, C., Ratschbacher, L., Minaev, V., Gadoev, M., Oimahmadov, I., Abdybachaev, U., Moldobekov, B., Orunbaev, S., Negmatullaev, S., 2012. Crustal and uppermost mantle velocity structure along a profile across the Pamir and southern Tien Shan as derived from project TIPAGE wide-angle seismic data. Geophys. J. Int. 188, 385–407. doi:10.1111/j.1365-246X.2011.05278.x

Mercader, J., Gosse, J.C., Bennett, T., Hidy, A.J., Rood, D.H., 2012. Cosmogenic nuclide age constraints on Middle Stone Age lithics from Niassa, Mozambique. Quat. Sci. Rev. 47, 116–130. doi:10.1016/j.quascirev.2012.05.018

Michel, L., Ehlers, T.A., Glotzbach, C., Adams, B.A., Stübner, K., 2018. Tectonic and glacial contributions to focused exhumation in the Olympic Mountains, Washington, USA. Geology 46, 491–494. doi:10.1130/G39881.1

Mohadjer, S., Ehlers, T.A., Bendick, R., Stübner, K., Strube, T., 2016. A Quaternary fault database for central Asia. Nat. Hazards Earth Syst. Sci. 16, 529–542. doi:10.5194/nhess-16-529-2016

Mohadjer, S., Ehlers, T.A., Bendick, R., Mutz, S.G., 2017. Review of GPS and Quaternary fault slip rates in the Himalaya-Tibet orogen. Earth-Science Rev. 174, 39–52. doi:10.1016/j.earscirev.2017.09.005

Narama, C., Kondo, R., Tsukamoto, S., Kajiura, T., Duishonakunov, M., Abdrakhmatov, K., 2009. Timing of glacier expansion during the Last Glacial in the inner Tien Shan, Kyrgyz Republic by OSL dating. Quat. Int. 199, 147–156. doi:10.1016/j.quaint.2008.04.010

Nikonov, A.A., Fin'ko, E.A., Pakhomov, M.M., Shumova, G.M., 1981. New data upon the Holocene of mountain regios of Middle Asia (Novye dannye po golotsenu gorkikh raionov Srednei Azii). Dokl. Akad. Nauk 257, 193–197.

Nikonov, A.A., Pakhomov, M.M., Romanova, E.A., Sulerzhitsky, I.D., 1989. The Holocene climatic optimum in the mountains of Pamiro-Alai (Klimaticheskyi optimum golotsena v gorah Pamiro-Alaya), in: Klimanov, V.A. (Ed.), Paleoclimates of Late Pleistocene and Holocene

(Paleoclimaty Pozdneledoikovya i Golotsena). Moscow, pp. 122–130.
Nishiizumi, K., 2004. Preparation of 26Al AMS standards. Nucl. Instruments Methods Phys. Res. Sect. B Beam Interact. with Mater. Atoms 223–224, 388–392. doi:10.1016/j.nimb.2004.04.075
Nishiizumi, K., Imamura, M., Caffee, M.W., Southon, J.R., Finkel, R.C., McAninch, J., 2007. Absolute calibration of 10Be AMS standards. Nucl. Instruments Methods Phys. Res. Sect. B Beam Interact. with Mater. Atoms 258, 403–413. doi:10.1016/j.nimb.2007.01.297
Onuchin, A.A., Burenina, T.A., 1996. Climatic and Geographic Patterns in Snow Density Dynamics, Northern Eurasia. Arct. Alp. Res. 28, 99–103. doi:10.2307/1552091
Ouimet, W.B., Whipple, K.X., Granger, D.E., 2009. Beyond threshold hillslopes: Channel adjustment to base-level fall in tectonically active mountain ranges. Geology 37, 579–582. doi:10.1130/G30013A.1
Owen, L. a., 2009. Latest Pleistocene and Holocene glacier fluctuations in the Himalaya and Tibet. Quat. Sci. Rev. 28, 2150–2164. doi:10.1016/j.quascirev.2008.10.020
Owen, L.A., Chen, J., Hedrick, K.A., Caffee, M.W., Robinson, A.C., Schoenbohm, L.M., Yuan, Z., Li, W., Imrecke, D.B., Liu, J., 2012. Quaternary glaciation of the Tashkurgan Valley, Southeast Pamir. Quat. Sci. Rev. 47, 56–72. doi:10.1016/j.quascirev.2012.04.027
Pavlis, T.L., Hamburger, M.W., Pavlis, G.L., 1997. Erosional processes as a control on the structural evolution of an actively deforming fold and thrust belt: An example from the Pamir-Tien Shan region, central Asia. Tectonics 16, 810–822. doi:10.1029/97TC01414
Pfeffer, W.T., Arendt, A.A., Bliss, A., Bolch, T., Cogley, J.G., Gardner, A.S., Hagen, J.-O., Hock, R., Kaser, G., Kienholz, C., Miles, E.S., Moholdt, G., Mölg, N., Paul, F., Radić, V., Rastner, P., Raup, B.H., Rich, J., Sharp, M.J., 2014. The Randolph Glacier Inventory: a globally complete inventory of glaciers. J. Glaciol. 60, 537–552. doi:10.3189/2014JoG13J176
Pohl, E., Gloaguen, R., Seiler, R., 2015a. Remote Sensing-Based Assessment of the Variability of Winter and Summer Precipitation in the Pamirs and Their Effects on Hydrology and Hazards Using Harmonic Time Series Analysis. Remote Sens. 7, 9727–9752. doi:10.3390/rs70809727
Pohl, E., Knoche, M., Gloaguen, R., Andermann, C., Krause, P., 2015b. Sensitivity analysis and implications for surface processes from a hydrological modelling approach in the Gunt catchment, high Pamir Mountains. Earth Surf. Dyn. 333–362.
Pritchard, D., Roberts, G.G., White, N.J., Richardson, C.N., 2009. Uplift histories from river profiles. Geophys. Res. Lett. 36, L24301. doi:10.1029/2009GL040928
Putkonen, J., Swanson, T., 2003. Accuracy of cosmogenic ages for moraines 59, 255–261. doi:10.1016/S0033-5894(03)00006-1
Reedy, R.C., 2013. Cosmogenic-nuclide production rates: Reaction cross section update. Nucl. Instruments Methods Phys. Res. Sect. B Beam Interact. with Mater. Atoms 294, 470–474. doi:10.1016/j.nimb.2011.08.034
Reuter, H.I., Nelson, A., Jarvis, A., 2007. An evaluation of void-filling

interpolation methods for SRTM data. Int. J. Geogr. Inf. Sci. 21, 983–1008. doi:10.1080/13658810601169899

Roe, G.H., Montgomery, D.R., Hallet, B., 2002. Effects of orographic precipitation variations on the concavity of steady-state river profiles. Geology 30, 143. doi:10.1130/0091-7613(2002)030<0143:EOOPVO>2.0.CO;2

Röhringer, I., Zech, R., Abramowski, U., Sosin, P., Aldahan, A., Kubik, P.W., Zöller, L., Zech, W., 2012. The late Pleistocene glaciation in the Bogchigir Valleys (Pamir, Tajikistan) based on 10Be surface exposure dating. Quat. Res. 78, 590–597. doi:10.1016/j.yqres.2012.09.002

Safran, E.B., Bierman, P.R., Aalto, R., Dunne, T., Whipple, K.X., Caffee, M., 2005. Erosion rates driven by channel network incision in the Bolivian Andes. Earth Surf. Process. Landforms 30, 1007–1024. doi:10.1002/esp.1259

Schaller, M., von Blankenburg, F., Veldkamp, A., Tebbens, L.A., Hovius, N., Kubik, P.W., 2002. A 30 000 yr record of erosion rates from cosmogenic 10Be in Middle European river terraces. Earth Planet. Sci. Lett. 204, 307–320.

Schaller, M., Ehrlers, T.A., Blum, J.D., Kallenberg, M.A., 2009. Quantifying glacial moraine age, denudation, and soil mixing with cosmogenic nuclide depth profiles. J. Geophys. Res. 114, F01012. doi:10.1029/2007JF000921

Scherler, D., Bookhagen, B., Wulf, H., Preusser, F., Strecker, M.R., 2015. Increased late Pleistocene erosion rates during fluvial aggradation in the Garhwal Himalaya, northern India. Earth Planet. Sci. Lett. 428, 255–266. doi:10.1016/j.epsl.2015.06.034

Schneider, F.M., Yuan, X., Schurr, B., Mechie, J., Sippl, C., Haberland, C., Minaev, V., Oimahmadov, I., Gadoev, M., Radjabov, N., Abdybachaev, U., Orunbaev, S., Negmatullaev, S., 2013. Seismic imaging of subducting continental lower crust beneath the Pamir. Earth Planet. Sci. Lett. 375, 101–112. doi:10.1016/j.epsl.2013.05.015

Schoenbohm, L.M., Whipple, K.., Burchfiel, B.C., Chen, L., 2004. Geomorphic constraints on surface uplift, exhumation, and plateau growth in the Red River region, Yunnan Province, China. Geol. Soc. Am. Bull. 116, 895. doi:10.1130/B25364.1

Schurr, B., Ratschbacher, L., Sippl, C., Gloaguen, R., Yuan, X., Mechie, J., 2014. Seismotectonics of the Pamir. Tectonics 33, 1501–1518. doi:10.1002/2014TC003576

Schwanghart, W., Scherler, D., 2014. Short Communication: TopoToolbox 2 – MATLAB-based software for topographic analysis and modeling in Earth surface sciences. Earth Surf. Dyn. 2, 1–7. doi:10.5194/esurf-2-1-2014

Seong, Y.B., Owen, L.A., Yi, C., Finkel, R.C., 2009. Quaternary glaciation of Muztag Ata and Kongur Shan: Evidence for glacier response to rapid climate changes throughout the late glacial and holocene in westernmost Tibet. Bull. Geol. Soc. Am. 121, 348–365. doi:10.1130/B26339.1

Sippl, C., Ratschbacher, L., Schurr, B., Krumbiegel, C., Rui, H., Abdybachaev, U., 2008. The 2008 Nura earthquake sequence at the Pamir-Tian Shan collision zone , southern Kyrgyzstan. doi:10.1002/2014TC003705

Sippl, C., Schurr, B., Yuan, X., Mechie, J., Schneider, F. M., Gadoev, M., et al. (2013). Geometry of the Pamir-Hindu Kush intermediate-depth

earthquake zone from local seismic data. Journal of Geophysical Research: Solid Earth, 118, 1438–1457. https://doi.org/10.1002/jgrb.50128

Snyder, N.P., Whipple, K.X., Tucker, G.E., Merritts, D.J., 2000. Landscape response to tectonic forcing: Digital elevation model analysis of stream profiles in the Mendocino triple junction region, northern California. Geol. Soc. Am. Bull. 112, 1250–1263. doi:10.1130/0016-7606(2000)112<1250:LRTTFD>2.0.CO;2

Stock, J.D., Dietrich, W.E., 2006. Erosion of steepland valleys by debris flows. Geol. Soc. Am. Bull. 118, 1125–1148. doi:10.1130/B25902.1

Stone, J.O., 2000. Air pressure and cosmogenic isotope production. J. Geophys. Res. 105, 23753. doi:10.1029/2000JB900181

Strahler, A. N. (1957), Quantitative analysis of watershed geomorphology, Eos Trans. AGU, 38(6), 913– 920, doi:10.1029/TR038i006p00913.

Svendsen, J.I., Alexanderson, H., Astakhov, V.I., Demidov, I., Dowdeswell, J.A., Funder, S., Gataullin, V., Henriksen, M., Hjort, C., Houmark-Nielsen, M., Hubberten, H., Ingo!lfsson, O., Jakobsson, M., Kjær, K.H., Larsen, E., Lokrantz, H., Lunkka, J.P., Lysa, A., Mangerud, J., Matiouchkov, A., Murray, A., Möller, P., Niessen, F., Nikolskaya, O., Polyak, L., Saarnisto, M., Siegert, C., Siegert, M.J., Spielhagen, R.F., Stein, R., 2004. Late Quaternary ice sheet history of northern Eurasia. Quat. Sci. Rev. 1229–1271. doi:10.1016/j.quascirev.2003.12.008

Thackray, G.D., Owen, L.A., Yi, C., 2008. Timing and nature of late quaternary mountain glaciation. J. Quat. Sci. 23, 503–508. doi:10.1002/jqs.1225

Vlasov, N.G., Dyakov, Y.A., S., C.E., 1991. Geological Map of the Tajik SSR and Adjacent Territories, 1:500,000.

von Blanckenburg, F., 2005. The control mechanisms of erosion and weathering at basin scale from cosmogenic nuclides in river sediment. Earth Planet. Sci. Lett. 237, 462–479. doi:10.1016/j.epsl.2005.06.030

Weiers, S., 1995. Zur Klimatologie des NW-Karakorum und angrenzender Gebiete. Bonner Geogr. Abhandlungen 156.

Whipple, K.X., 2004. Bedrock rivers and the geomorphology of active orogens. Annu. Rev. Earth Planet. Sci. 32, 151–185. doi:10.1146/annurev.earth.32.101802.120356

Whipple, K.X., 2009. The influence of climate on the tectonic evolution of mountain belts. Nat. Geosci. 2, 97–104. doi:10.1038/ngeo413

Whipple, K.X., DiBiase, R.A., Crosby, B.T., 2013. 9.28 Bedrock Rivers, in: Treatise on Geomorphology. Elsevier, pp. 550–573. doi:10.1016/B978-0-12-374739-6.00254-2

Whipple, K.X., Tucker, G.E., 2002. Implications of sediment-flux-dependent river incision models for landscape evolution. J. Geophys. Res. Solid Earth 107, ETG 3-1-ETG 3-20. doi:10.1029/2000JB000044

Whittaker, A.C., 2012. How do landscapes record tectonics and climate? Lithosphere 4, 160–164. doi:10.1130/RF.L003.1

Whittaker, A.C., Cowie, P.A., Attal, M., Tucker, G.E., Roberts, G.P., 2007. Bedrock channel adjustment to tectonic forcing: Implications for predicting river incision rates. Geology 35, 103. doi:10.1130/G23106A.1

Willenbring, J.K., von Blanckenburg, F., 2010. Meteoric cosmogenic Beryllium-10 adsorbed to river sediment and soil: Applications for Earth-

surface dynamics. Earth-Science Rev. 98, 105–122. doi:10.1016/j.earscirev.2009.10.008

Willett, S.D., 1999. Orogeny and orography: The effects of erosion on the structure of mountain belts. J. Geophys. Res. Solid Earth 104, 28957–28981. doi:10.1029/1999JB900248

Willett, S.D., McCoy, S.W., Perron, J.T., Goren, L., Chen, C.-Y., 2014. Dynamic Reorganization of River Basins. Science (80-.). 343, 1248765–1248765. doi:10.1126/science.1248765

Williams, M.W., Konovalov, V.G., 2008. Central Asia Temperature and Precipitation Data, 1879-2003, [January 1960 - December 1990]. NSIDC, Boulder, Colorado: USA National Snow and Ice Data Center. doi:http://dx.doi.org/10.7265/N5NK3BZ8

Wittmann, H., von Blanckenburg, F., Kruesmann, T., Norton, K.P., Kubik, P.W., 2007. Relation between rock uplift and denudation from cosmogenic nuclides in river sediment in the Central Alps of Switzerland. J. Geophys. Res. 112, F04010. doi:10.1029/2006JF000729

Wittmann, H., von Blanckenburg, F., Maurice, L., Guyot, J.L., Kubik, P.W., 2011. Recycling of Amazon floodplain sediment quantified by cosmogenic 26Al and 10Be. Geology 39, 467–470. doi:10.1130/G31829.1

Wobus, C., Whipple, K.X., Kirby, E., Snyder, N., Johnson, J., Spyropolou, K., Crosby, B., Sheehan, D., 2006. Tectonics from topography: procedurses, promise, and pitfalls. Geol. Soc. Am. Spec. Pap. 398, 55–74. doi:10.1130/2006.2398(04)

Xu, X., Hu, G., Qiao, B., 2013. Last glacial maximum climate based on cosmogenic 10Be exposure ages and glacier modeling for the head of Tashkurgan Valley, northwest Tibetan Plateau. Quat. Sci. Rev. 80, 91–101. doi:10.1016/j.quascirev.2013.09.004

Zech, R., Abramowski, U., Glaser, B., Sosin, P., Kubik, P.W., Zech, W., 2005a. Late Quaternary glacial and climate history of the Pamir Mountains derived from cosmogenic 10Be exposure ages. Quat. Res. 64, 212–220. doi:10.1016/j.yqres.2005.06.002

Zech, R., Glaser, B., Sosin, P., Kubik, P.W., Zech, W., 2005b. Evidence for long-lasting landform surface instability on hummocky moraines in the Pamir Mountains (Tajikistan) from 10Be surface exposure dating. Earth Planet. Sci. Lett. 237, 453–461. doi:10.1016/j.epsl.2005.06.031

Zech, R., 2012. A late Pleistocene glacial chronology from the Kitschi-Kurumdu Valley, Tien Shan (Kyrgyzstan), based on 10Be surface exposure dating. Quat. Res. 77, 281–288. doi:10.1016/j.yqres.2011.11.008

Zech, R., Röhringer, I., Sosin, P., Kabgov, H., Merchel, S., Akhmadaliev, S., Zech, W., 2013. Late Pleistocene glaciations in the Gissar Range, Tajikistan, based on 10Be surface exposure dating. Palaeogeogr. Palaeoclimatol. Palaeoecol. 369, 253–261. doi:10.1016/j.palaeo.2012.10.031

Zubovich, A.V., Wang, X., Scherba, Y.G., Schelochkov, G.G., Reilinger, R., Reigber, C., Mosienko, O.I., Molnar, P., Michajljow, W., Makarov, V.I., Li, J., Kuzikov, S.I., Herring, T.A., Hamburger, M.W., Hager, B.H., Dang, Y., Bragin, V.D., Beisenbaev, R.T., 2010. GPS velocity field for the Tien Shan and surrounding regions. Tectonics 29. doi:10.1029/2010TC002772

8 Appendices

The data presented in this thesis can also be found on the University of Tübingen server: smb://134.2.5.43/esd01/docs/egrin

All data generated and used during this project, which cannot be printed in the appendix (MatLab codes, ArcGIS files, etc.) are stored in separate folders for each application at:

smb://134.2.5.43/esd01/docs/egrin/data_small

Documentation of first-author submissions are located at:

smb://134.2.5.43/esd01/docs/egrin/papers

Data (text, tables, and figures in different file formats) concerning this thesis are located at: smb://134.2.5.43/esd01/docs/egrin/thesis

Appendix Table 1: Sample locations.

sample ID	N	E	Altitude	utm	utm	notes
river sand samples	**Lat. in ˚**	**Long. in ˚**	**in m**	**zone 42 S**		105 samples
12 mod7 001	38.74477	69.83218	1034	572314	4288778	
12 mod7 002	38.86478	70.00610	1137	587285	4302257	
12 mod7 003	38.86478	69.97709	1134	584786	4300710	
12 mod7 004	38.94810	70.12465	1210	597449	4311622	
12 mod7 005	39.01980	70.37091	1327	618681	4319875	
12 mod7 006	39.16610	71.08647	1660	680258	4337282	
12 mod7 007	39.19270	71.20881	1720	690761	4340482	
12 mod7 008	38.38266	69.34405	636	530048	4248326	
12 mod6 001	38.85989	70.10363	1218	595754	4301810	
12 mod6 002	39.24385	71.22711	1785	692195	4346205	
12 mod6 003	39.30426	71.43349	1876	709835	4353356	
12 mod6 004	39.17273	71.55499	1940	720714	4339164	
12 mod6 005	39.26691	71.37693	1842	705058	4349088	
12 mod5 001	39.03497	70.18875	1270	602893	4321334	
12mod5 002	39.20391	70.85537	1594	660203	4341044	
12 mod5 003	39.29609	71.23148	1876	692429	4352003	
12 mod5 004	39.29603	71.22601	1871	691966	4351998	
terrace depth profile						
12 S7 001	38.84832	69.97050	1153	584218	4300392	T1
12 S7 003	38.84336	69.96070	1068	583370	4299830	T3
12 S7 002	38.84755	69.97125	1088	584283	4300308	T5
12 S7 004	38.84645	69.96555	1275	583790	4300177	AF
terrace klasts						
12 S7 001 K	38.84832	69.97050	1159	584218	4300392	not enough material
12 S7 003 K	38.84336	69.96070	1288	583370	4299830	not enough material
moraine boulder samples						
12 ER 001	39.28185	71.42316	2068	709009	4350852	
12 ER 002	39.28128	71.42244	2072	708949	4350791	
12 ER 003	39.28107	71.42232	2078	708932	4350765	
12 ER 004	39.28098	71.42111	2068	708831	4350752	
12 ER 005	39.28098	71.42111	2068	708831	4350752	not enough material
12 ER 006	39.28064	71.41969	2075	708709	4350710	
12 ER 007	39.28092	71.41677	2048	708456	4350735	not enough material
12 ER 008	39.28021	71.41484	2059	708291	4350652	
12 ER 009	39.28021	71.41484	2059	708291	4350652	
12 ER 010	39.28001	71.41446	2062	708256	4350625	
12 ER 011	39.28207	71.42548	2078	709208	4350883	
12 ER 012	39.28186	71.42601	2078	709243	4350859	not enough material
12 ER 013	39.28186	71.42601	2078	709243	4350859	

12 ER 014	39.28164	71.42662	2082	709306	4350844	
12 ER 015	39.28188	71.42793	2090	709413	4350869	
12 ER 016	39.28175	71.42785	2090	709407	430855	
12 ER 017	39.28307	71.42754	2069	709579	4351000	
12 ER 018	39.28304	71.42744	2069	709370	4351001	
12 ER 019	39.28304	71.42702	2077	709334	4350995	
12 ER 020	39.28411	71.42448	2060	709110	4351110	
12 LMA 001	39.23167	71.45860	2265	712214	4345370	not enough material
12 LMA 002	39.23157	71.45891	2258	712238	4345357	
12 LMA 003	39.23128	71.45942	2258	712288	4345327	
12 LMA 004	39.23128	71.45942	2258	712288	4345327	
12 LMA 005	39.23098	71.46027	2264	712357	4345295	
12 LMA 006	39.23074	71.46067	2271	712395	4345267	not enough material
12 LMA 007	39.23051	71.46122	2270	712441	4345247	not enough material
12 LMA 008	39.23011	71.46222	2276	712529	4345206	
12 LMA 009	39.22859	71.46568	2315	712832	4345041	
12 LMA 010	39.22761	71.46804	2337	713039	4344938	
12 LMB 001	39.23146	71.46003	2262	712334	4345347	
12 LMB 002	39.22726	71.47054	2313	713249	4344907	
12 LMB 003	39.22668	71.47169	2316	713356	4344849	not enough material
12 LMB 004	39.22653	71.47211	2315	713392	4344826	
12 LMB 005	39.23091	71.46139	2266	712455	4345290	
12 LMB 006	39.22257	71.47916	2316	714013	4344405	
12 LMB 007	39.22294	71.47839	2316	713946	4344445	
12 LMB 008	39.22361	71.47729	2318	713845	4344519	
12 LMC 001	39.22558	71.47550	2303	713683	4344735	
12 LMC 002	39.22879	71.46790	2311	713018	4345070	
12 LMC 003	39.23003	71.46506	2293	712775	4345198	
12 LMC 004	39.23003	71.46506	2293	712775	4345198	
12 LMC 005	39.23090	71.46325	2285	712611	4345291	
12 LMC 006	39.23096	71.46301	2279	712594	4345302	
12 LMC 007	39.23096	71.46301	2279	712594	4345302	
12 LMC 008	39.23105	71.46276	2278	712574	4345305	
12 LMC 009	39.23118	71.46252	2278	712553	4345320	
12 LMC 010	39.23162	71.46124	2271	712441	4345364	
12 LMD 001	39.23211	71.46103	2251	712418	4345421	
12 LMD 002	39.23184	71.46165	2255	712477	4345391	
12 LMD 003	39.23448	71.45472	2241	711868	4345672	
12 LME 001	39.22285	71.48200	2262	714255	434442	not enough material
12 LME 002	39.22435	71.47972	2283	714056	434604	not enough material
12 LME 003	39.22499	71.47882	2281	713977	4344670	

12 LME 004	39.22603	71.47704	2284	713821	4344785	not enough material
12 LME 005	39.22637	71.47633	2288	713754	4344818	
12 LME 006	39.22657	71.47598	2293	713729	4344840	not enough material
12 LME 007	39.22820	71.47279	2305	713450	4345014	
12 LME 008	39.23026	71.46711	2306	712951	4345230	not enough material
12 LME 009	39.23026	71.46711	2306	712951	4345230	not enough material
12 LME 010	39.23125	71.46468	2285	712735	4345335	
12 LME 011	39.23259	71.46098	2255	712414	4345481	not enough material
12 LME 012	39.23259	71.46098	2255	712414	4345481	
12 LME 013	39.23293	71.46049	2252	7123772	4345511	not enough material
moraine depth profiles						
12 LMDP	39.23162	71.45874	2256	712219	4345362	not enough quartz
12 LMK 001	39.23162	71.45874	2256	712219	4345362	not enough quartz
river sand samples						
13 mod7 001	38.74475	69.83133	1039	-	-	resampled
13 mod7 002	38.85148	69.97854	1150	-	-	locations
13 mod7 003	39.02029	70.37051	1320	-	-	from last year
13 mod4 001	39.02029	70.37051	1320	-	-	
13 mod4 002	39.42830	71.22105	2164	-	-	
13 mod4 003	39.42527	71.22238	2168	-	-	
13 mod4 004	39.30993	71.22173	1893	-	-	
13 mod4 005	39.22115	70.85117	1623	-	-	
13 mod4 006	39.31816	70.63783		-	-	
13 mod4 007	39.31721	70.63815	1992	-	-	
13 mod4 008	39.31421	70.65121	1982	-	-	
13 mod4 009	39.17378	70.82201	1613	-	-	
13 mod4 010	39.13214	70.19888	1346	-	-	
13 mod4 011	39.13641	70.19878	1341	-	-	
13 mod4 012	39.01307	70.14259	1271	-	-	
13 mod4 013	39.01190	70.13979	1267	-	-	

Appendix Table 2: Moraine boulder characteristics and shielding correction in ˚.

Sample ID	boulder height(cm)	lithology	0°N	60°	120°	180°	240°	300°
ER001	180	Granodiorite	15	4	7	4	3	4
ER002	70	Granodiorite	16	5	4	8	4	13
ER003	110	Granodiorite	15	6	5	9	5	12
ER004	140	Granodiorite	15	7	5	9	4	15
ER006	50	Granodiorite	15	5	5	9	3	5
ER008	220	Granodiorite	12	5	5	8	6	6
ER009	140	Granodiorite	12	5	5	8	6	6
ER010	500	Granodiorite	12	5	5	8	6	6
ER11	90	Granodiorite	16	5	7	6	4	14
ER013	100	Granodiorite	17	5	5	7	5	5
ER014	150	Granodiorite	15	4	5	8	3	13
ER015	400	Granodiorite	14	5	4	7	4	15
ER016	100	Quartz vein	11	2	5	8	2	13
ER017	100	Granodiorite	14	2	8	7	3	16
ER019	100	Granodiorite	13	5	6	9	5	15
ER020	100	Red Sandstone Conglomerat	14	6	5	8	4	14
LMA002	110	Granodiorite	10	6	7	19	11	10
LMA003	110	Granodiorite	8	4	5	20	12	7
LMA004	80	Granodiorite	8	4	5	20	12	7
LMA005	80	Granodiorite	8	4	6	20	11	7
LMA008	70	Granodiorite	8	4	6	20	13	7
LMA009	150	Granodiorite	8	5	5	20	15	8
LMA010	60	Granodiorite	8	5	4	20	15	6
LMB001	90	Granodiorite	7	5	6	19	14	6
LMB002	60	Red Sandstone Conglomerat	6	4	6	24	15	5
LMB004	90	Granodiorite	8	3	5	23	18	5
LMB005	50	Granodiorite	6	4	6	19	11	5
LMB006	110	Granodiorite	7	4	6	24	20	4
LMB007	80	Granodiorite	6	5	5	21	23	5
LMB008	120	Red Sandstone Conglomerat	7	4	7	25	12	4
LMC001	100	Granodiorite	7	5	4	21	13	5
LMC002	80	Quartz vein	7	3	5	19	15	6
LMC003	120	Quartz vein	3	5	5	19	13	5
LMC004	120	Granodiorite	3	5	5	19	13	5
LMC005	70	Granodiorite	7	5	5	18	13	6
LMC006	110	Granodiorite	8	4	5	18	14	5
LMC008	90	Red Sandstone Conglomerat	7	5	7	18	14	5
LMC009	50	Granodiorite	7	4	5	19	14	5
LMC010	110	Red Sandstone Conglomerat	6	4	4	19	12	5
LMD001	130	Granodiorite	8	4	6	18	13	6
LMD002	90	Granodiorite	6	3	5	19	14	6
LMD003	50	Granodiorite	8	4	5	17	14	7
LME003	130	Quartz veign	5	5	5	20	16	6
LME005	110	Red Sandstone Conglomerat	5	5	5	18	11	6
LME007	110	Quartz vein	7	4	5	20	15	6
LME010	80	Granodiorite	8	4	5	17	14	6
LME012	80	Granodiorite	7	5	5	22	13	6

Appendix Table 3: Purified quartz and Beryllium-9 carrier weights.

Date	Sample ID	Sample Lab ID	beaker (g)	qtz (g)	weight(tot)	difference (g)	weight(leached)	leach loss (g)	leached qtz (g)	Be carrier fluid(g)	0.8 ml in g	blank(Al)
10.05.13	ER 001	EG 1	94.28	20	117.840	3.56	115.082	2.758	17.242	16.8093	0.8797	
	ER 002	EG 2	91.92	20	116.260	4.34	114.611	1.649	18.351	15.9323	0.8745	
	12 S7 003 a	EG 3	92.92	25	120.140	2.22	117.890	2.25	22.75	15.0578	0.8745	
	blank	EG 4	93.66	0	93.670	0.01	93.666	0.004	-0.004	20.3883	0.8773	
	12 S7 001 c	EG 5	311.87	30	345.380	3.51	339.820	5.56	24.44	19.5136	0.8746	
	12 S7 001 d	EG 6	303.39	30	335.230	1.84	329.835	5.395	24.605	18.639	0.8744	
	blank	EG 7	299.63	0	299.620	-0.01	299.608	0.012	-0.012	17.7646	0.8739	
	12 mod6 004	EG 8	310.22	60	373.940	3.72	367.368	6.572	53.428	16.8907	0.8745	
	12 mod6 005	EG 9	307.27	60	371.500	4.23	366.143	5.357	54.643	16.0162	0.8726	
	blank	EG 10	93.94	0	93.940	0	93.950	-0.01	0.01	15.1436	0.8726	
12.08.13	ER 002	EG 11	92.44	20	112.500	0.06	111.118	1.382	18.618	20.0909	0.8802	
	12 mod6 005	EG 12	307.02	60	366.680	-0.34	361.366	5.314	54.686	19.2119	0.8769	
	blank	EG 13	93.22	0	93.220	0	93.257	-0.037	0.037	18.335	0.8735	
	12 mod7 001	EG 14	312.36	40	352.180	-0.18	347.444	4.736	35.264	17.4615	0.8742	
	12 mod7 005	EG 15	314.23	40	354.370	0.14	349.333	5.037	34.963	16.5873	0.8742	
	12 mod7 007	EG 16	305.23	40	345.290	0.06	341.595	3.695	36.305	19.9017	0.8766	
	blank	EG 17	94.13	0	94.130	0	94.174	-0.044	0.044	19.0256	0.873	
	12 S7 001 d	EG 18	93.99	30	124.070	0.08	122.072	1.998	28.002	18.1526	0.874	
	12 S7 002 b	EG 19	93.43	25	118.440	0.01	116.692	1.748	23.252	17.2786	0.8731	
	blank	EG 20	94.11	0	94.110	0	94.169	-0.059	0.059	16.4055	-1.928	
10.10.13	12 S7 002 b	EG 21	185.74	40	225.670	-0.07	221.580	4.09	35.91	18.3335	0.8781	
	12 S7 002 c	EG 22	93.51	30	123.490	-0.02	120.040	3.45	26.55	17.4554	0.8763	
	12 S7 002 d	EG 23	292.37	45	338.260	0.89	329.740	8.52	36.48	16.5791	0.8763	
	blank	EG 24	92.44	0	92.440	0	92.440	0	0	19.7014	0.8768	
	12 S7 004 a	EG 25	93.32	30	123.290	-0.03	120.220	3.07	26.93	18.8246	0.8743	
	12 S7 004 b	EG 26	92.52	30	122.460	-0.06	119.290	3.17	26.83	17.9503	0.8737	
	12 S7 004 c	EG 27	95.28	30	125.360	0.08	122.260	3.1	26.9	17.0766	0.8737	
	12 S7 004 d	EG 28	290.54	40	330.510	-0.03	332.340	-1.83	41.83	21.1243	0.8761	
	12 S7 004 e	EG 29	310.88	56	367.480	0.6	359.660	7.82	48.18	20.2482	0.8736	
	blank	EG 30	93.01	0	93.010	0	93.010	0	0	19.3746	0.8721	
15.11.13	12 mod 002	EG 31	92.73	51.440	144.170	0	140.550	3.62	47.82	16.1372	0.8948	
	12 mod7 003	EG 32	91.39	50.330	141.720	0	134.700	7.02	43.31	15.2459	0.8913	
	12 mod 6 001	EG 33	92.28	50.770	143.050	0	139.570	3.48	47.29	14.3576	0.8883	
	12 mod 6 002	EG 34	92.06	50.830	142.890	0	139.310	3.58	47.25	13.4709	0.8867	
	12 mod 6 003	EG 35	91.77	39.060	130.830	0	127.600	3.23	35.83	12.5821	0.8888	
	blank	EG 36	92.96	0.000	92.960	0	92.950	0.01	-0.01	11.6934	0.8887	
	12 mod 6 004	EG 37	93.57	36.270	129.840	0	127.140	2.7	33.57	15.97	0.8886	
	12 mod 5 003	EG 38	92.2	52.910	145.110	0	138.550	6.56	46.35	15.0836	0.8864	
	12 mod 5 004	EG 39	91.95	51.480	143.430	0	139.660	3.77	47.71	14.1963	0.8873	
	blank	EG 40	94.44	0.000	94.440	0	94.440	0	0			

04.12.13	12 S7 001 a	EG 41	94.784	22.3	117.611	-0.527	113.612	3.999	18.301	20.8094	0.8832	
	12 S7 001 c	EG 42	93.564	29.6	123.211	-0.047	118.292	4.919	24.681	19.934	0.8754	
	12 S7 001 e	EG 43	242.151	51.1	293.266	-0.015	283.046	10.22	40.88	19.0567	0.8773	
	12 S7 002 a	EG 44	94.463	21	115.418	0.045	111.454	3.964	17.036	18.1814	0.8753	
	blank	EG 45	93.834	0	93.835	-0.001	93.816	0.019	-0.019	17.3059	0.8755	
	12 S7 003 a	EG 46	93.581	20.8	114.367	0.014	110.292	4.075	16.725	16.4302	0.8757	
	12 S7 003 c	EG 47	94.354	30.4	124.788	-0.034	119.551	5.237	25.163	15.5555	0.8747	
	12 mod7 006	EG 48	93.915	31.9	125.819	-0.004	120.755	5.064	26.836	20.7835	0.8762	
	12 mod 5 001	EG 49	246.555	53.6	300.109	0.046	287.255	12.854	40.746	19.9109	0.8726	
	db blank	EG 50	93.55	0	93.551	-0.001	93.539	0.012	-0.012	19.0365	0.8744	5.0798
	12 S7 001 b	EG 51	93.7059	31.1	124.809	-0.0031	122.244	2.565	28.535	13.6745	0.8899	
	12 S7 002 e	EG 52	241.05	61.66	302.702	0.008	295.166	7.536	54.124	12.7928	0.8817	
	12 S7 003 e	EG 53	239.911	64.03	303.931	0.01	297.827	6.104	57.926	16.036	0.8867	
	12 S7 003 b	EG 54	92.197	31.6	123.796	0.001	120.478	3.318	28.282	15.1556	0.8804	
	blank	EG 55	90.868	0	90.868	0	90.857	0.011	-0.011	14.2771	0.8785	
	12 LMA 008	EG 56	93.785	0	93.785	0	93.780	0.005	-0.005	13.3977	0.8794	
	12 LME 010	EG 57	93.53	29.49	123.022	-0.002	121.166	1.856	27.634	12.5202	0.8775	
	12 ER 016	EG 58	93.639	30	123.891	-0.252	122.035	1.856	28.144	16.2667	0.8853	
	12 ER 018	EG 59	93.929	26.406	120.325	0.01	116.958	3.367	23.039	15.3887	0.878	
	db blank	EG 60	92.481	28.49	121.104	-0.133	118.208	2.896	25.594	14.5102	0.8785	
	12 ER 001	EG 61	93.659	21.602	115.252	0.009	113.664	1.588	20.014	16.8272	0.893	
	12 ER 003	EG 62	92.04	20.521	112.545	0.016	111.027	1.518	19.003	15.9377	0.8895	
	12 ER 004	EG 63	94.433	20.538	114.952	0.019	113.503	1.449	19.089	15.0505	0.8872	
	12 ER 006	EG 64	94.858	21.752	116.587	0.023	113.686	2.901	18.851	14.1618	0.8887	
	12 ER 007	EG 65	94.432	20.154	114.586	0	111.941	2.645	17.509	13.2724	0.8894	
	blank	EG 66	92.281	0	92.282	-0.001	92.295	-0.013	0.013	12.3855	0.8869	
	12 ER 010	EG 67	94.669	21.474	116.131	0.012	114.703	1.428	20.046	11.4997	0.8858	
	12 ER 015	EG 68	93.559	20.351	113.865	0.045	111.056	2.809	17.542	10.6138	0.8859	
	12 ER 018	EG 69	92.481	28.49	121.104	-0.133	118.208	2.896	25.594	15.3887	0.878	
	dbblank	EG 70	92.5	0	92.500	0	92.509	-0.009	0.009	15.3048	0.0839	5.1026
	13 mod7 001	EG 71	240.993	50.306	291.297	0.002	279.997	11.3	39.006	13.3137	0.8935	
	12 S7 003 d	EG 72	239.85	46.036	285.884	0.002	275.755	10.129	35.907	12.427	0.8867	
	12 ER 11	EG 73	92.453	27.398	119.860	-0.009	116.658	3.202	24.196	11.5375	0.8895	
	12 ER 013	EG 74	92.025	27.655	119.666	0.014	115.645	4.021	23.634	15.4594	0.8891	
	12 ER 014	EG 75	93.491	28.1	121.574	0.017	117.812	3.762	24.338	14.573	0.8864	
	blank	EG 76	93.407	0	93.407	0	93.403	0.004	-0.004	13.6868	0.8862	
	12 LMA 003	EG 77	93.884	27.681	121.570	-0.005	117.618	3.952	23.729	12.8003	0.8865	
	12 LMA 004	EG 78	94.415	27.688	122.085	0.018	118.552	3.533	24.155	11.9148	0.8855	
	12 LME 003	EG 79	93.777	16.422	110.199	0	106.639	3.56	12.862	11.0292	0.8856	
	db blank	EG 80	94.299	0	94.299	0	94.293	0.006	-0.006	10.1463	0.8829	5.0405

12 ER 002	EG 81	92.431	25.403	117.836	-0.002	116.364	1.472	23.931	15.2866	0.8915	
12 ER 008	EG 82	93.591	25.19	118.768	0.013	117.356	1.412	23.778	14.3962	0.8904	
12 ER 009	EG 83	93.664	25.367	119.027	0.004	117.417	1.61	23.757	13.4991	0.8971	
12 ER 017	EG 84	93.152	21.502	113.641	1.013	112.367	1.274	20.228	12.6122	0.8869	
12 ER 020	EG 85	93.493	17.945	111.438	0	109.698	1.74	16.205	11.7211	0.8911	
blank	EG 86	93.746	0	93.751	-0.005	93.738	0.013	-0.013	10.8319	0.8892	
12 LMA 005	EG 87	92.269	26.274	118.542	0.001	117.130	1.412	24.862	15.587	0.8925	
12 LMB 005	EG 88	91.669	25.01	116.672	0.007	115.265	1.407	23.603	14.6998	0.8872	
12 LMD 001	EG 89	93.774	27.261	121.027	0.008	119.431	1.596	25.665	13.821	0.8788	
db blank	EG 90	93.87	0	93.870	0	93.866	0.004	-0.004			5.1403
LMA 009	EG 91	91.662	29.09	120.769	-0.017	119.187	1.582	27.508	14.7826	0.8845	
LME 007	EG 92	93.79	28.035	121.803	0.022	119.519	2.284	25.751	13.9016	0.881	
LMB 006	EG 93	96.101	30.788	126.894	-0.005	125.028	1.866	28.922	13.0221	0.8795	
LMB 007	EG 94	93.875	30.738	124.609	0.004	122.659	1.95	28.788	12.1419	0.8802	
LMC 006	EG 95	91.481	30.131	121.612	0	119.350	2.262	27.869	11.2622	0.8797	
blank	EG 96	92.621	0	92.621	0	92.619	0.002	-0.002	15.7445	0.883	
LMD 002	EG 97	92.355	30.184	122.533	0.006	120.702	1.831	28.353	14.8647	0.8798	
LMD 003	EG 98	92.271	27.859	120.136	-0.006	118.430	1.706	26.153	13.9855	0.8792	
LME 005	EG 99	93.745	29.735	123.459	0.021	121.684	1.775	27.96	13.106	0.8795	
db blank	EG 100	93.869	0	93.869	0	93.878	-0.009	0.009	12.227	0.879	5.1456
12 ER 019	EG 101	93.624	27.793	121.419	-0.002	117.141	4.278	23.515	17.9786	0.8906	
12 LMA 010	EG 102	93.702	32.717	126.402	0.017	121.347	5.055	27.662	17.0924	0.8862	
12 LMB 001	EG 103	92.003	23.541	115.539	0.005	111.959	3.58	19.961	16.2083	0.8841	
12 LMB 004	EG 104	94.651	28.084	112.721	10.014	118.391	-5.67	33.754	15.3252	0.8831	
12 LMB 008	EG 105	94.817	28.43	123.237	0.01	118.205	5.032	23.398	14.4408	0.8844	
blank	EG 106	91.729	0	91.729	0	91.682	0.047	-0.047	13.5616	0.8792	
12 LMC 007	EG 107	94.416	27.663	112.050	10.029	117.532	-5.482	33.145	12.6755	0.8861	
12 LME 012	EG 108	92.196	30.802	122.975	0.023	118.299	4.676	26.126	11.7917	0.8838	
12 ER 018	EG 109	93.529	28.68	122.141	0.068	188.183	-66.042	94.722	10.9085	0.8832	
db blank	EG 110	93.53	0	93.530	0	93.530	0	0	10.0242	0.8843	5.1807
12 S7 001 b	EG 111	93.699	31	124.765	-0.066	124.765	0	31	17.8547	0.8928	
12 S7 003 e	EG 112	92.182	39.491	131.668	0.005	131.668	0	39.491	16.9716	0.8831	
12 S7 003 b	EG 113	93.846	29.573	123.427	-0.008	123.247	0.18	29.393	16.0895	0.8821	
12 ER 006	EG 114	94.132	27.338	121.475	-0.005	121.475	0	27.338	15.2095	0.88	
blank	EG 115	93.524	0	93.524	0	93.524	0	0	14.3277	0.8818	
12 ER 007	EG 116	91.682	29.158	120.846	-0.006	120.846	0	29.158	13.4451	0.8826	
12 ER 016	EG 117	92.091	27.66	119.738	0.013	119.738	0	27.66	12.5649	0.8802	
12 LMA 008	EG 118	92.317	28.236	120.555	-0.002	120.555	0	28.236	11.6835	0.8814	
12 LME 010	EG 119	94.464	29.675	124.126	0.013	124.126	0	29.675	10.8019	0.8816	
db blank	EG 120	92.488	0	92.488	0	92.488	0	0	9.9221	0.8798	5.1533

	12 S7 1a	EG 121	94.391	36.458	130.876	-0.027	128.035	2.841	33.617	16.5548	0.893	
	12 S7 2a	EG 122	93.982	41.301	135.138	0.145	132.428	2.71	38.591	15.6716	0.8832	
	12 S7 2e	EG 123	91.986	60.613	152.619	-0.02	149.017	3.602	57.011	14.7885	0.8831	
	12 S7 3a	EG 124	93.527	39.513	133.063	-0.023	130.430	2.633	36.88	13.9071	0.8814	
	blank	EG 125	92.434	0	0.000	92.434	92.430	-92.43	92.43	13.026	0.8811	
	12 LMC 001	EG 126	93.703	31.945	125.656	-0.008	123.763	1.893	30.052	12.1454	0.8806	
	12 LMC 002	EG 127	92.778	33.336	126.132	-0.018	123.477	2.655	30.681	11.2631	0.8823	
	!2 LMB 002	EG 128	92.176	29	121.773	-0.597	119.443	2.33	26.67	10.4094	0.8537	
	12 mod 7 006	EG 129	93.518	29.329	122.857	-0.01	120.513	2.344	26.985	13.6644	0.8851	
	db blank	EG 130	91.685	0	91.685	0	91.679	0.006	-0.006	12.7838	0.8806	5.1073
	12S7 1b	EG 131	307.704	30.808	338.598	-0.086	333.996	4.602	26.206	16.8835	0.8948	
	12 LMA 002	EG 132	312.016	35.35	347.408	-0.042	343.874	3.534	31.816	16.0036	0.8799	
	12 LMC 003	EG 133	239.939	35.297	275.240	-0.004	271.993	3.247	32.05	15.1255	0.8781	
	12 LMC 004	EG 134	242.491	33.121	275.597	0.015	271.130	4.467	28.654	14.2458	0.8797	
	blank	EG 135	241.06	0	241.060	0	241.049	0.011	-0.011	13.3651	0.8807	
	12 LMC 005	EG 136	299.91	34.418	334.403	-0.075	330.372	4.031	30.387	12.4866	0.8785	
	12 LMC 008	EG 137	247.591	32.858	280.446	0.003	276.982	3.464	29.394	17.0075	0.7708	
	12 LMC 009	EG 138	291.012	35.844	326.835	0.021	323.026	3.809	32.035	16.1321	0.8754	
	12 LMC 010	EG 139	291.442	31.007	322.491	-0.042	315.545	6.946	24.061	15.2545	0.8776	
	db blank	EG 140	247.062	0	247.062	0	247.051	0.011	-0.011			5.0996
dagmar	13 mod 7 003	EG 141		38.0644							891.5	
	13 mod 7 007	EG 142		40.1465							881.1	
	13 mod 4001	EG 143		39.6698							880	
	13 mod 4002	EG 144		39.9474							874.6	
	blank	EG 145		0							879.9	
	13 mod 4003	EG 146		39.0402							881.3	
	13 mod 4004	EG 147		40.0699							883.2	
	13 mod 4011	EG 148		37.42							879.1	
	13 mod 4012	EG 149		38.6635							882.1	
	dbblank	EG 150		0							881.5	5.1387

Appendix Table 4: $^{10}Be/^{9}Be$ AMS measurements raw data.

AMS ID	Lab ID	$^{10}Be/^{9}Be$	$^{10}Be/^{9}Be$ 1s	$^{10}Be/^{9}Be$ 1s (%)	avg. ^{9}Be current (A)	Sample ID
EG 01-EG10: wasserschaden						
s02499	EG11	2.85E-13	9.93E-15	3.49	1.32E-06	ER 002
s02500	EG12	5.96E-14	4.29E-15	7.19	3.02E-07	12 mod6 005
s02501	EG13	1.73E-15	4.12E-16	23.76	1.26E-06	blank
s02502	EG14	4.24E-14	2.35E-15	5.55	1.09E-06	12 mod7 001
s02503	EG15	3.91E-14	2.23E-15	5.69	1.44E-06	12 mod7 005
s02504	EG16	3.78E-14	2.53E-15	6.7	8.82E-07	12 mod7 007
s02505	EG17	2.02E-15	4.18E-16	20.63	1.40E-06	blank
s02506	EG18	2.48E-14	1.59E-15	6.4	1.14E-06	12 S7 001 d
s02508	EG20	2.10E-15	4.52E-16	21.53	1.29E-06	blank
s02957	EG21	4.44E-14	2.72E-15	6.11	1.31E-06	12 S7 002 b
s02958	EG22	3.21E-14	2.22E-15	6.93	1.31E-06	12 S7 002 c
s02959	EG23	3.51E-14	2.50E-15	7.13	1.12E-06	12 S7 002 d
s02960	EG24	3.23E-15	6.19E-16	19.14	1.41E-06	blank
s02961	EG25	4.07E-14	2.45E-15	6.03	1.49E-06	12 S7 004 a
s02962	EG26	3.15E-14	2.13E-15	6.77	1.42E-06	12 S7 004 b
s02963	EG27	2.69E-14	2.26E-15	8.38	9.93E-07	12 S7 004 c
s02964	EG28	3.65E-14	2.36E-15	6.46	1.38E-06	12 S7 004 d
s02965	EG29	4.46E-14	2.61E-15	5.85	1.47E-06	12 S7 004 e
s02966	EG30	1.90E-15	5.11E-16	26.9	1.20E-06	blank
s03441	EG31	5.03E-14	2.48E-15	4.93	1.73E-06	12 mod 002
s03442	EG32	3.46E-14	2.29E-15	6.61	1.10E-06	12 mod7 003
s03443	EG33	3.72E-14	1.84E-15	4.96	2.29E-06	12 mod 6 001
s03444	EG34	4.20E-14	2.10E-15	5	1.98E-06	12 mod 6 002
s03445	EG35	5.09E-14	2.34E-15	4.6	2.15E-06	12 mod 6 003
s03446	EG36	1.05E-15	2.43E-16	23.14	2.39E-06	blank
s03447	EG37	3.98E-14	1.97E-15	4.96	2.14E-06	12 mod 6 004
s03448	EG38	1.50E-13	5.44E-15	3.64	2.14E-06	12 mod 5 003
s03449	EG39	3.49E-14	2.12E-15	6.08	1.36E-06	12 mod 5 004
s03450	EG40	6.31E-16	2.01E-16	31.77	2.10E-06	blank
s03451	EG41	1.94E-14	1.58E-15	8.14	1.19E-06	12 S7 001 a
s03452	EG42	2.71E-14	1.52E-15	5.63	2.16E-06	12 S7 001 c
s03453	EG43	3.54E-14	1.78E-15	5.03	2.31E-06	12 S7 001 e
s03454	EG44	1.96E-14	1.45E-15	7.39	1.48E-06	12 S7 002 a
s03455	EG45	3.24E-15	6.83E-16	21.07	9.39E-07	blank
s03456	EG46	1.48E-14	1.93E-15	13.05	5.55E-07	12 S7 003 a
s03457	EG47	3.30E-14	1.91E-14	57.81	1.27E-08	12 S7 003 c
s03458	EG48	2.26E-14	1.58E-15	6.99	1.56E-06	12 mod7 006
s03459	EG49	7.46E-14	3.38E-15	4.53	1.63E-06	12 mod 5 001
s03460	EG50	1.88E-15	5.68E-16	30.3	8.19E-07	db blank
EG 51-EG60: lost by Post						
EG 61-EG8	EG90: kein Be carrier, reiner AL bla		EG 64,65,69: Be precipittion failed			
s04155	EG61	4.70E-13	1.59E-14	3.38	1.70E-06	12 ER 001
s04156	EG62	2.00E-13	7.85E-15	3.92	1.46E-06	12 ER 003
s04157	EG63	6.42E-13	2.12E-14	3.3	1.63E-06	12 ER 004
s04158	EG66	6.96E-16	2.64E-16	37.92	1.82E-06	blank
s04159	EG67	3.17E-13	1.12E-14	3.52	1.76E-06	12 ER 010
s04160	EG68	2.81E-13	1.01E-14	3.61	1.67E-06	12 ER 015
s04161	EG70	2.36E-15	4.98E-16	21.07	1.76E-06	dbblank
s04136	EG71	4.71E-14	2.42E-15	5.13	2.09E-06	13 mod7 001
s04137	EG72	1.27E-14	9.71E-16	7.66	2.70E-06	12 S7 003 d
s04138	EG73	3.07E-13	1.03E-14	3.35	2.76E-06	12 ER 11

s04139	EG74	3.67E-13	1.22E-14	3.34	2.34E-06	12 ER 013
s04140	EG75	4.41E-13	1.43E-14	3.25	2.80E-06	12 ER 014
s04141	EG76	5.33E-16	1.78E-16	33.47	2.86E-06	blank
s04142	EG77	3.50E-13	1.70E-14	4.84	3.73E-07	12 LMA 003
s04143	EG78	2.22E-13	7.64E-15	3.44	3.08E-06	12 LMA 004
s04144	EG79	1.07E-13	4.36E-15	4.08	2.71E-06	12 LME 003
s04145	EG80	2.10E-15	3.88E-16	18.51	2.59E-06	db blank
s04146	EG81	3.68E-13	1.23E-14	3.35	2.43E-06	12 ER 002
s04147	EG82	3.64E-13	1.25E-14	3.43	1.98E-06	12 ER 008
s04148	EG83	3.62E-13	1.23E-14	3.4	2.20E-06	12 ER 009
s04149	EG84	5.40E-13	1.76E-14	3.25	2.38E-06	12 ER 017
s04150	EG85	1.81E-13	6.79E-15	3.76	2.29E-06	12 ER 020
s04151	EG86	9.79E-16	2.84E-16	29.03	2.22E-06	blank
s04152	EG87	3.80E-13	1.28E-14	3.36	2.24E-06	12 LMA 005
s04153	EG88	3.30E-13	1.14E-14	3.47	1.92E-06	12 LMB 005
s04154	EG89	3.82E-13	1.29E-14	3.36	2.22E-06	12 LMD 001
s05129	EG91	4.53E-13	1.61E-14	3.57	3.19E-06	LMA 009
s05130	EG92	2.62E-13	1.03E-14	3.94	2.49E-06	LME 007
s05131	EG93_EG99	4.27E-13	1.55E-14	3.62	2.91E-06	LMB 006
s05132	EG94	4.30E-13	1.57E-14	3.66	2.62E-06	LMB 007
s05133	EG95	2.79E-13	1.14E-14	4.08	1.98E-06	LMC 006
s05134	EG96	1.33E-15	3.87E-16	29.05	3.06E-06	blank
s05135	EG97	0.00E+00	0.00E+00	100	2.52E-06	LMD 002
s05136	EG98	3.78E-13	1.39E-14	3.68	2.91E-06	LMD 003
s05137	EG99_EG93	2.99E-13	1.14E-14	3.82	2.67E-06	LME 005
s05138	EG100	3.54E-15	7.03E-16	19.87	2.49E-06	db blank
s05119	EG101	3.02E-13	1.31E-14	4.32	1.20E-06	12 ER 019
s05120	EG102	2.33E-13	1.15E-14	4.92	9.48E-07	12 LMA 010
s05121	EG103	5.04E-13	2.03E-14	4.03	1.02E-06	12 LMB 001
s05122	EG104	3.88E-13	1.76E-14	4.53	8.61E-07	12 LMB 004
s05123	EG105	4.94E-13	2.00E-14	4.04	1.16E-06	12 LMB 008
s05124	EG106	1.37E-15	5.62E-16	40.95	1.49E-06	blank
s05125	EG107	5.35E-13	2.03E-14	3.8	1.59E-06	12 LMC 007
s05126	EG108	4.13E-13	1.67E-14	4.04	1.39E-06	12 LME 012
s05127	EG109	4.48E-13	1.71E-14	3.81	1.82E-06	12 ER 018
s05128	EG110	4.27E-15	9.22E-16	21.56	1.75E-06	db blank
s04693	EG111	4.95E-13	1.58E-14	3.19	3.58E-06	12 S7 001 b
s04694	EG112	2.17E-15	3.89E-16	17.94	3.17E-06	12 S7 003 e
s04695	EG113	1.96E-14	1.21E-15	6.18	3.12E-06	12 S7 003 b
s04696	EG114	2.87E-13	9.48E-15	3.3	3.62E-06	12 ER 006
s04697	EG115	1.17E-15	2.41E-16	20.64	3.64E-06	blank
s04698	EG116	5.25E-14	2.39E-15	4.55	3.53E-06	12 ER 007
s04699	EG117	2.88E-13	9.46E-15	3.29	3.73E-06	12 ER 016
s04700	EG118	2.96E-13	9.77E-15	3.30	3.51E-06	12 LMA 008
s04701	EG119	3.86E-13	1.24E-14	3.22	3.83E-06	12 LME 010
s04702	EG120	2.68E-15	3.77E-16	14.07	3.46E-06	db blank
s05145	EG121	3.75E-14	5.01E-15	13.35	3.99E-07	12 S7 1a
s05146	EG122	3.88E-14	6.78E-15	17.49	2.18E-07	12 S7 2a
s05147	EG123	8.06E-14	9.27E-15	11.5	2.57E-07	12 S7 2e
s05148	EG124	4.15E-14	6.48E-15	15.63	2.84E-07	12 S7 3a
s05149	EG125	0.00E+00	0.00E+00	100	2.34E-07	blank
s05150	EG126	4.66E-13	2.68E-14	5.74	2.75E-07	12 LMC 001
s05151	EG127	4.97E-13	2.65E-14	5.33	3.32E-07	12 LMC 002

s05152	EG128	2.33E-13	1.93E-14	8.26	2.07E-07	!2 LMB 002
s05153	EG130	1.24E-15	1.24E-15	100	2.20E-07	12 mod 7 006
s05154	EG129	2.88E-14	1.99E-15	6.9	2.66E-06	db blank
s05155	EG131	3.28E-14	2.16E-15	6.57	2.67E-06	12S7 1b
s05156	EG132	4.14E-13	1.58E-14	3.81	2.36E-06	12 LMA 002
s05157	EG133	5.10E-13	1.94E-14	3.81	1.89E-06	12 LMC 003
s05158	EG135	5.21E-13	1.93E-14	3.7	2.64E-06	12 LMC 004
s05159	EG136	3.65E-13	1.40E-14	3.84	2.47E-06	blank
s05160	EG137	2.57E-13	1.05E-14	4.08	2.26E-06	12 LMC 005
s05161	EG138	4.09E-13	1.56E-14	3.81	2.35E-06	12 LMC 008
s05162	EG139	3.24E-13	1.30E-14	4.02	1.90E-06	12 LMC 009
s05163	EG140	2.37E-15	5.13E-16	21.59	2.55E-06	12 LMC 010
s05912	EG141	3.98E-14	2.10E-15	5.27	2.94E-06	db blank
s05913	EG142	8.58E-14	3.61E-15	4.20	3.14E-06	13 mod 7 007
s05914	EG143	1.56E-13	5.58E-15	3.58	3.28E-06	13 mod 4001
s05915	EG144	5.47E-14	2.51E-15	4.59	3.42E-06	13 mod 4002
s05916	EG145	5.62E-16	2.13E-16	37.92	2.87E-06	blank
s05917	EG146	3.95E-14	1.95E-15	4.94	3.06E-06	13 mod 4003
s05918	EG147	1.68E-15	4.00E-16	23.76	3.37E-06	13 mod 4004
s05919	EG148	5.49E-14	2.42E-15	4.42	3.20E-06	13 mod 4011
s05920	EG149	6.99E-14	2.99E-15	4.27	3.41E-06	13 mod 4012
s05921	EG150	2.31E-15	4.28E-16	18.51	3.10E-06	dbblank

There were sample(s) with 0 counts.
If we assume one count, then the isotopic ratios are:
s05135 3.015915e-16
Note: The statistical uncertainty for one count is 100%.

Appendix Table 5: $^{26}Al/^{27}Al$ AMS measurements raw data.

AMS ID	Sample ID	$^{26}Al/^{27}Al$	$^{26}Al/^{27}Al$ 1σ	$^{26}Al/^{27}Al$ 1σ (%)	avg. ^{27}Al current (A)
s06060	EG12a	5.60E-14	6.23E-15	11.11	2.70E-07
s06061	EG12b	5.94E-14	6.38E-15	10.74	2.74E-07
s06062	EG12c	5.58E-14	6.20E-15	11.11	2.71E-07
s06063	EG12d	6.12E-14	6.67E-15	10.89	2.58E-07
s06064	EG15a	3.04E-14	4.51E-15	14.85	2.90E-07
s06065	EG15b	2.27E-14	3.86E-15	17.03	2.91E-07
s06066	EG15c	3.12E-14	4.69E-15	15	2.76E-07
s06067	EG15d	2.82E-14	4.32E-15	15.31	2.92E-07
s06068	EG32	3.48E-14	6.01E-15	17.26	1.84E-07
s06069	EG33a	4.48E-14	6.09E-15	13.59	2.37E-07
s06070	EG33b	5.86E-14	6.90E-15	11.78	2.47E-07
s06071	EG33c	3.89E-14	5.62E-15	14.43	2.40E-07
s06072	EG34a	3.85E-14	5.15E-15	13.38	2.86E-07
s06073	EG34b	3.64E-14	5.15E-15	14.18	2.67E-07
s06074	EG34c	4.26E-14	5.78E-15	13.59	2.50E-07
s06075	EG34d	3.43E-14	4.91E-15	14.3	2.78E-07
s06076	EG37	5.88E-14	8.49E-15	14.43	1.59E-07
s06077	EG38a	1.52E-13	1.41E-14	9.29	1.63E-07
s06078	EG38b	2.12E-13	1.60E-14	7.54	1.94E-07
s06079	EG39a	2.39E-14	4.13E-15	17.26	2.69E-07
s06080	EG39b	3.38E-14	5.54E-15	16.39	2.12E-07
s06081	EG39c	3.29E-14	4.84E-15	14.71	2.73E-07
s06082	EG48	2.68E-14	4.29E-15	16.01	2.80E-07
s06083	EG49	1.14E-13	9.50E-15	8.35	2.80E-07
s06084	EG70a	0.00E+00	0.00E+00	100	2.18E-07
s06085	EG70b	0.00E+00	0.00E+00	100	2.23E-07
s06086	Al-STDa	0.00E+00	0.00E+00	100	2.98E-07
s06087	Al-STDb	1.31E-15	9.27E-16	70.8	2.80E-07
s06088	Al-STDc	1.22E-15	8.63E-16	70.8	3.01E-07
s06089	Al-STDd	0.00E+00	0.00E+00	100.00	3.01E-07

Appendix Table 6: Aluminium aliquot preparation.

Sample ID	empty tube(g)	tube+sample(g)	sample weight(g)	empty bottle(g)	200µl in bottle(g)	200µl transfer loss(g)	5 ml in g
EG 11	6.4860	16.7285	10.2425	19.2334	0.2145	0.0028	5.4463
EG 12	6.4857	17.4951	11.0094	19.2891	0.2177	0.0002	5.4533
EG 13	6.4646	17.3966	10.9320	19.4935	0.2171	0.0007	4.4468
EG 14	6.5014	17.3239	10.8225	19.4523	0.2110	0.0073	5.4670
EG 15	6.4820	17.3527	10.8707	19.7043	0.2158	0.0011	5.4653
EG 16	6.4815	17.4498	10.9683	19.2693	0.2154	0.0020	5.4686
EG 17	6.4654	17.4798	11.0144	19.2602	0.2175	-0.0003	5.4257
EG 18	6.4742	17.4365	10.9623	19.5342	0.2168	0.0000	5.4677
EG 19	6.4651	17.3802	10.9151	19.4931	0.2148	0.0027	5.4723
EG 20	6.4776	17.4722	10.9946	19.3830	0.2172	-0.0001	5.4604
EG 21	6.4933	17.4218	10.9285	14.3399	0.2148	0.0007	5.4548
EG 22	6.4830	17.4113	10.9283	14.3474	0.2156	0.0004	5.4863
EG 23	6.4668	17.3216	10.8548	14.3173	0.2152	0.0003	5.4827
EG 24	6.5224	17.3697	10.8473	14.3594	0.2159	0.0005	5.4296
EG 25	6.4503	17.3714	10.9211	14.3205	0.2156	0.0012	5.4794
EG 26	6.4141	17.3172	10.9031	14.3500	0.2164	0.0009	5.4766
EG 27	6.4997	17.4715	10.9718	14.3326	0.2168	0.0007	5.4649
EG 28	6.4670	17.3678	10.9008	14.3112	0.2149	0.0116	5.4662
EG 29	6.4504	17.3167	10.8663	14.3194	0.2148	0.0020	5.4962
EG 30	6.4851	17.3389	10.8538	14.3064	0.2150	0.0007	5.4504
EG 31	6.4663	17.3321	10.8658	14.3865	0.2172	0.0000	5.4332
EG 32	6.3364	17.1746	10.8382	14.3753	0.2157	0.0017	5.3351
EG 33	6.4506	17.2522	10.8017	14.3475	0.2146	0.0010	5.3863
EG 34	6.5343	17.3672	10.8329	14.2756	0.2155	0.0004	5.3540
EG 35	6.4446	17.2957	10.8511	14.3312	0.2163	0.0001	5.3982
EG 36	6.4640	17.0543	10.5903	14.3490	0.2163	-1.0001	5.3755
EG 37	6.4766	17.3256	10.8490	14.3776	0.2153	0.0009	5.3770
EG 38	6.3477	17.0720	10.7243	14.3533	0.2201	-0.0014	5.3857
EG 39	6.4377	17.3373	10.8996	14.3207	0.2180	0.0008	5.3991
EG 40	6.4824	17.2906	10.8082	14.3189	0.2156	-0.0002	5.4075
EG 41	6.4513	17.2368	10.7855	14.3605	-14.3605	14.3605	0.0000
EG 42	6.4633	17.2804	10.8171	14.3648	-14.3648	14.3648	0.0000
EG 43	6.4637	17.2026	10.7389	14.3389	-14.3389	14.3389	0.0000
EG 44	6.4668	17.0640	10.5972	14.3370	-14.3370	14.3370	0.0000
EG 45	6.4621	17.0550	10.5929	14.3287	-14.3287	14.3287	0.0000
EG 46	6.4879	17.9162	11.4283	14.3672	-14.3672	14.3672	0.0000
EG 47	6.4391	17.0096	10.5705	14.3427	-14.3427	14.3427	0.0000
EG 48	6.3484	17.1211	10.7727	14.4578	-14.4578	14.4578	0.0000
EG 49	6.4505	17.2267	10.7762	14.3752	-14.3752	14.3752	0.0000
EG 50	6.4539	17.2064	10.7525	14.3916	-14.3916	14.3916	0.0000
EG 51	6.5624	17.2493	10.6869	14.3255	0.2150	-0.0001	5.4121
EG 52	6.5164	17.0953	10.5789	14.3802	0.2151	0.0000	5.3992
EG 53	6.6009	17.2374	10.6365	14.3788	0.2138	0.0008	5.3751
EG 54	6.5313	17.2035	10.6722	14.3642	0.2151	0.0010	5.3515
EG 55	6.4085	17.2077	10.7992	14.3519	0.2123	0.0016	5.3369
EG 56	6.5774	17.3498	10.7724	14.3725	0.2133	0.0003	5.4034
EG 57	6.4310	17.1580	10.7270	14.3422	0.2135	0.0009	5.3826
EG 58	6.5723	17.3606	10.7883	14.3442	0.2089	0.0063	5.3654
EG 59	6.5990	17.3264	10.7274	14.3396	0.2375	-0.0233	5.3992
EG 60	6.5799	17.4911	10.9112	14.3614	0.2157	0.0011	5.4087
EG 61	13.3026	34.4085	21.1059	14.3696	0.1885	-0.1885	5.4248
EG 62	6.5640	14.8606	8.2966	14.3241	0.2147	-0.2147	5.4827
EG 63	6.5557	17.1528	10.5971	14.3156	0.2176	-0.2176	5.4161
EG 64	6.9238	17.6058	10.6820	14.2934	0.2179	-0.2179	5.4572
EG 65	9.5509	17.6547	8.1038	14.3116	0.2249	-0.2249	5.4757
EG 66	6.5201	16.9609	10.4408	14.3526	0.2143	-0.2143	5.4303
EG 67	6.5667	17.1497	10.5830	14.3267	0.2140	-0.2140	5.4337
EG 68	6.6609	17.0359	10.3750	14.3656	0.2127	-0.2127	5.4321
EG 69	8.5342	18.9630	10.4288	14.4251	0.2217	-0.2217	5.4430
EG 70	6.5653	16.9628	10.3975	14.7175	0.0291	-0.0291	5.2448
EG 71	6.4000	17.2454	10.8454	14.3419	0.2153	-0.0006	5.4516
EG 72	6.4000	17.1745	10.7745	14.3714	0.2165	-0.0001	5.4611
EG 73	6.4000	17.2762	10.8762	14.3265	0.2161	0.0008	5.3928
EG 74	6.4000	17.3582	10.9582	14.3757	0.2143	0.0011	5.4085
EG 75	6.4000	17.3576	10.9576	14.2958	0.2184	0.0001	5.3789
EG 76	6.4000	17.3020	10.9020	14.3035	0.2155	-0.0001	5.3666
EG 77	6.4000	17.2682	10.8682	14.3017	0.2146	0.0006	5.4299
EG 78	6.4000	17.3183	10.9183	14.3209	0.2271	0.0003	5.4166
EG 79	6.4000	17.2084	10.8084	14.3296	0.2150	-0.0004	5.3956

EG 80	6.4000	17.3890	10.9890	14.2986	0.2194	-0.0003	5.4156
EG 81	6.4656	17.2413	10.7757	14.3823	0.2203	0.0006	5.4380
EG 82	6.4823	17.1233	10.6410	14.4400	0.2216	0.0006	5.4250
EG 83	6.4635	17.1499	10.6864	14.3260	0.2218	0.0001	5.3569
EG 84	6.4777	17.2564	10.7787	14.3717	0.2228	-0.0008	5.4114
EG 85	6.4459	17.0611	10.6152	14.3639	0.2221	0.0011	5.4419
EG 86	6.5318	17.3269	10.7951	14.3778	0.2599	-0.0008	5.4188
EG 87	6.3973	17.0890	10.6917	14.3772	0.2226	0.0000	5.4297
EG 88	6.4498	16.9351	10.4853	14.3527	0.2224	0.0010	5.4423
EG 89	6.4047	17.0516	10.6469	14.3728	0.2209	0.0011	5.4135
EG 90	6.3937	17.1932	10.7995	14.3349	0.2234	-0.0022	5.4569
EG 91	6.4000	17.4752	11.0752	14.3227	0.2180	0.0012	5.4874
EG 92	6.4000	17.4351	11.0351	14.3224	0.2149	0.0014	5.4353
EG 93	6.4000	17.2402	10.8402	14.3292	0.2157	0.0000	5.4981
EG 94	6.4000	17.5443	11.1443	14.3050	0.2157	0.0008	5.4188
EG 95	6.4000	17.4803	11.0803	14.2908	0.2170	0.0000	5.3916
EG 96	6.4000	17.3991	10.9991	14.3395	0.1954	0.0196	4.4119
EG 97	6.4000	17.5051	11.1051	14.3587	0.1899	0.0269	5.4243
EG 98	6.4000	17.5241	11.1241	14.3858	0.2579	-0.0408	5.4499
EG 99	6.4000	17.4349	11.0349	14.3451	0.2245	-0.0082	5.4605
EG 100	6.4000	17.4421	11.0421	14.3362	0.2811	-0.2811	5.4491
EG 101	6.4701	17.2139	10.7438	14.2734	0.2194	-0.0022	-14.4928
EG 102	6.4524	17.4253	10.9729	14.3345	0.2156	0.0010	-14.5501
EG 103	6.4524	17.2529	10.8005	14.3644	0.2167	-0.0002	-14.5811
EG 104	6.4536	17.3906	10.9370	14.2973	0.2180	-0.0047	-14.5153
EG 105	6.4549	17.3387	10.8838	14.3319	0.2192	-0.0008	-14.5511
EG 106	6.3936	17.3448	10.9512	14.3456	0.2153	0.0007	-14.5609
EG 107	6.4485	17.4039	10.9554	14.3308	0.2170	0.0000	-14.5478
EG 108	6.4469	17.4325	10.9856	14.3070	0.2187	-0.0010	-14.5257
EG 109	6.4573	17.3369	10.8796	14.2885	0.2190	-0.0009	-14.5075
EG 110	6.5514	17.5205	10.9691	14.3765	0.2177	0.0004	-14.5942
EG 111	6.4490			13.8486	0.2224		5.4575
EG 112	6.4646			13.7900	0.2209		5.4154
EG 113	6.4813			13.7082	0.2310		5.3454
EG 114	6.4759			13.7799	0.2296		5.3685
EG 115	6.4573			13.7026	0.2327		5.3488
EG 116	6.4750			13.7723	0.2223		5.3653
EG 117	6.4618			13.6521	0.2200		5.3620
EG 118	6.4575			13.7746	0.2224		5.3531
EG 119	6.4830			13.6423	0.2214		5.4072
EG 120	6.4584			13.8450	0.2253		5.4218
EG 121	6.3919	17.2852	10.8933	13.7852	0.2175	0.0007	5.3867
EG 122	6.4827	17.4262	10.9435	13.6719	0.2177		5.4033
EG 123	6.4090	17.3953	10.9863	13.6671	0.2171	0.0002	5.3602
EG 124	6.4102	17.2629	10.8527	13.8050	0.2172	0.0005	5.4325
EG 125	6.4624	17.3935	10.9311	13.7364	0.2179	0.0003	5.3306
EG 126	6.4635	17.3578	10.8943	13.6879	0.2180	0.0005	5.3267
EG 127	6.3928	17.5861	11.1933	13.7758	0.2173	0.0013	5.3326
EG 128	6.5519	17.5097	10.9578	13.7430	0.2185	0.0009	5.3911
EG 129	6.4537	17.4148	10.9611	13.7708	0.1794	0.0538	5.3405
EG 130	6.4646	17.4543	10.9897	13.6269	0.2174	0.0003	5.4504
EG 131	6.4486			13.6483	0.2235	-0.2235	5.4320
EG 132	6.4702			13.8470	0.2229	-0.2229	5.4316
EG 133	6.4630			13.6504	0.2206	-0.2206	5.4000
EG 134	6.4540			13.6378	0.2213	-0.2213	5.3998
EG 135	6.3312			13.7735	0.2207	-0.2207	5.4044
EG 136	6.4597			13.7770	0.2223	-0.2223	5.3745
EG 137	6.4577			13.6267	0.2211	-0.2211	5.3001
EG 138	6.4718			13.6472	0.2222	-0.2222	5.4311
EG 139	6.4549			13.7042	0.2212	-0.2212	5.4465
EG 140	6.4636			13.6573	0.2208	-0.2208	5.3799
EG 141	6.5179	17.0151	10.4972	19.3846	0.2116	0.0085	-0.3565
EG 142	6.4038	16.8740	10.4702	19.4147	0.2175	0.0016	-0.3972
EG 143	6.6078	16.9288	10.3210	19.3964	0.2178	0.0019	-0.3838
EG 144	6.4553	16.7880	10.3327	19.3048	0.2170	0.0037	-0.2961
EG 145	6.5225	16.9899	10.4674	19.4408	0.1987	0.0208	-0.4184
EG 146	6.5211	16.9923	10.4712	19.5935	0.2106	0.0092	-0.5877
EG 147	6.4083	16.9692	10.5609	19.3793	0.2124	0.0065	-0.3799
EG 148	6.4590	16.8963	10.4373	19.4345	0.2051	0.0144	-0.4324
EG 149	6.4421	16.8105	10.3684	19.3543	0.2151	0.0032	-0.3669
EG 150	6.4480	16.9573	10.5093	19.4717	0.2150	0.0041	-0.4888

Appendix Table 7: Standard addition for aluminium ICP-OES-MS measurements preparation.

Sample ID	Lab ID	sample in g	STD conc ppm	STD liq in g	HNO3 in g	weight(tot) in g	factor STD in tube	sample dilut. fac.	STD adjustment x-axis
ER 011	EG 11	5.9814	1	0	5.9771	11.9585	0.0000	0.5002	0.0000
		5.956		1.9717	3.9714	11.8991	0.1657		0.1657
		5.971		3.9577	1.9695	11.8982	0.3326		0.3326
		5.9119		5.9572	0	11.8691	0.5019		0.5019
12 mod6 005	EG 12	5.9704	2	0	5.9589	11.9293	0.0000	0.5005	0.0000
		5.9943		1.9443	3.9358	11.8744	0.1637		0.3275
		5.9726		3.8161	1.9729	11.7616	0.3245		0.6489
		5.9765		5.6944	0	11.6709	0.4879		0.9758
12 mod 7 001	EG 14	5.9168	2	0	5.9349	11.8517	0.0000	0.4992	0.0000
		5.9026		2.0619	3.9305	11.895	0.1733		0.3467
		5.889		4.018	1.9604	11.8674	0.3386		0.6771
		5.9368		6.0095	0	11.9463	0.5030		1.0061
12 mod7 005	EG 15	5.9293	2	0	5.979	11.9083	0.0000	0.4979	0.0000
		5.924		2.0741	3.9167	11.9148	0.1741		0.3482
		5.8582		4.1109	1.9648	11.9339	0.3445		0.6889
		5.91		6.096	0	12.006	0.5077		1.0155
12 mod 7 007	EG16	5.9868	2	0	5.9474	11.9342	0.0000	0.5017	0.0000
		5.9725		1.9887	3.9423	11.9035	0.1671		0.3341
		6.0111		3.9798	1.9644	11.9553	0.3329		0.6658
		5.9889		5.8869	0	11.8758	0.4957		0.9914
12 S7 001 d	EG 18	5.9691	1	0	5.7486	11.7177	0.0000	0.5094	0.0000
		5.9826		2.0057	3.9106	11.8989	0.1686		0.1686
		5.9889		4.0181	1.9524	11.9594	0.3360		0.3360
		5.9393		6.0467	0	11.986	0.5045		0.5045
ER 011	EG 11	5.9814	1	0	5.9771	11.9585	0.0000	0.5002	0.0000
		5.956		1.9717	3.9714	11.8991	0.1657		0.1657
		5.971		3.9577	1.9695	11.8982	0.3326		0.3326
		5.9119		5.9572	0	11.8691	0.5019		0.5019
12 mod6 005	EG 12	5.9704	2	0	5.9589	11.9293	0.0000	0.5005	0.0000
		5.9943		1.9443	3.9358	11.8744	0.1637		0.3275
		5.9726		3.8161	1.9729	11.7616	0.3245		0.6489
		5.9765		5.6944	0	11.6709	0.4879		0.9758
12 mod 7 001	EG 14	5.9168	2	0	5.9349	11.8517	0.0000	0.4992	0.0000
		5.9026		2.0619	3.9305	11.895	0.1733		0.3467
		5.889		4.018	1.9604	11.8674	0.3386		0.6771
		5.9368		6.0095	0	11.9463	0.5030		1.0061
12 mod7 005	EG 15	5.9293	2	0	5.979	11.9083	0.0000	0.4979	0.0000
		5.924		2.0741	3.9167	11.9148	0.1741		0.3482
		5.8582		4.1109	1.9648	11.9339	0.3445		0.6889
		5.91		6.096	0	12.006	0.5077		1.0155
12 mod 7 007	EG16	5.9868	2	0	5.9474	11.9342	0.0000	0.5017	0.0000
		5.9725		1.9887	3.9423	11.9035	0.1671		0.3341
		6.0111		3.9798	1.9644	11.9553	0.3329		0.6658
		5.9889		5.8869	0	11.8758	0.4957		0.9914
12 S7 001 d	EG 18	5.9691	1	0	5.7486	11.7177	0.0000	0.5094	0.0000
		5.9826		2.0057	3.9106	11.8989	0.1686		0.1686

		5.9889		4.0181	1.9524	11.9594	0.3360		0.3360
		5.9393		6.0467	0	11.986	0.5045		0.5045
12 S7002b	EG 21	5.9157	2	0	5.9429	11.8586	0.0000	0.4989	0.0000
		5.8678		1.9645	3.9731	11.8054	0.1664		0.3328
		5.9287		3.9438	1.9522	11.8247	0.3335		0.6670
		5.946		5.9727	0	11.9187	0.5011		1.0022
12 S7 002c	EG 22	5.8774	1	0	5.9092	11.7866	0.0000	0.4965	0.0000
		5.8583		2.0013	3.9975	11.8571	0.1688		0.1688
		5.9291		3.9693	1.9605	11.8589	0.3347		0.3347
		5.8658		5.9372	0	11.803	0.5030		0.5030
12 S7 002d	EG 23	5.8477	2	0	5.9803	11.828	0.0000	0.4944	0.0000
		5.8308		1.9969	3.946	11.7737	0.1696		0.3392
		5.7936		3.9491	2.0431	11.7858	0.3351		0.6701
		5.8414		5.9771	0	11.8185	0.5057		1.0115
12 S7 004 a	EG 25	5.8693	1	0	5.9234	11.7927	0.0000	0.4977	0.0000
		5.8992		2.0143	3.9516	11.8651	0.1698		0.1698
		5.877		4.0189	2.0015	11.8974	0.3378		0.3378
		5.9337		5.9667	0	11.9004	0.5014		0.5014
12 S7 004b	EG 26	5.88	1	0	5.9258	11.8058	0.0000	0.4981	0.0000
		5.8673		2.0136	3.9669	11.8478	0.1700		0.1700
		5.8976		4.0171	1.9937	11.9084	0.3373		0.3373
		5.8928		6.0207	0	11.9135	0.5054		0.5054
12 S7 004 c	EG 27	5.8509	1	0	5.9432	11.7941	0.0000	0.4961	0.0000
		5.8472		2.0088	4.0296	11.8856	0.1690		0.1690
		5.8578		3.9523	2.0205	11.8306	0.3341		0.3341
		5.724		5.9623	0	11.6863	0.5102		0.5102
12 S7 004 d	EG28	5.8897	2	0	5.9698	11.8595	0.0000	0.4966	0.0000
		5.8937		2.0005	4.0059	11.9001	0.1681		0.3362
		5.8793		3.9941	2.0034	11.8768	0.3363		0.6726
		5.8898		5.9687	0	11.8585	0.5033		1.0067
12 S7 004 e	EG29	5.8296	2	0	5.8993	11.7289	0.0000	0.4970	0.0000
		5.8984		1.9799	3.9806	11.8589	0.1670		0.3339
		5.8597		3.9624	2.0184	11.8405	0.3346		0.6693
		5.8461		5.9544	0	11.8005	0.5046		1.0092
blank	EG30	5.8637	50ppb	0	5.8996	11.7633	0.0000	0.4985	0.0000
		5.8676		2.032	3.9959	11.8955	0.1708		0.0085
		5.9229		4.026	2.0035	11.9524	0.3368		0.0168
		5.8964		6.011	0	11.9074	0.5048		0.0252
12 mod7 002	EG 31	5.9507	2	0	6.0603	12.011	0.0000	0.4954	0.0000
		5.9003		2.0152	4.0197	11.9352	0.1688		0.3377
		5.9088		3.9762	2.0162	11.9012	0.3341		0.6682
		5.9121		5.9232	0	11.8353	0.5005	0.4995	1.0009
12 mod7 003	EG 32	5.9212	2	0	6.0069	11.9281	0.0000	0.4964	0.0000
		5.8792		2.0306	4.0067	11.9165	0.1704		0.3408
		5.9453		3.9839	1.9926	11.9218	0.3342		0.6683
		5.9313		5.9914	0	11.9227	0.5025		1.0050
12 mod 6 001	EG 33	5.8761	2	0	5.998	11.8741	0.0000	0.4949	0.0000
		5.9938		1.9941	4.0077	11.9956	0.1662		0.3325
		5.9954		4.011	1.9952	12.0016	0.3342		0.6684

		5.9746		6.0133	0	11.9879	0.5016		1.0032
12 mod 6 002	EG 34	5.9388	2	0	5.9914	11.9302	0.0000	0.4978	0.0000
		5.9248		1.9918	3.9927	11.9093	0.1672		0.3345
		5.9368		3.9828	2.0063	11.9259	0.3340		0.6679
		5.953		5.9907	0	11.9437	0.5016		1.0032
12 mod 6 003	EG 35	5.8743	2	0	5.8873	11.7616	0.0000	0.4994	0.0000
		5.861		2.0329	3.7788	11.6727	0.1742		0.3483
		5.8447		4.0634	1.9999	11.908	0.3412		0.6825
		5.8521		6.0104	0	11.8625	0.5067		1.0133
12 mod 5 003	EG 36	5.9337	50ppb	0	5.9101	11.8438	0.0000	0.5010	0.0000
		5.97		1.8637	3.9854	11.8191	0.1577		0.0079
		5.9728		3.7797	1.9871	11.7396	0.3220		0.0161
		5.9396		5.6689	0	11.6085	0.4883		0.0244
12 mod 5 003	EG 37	5.9598	1	0	5.8855	11.8453	0.0000	0.5031	0.0000
		5.9411		2.0515	3.9845	11.9771	0.1713		0.1713
		5.9594		4.0659	1.993	12.0183	0.3383		0.3383
		5.9867		6.008	0	11.9947	0.5009		0.5009
12 mod 5 003	EG 38	5.9197	2	0	5.8443	11.764	0.0000	0.5032	0.0000
		5.9243		2.0072	4.0266	11.9581	0.1679		0.3357
		5.9457		4.0061	1.995	11.9468	0.3353		0.6707
		5.9549		6.0238	0	11.9787	0.5029		1.0058
12 mod 5 003	EG 39	6.0605	2	0	5.9362	11.9967	0.0000	0.5052	0.0000
		5.9848		1.9989	3.9576	11.9413	0.1674		0.3348
		5.9833		3.9828	1.9397	11.9058	0.3345		0.6691
		5.9634		5.971	0	11.9344	0.5003		1.0006
12 mod 5 003	EG 41	5.9289	1	0	5.8995	11.8284	0.0000	0.5012	0.0000
		5.9741		2.0045	3.989	11.9676	0.1675		0.1675
		5.9785		3.9854	1.9486	11.9125	0.3346		0.3346
		5.9561		5.9684	0	11.9245	0.5005		0.5005
12 S7 001 c	EG 42	5.9183	1	0	5.9704	11.8887	0.0000	0.4978	0.0000
		5.9561		2.2104	3.9952	12.1617	0.1818		0.1818
		5.9682		3.9825	1.9579	11.9086	0.3344		0.3344
		5.9887		5.939	0	11.9277	0.4979		0.4979
12 S7 001 e	EG 43	6.1271	2	0	5.7712	11.8983	0.0000	0.5150	0.0000
		6.0092		2.0043	3.9894	12.0029	0.1670		0.3340
		5.9855		3.9812	1.9653	11.932	0.3337		0.6673
		5.9379		6.0179	0	11.9558	0.5033		1.0067
12 S7 002 a	EG 44	5.9739	1	0	5.9814	11.9553	0.0000	0.4997	0.0000
		5.9631		1.9911	3.9977	11.9519	0.1666		0.1666
		5.9926		3.9284	1.9513	11.8723	0.3309		0.3309
		6.0078		5.8976	0	11.9054	0.4954		0.4954
12 S7 003 a	EG 46	5.9093	1	0	5.9592	11.8685	0.0000	0.4979	0.0000
		5.9671		1.9744	3.905	11.8465	0.1667		0.1667
		5.9316		3.9316	1.9578	11.821	0.3326		0.3326
		5.9559		5.9142	0	11.8701	0.4982		0.4982
12 S7 003 c	EG 47	5.9265	1	0	5.9587	11.8852	0.0000	0.4986	0.0000
		5.9214		1.9806	3.9733	11.8753	0.1668		0.1668
		5.9497		3.9763	1.9658	11.8918	0.3344		0.3344
		5.9611		5.9564	0	11.9175	0.4998		0.4998

12 mod7 006	EG 48	5.9142	1	0	5.9537	11.8679	0.0000	0.4983	0.0000
		5.9475		1.9929	3.9318	11.8722	0.1679		0.1679
		5.9655		3.9786	1.9915	11.9356	0.3333		0.3333
		5.941		5.9449	0	11.8859	0.5002		0.5002
12 mod 5 001	EG 49	5.9564	2	0	5.9835	11.9399	0.0000	0.4989	0.0000
		5.9493		1.9855	3.9662	11.901	0.1668		0.3337
		5.9557		3.9606	1.9689	11.8852	0.3332		0.6665
		5.9256		5.915	0	11.8406	0.4996		0.9991
db blank	EG 50	5.9158	5	0	5.9853	11.9011	0.0000	0.4971	0.0000
		5.9158		1.9873	3.975	11.8781	0.1673		0.8365
		5.8982		3.9601	1.9962	11.8545	0.3341		1.6703
		5.9074		5.9708	0	11.8782	0.5027		2.5133
12 S7 001 b	EG 51	5.9096	1	0	5.7995	11.7091	0.0000	0.5047	0.0000
		5.928		2.0183	3.9666	11.9129	0.1694		0.1694
		5.9318		3.9651	1.983	11.8799	0.3338		0.3338
		5.9376		6.0045	0	11.9421	0.5028		0.5028
12 S7 002 e	EG 52	5.9251	2	0	5.7907	11.7158	0.0000	0.5057	0.0000
		5.9573		1.9943	3.9655	11.9171	0.1673		0.3347
		5.9565		3.9782	1.9752	11.9099	0.3340		0.6680
		5.9276		5.9823	0	11.9099	0.5023		1.0046
12 S7 003 e	EG 53	5.8735	2	0	5.7894	11.6629	0.0000	0.5036	0.0000
		5.8892		1.986	3.9808	11.856	0.1675		0.3350
		5.8584		3.9899	1.9563	11.8046	0.3380		0.6760
		5.8973		5.9914	0	11.8887	0.5040		1.0079
12 S7 003 b	EG 54	5.9209	1	0	5.8103	11.7312	0.0000	0.5047	0.0000
		5.9401		2.0082	3.9895	11.9378	0.1682	0.4976	0.1682
		5.9337		4.0304	1.9783	11.9424	0.3375	0.4969	0.3375
		5.9137		6.0725	0	11.9862	0.5066	0.4934	0.5066
blank	EG 55	5.9283	50ppb	0	5.8097	11.738	0.0000	0.5051	0.0000
		5.9504		1.9839	3.9158	11.8501	0.1674	0.5021	0.0084
		5.8891		3.9546	1.9581	11.8018	0.3351	0.4990	0.0168
		5.885		5.8958	0	11.7808	0.5005	0.4995	0.0250
12 LMA 008	EG 56	5.8924	5	0	5.8609	11.7533	0.0000	0.5013	0.0000
		5.8865		2.0038	3.9796	11.8699	0.1688	0.4959	0.8441
		5.8917		3.9944	1.9624	11.8485	0.3371	0.4973	1.6856
		5.9259		6.0183	0	11.9442	0.5039	0.4961	2.5193
12 LME 010	EG 57	5.811	1	0	5.9556	11.7666	0.0000	0.4939	0.0000
		5.8369		1.9547	3.9085	11.7001	0.1671	0.4989	0.1671
		5.8347		3.9483	1.9759	11.7589	0.3358	0.4962	0.3358
		5.854		5.9088	0	11.7628	0.5023	0.4977	0.5023
12 ER 016	EG 58	5.8819	1	0	5.9122	11.7941	0.0000	0.4987	0.0000
		5.9063		1.9805	3.9317	11.8185	0.1676	0.4998	0.1676
		5.9064		3.9676	1.9583	11.8323	0.3353	0.4992	0.3353
		5.8861		5.9595	0	11.8456	0.5031	0.4969	0.5031
12 ER 018	EG 59	5.9541	1	0	5.8581	11.8122	0.0000	0.5041	0.0000
		5.9583		1.9864	3.9589	11.9036	0.1669	0.5005	0.1669
		5.9572		3.9923	1.9661	11.9156	0.3350	0.4999	0.3350
		5.9332		6.0301	0	11.9633	0.5040	0.4960	0.5040

blank	EG 60	5.9257	50ppb	0	5.8728	11.7985	0.0000	0.5022	0.0000
		5.9139		1.953	4.146	12.0129	0.1626	0.4923	0.0081
		5.8647		3.9096	1.9902	11.7645	0.3323	0.4985	0.0166
		5.8899		5.8689	0	11.7588	0.4991	0.5009	0.0250
12 ER 001	EG 61	5.9055	1	0	5.919	11.8245	0.0000	0.4994	0.0000
		5.9041		1.9923	3.9262	11.8226	0.1685	0.4994	0.1685
		5.9179		3.9523	1.9761	11.8463	0.3336	0.4996	0.3336
		5.9623		5.9202	0	11.8825	0.4982	0.5018	0.4982
12 ER 003	EG 62	5.914	1	0	5.9199	11.8339	0.0000	0.4998	0.0000
		5.9529		1.7659	3.9268	11.6456	0.1516	0.5112	0.1516
		5.9549		3.9559	1.9937	11.9045	0.3323	0.5002	0.3323
		5.9872		5.9672	0	11.9544	0.4992	0.5008	0.4992
12 ER 004	EG 63	5.9226	1	0	5.9004	11.823	0.0000	0.5009	0.0000
		5.9265		1.9782	3.9247	11.8294	0.1672	0.5010	0.1672
		5.9531		3.9459	2.0093	11.9083	0.3314	0.4999	0.3314
		5.9334		5.9096	0	11.843	0.4990	0.5010	0.4990
12 ER 006	EG 64	5.9206	1	0	5.952	11.8726	0.0000	0.4987	0.0000
		5.8952		1.9713	3.9858	11.8523	0.1663	0.4974	0.1663
		5.8798		3.9406	2.0124	11.8328	0.3330	0.4969	0.3330
		5.8843		5.9285	0	11.8128	0.5019	0.4981	0.5019
12 ER 007	EG 65	5.9373	1	0	6.0043	11.9416	0.0000	0.4972	0.0000
		5.9607		1.4359	5.0088	12.4054	0.1157	0.4805	0.1157
		5.9267		3.9903	2.0004	11.9174	0.3348	0.4973	0.3348
		5.9282		6.0289	0	11.9571	0.5042	0.4958	0.5042
blank	EG 66	5.9664	50 ppb	0	5.9971	11.9635	0.0000	0.4987	0.0000
		5.9749		1.978	3.92	11.8729	0.1666	0.5032	0.0083
		5.982		3.9341	1.9932	11.9093	0.3303	0.5023	0.0165
		5.9796		5.8767	0	11.8563	0.4957	0.5043	0.0248
12 ER 010	EG 67	5.8947	1	0	5.9675	11.8622	0.0000	0.4969	0.0000
		5.8917		2.0011	3.8952	11.788	0.1698	0.4998	0.1698
		5.9036		4.0008	1.9929	11.8973	0.3363	0.4962	0.3363
		5.8761		5.976	0	11.8521	0.5042	0.4958	0.5042
12 ER 015	EG 68	5.9227	1	0	6.0102	11.9329	0.0000	0.4963	0.0000
		5.9205		1.9785	3.8955	11.7945	0.1677	0.5020	0.1677
		5.9161		3.9255	2.0012	11.8428	0.3315	0.4996	0.3315
		5.8855		5.928	0	11.8135	0.5018	0.4982	0.5018
12 ER 018	EG 69	5.9209	1	0	5.9677	11.8886	0.0000	0.4980	0.0000
		5.9348		2.0372	3.9406	11.9126	0.1710	0.4982	0.1710
		5.9179		3.9865	2.003	11.9074	0.3348	0.4970	0.3348
		5.9301		5.9576	0	11.8877	0.5012	0.4988	0.5012

Appendix Table 8: Al ICP-OES-MS raw data.

Sample ID	Analyte Name	RSD (Corr Int)	Conc (Samp)	QC Recovery	Int (Corr)
Blanc	Al 396.153	11.35935458			-344.6396731
Blanc	Al 394.401	315.1819554			-6.788193129
St 50 ppb	Al 396.153	0.807111437			5544.678223
St 50 ppb	Al 394.401	1.607495017			1555.184475
St 100 ppb	Al 396.153	0.930271547			11015.66775
St 100 ppb	Al 394.401	1.258754007			3043.641249
St 500 ppb	Al 396.153	2.05229717			54421.49405
St 500 ppb	Al 394.401	2.453563327			15044.67144
St 1 ppm	Al 396.153	1.583164119			109424.3086
St 1 ppm	Al 394.401	1.367915297			30321.15509
St 10 ppm	Al 396.153	2.203194755			1114264.781
St 10 ppm	Al 394.401	2.176187785			313903.1617
St 2 ppm	Al 396.153	1.600971663	1.9527444	97.63722002	217536.0958
St 2 ppm	Al 394.401	1.965002821	1.930109842	96.5054921	60559.98473
Blanc	Al 396.153	6.86106531			-392.1713022
Blanc	Al 394.401	14.3008066			-56.62954221
St 1 ppm	Al 396.153	0.510630379			11045.88525
St 1 ppm	Al 394.401	0.942208869			3045.243471
NWG	Al 396.153	155.6508723	-0.000138387		-15.28611958
NWG	Al 394.401	107.4466074	0.000446763		13.60500814
BG	Al 396.153	767.4560853	5.84E-05		6.453543542
BG	Al 394.401	110.4626487	0.000185107		5.636970371
Blanc	Al 396.153	60.18741907	0.032301268		3570.751624
Blanc	Al 394.401	61.92796	0.032662448		1010.740685
St 1 ppm	Al 396.153	1.192379993	0.098115291		10846.17896
St 1 ppm	Al 394.401	1.384528516	0.097466393		3016.101201
St 2 ppm	Al 396.153	4.734700601	2.066921599	103.3460799	228488.3551
St 2 ppm	Al 394.401	2.543303318	2.030405629	101.5202814	62830.97864
EG 11/1	Al 396.153	0.554643137	0.078323069		8658.24286
EG 11/1	Al 394.401	1.956098928	0.078669817		2434.440449
EG11/2	Al 396.153	0.754520739	0.241539079		26700.99675
EG11/2	Al 394.401	0.620154086	0.242267537		7496.978038
EG11/3	Al 396.153	0.899478143	0.412319564		45579.96738
EG11/3	Al 394.401	0.612074272	0.408210702		12632.09554
EG11/4	Al 396.153	0.449596599	0.572235125		63257.87227
EG11/4	Al 394.401	0.228272253	0.569845528		17633.89131
EG12/1	Al 396.153	0.822382546	1.423874222		157402.5252
EG12/1	Al 394.401	1.036352659	1.414104396		43759.51378
Blanc	Al 396.153	14.1016287			-330.0951813
Blanc	Al 394.401	14.57644222			-48.56775647
St 1 ppm	Al 396.153	1.689311506			10881.28944
St 1 ppm	Al 394.401	1.254544448			3054.210085
EG12/2	Al 396.153	1.122235939	1.751799721		190618.398
EG12/2	Al 394.401	1.077148215	1.7453043		53305.25993
EG12/3	Al 396.153	1.509058056	2.102761175		228807.5297
EG12/3	Al 394.401	0.501098658	2.110982851		64473.85113
EG12/4	Al 396.153	1.332592276	2.422681059		263618.9381
EG12/4	Al 394.401	0.993445475	2.448097423		74770.03837
EG14/1	Al 396.153	1.101326263	1.302680545		141748.4406
EG14/1	Al 394.401	1.095954096	1.296346857		39593.15644
EG14/2	Al 396.153	0.696672505	1.646953858		179209.8162
EG14/2	Al 394.401	0.999375798	1.634983337		49935.82595
EG14/3	Al 396.153	1.415469652	1.970362983		214400.8992
EG14/3	Al 394.401	0.864853462	1.994851153		60926.94509
EG14/4	Al 396.153	1.021549848	2.320064677		252452.9527
EG14/4	Al 394.401	0.389055268	2.346396669		71663.88369
EG15/1	Al 396.153	0.690549701	1.599605063		174057.6568

EG15/1	Al 394.401	0.81918998	1.592690776		48644.12229
EG15/2	Al 396.153	0.461104114	1.936527242		210719.1342
EG15/2	Al 394.401	1.330408945	1.959039439		59833.1801
EG15/3	Al 396.153	1.599953524	2.284388074		248570.8782
EG15/3	Al 394.401	0.842077368	2.309120193		70525.38182
EG15/4	Al 396.153	1.70735604	2.598118048		282708.7447
EG15/4	Al 394.401	0.791195728	2.657624378		81169.43177
St 2 ppm	Al 396.153	1.212568304	1.974686422	98.7343211	214871.345
St 2 ppm	Al 394.401	1.235797938	1.996380714	99.81903569	60973.66109
EG16/1	Al 396.153	0.622273179	1.486339942		161732.9511
EG16/1	Al 394.401	0.752433099	1.477929471		45139.07095
EG16/2	Al 396.153	1.355763995	1.77707125		193368.2662
EG16/2	Al 394.401	1.449363649	1.769733928		54051.3921
EG16/3	Al 396.153	1.472001696	2.104536438		229000.7011
EG16/3	Al 394.401	1.081982945	2.137352222		65279.22711
EG16/4	Al 396.153	1.355058049	2.442885679		265817.4613
EG16/4	Al 394.401	1.097996789	2.47948726		75728.74995
EG18/1	Al 396.153	2.066128208	0.841413872		91556.67873
EG18/1	Al 394.401	1.490618765	0.857476397		26189.13061
EG18/2	Al 396.153	2.321503863	1.013768854		110311.1233
EG18/2	Al 394.401	1.108637262	1.033480462		31564.66449
EG18/3	Al 396.153	1.606902537	1.160780613		126307.8982
EG18/3	Al 394.401	1.602134449	1.155409987		35288.64836
EG18/4	Al 396.153	1.335871269	1.330108967		144733.0066
EG18/4	Al 394.401	1.45176029	1.322418859		40389.45016
EG21/1	Al 396.153	0.336134151	1.036980264		112836.8239
EG21/1	Al 394.401	0.294574701	1.054729341		32213.64991
EG21/2	Al 396.153	1.938751414	1.355086295		147450.8618
EG21/2	Al 394.401	2.431895436	1.354331561		41364.13111
EG21/3	Al 396.153	1.427257451	1.692113189		184123.7337
EG21/3	Al 394.401	1.328134201	1.685386922		51475.25735
EG21/4	Al 396.153	1.548390665	2.023597066		220193.4538
EG21/4	Al 394.401	0.678310588	2.041398733		62348.60598
EG22/1	Al 396.153	0.726068604	0.800702844		87126.79403
EG22/1	Al 394.401	1.015235365	0.820063958		25046.47611
EG22/2	Al 396.153	1.177586124	0.967214313		105245.3888
EG22/2	Al 394.401	0.542825684	0.977213905		29846.16562
EG22/3	Al 396.153	0.316167975	1.133876417		123380.3748
EG22/3	Al 394.401	0.201434386	1.138420659		34769.75858
EG22/4	Al 396.153	1.144131778	1.297202919		141152.4042
EG22/4	Al 394.401	1.279365969	1.302454641		39779.70101
EG23/1	Al 396.153	1.054178761	1.177890322		128169.6552
EG23/1	Al 394.401	0.934910694	1.178050356		35980.13279
EG23/2	Al 396.153	1.075927372	1.527054012		166163.1669
EG23/2	Al 394.401	1.076032514	1.521642886		46474.17047
EG23/3	Al 396.153	1.314750122	1.847765011		201060.659
EG23/3	Al 394.401	1.216602466	1.838079466		56138.80841
Blanc	Al 396.153	15.67026481			-292.8506043
Blanc	Al 394.401	16.36905342			-53.96100181
St 1 ppm	Al 396.153	0.971213022			10880.12205
St 1 ppm	Al 394.401	0.511158233			3054.47491
EG23/4	Al 396.153	1.27063135	2.199439614		239301.7146
EG23/4	Al 394.401	0.73266133	2.199653975		67187.87877
EG25/1	Al 396.153	1.522431971	1.007018841		109564.879
EG25/1	Al 394.401	0.924201577	1.022314188		31226.33037
EG25/2	Al 396.153	0.833110194	1.188829993		129346.1543
EG25/2	Al 394.401	0.521614974	1.189773215		36341.32435
EG25/3	Al 396.153	0.751557517	1.330880287		144801.3996
EG25/3	Al 394.401	1.02919667	1.332839769		40711.25633

EG25/4	Al 396.153	1.259810308	1.500663413		163274.011
EG25/4	Al 394.401	1.08401946	1.507758374		46054.10123
EG26/1	Al 396.153	1.730124492	1.072745457		116716.015
EG26/1	Al 394.401	1.834803826	1.118949973		34178.04617
St 2 ppm	Al 396.153	0.707794843	1.981076824	99.05384121	215543.5765
St 2 ppm	Al 394.401	0.300043949	1.999570351	99.97851754	61076.37467
EG26/2	Al 396.153	1.463180213	1.240353241		134951.9465
EG26/2	Al 394.401	1.450293967	1.267398425		38712.36688
EG26/3	Al 396.153	1.388382219	1.410210593		153432.6338
EG26/3	Al 394.401	1.359650241	1.441038664		44016.16443
EG26/4	Al 396.153	1.262452142	1.591770386		173186.5608
EG26/4	Al 394.401	1.211390695	1.627700074		49717.69035
EG27/1	Al 396.153	2.429129037	0.879866425		95730.54092
EG27/1	Al 394.401	1.259903717	0.915090823		27951.21959
EG27/2	Al 396.153	1.305027625	1.05532778		114820.9505
EG27/2	Al 394.401	1.706383393	1.106869801		33809.06034
EG27/3	Al 396.153	1.607058547	1.218454101		132569.2933
EG27/3	Al 394.401	1.49895166	1.244668797		38018.09612
EG27/4	Al 396.153	0.651286705	1.386259805		150826.7588
EG27/4	Al 394.401	0.851589406	1.41342734		43172.78348
EG28/1	Al 396.153	1.116036969	1.078460975		117337.8704
EG28/1	Al 394.401	1.128212106	1.077806972		32921.34353
EG28/2	Al 396.153	1.218032004	1.419992175		154496.8818
EG28/2	Al 394.401	1.205152154	1.412464991		43143.38875
EG28/3	Al 396.153	1.462675011	1.75058105		190465.3549
EG28/3	Al 394.401	1.461287084	1.748009295		53392.50534
EG28/4	Al 396.153	1.483229309	2.09035073		227432.7108
EG28/4	Al 394.401	0.716268564	2.104136703		64270.32765
EG29/1	Al 396.153	1.310831865	1.800737286		195922.4146
EG29/1	Al 394.401	1.270350748	1.801588779		55029.07722
EG29/2	Al 396.153	1.466243129	2.12474641		231175.0027
EG29/2	Al 394.401	0.168858863	2.163678538		66089.01807
EG29/3	Al 396.153	2.122051172	2.465023492		268197.5646
EG29/3	Al 394.401	1.225077317	2.506814998		76570.03515
EG29/4	Al 396.153	2.084327605	2.824815987		307343.4271
EG29/4	Al 394.401	1.305316808	2.864681025		87500.96316
EG30/1	Al 396.153	15.67954791	0.001479521		160.9737397
EG30/1	Al 394.401	20.93244016	0.002188827		66.85717034
EG30/2	Al 396.153	4.085664175	0.011379646		1238.119359
EG30/2	Al 394.401	1.518094009	0.012647683		386.3203066
EG30/3	Al 396.153	4.40396649	0.018419319		2004.044369
EG30/3	Al 394.401	1.097143696	0.019830733		605.7247609
EG30/4	Al 396.153	1.191660515	0.027012722		2939.017155
EG30/4	Al 394.401	0.952013321	0.028676484		875.9159984
St 2 ppm	Al 396.153	2.593377479	1.995239034	99.76195172	217084.4422
St 2 ppm	Al 394.401	1.181029766	2.003624974	100.1812487	61200.2221

Sample ID	Analyte Name	RSD (Corr Int)	Conc (Samp)	QC Recovery	Int (Corr)
Blanc	Al 396.153	8.608465315			-533.3806225
Blanc	Al 394.401	17.81326693			-108.0665527
St 50 ppb	Al 396.153	1.088301649			5497.230151
St 50 ppb	Al 394.401	1.553221411			1596.824016
St 100 ppb	Al 396.153	0.630492806			10811.65861
St 100 ppb	Al 394.401	0.396196725			3075.274645
St 500 ppb	Al 396.153	0.632388985			54008.62268
St 500 ppb	Al 394.401	0.553101622			15659.05474
St 1 ppm	Al 396.153	1.433263727			100042.6147
St 1 ppm	Al 394.401	0.717939983			29139.31067
St 10 ppm	Al 396.153	1.181862875			1052278.72

St 10 ppm	Al 394.401	0.590800215			309832.3997
St 2 ppm	Al 396.153	0.684130749	1.960745561	98.03727805	206238.9711
St 2 ppm	Al 394.401	0.248127562	1.937040733	96.85203666	59982.12844
Blanc	Al 396.153	3.914410705			-477.9264568
Blanc	Al 394.401	9.406917754			-87.99990819
St 100 ppb	Al 396.153	0.29771931			10857.63347
St 100 ppb	Al 394.401	0.810234306			3103.00762
31-1	Al 396.153	0.501422714	1.454224477		157894.3636
31-1	Al 394.401	0.381586536	1.494523072		46375.16479
31-2	Al 396.153	0.857925646	1.793012043		194678.6757
31-2	Al 394.401	0.409601986	1.830750451		56808.32598
31-3	Al 396.153	0.7140352	2.146038253		233008.9677
31-3	Al 394.401	1.094269541	2.197472256		68187.73153
31-4	Al 396.153	0.2110516	2.477549476		269003.2413
31-4	Al 394.401	0.378326117	2.546665234		79023.21626
32-1	Al 396.153	0.466231896	1.19093557		129307.4191
32-1	Al 394.401	0.393116856	1.205705929		37413.14684
32-2	Al 396.153	0.595210358	1.528315705		165938.9175
32-2	Al 394.401	0.66427077	1.553638938		48209.53463
32-3	Al 396.153	0.575466001	1.87526005		203608.8629
32-3	Al 394.401	0.318069124	1.918657156		59536.07774
32-4	Al 396.153	0.792896203	2.193448117		238156.5569
32-4	Al 394.401	0.323964569	2.229450301		69180.01273
33-1	Al 396.153	0.33070113	1.095831213		118981.3366
33-1	Al 394.401	0.586598444	1.103196294		34232.26505
33-2	Al 396.153	0.725329533	1.426385573		154871.7175
33-2	Al 394.401	0.316166441	1.452380948		45067.49147
33-3	Al 396.153	1.02079995	1.748934932		189892.9446
33-3	Al 394.401	0.397224127	1.782722822		55318.025
33-4	Al 396.153	0.821720255	2.090292001		226956.244
33-4	Al 394.401	0.180785115	2.132378245		66167.85942
34-1	Al 396.153	1.062775587	1.3862926		150518.5694
34-1	Al 394.401	0.113723353	1.420956342		44092.38356
34-2	Al 396.153	0.846149252	1.720740266		186831.6711
34-2	Al 394.401	0.786595056	1.754410519		54439.49209
34-3	Al 396.153	0.769923613	2.059507561		223613.7823
34-3	Al 394.401	0.784903299	2.108879981		65438.70648
34-4	Al 396.153	0.689736017	2.397124439		260270.9854
34-4	Al 394.401	0.279912854	2.447271088		75939.00832
35-1	Al 396.153	0.497388438	1.151211285		124994.3019
35-1	Al 394.401	0.708809335	1.166771138		36204.99732
35-2	Al 396.153	1.098865407	1.470994845		159715.2287
35-2	Al 394.401	0.548305007	1.511856618		46913.02605
35-3	Al 396.153	0.982409972	1.788996104		194242.6398
35-3	Al 394.401	0.356061706	1.838207464		57039.71766
35-4	Al 396.153	0.880706859	2.116717592		229825.4378
35-4	Al 394.401	0.640032309	2.175052819		67492.05469
36-1	Al 396.153	14.43331143	0.002271228		246.6016621
36-1	Al 394.401	32.18813647	0.003330407		103.3427962
36-2	Al 396.153	3.638806937	0.01033655		1122.304732
36-2	Al 394.401	7.214976502	0.011374837		352.9620507
36-3	Al 396.153	2.675105213	0.018034996		1958.173726
36-3	Al 394.401	2.409001321	0.018380105		570.3360618
36-4	Al 396.153	1.413083123	0.025580698		2777.458434
36-4	Al 394.401	5.852959364	0.025822427		801.2718685

Sample ID	Analyte Name	RSD (Corr Int)	Conc (Samp)	QC Recovery	Int (Corr)
St 2 ppm	Al 396.153	0.341574928	1.878419849	93.92099243	199274.5123
St 2 ppm	Al 394.401	0.494628909	1.868272581	93.41362906	58300.05682

Blanc	Al 396.153	12.96324259			-475.7170222
Blanc	Al 394.401	53.33066515			-81.87644795
St 100 ppb	Al 396.153	0.983096843			10419.70443
St 100 ppb	Al 394.401	1.331789482			3000.085322
35-4	Al 396.153	0.64265611	2.178353879		226978.0356
35-4	Al 394.401	0.181886145	2.233569474		67008.98994
36-1	Al 396.153	16.5521448	0.002559869		266.7308242
36-1	Al 394.401	36.74700888	0.002284817		68.54647147
36-2	Al 396.153	0.089184565	0.010590811		1103.53124
36-2	Al 394.401	10.13476646	0.010085945		302.5869568
36-3	Al 396.153	1.01034103	0.019292334		2010.204155
36-3	Al 394.401	1.546827302	0.018759036		562.7870937
36-4	Al 396.153	0.58275607	0.02694364		2807.447677
36-4	Al 394.401	3.216916255	0.027258652		817.7828224
37-1	Al 396.153	0.425802365	0.996721452		103855.4293
37-1	Al 394.401	0.457587446	1.021176059		30636.15306
37-2	Al 396.153	0.481732596	1.167124522		121610.9255
37-2	Al 394.401	0.437860568	1.177047625		35312.43304
37-3	Al 396.153	0.804777549	1.334689205		139070.6702
37-3	Al 394.401	0.725664298	1.352169327		40566.23351
37-4	Al 396.153	0.608017045	1.512862266		157635.7766
37-4	Al 394.401	0.563171857	1.539759892		46194.1105
38-1	Al 396.153	0.744171511	1.11882584		116578.3456
38-1	Al 394.401	0.659997242	1.159379256		34782.36688
Blanc	Al 396.153	13.10555726			-487.8174832
Blanc	Al 394.401	27.92267848			-61.45952207
St 100 ppb	Al 396.153	0.879143955			10440.49831
St 100 ppb	Al 394.401	1.129720487			3015.03577
38-2	Al 396.153	0.779423215	1.439819065		150324.2851
38-2	Al 394.401	0.812555778	1.481512142		44668.12101
38-3	Al 396.153	0.833701932	1.775220334		185341.8489
38-3	Al 394.401	0.558502761	1.84760401		55705.92178
38-4	Al 396.153	1.014905474	2.120185668		221357.9487
38-4	Al 394.401	0.268171261	2.204181001		66456.84562
39-1	Al 396.153	0.367221979	1.486600682		155208.519
39-1	Al 394.401	0.559770751	1.547273064		46650.83633
39-2	Al 396.153	0.862493141	1.84021863		192127.9949
39-2	Al 394.401	0.245011717	1.911300411		57626.39107
39-3	Al 396.153	0.361330573	2.178298732		227425.2423
39-3	Al 394.401	0.444158698	2.257782589		68072.95268
39-4	Al 396.153	0.852146963	2.495732739		260566.9343
39-4	Al 394.401	0.391603788	2.613001633		78782.93392
41-1	Al 396.153	0.724379512	0.591093371		61713.09339
41-1	Al 394.401	0.403748607	0.604491421		18225.63256
41-2	Al 396.153	0.525728394	0.764064085		79772.09788
41-2	Al 394.401	0.803475995	0.777883678		23453.47113
41-3	Al 396.153	0.421573589	0.93517558		97636.99055
41-3	Al 394.401	0.38980175	0.959010143		28914.49884
41-4	Al 396.153	0.55914443	1.099204958		114762.475
41-4	Al 394.401	0.63879214	1.112030034		33528.10331
42-1	Al 396.153	0.5963161	0.834539673		87130.10036
42-1	Al 394.401	0.330085327	0.854078954		25750.78596
42-2	Al 396.153	1.169594286	1.008196956		105260.7861
42-2	Al 394.401	0.454663096	1.032354987		31125.87214
42-3	Al 396.153	0.756723432	1.190432492		124287.0841
42-3	Al 394.401	0.570837966	1.199104534		36153.43062
42-4	Al 396.153	0.653969798	1.35718556		141696.9354
42-4	Al 394.401	0.561109218	1.369066513		41277.84508
St 2 ppm	Al 396.153	0.405922809	1.910049589	95.50247944	199418.695

St 2 ppm	Al 394.401	0.862753802	1.94645428	97.32271398	58686.29278
43-1	Al 396.153	1.148009926	1.124899293		117445.0916
43-1	Al 394.401	0.710031544	1.139146051		34345.66091
43-2	Al 396.153	1.150400002	1.468560701		153325.0551
43-2	Al 394.401	0.776059669	1.506110012		45409.7556
43-3	Al 396.153	0.547556805	1.795205116		187428.3597
43-3	Al 394.401	0.49738527	1.836129381		55359.95763
43-4	Al 396.153	0.771954791	2.144653783		223912.5419
43-4	Al 394.401	0.624029595	2.186536858		65924.8684
44-1	Al 396.153	0.150813299	0.518765113		54161.66282
44-1	Al 394.401	0.394592696	0.530750402		16002.31446
St 2 ppm	Al 396.153	0.878586239	1.914523796	95.7261898	199885.8245
St 2 ppm	Al 394.401	0.45552348	1.953249268	97.66246341	58891.16412
44-2	Al 396.153	0.635957104	0.694346117		72493.19461
44-2	Al 394.401	0.413022149	0.71221554		21473.55328
44-3	Al 396.153	1.100669131	0.86590539		90404.83761
44-3	Al 394.401	0.85227607	0.892677335		26914.54096
44-4	Al 396.153	1.149271964	1.045083705		109111.9465
44-4	Al 394.401	0.726127348	1.066968935		32169.49504
46-1	Al 396.153	0.863897038	0.323702439		33796.14769
46-1	Al 394.401	0.14602127	0.335800153		10124.49473
46-2	Al 396.153	0.896198991	0.491997425		51366.98282
46-2	Al 394.401	0.772403695	0.514505395		15512.52171
46-3	Al 396.153	0.918122758	0.664850467		69413.7017
46-3	Al 394.401	0.537288213	0.69466962		20944.53753
46-4	Al 396.153	1.164780567	0.832227377		86888.68523
46-4	Al 394.401	0.766080028	0.875394926		26393.47016
47-1	Al 396.153	0.699643195	0.199489697		20827.7184
47-1	Al 394.401	0.601988664	0.203822857		6145.332047
47-2	Al 396.153	0.342367967	0.37306331		38949.66854
47-2	Al 394.401	0.353465716	0.382537747		11533.64992
47-3	Al 396.153	0.894076782	0.539571486		56333.95187
47-3	Al 394.401	0.228801005	0.554011426		16703.64266
Blanc	Al 396.153	10.6037499			-438.3344262
Blanc	Al 394.401	9.079212891			-92.36758433
St 100 ppb	Al 396.153	0.48347599			10520.63365
St 100 ppb	Al 394.401	0.252067029			3087.169425
47-4	Al 396.153	0.700211009	0.705723286		74246.5615
47-4	Al 394.401	0.702528173	0.710673417		21939.69245
48-1	Al 396.153	0.96515286	1.151929407		121190.2728
48-1	Al 394.401	0.960415868	1.146250858		35386.70604
48-2	Al 396.153	0.455291338	1.338916375		140862.4867
48-2	Al 394.401	0.506370522	1.33716779		41280.63517
48-3	Al 396.153	0.544676141	1.494821169		157264.6589
48-3	Al 394.401	0.400065819	1.502736394		46392.01851
48-4	Al 396.153	0.740630169	1.668302832		175516.0291
48-4	Al 394.401	0.387028451	1.682830224		51951.82016
49-1	Al 396.153	1.122400857	0.853399794		89783.06586
49-1	Al 394.401	0.397522557	0.856770568		26449.95902
49-2	Al 396.153	0.616206397	1.194640919		125683.7945
49-2	Al 394.401	0.368757859	1.19427942		36869.4291
49-3	Al 396.153	0.701453789	1.52093823		160012.3392
49-3	Al 394.401	0.37318996	1.546927531		47756.27376
49-4	Al 396.153	0.458289601	1.848767211		194502.0254
49-4	Al 394.401	0.886016826	1.86844481		57682.0569
50-1	Al 396.153	0.993836219	0.834747357		87820.7113
50-1	Al 394.401	0.317801793	0.841908229		25991.13342
50-2	Al 396.153	0.688136144	2.486852022		261632.5906
50-2	Al 394.401	0.516688079	2.504408131		77315.32211

50-3	Al 396.153	0.831842265	4.140659464		435623.6129
50-3	Al 394.401	0.586050366	4.17267913		128817.6743
50-4	Al 396.153	0.502782996	5.845543914		614988.2601
50-4	Al 394.401	1.197668726	5.927911352		183004.6668
51-1	Al 396.153	0.844842775	1.047207288		110172.8423
51-1	Al 394.401	0.650717903	1.060857676		32750.47381
51-2	Al 396.153	0.437479873	1.212981028		127613.2902
51-2	Al 394.401	0.618619867	1.211324769		37395.6479
St 2 ppm	Al 396.153	0.67927917	1.914066177	95.70330883	201371.8903
St 2 ppm	Al 394.401	0.646473418	1.927098578	96.3549289	59492.7981
51-3	Al 396.153	0.629898189	1.389818669		146217.7306
51-3	Al 394.401	0.457292508	1.390161193		42916.6313
51-4	Al 396.153	0.921094132	1.535134516		161505.8784
51-4	Al 394.401	1.020944466	1.539521248		47527.62928
52-1	Al 396.153	1.040238746	2.393778223		251840.6372
52-1	Al 394.401	0.412275692	2.415904159		74583.05455
52-2	Al 396.153	0.980718382	2.671642726		281073.7437
52-2	Al 394.401	0.667736454	2.746407561		84786.25453
52-3	Al 396.153	0.946394063	3.019141705		317632.8382
52-3	Al 394.401	0.717721495	3.062587845		94547.27559
52-4	Al 396.153	0.90980466	3.353293827		352787.7587
52-4	Al 394.401	0.712206912	3.380360626		104357.4597
53-1	Al 396.153	0.372525432	0.670483066		70539.06704
53-1	Al 394.401	1.028718736	0.681947459		21052.87346
53-2	Al 396.153	1.185102595	1.006584852		105899.1047
53-2	Al 394.401	0.633929697	1.014036342		31305.01992
53-3	Al 396.153	0.119482996	1.347320287		141746.6314
53-3	Al 394.401	0.549246121	1.344848442		41517.74993
53-4	Al 396.153	0.975144562	1.673621332		176075.5691
53-4	Al 394.401	0.354047133	1.683337863		51967.49183
54-1	Al 396.153	0.399095022	0.434870723		45751.15559
54-1	Al 394.401	0.571693563	0.440879862		13610.70831
54-2	Al 396.153	0.987422674	0.599395275		63060.18094
54-2	Al 394.401	0.640998698	0.61505035		18987.64637
54-3	Al 396.153	0.838670885	0.774420858		81473.98135
54-3	Al 394.401	0.554968132	0.797138292		24609.00964
54-4	Al 396.153	0.780191711	0.944445393		99361.6398
54-4	Al 394.401	0.794007175	0.964396746		29772.56149
55-1	Al 396.153	16.24049772	0.00170666		179.5514627
55-1	Al 394.401	7.907019696	0.003220875		99.43387413
Blanc	Al 396.153	2.337631848			-452.8213604
Blanc	Al 394.401	17.30336675			-68.90994539
St 100 ppb	Al 396.153	0.514272302			10494.6893
St 100 ppb	Al 394.401	1.573652616			3047.227689
55-2	Al 396.153	1.459083332	0.010446128		1096.288658
55-2	Al 394.401	10.88964114	0.010815279		329.5661907
55-3	Al 396.153	1.232354901	0.018998845		1993.869722
55-3	Al 394.401	4.621475597	0.018262104		556.4879024
55-4	Al 396.153	2.29297143	0.027569315		2893.313974
55-4	Al 394.401	2.58937471	0.027414024		835.3677222
56-1	Al 396.153	0.363306638	0.99436224		104355.2276
56-1	Al 394.401	0.464356239	1.013438773		30881.7869
56-2	Al 396.153	1.034518281	2.647508788		277847.8216
56-2	Al 394.401	0.767223055	2.718188747		82829.40012
56-3	Al 396.153	0.664448251	4.296652396		450920.3194
56-3	Al 394.401	0.294744902	4.451488261		135646.9828
56-4	Al 396.153	0.717806595	6.018602956		631633.6806
56-4	Al 394.401	0.118607432	6.222682698		189619.3102
57-1	Al 396.153	0.532325908	0.593383735		62273.77941

57-1	Al 394.401	0.318300027	0.603181912		18380.32623
57-2	Al 396.153	0.924286386	0.76727418		80523.04131
57-2	Al 394.401	0.486549244	0.787178805		23987.13051
57-3	Al 396.153	1.189362973	0.948366234		99528.08966
57-3	Al 394.401	0.385048696	0.967511673		29482.28358
St 2 ppm	Al 396.153	0.399853581	1.934372852	96.71864262	203006.4208
St 2 ppm	Al 394.401	0.510786317	1.973767269	98.68836347	60145.18275
57-4	Al 396.153	1.035496604	1.125593226		118127.5118
57-4	Al 394.401	0.870119661	1.135176323		34591.40722
58-1	Al 396.153	0.91423292	0.697238245		73172.98747
58-1	Al 394.401	0.607337176	0.710049245		21636.81721
58-2	Al 396.153	1.050881976	0.874785253		91805.99441
58-2	Al 394.401	0.494002951	0.887527161		27044.97338
58-3	Al 396.153	0.549947386	1.037558835		108888.576
58-3	Al 394.401	0.787812952	1.048099077		31937.96528
58-4	Al 396.153	0.660868545	1.223780732		128431.9856
58-4	Al 394.401	0.629478016	1.230746135		37503.637
59-1	Al 396.153	0.644018211	0.168695703		17704.08988
59-1	Al 394.401	0.900329533	0.171541788		5227.268861
59-2	Al 396.153	0.991990829	0.339753445		35656.06839
59-2	Al 394.401	0.770785448	0.346850696		10569.33044
59-3	Al 396.153	0.687553334	0.512374694		53772.13217
59-3	Al 394.401	0.159661595	0.520862623		15871.87008
59-4	Al 396.153	1.095154069	0.687563268		72157.62871
59-4	Al 394.401	0.832623244	0.701768274		21384.47716
60-1	Al 396.153	1.109928197	0.458469004		48114.89751
60-1	Al 394.401	1.2649703	0.467233736		14237.67576
60-2	Al 396.153	0.647476666	0.458175869		48084.13394
60-2	Al 394.401	0.670774273	0.468542094		14277.54443
60-3	Al 396.153	0.796801175	0.471083823		49438.78355
60-3	Al 394.401	0.497376558	0.480368055		14637.90839
60-4	Al 396.153	0.81880457	0.481247941		50505.47616
60-4	Al 394.401	0.124523128	0.495952277		15112.79511
61-1	Al 396.153	1.358608045	0.219313918		23016.3143
61-1	Al 394.401	1.593627565	0.225674766		6876.82395
61-2	Al 396.153	0.744119896	0.396515293		41613.04799
61-2	Al 394.401	0.278952386	0.403855691		12306.40245
61-3	Al 396.153	0.446387465	0.562265413		59008.00812
61-3	Al 394.401	1.222235287	0.585558821		17843.31051
61-4	Al 396.153	0.091351535	0.736089851		77250.34283
61-4	Al 394.401	0.404047278	0.769153759		23437.86632
62-1	Al 396.153	0.711590864	0.407430641		42758.57989
62-1	Al 394.401	0.793908343	0.409969327		12492.69886
62-2	Al 396.153	0.591961441	0.568416771		59653.57406
62-2	Al 394.401	0.360279252	0.584467924		17810.06842
62-3	Al 396.153	0.441062361	0.753129989		79038.65237
62-3	Al 394.401	0.153378367	0.767461822		23386.30913
Blanc	Al 396.153	10.69672527			-425.6780121
Blanc	Al 394.401	23.00677107			-97.42033159
St 100 ppb	Al 396.153	1.131394482			10608.62472
St 100 ppb	Al 394.401	1.47756912			3127.612302
62-4	Al 396.153	0.568582475	0.907127555		96233.75804
62-4	Al 394.401	0.948250662	0.920702958		28796.01898
63-1	Al 396.153	1.234432988	0.185558249		19685.17828
63-1	Al 394.401	0.725834493	0.190670976		5963.448899
63-2	Al 396.153	0.755643683	0.357547746		37930.89852
63-2	Al 394.401	0.937880511	0.36740282		11490.93579
63-3	Al 396.153	0.757482164	0.520187161		55184.70374
63-3	Al 394.401	0.92685281	0.528143126		16518.26938

63-4	Al 396.153	1.091733151	0.691382606		73346.18606
63-4	Al 394.401	0.328103068	0.70532081		22059.70041
St 2 ppm	Al 396.153	1.202719658	1.912613515	95.63067573	202901.99
St 2 ppm	Al 394.401	0.542804616	1.897921718	94.89608589	59359.63313
64-1	Al 396.153	1.116371342	6.605669239		700770.6594
64-1	Al 394.401	1.086417713	6.725660341		210352.5802
64-2	Al 396.153	0.722256632	6.758548492		716989.0457
64-2	Al 394.401	0.678676793	6.860753013		214577.7552
64-3	Al 396.153	0.584198112	6.874786193		729320.2672
64-3	Al 394.401	0.093069816	7.000569882		218950.6849
64-4	Al 396.153	0.978918433	7.084127068		751528.455
64-4	Al 394.401	0.705538626	7.228176802		226069.3469
65-1	Al 396.153	0.34934751	27.76784569		2945786.54
65-1	Al 394.401	0.940421879	28.82049096		901393.221
65-2	Al 396.153	1.080848964	24.97125449		2649106.675
65-2	Al 394.401	0.834317918	25.77039296		805997.9806
65-3	Al 396.153	0.717509063	28.12970392		2984174.723
65-3	Al 394.401	1.14801767	29.10163924		910186.4489
65-4	Al 396.153	0.907257116	28.23251155		2995081.198
65-4	Al 394.401	0.264304323	29.37058376		918597.991
66-1	Al 396.153	41.09803427	0.005496789		583.1336745
66-1	Al 394.401	8.937526753	0.006156031		192.5367937
66-2	Al 396.153	2.120420681	0.01110494		1178.081379
66-2	Al 394.401	5.765188916	0.011735196		367.0314407
66-3	Al 396.153	5.277516635	0.018553817		1968.304827
66-3	Al 394.401	2.23953096	0.019972982		624.6774506
66-4	Al 396.153	1.612629959	0.025676219		2723.893718
66-4	Al 394.401	2.418896687	0.025302482		791.3635335
67-1	Al 396.153	1.10068499	0.106990199		11350.18867
67-1	Al 394.401	1.050842738	0.106033456		3316.315406
67-2	Al 396.153	0.618270098	0.444559326		47161.63055
67-2	Al 394.401	0.097528617	0.440594573		13780.09006
67-3	Al 396.153	0.987218975	0.775367252		82255.80193
67-3	Al 394.401	0.345417845	0.776050523		24271.85164
67-4	Al 396.153	0.524744071	1.117625531		118564.6983
67-4	Al 394.401	0.88368795	1.107694322		34644.38388
68-1	Al 396.153	0.799356679	0.098177878		10415.32262
68-1	Al 394.401	1.988496995	0.096970587		3032.864001
68-2	Al 396.153	0.469161453	0.436474065		46303.8955
68-2	Al 394.401	1.028880506	0.43027992		13457.4877
68-3	Al 396.153	0.815399052	0.764300488		81081.77042
68-3	Al 394.401	0.53772424	0.765250657		23934.07368
68-4	Al 396.153	0.257889665	1.109042277		117654.1331
68-4	Al 394.401	0.603231788	1.105246451		34567.82398
69-1	Al 396.153	0.7783133	23.55171856		2498513.436
69-1	Al 394.401	0.42757899	24.28276012		759470.5927
69-2	Al 396.153	1.010285999	23.62094239		2505857.133
69-2	Al 394.401	0.302567867	24.48907203		765923.2296
69-3	Al 396.153	1.079279251	23.7084096		2515136.2
69-3	Al 394.401	0.958823869	24.70517522		772682.0995
69-4	Al 396.153	0.910202208	29.31329377		3109737.328
69-4	Al 394.401	0.24851539	30.68908367		959835.5564
St 2 ppm	Al 396.153	1.181543741	1.933580168	96.67900839	205126.2636
St 2 ppm	Al 394.401	0.350001048	1.95726609	97.8633045	61215.69502

Appendix Table 9: Al, Ca, K, Na, Ti ICP-OES-MS raw data.

Sample ID	Analyte Name	Reported Conc (Calib)	Reported Conc (Samp)	RSD (Conc)	QC Recovery
Blanc	Al 396.153	[0.00]		0	
Blanc	Ca 317.933	[0.00]		0	
Blanc	K 766.490	[0.00]		0	
Blanc	Na 589.592	[0.00]		0	
Blanc	Ti 334.940	[0.00]		0	
St 10 mg/l Roth IV	Al 396.153	[10]		0	
St 10 mg/l Roth IV	Ca 317.933	[10]		0	
St 10 mg/l Roth IV	K 766.490	[10]		0	
St 10 mg/l Roth IV	Na 589.592	[10]		0	
St 1 mg/l Titan	Ti 334.940	[1]		0	
2 mg/l Alu	Al 396.153	2.083	2.083	0.118574256	104.1553564
2 mg/l Alu	Ca 317.933	-0.001	-0.001	137.7463683	
2 mg/l Alu	K 766.490	0.005	0.005	257.7362797	
2 mg/l Alu	Na 589.592	0.034	0.034	10.44284037	
2 mg/l Alu	Ti 334.940	0.001	0.001	29.67750166	
71	Al 396.153	3.306	3.306	0.259733061	
71	Ca 317.933	0.713	0.713	0.487707222	
71	K 766.490	0.774	0.774	2.563420068	
71	Na 589.592	0.529	0.529	1.723692264	
71	Ti 334.940	1.23	1.23	0.134058774	
72	Al 396.153	0.903	0.903	0.167986211	
72	Ca 317.933	0.332	0.332	0.38995642	
72	K 766.490	0.134	0.134	5.211500457	
72	Na 589.592	0.093	0.093	3.993012063	
72	Ti 334.940	0.728	0.728	0.266335921	
76	Al 396.153	0.009	0.009	6.733013265	
76	Ca 317.933	0.279	0.279	1.454332018	
76	K 766.490	0.022	0.022	23.67866458	
76	Na 589.592	0.007	0.007	18.55708369	
76	Ti 334.940	0.001	0.001	33.80850888	
78	Al 396.153	0.976	0.976	0.431202565	
78	Ca 317.933	0.621	0.621	0.688052766	
78	K 766.490	0.607	0.607	1.801144687	
78	Na 589.592	0.305	0.305	3.300400776	
78	Ti 334.940	0.251	0.251	0.52641327	
80	Al 396.153	2.104	2.104	0.122861995	
80	Ca 317.933	0.246	0.246	0.490051656	
80	K 766.490	0.016	0.016	62.58972516	
80	Na 589.592	0.002	0.002	274.3717803	
80	Ti 334.940	0.001	0.001	23.52771343	
88	Al 396.153	1.737	1.737	0.471021738	
88	Ca 317.933	0.703	0.703	0.858162781	
88	K 766.490	0.73	0.73	3.616224471	
88	Na 589.592	0.253	0.253	2.093452912	
88	Ti 334.940	0.823	0.823	0.486804242	
98	Al 396.153	1.67	1.67	0.263625641	
98	Ca 317.933	0.489	0.489	1.043017545	
98	K 766.490	0.873	0.873	1.515230017	
98	Na 589.592	0.441	0.441	0.978654282	
98	Ti 334.940	0.328	0.328	0.160432088	
111	Al 396.153	1.741	1.741	0.306876621	
111	Ca 317.933	0.234	0.234	0.596942168	
111	K 766.490	0.934	0.934	2.359690075	
111	Na 589.592	0.586	0.586	0.884387755	
111	Ti 334.940	0.521	0.521	0.267726693	
112	Al 396.153	0.663	0.663	3.110963935	
112	Ca 317.933	0.223	0.223	0.994960113	
112	K 766.490	8.188	8.188	0.953414379	
112	Na 589.592	0.093	0.093	6.571751027	
112	Ti 334.940	0.349	0.349	0.336343462	
113	Al 396.153	0.906	0.906	0.243942682	

113	Ca 317.933	0.235	0.235	0.329109554	
113	K 766.490	31.03	31.03	0.572532952	
113	Na 589.592	0.113	0.113	2.040603605	
113	Ti 334.940	0.822	0.822	0.198916586	
119	Al 396.153	1.424	1.424	0.215667083	
119	Ca 317.933	0.594	0.594	0.76093437	
119	K 766.490	0.875	0.875	0.634966546	
119	Na 589.592	0.419	0.419	1.027081463	
119	Ti 334.940	0.452	0.452	0.262164698	
121	Al 396.153	2.112	2.112	0.53245663	
121	Ca 317.933	0.512	0.512	0.813397285	
121	K 766.490	0.451	0.451	1.150247125	
121	Na 589.592	0.453	0.453	0.856374241	
121	Ti 334.940	0.55	0.55	0.421302519	
2 mg/l Alu	Al 396.153	2.096	2.096	0.250523506	104.8095574
2 mg/l Alu	Ca 317.933	-0.003	-0.003	1.521900572	
2 mg/l Alu	K 766.490	0.013	0.013	49.81089197	
2 mg/l Alu	Na 589.592	0.002	0.002	34.83676537	
2 mg/l Alu	Ti 334.940	0.001	0.001	18.05923064	
122	Al 396.153	2.35	2.35	0.158228598	
122	Ca 317.933	0.551	0.551	0.866978909	
122	K 766.490	0.437	0.437	6.639067517	
122	Na 589.592	0.488	0.488	0.797964818	
122	Ti 334.940	0.642	0.642	0.193813175	
123	Al 396.153	4.801	4.801	0.41253456	
123	Ca 317.933	0.888	0.888	0.845133422	
123	K 766.490	0.952	0.952	1.202815273	
123	Na 589.592	0.814	0.814	0.820507008	
123	Ti 334.940	1.605	1.605	0.291651565	
124	Al 396.153	0.845	0.845	0.302419349	
124	Ca 317.933	0.202	0.202	0.355036405	
124	K 766.490	0.056	0.056	25.71362524	
124	Na 589.592	0.082	0.082	3.743123035	
124	Ti 334.940	0.476	0.476	0.333865901	
125	Al 396.153	0.008	0.008	1.839219764	
125	Ca 317.933	0.116	0.116	1.270592391	
125	K 766.490	0.023	0.023	27.87359069	
125	Na 589.592	0.003	0.003	304.624245	
125	Ti 334.940	0.001	0.001	24.2836099	
126	Al 396.153	1.121	1.121	0.20720189	
126	Ca 317.933	0.725	0.725	0.071173295	
126	K 766.490	0.542	0.542	6.480502515	
126	Na 589.592	0.267	0.267	1.560955389	
126	Ti 334.940	0.172	0.172	0.175297085	
127	Al 396.153	4.849	4.849	0.271039908	
127	Ca 317.933	1.778	1.778	0.480857564	
127	K 766.490	1.954	1.954	1.145484983	
127	Na 589.592	0.349	0.349	1.249552917	
127	Ti 334.940	0.601	0.601	0.00780435	
128	Al 396.153	2.867	2.867	0.22998244	
128	Ca 317.933	0.492	0.492	0.146206749	
128	K 766.490	0.543	0.543	0.072818576	
128	Na 589.592	0.588	0.588	0.826250302	
128	Ti 334.940	4.968	4.968	0.20467946	
129	Al 396.153	2.213	2.213	0.197033474	
129	Ca 317.933	0.322	0.322	1.277618063	
129	K 766.490	0.357	0.357	5.332560896	
129	Na 589.592	0.442	0.442	1.575381242	
129	Ti 334.940	0.784	0.784	0.422710492	
130	Al 396.153	2.259	2.259	0.257679688	
130	Ca 317.933	0.072	0.072	2.042844632	
130	K 766.490	0	0	7360.877593	
130	Na 589.592	0.005	0.005	57.16136449	
130	Ti 334.940	0.003	0.003	18.28811439	

131	Al 396.153	2.123	2.123	0.199185098	
131	Ca 317.933	0.463	0.463	0.677792616	
131	K 766.490	0.358	0.358	3.440463781	
131	Na 589.592	0.359	0.359	1.223058372	
131	Ti 334.940	0.896	0.896	0.036648708	
134	Al 396.153	1.075	1.075	0.426038083	
134	Ca 317.933	0.694	0.694	0.440375551	
134	K 766.490	0.562	0.562	2.461654226	
134	Na 589.592	0.24	0.24	1.32929141	
134	Ti 334.940	0.166	0.166	0.615750354	
2 mg/l Alu	Al 396.153	2.098	2.098	0.656950387	104.9211699
2 mg/l Alu	Ca 317.933	-0.001	-0.001	46.54171613	
2 mg/l Alu	K 766.490	0	0	4218.043376	
2 mg/l Alu	Na 589.592	-0.005	-0.005	69.3322427	
2 mg/l Alu	Ti 334.940	0.001	0.001	11.31795917	

Appendix Table 10: Aluminium concentration in samples.

STD anpassung x-achse	E	slope	intercept	konz rohr in mg/L	sample dilut. fac.	mg/L VF corr	mg in 0.2ml	in 10 ml	QTZ in g	ppm in sample	Sample ID	rsq	Lab ID
0	0.078669817	0.9801	0.0797	0.0813	0.5002	0.1625	0.0082	0.4078	18.62	21.91	ER 011	0.9999	EG 11
0.165701608	0.242267537												
0.332630146	0.408210702												
0.501908317	0.569845528												
0	1.414104396	1.0672	1.4088	1.3200	0.5005	2.6374	0.1324	6.6200	54.69	121.05	12 mod6 005	0.9995	EG 12
0.327477599	1.7453043												
0.648908312	2.110982851												
0.975828771	2.448097423												
0	1.296346857	1.0479	1.2864	1.2276	0.4992	2.4590	0.1234	6.1721	35.26	175.03	12 mod 7 001	0.9994	EG 14
0.34668348	1.634983337												
0.677149165	1.994851153												
1.006085566	2.346396669												
0	1.592690776	1.0465	1.5926	1.5219	0.4979	3.0565	0.1534	7.6719	34.96	219.43	12 mod7 005	1.0000	EG 15
0.348155236	1.959039439												
0.688944938	2.309120193												
1.015492254	2.657624378												
0	1.477929471	1.0199	1.4584	1.4299	0.5017	2.8505	0.1431	7.1547	36.31	197.07	12 mod 7 007	0.9976	EG16
0.334137019	1.769733928												
0.665780031	2.137352222												
0.991411105	2.47948726												
0	0.857476397	0.9024	0.8645	0.9580	0.5094	1.8806	0.0944	4.7204	28.00	168.57	12 S7 001 d	0.9957	EG 18
0.1685618	1.033480462												
0.335978394	1.155409987												
0.504480227	1.322418859												
0	1.054729341	0.9851	1.0409	1.0566	0.4989	2.1181	0.1063	5.3163	36.00	147.68	12 S7002b	0.9986	EG 21
0.332813797	1.354331561												
0.667044407	1.685386922												
1.002240177	2.041398733												
0	0.820063958	0.9602	0.8179	0.8518	0.4987	1.7082	0.0858	4.2877	26.51	161.74	12 S7 002c	0.9999	EG 22
0.168784947	0.977213905												
0.334710639	1.138420659												
0.503024655	1.302454641												
0	1.178050356	1.0048	1.1767	1.1711	0.4944	2.3687	0.1189	5.9454	36.40	163.34	12 S7 002d	0.9996	EG 23
0.339213671	1.521642886												
0.670145429	1.838079466												
1.011481999	2.199653975												
0	1.022314188	0.9563	1.0220	1.0687	0.4977	2.1473	0.1078	5.3896	26.90	200.36	12 S7 004 a	0.9983	EG 25
0.169766795	1.189773215												
0.337796493	1.332839769												
0.501386508	1.507758374												
0	1.118949973	1.0096	1.1082	1.0976	0.4981	2.2038	0.1106	5.5317	26.80	206.41	12 S7 004b	0.9971	EG 26
0.169955604	1.267398425												
0.337333311	1.441038664												
0.50536786	1.627700074												
0	0.915090823	0.9629	0.9261	0.9617	0.4961	1.9386	0.0973	4.8659	26.90	180.89	12 S7 004 c	0.9965	EG 27
0.16901124	1.106869801												
0.33407435	1.244668797												
0.510195699	1.41342734												
0	1.077806972	1.0173	1.0730	1.0548	0.4966	2.1239	0.1066	5.3309	41.20	129.39	12 S7 004 d	0.9997	EG28
0.336215662	1.412464991												
0.672588576	1.748009295												
1.006653455	2.104136703												
0	1.801588779	1.0504	1.8057	1.7191	0.4970	3.4588	0.1736	8.6817	48.20	180.12	12 S7 004 e	0.9999	EG29
0.333909553	2.163678538												
0.66929606	2.506814998												
1.009177577	2.864681025												
0	0.002188827	1.0316	0.0028	0.0027	0.4985	0.0054	0.0003	0.0136	1000.00	0.01	blank	0.9958	EG30
0.008541045	0.012647683												
0.016841806	0.019830733												
0.025240607	0.028676484												
0	1.494523072	1.0569	1.4871	1.4071	0.4954	2.8401	0.1426	7.1288	47.82	149.07	12 mod7 002	0.9996	EG 31
0.337690194	1.830750451												
0.668201526	2.197472256												
1.000937872	2.546665234												
0	1.205705929	1.0279	1.2093	1.1765	0.4964	2.3700	0.1190	5.9487	43.31	137.35	12 mod7 003	0.9988	EG 32
0.340804767	1.553638938												
0.668338674	1.918657156												
1.005040805	2.229450301												

0	1.103196294	1.0216	1.1058	1.0825	0.4949	2.1874	0.1098	5.4904	47.29	116.10	12 mod 6 001	0.9998	EG 33
0.332471906	1.452380948												
0.668410879	1.782722822												
1.003228255	2.132378245												
0	1.420956342	1.0271	1.4179	1.3805	0.4978	2.7733	0.1392	6.9610	47.25	147.32	12 mod 6 002	0.9999	EG 34
0.334494891	1.754410519												
0.667924433	2.108879981												
1.003156476	2.447271088												
0	1.166771138	1.0448	1.1537	1.1043	0.4994	2.2110	0.1110	5.5495	35.83	154.89	12 mod 6 003	0.9976	EG 35
0.348317013	1.511856618												
0.682465569	1.838207464												
1.013344573	2.233569474												
0	0.002284817	1.0263	0.0022	0.0021	0.5010	0.0042	0.0002	0.0106	1000.00	0.01	blank	0.9999	EG 36
0.007884272	0.010085945												
0.016098078	0.018759036												
0.024417022	0.027258652												
0	1.021176059	1.0360	1.0108	0.9757	0.5031	1.9392	0.0973	4.8674	33.57	144.99	12 mod 6 004	0.9972	EG 37
0.171285203	1.177047625												
0.338309079	1.352169327												
0.500887892	1.539759892												
0	1.159379256	1.0442	1.1479	1.0993	0.5032	2.1846	0.1097	5.4833	46.35	118.30	12 mod 5 003	0.9993	EG 38
0.335705505	1.481512142												
0.670656577	1.84760401												
1.005751876	2.204181001												
0	1.547273064	1.0622	1.5501	1.4593	0.5052	2.8886	0.1450	7.2505	47.71	151.97	12 mod 5 004	0.9999	EG 39
0.33478767	1.911300411												
0.669052059	2.257782589												
1.000636815	2.613001633												
0	0.604491421	1.0211	0.6074	0.5949	0.5012	1.1868	0.0596	2.9788	18.30	162.77	12 S7 001 a	0.9990	EG 41
0.1674939	0.777883678												
0.334556139	0.959010143												
0.500515745	1.112030034												
0	0.854078954	1.0389	0.8503	0.8184	0.4978	1.6441	0.0825	4.1266	29.60	139.41	12 S7 001 c	0.9996	EG 42
0.181750907	1.032354987												
0.334422182	1.199104534												
0.497916614	1.369066513												
0	1.139146051	1.0354	1.1472	1.1080	0.5150	2.1516	0.1080	5.4006	51.10	105.69	12 S7 001 e	0.9996	EG 43
0.333969291	1.506110012												
0.667314784	1.836129381												
1.006691313	2.186536858												
0	0.530750402	1.0841	0.5316	0.4904	0.4997	0.9813	0.0493	2.4631	21.00	117.29	12 S7 002 a	0.9999	EG 44
0.166592759	0.71221554												
0.330887865	0.892677335												
0.495371848	1.066968935												
0	0.335800153	1.0833	0.3350	0.3092	0.4979	0.6210	0.0312	1.5588	20.80	74.94	12 S7 003 a	1.0000	EG 46
0.16666526	0.514505395												
0.332594535	0.69466962												
0.498243486	0.875394926												
0	0.203822857	1.0151	0.2088	0.2057	0.4986	0.4124	0.0207	1.0352	30.40	34.05	12 S7 003 c	0.9992	EG 47
0.166783155	0.382537747												
0.334373266	0.554011426												
0.499802811	0.710673417												
0	1.146250858	1.0657	1.1505	1.0795	0.4983	2.1663	0.1087	5.4374	31.90	170.45	12 mod7 006	0.9994	EG 48
0.167862738	1.33716779												
0.333338919	1.502736394												
0.50016406	1.682830224												
0	0.856770568	1.0173	0.8582	0.8436	0.4989	1.6910	0.0849	4.2444	53.60	79.19	12 mod 5 001	0.9997	EG 49
0.33366944	1.19427942												
0.666475953	1.546927531												
0.999104775	1.86844481												
0	0.841908229	2.0214	0.8248	0.4080	0.4971	0.8209	0.0412	2.0604	1000.00	2.06	db blank	0.9999	EG 50
0.836539514	2.504408131												
1.670293981	4.17267913												
2.513343773	5.927911352												
0	1.060857676	0.9651	1.0577	1.0959	0.5047	2.1715	0.1090	5.4504	31.10	175.25	12 S7 001 b	0.9983	EG 51
0.169421384	1.211324769												
0.333765436	1.390161193												
0.502801015	1.539521248												
0	2.415904159	0.9589	2.4201	2.5239	0.5057	4.9905	0.2505	12.5261	61.66	203.15	12 S7 002 e	0.9999	EG 52
0.334695522	2.746407561												
0.66804927	3.062587845												
1.004592818	3.380360626												

0	0.681947459	0.9911	0.6808	0.6869	0.5036	1.3640	0.0685	3.4235	64.03	53.47	12 S7 003 e	0.9999	EG 53
0.335020243	1.014036342												
0.675990715	1.344848442												
1.007915079	1.683337863												
0	0.440879862	1.0376	0.4418	0.4258	0.5047	0.8436	0.0423	2.1174	31.60	67.01	12 S7 003 b	0.9997	
0.16822195	0.61505035												EG 54
0.337486602	0.797138292												
0.506624285	0.964396746												
0	0.003220875	0.9588	0.0029	0.0030	0.5051	0.0060	0.0003	0.0151	1000.00	0.02	blank	0.9973	
0.008370815	0.010815279												
0.016754224	0.018262104												EG 55
0.025022919	0.027414024												
0	1.013438773	2.0668	0.9926	0.4802	0.5013	0.9579	0.0481	2.4044	29.49	81.53	12 LMA 008	0.9999	
0.844067768	2.718188747												
1.685614213	4.451488261												
2.519339931	6.222682698												EG 56
0	0.603181912	1.0601	0.6069	0.5725	0.4939	1.1592	0.0582	2.9096	30.00	96.99	12 LME 010	0.9996	
0.167066948	0.787178805												
0.335771203	0.967511673												
0.502329377	1.135176323												
0	0.710049245	1.0272	0.7108	0.6919	0.4987	1.3874	0.0696	3.4825	26.41	131.88	12 ER 016	0.9994	EG 57
0.167576258	0.887527161												
0.335319422	1.048099077												
0.503098197	1.230746135												
0	0.171541788	1.0502	0.1711	0.1629	0.5041	0.3233	0.0162	0.8114	25.59	31.70	12 ER 018	1.0000	
0.166873887	0.346850696												EG 58
0.335048172	0.520862623												
0.504049886	0.701768274												
0	0.467233736	1.1781	0.4634	0.3933	0.5022	0.7832	0.0393	1.9658	1000.00	1.97	dbblank	0.9042	
0.008128762	0.468542094												
0.016616091	0.480368055												EG 59
0.024955353	0.495952277												
0	0.225674766	1.0917	0.2230	0.2043	0.4994	0.4091	0.0205	1.0267	21.60	47.53	12 ER 001	0.9999	
0.168516232	0.403855691												
0.333631598	0.585558821												
0.498228487	0.769153759												EG 60
0	0.409969327	1.0210	0.4197	0.4111	0.4998	0.8226	0.0413	2.0647	20.52	100.61	12 ER 003	0.9977	
0.15163667	0.584467924												
0.332302911	0.767461822												
0.499163488	0.920702958												
0	0.190670976	1.0263	0.1919	0.1870	0.5009	0.3733	0.0187	0.9371	20.54	45.63	12 ER 004	0.9998	EG 61
0.167227416	0.36740282												
0.331357121	0.528143126												
0.498995187	0.70532081												
0	6.725660341	0.9855	6.7071	6.8055	0.4987	13.6471	0.6851	34.2543	21.75	1574.76	12 ER 006	0.9829	
0.166322148	6.860753013												EG 62
0.33302346	7.000569882												
0.501870852	7.228176802												
0	28.82049096	3.6099	27.4041	7.5915	0.4972	15.2686	0.7665	38.3242	20.15	1901.57	12 ER 007	0.2340	
0.115747981	25.77039296												
0.334829745	29.10163924												EG 63
0.504210887	29.37058376												
0	0.006156031	0.7956	0.0059	0.0074	0.4987	0.0149	0.0007	0.0375	1000.00	0.04	blank	0.9924	
0.008329894	0.011735196												
0.016516924	0.019972982												
0.024783027	0.025302482												EG 64
0	0.106033456	1.9893	0.1052	0.0529	0.4969	0.1064	0.0053	0.2670	21.47	12.43	12 ER 010	1.0000	
0.16975738	0.440594573												
0.336277979	0.776050523												
0.504214443	1.107694322												
0	0.096970587	2.0129	0.0957	0.0476	0.4963	0.0958	0.0048	0.2405	20.35	11.82	12 ER 015	1.0000	EG 65
0.167747679	0.43027992												
0.331467221	0.765250657												
0.50179879	1.105246451												
0	24.28276012	11.6282	23.1142	1.9878	0.4980	3.9913	0.2004	10.0181	28.49	351.64	12 ER 018	0.6506	
0.171012206	24.48907203												EG 66
0.33479181	24.70517522												
0.501156658	30.68908367												

Appendix Table 11: Al, Ca, K, Na, Ti concentration in samples.

tube in g	tube +sample	messloesung in g	HNO3 in sample	messloesung in in g	conc in rohr mg/L	dilution factor	conc in probe mg/L	in 0.2 ml in 50 ml mg/L	in 10 ml anfangsloesung mg/L	qtz in sample in g	element in ppm		Sample ID EG
6.5227	18.5235	12.0008	0	12.0008	3.306	1	3.306	13.7741	688.7041	39.006	17.66	Al	71
6.5227	18.5235	12.0008	0	12.0008	0.713	1	0.713	2.9706	148.5318	39.006	3.81	Ca	71
6.5227	18.5235	12.0008	0	12.0008	0.774	1	0.774	3.2248	161.2393	39.006	4.13	K	71
6.5227	18.5235	12.0008	0	12.0008	0.529	1	0.529	2.2040	110.2010	39.006	2.83	Na	71
6.5227	18.5235	12.0008	0	12.0008	1.23	1	1.23	5.1247	256.2329	39.006	6.57	Ti	71
6.495	18.0773	11.5823	0	11.5823	0.903	1	0.903	3.8982	194.9095	35.907	5.43	Al	72
6.495	18.0773	11.5823	0	11.5823	0.332	1	0.332	1.4332	71.6611	35.907	2.00	Ca	72
6.495	18.0773	11.5823	0	11.5823	0.134	1	0.134	0.5785	28.9234	35.907	0.81	K	72
6.495	18.0773	11.5823	0	11.5823	0.093	1	0.093	0.4015	20.0737	35.907	0.56	Na	72
6.495	18.0773	11.5823	0	11.5823	0.728	1	0.728	3.1427	157.1363	35.907	4.38	Ti	72
6.4258	18.3856	11.9598	0	11.9598	0.009	1	0.009	0.0376	1.8813	1000	0.00	Al	76
6.4258	18.3856	11.9598	0	11.9598	0.279	1	0.279	1.1664	58.3204	1000	0.06	Ca	76
6.4258	18.3856	11.9598	0	11.9598	0.022	1	0.022	0.0920	4.5987	1000	0.00	K	76
6.4258	18.3856	11.9598	0	11.9598	0.007	1	0.007	0.0293	1.4632	1000	0.00	Na	76
6.4258	18.3856	11.9598	0	11.9598	0.001	1	0.001	0.0042	0.2090	1000	0.00	Ti	76
6.4284	18.3407	11.9123	0	11.9123	0.976	1	0.976	4.0966	204.8303	24.155	8.48	Al	78
6.4284	18.3407	11.9123	0	11.9123	0.621	1	0.621	2.6065	130.3275	24.155	5.40	Ca	78
6.4284	18.3407	11.9123	0	11.9123	0.607	1	0.607	2.5478	127.3893	24.155	5.27	K	78
6.4284	18.3407	11.9123	0	11.9123	0.305	1	0.305	1.2802	64.0095	24.155	2.65	Na	78
6.4284	18.3407	11.9123	0	11.9123	0.251	1	0.251	1.0535	52.6766	24.155	2.18	Ti	78
6.4435	18.4084	11.9649	0	11.9649	2.104	1	2.104	8.7924	439.6192	1000	0.44	Al	80
6.4435	18.4084	11.9649	0	11.9649	0.246	1	0.246	1.0280	51.4003	1000	0.05	Ca	80
6.4435	18.4084	11.9649	0	11.9649	0.016	1	0.016	0.0669	3.3431	1000	0.00	K	80
6.4435	18.4084	11.9649	0	11.9649	0.002	1	0.002	0.0084	0.4179	1000	0.00	Na	80
6.4435	18.4084	11.9649	0	11.9649	0.001	1	0.001	0.0042	0.2089	1000	0.00	Ti	80
6.4441	18.4724	12.0283	0	12.0283	1.737	1	1.737	7.2205	361.0236	23.603	15.30	Al	88
6.4441	18.4724	12.0283	0	12.0283	0.703	1	0.703	2.9223	146.1137	23.603	6.19	Ca	88
6.4441	18.4724	12.0283	0	12.0283	0.73	1	0.73	3.0345	151.7255	23.603	6.43	K	88
6.4441	18.4724	12.0283	0	12.0283	0.253	1	0.253	1.0517	52.5843	23.603	2.23	Na	88
6.4441	18.4724	12.0283	0	12.0283	0.823	1	0.823	3.4211	171.0549	23.603	7.25	Ti	88

6.4414	18.4249	11.9835	0	11.9835	1.67	1	1.67	6.9679	348.3957	26.153	13.32	Al	98
6.4414	18.4249	11.9835	0	11.9835	0.489	1	0.489	2.0403	102.0153	26.153	3.90	Ca	98
6.4414	18.4249	11.9835	0	11.9835	0.873	1	0.873	3.6425	182.1254	26.153	6.96	K	98
6.4414	18.4249	11.9835	0	11.9835	0.441	1	0.441	1.8400	92.0015	26.153	3.52	Na	98
6.4414	18.4249	11.9835	0	11.9835	0.328	1	0.328	1.3685	68.4274	26.153	2.62	Ti	98
6.4051	18.3762	11.9711	0	11.9711	1.741	1	1.741	7.2717	363.5840	31	11.73	Al	111
6.4051	18.3762	11.9711	0	11.9711	0.234	1	0.234	0.9774	48.8677	31	1.58	Ca	111
6.4051	18.3762	11.9711	0	11.9711	0.934	1	0.934	3.9011	195.0531	31	6.29	K	111
6.4051	18.3762	11.9711	0	11.9711	0.586	1	0.586	2.4476	122.3781	31	3.95	Na	111
6.4051	18.3762	11.9711	0	11.9711	0.521	1	0.521	2.1761	108.8037	31	3.51	Ti	111
6.4263	18.3953	11.969	0	11.969	0.663	1	0.663	2.7697	138.4827	39.491	3.51	Al	112
6.4263	18.3953	11.969	0	11.969	0.223	1	0.223	0.9316	46.5787	39.491	1.18	Ca	112
6.4263	18.3953	11.969	0	11.969	8.188	1	8.188	34.2050	1710.2515	39.491	43.31	K	112
6.4263	18.3953	11.969	0	11.969	0.093	1	0.093	0.3885	19.4252	39.491	0.49	Na	112
6.4263	18.3953	11.969	0	11.969	0.349	1	0.349	1.4579	72.8966	39.491	1.85	Ti	112
6.4179	18.7458	12.3279	0	12.3279	0.906	1	0.906	3.6746	183.7296	29.393	6.25	Al	113
6.4179	18.7458	12.3279	0	12.3279	0.235	1	0.235	0.9531	47.6561	29.393	1.62	Ca	113
6.4179	18.7458	12.3279	0	12.3279	31.03	1	31.03	125.8527	6292.6370	29.393	214.09	K	113
6.4179	18.7458	12.3279	0	12.3279	0.113	1	0.113	0.4583	22.9155	29.393	0.78	Na	113
6.4179	18.7458	12.3279	0	12.3279	0.822	1	0.822	3.3339	166.6951	29.393	5.67	Ti	113
6.493	18.449	11.956	0	11.956	1.424	1	1.424	5.9552	297.7584	29.675	10.03	Al	119
6.493	18.449	11.956	0	11.956	0.594	1	0.594	2.4841	124.2054	29.675	4.19	Ca	119
6.493	18.449	11.956	0	11.956	0.875	1	0.875	3.6593	182.9625	29.675	6.17	K	119
6.493	18.449	11.956	0	11.956	0.419	1	0.419	1.7523	87.6129	29.675	2.95	Na	119
6.493	18.449	11.956	0	11.956	0.452	1	0.452	1.8903	94.5132	29.675	3.18	Ti	119
6.6137	18.4649	11.8512	0	11.8512	2.112	1	2.112	8.9105	445.5245	33.617	13.25	Al	121
6.6137	18.4649	11.8512	0	11.8512	0.512	1	0.512	2.1601	108.0059	33.617	3.21	Ca	121
6.6137	18.4649	11.8512	0	11.8512	0.451	1	0.451	1.9028	95.1380	33.617	2.83	K	121
6.6137	18.4649	11.8512	0	11.8512	0.453	1	0.453	1.9112	95.5599	33.617	2.84	Na	121
6.6137	18.4649	11.8512	0	11.8512	0.55	1	0.55	2.3204	116.0220	33.617	3.45	Ti	121
6.4592	18.2354	11.7762	0	11.7762	2.35	1	2.35	9.9778	498.8876	38.591	12.93	Al	122
6.4592	18.2354	11.7762	0	11.7762	0.551	1	0.551	2.3395	116.9732	38.591	3.03	Ca	122
6.4592	18.2354	11.7762	0	11.7762	0.437	1	0.437	1.8554	92.7719	38.591	2.40	K	122
6.4592	18.2354	11.7762	0	11.7762	0.488	1	0.488	2.0720	103.5988	38.591	2.68	Na	122
6.4592	18.2354	11.7762	0	11.7762	0.642	1	0.642	2.7258	136.2918	38.591	3.53	Ti	122

6.4265	18.3421	11.9156	0	11.9156	4.801	1	4.801	20.1459	1007.2930	57.011	17.67	Al	123
6.4265	18.3421	11.9156	0	11.9156	0.888	1	0.888	3.7262	186.3104	57.011	3.27	Ca	123
6.4265	18.3421	11.9156	0	11.9156	0.952	1	0.952	3.9948	199.7382	57.011	3.50	K	123
6.4265	18.3421	11.9156	0	11.9156	0.814	1	0.814	3.4157	170.7845	57.011	3.00	Na	123
6.4265	18.3421	11.9156	0	11.9156	1.605	1	1.605	6.7349	336.7434	57.011	5.91	Ti	123
6.4584	18.3569	11.8985	0	11.8985	0.845	1	0.845	3.5509	177.5434	36.88	4.81	Al	124
6.4584	18.3569	11.8985	0	11.8985	0.202	1	0.202	0.8488	42.4423	36.88	1.15	Ca	124
6.4584	18.3569	11.8985	0	11.8985	0.056	1	0.056	0.2353	11.7662	36.88	0.32	K	124
6.4584	18.3569	11.8985	0	11.8985	0.082	1	0.082	0.3446	17.2291	36.88	0.47	Na	124
6.4584	18.3569	11.8985	0	11.8985	0.476	1	0.476	2.0003	100.0126	36.88	2.71	Ti	124
6.4734	18.439	11.9656	0	11.9656	0.008	1	0.008	0.0334	1.6715	1000	0.00	Al	125
6.4734	18.439	11.9656	0	11.9656	0.116	1	0.116	0.4847	24.2361	1000	0.02	Ca	125
6.4734	18.439	11.9656	0	11.9656	0.023	1	0.023	0.0961	4.8054	1000	0.00	K	125
6.4734	18.439	11.9656	0	11.9656	0.003	1	0.003	0.0125	0.6268	1000	0.00	Na	125
6.4734	18.439	11.9656	0	11.9656	0.001	1	0.001	0.0042	0.2089	1000	0.00	Ti	125
6.4375	18.3155	11.878	0	11.878	1.121	1	1.121	4.7188	235.9404	30.052	7.85	Al	126
6.4375	18.3155	11.878	0	11.878	0.725	1	0.725	3.0519	152.5930	30.052	5.08	Ca	126
6.4375	18.3155	11.878	0	11.878	0.542	1	0.542	2.2815	114.0764	30.052	3.80	K	126
6.4375	18.3155	11.878	0	11.878	0.267	1	0.267	1.1239	56.1963	30.052	1.87	Na	126
6.4375	18.3155	11.878	0	11.878	0.172	1	0.172	0.7240	36.2014	30.052	1.20	Ti	126
6.4364	18.3801	11.9437	0	11.9437	4.849	1	4.849	20.2994	1014.9702	30.681	33.08	Al	127
6.4364	18.3801	11.9437	0	11.9437	1.778	1	1.778	7.4433	372.1627	30.681	12.13	Ca	127
6.4364	18.3801	11.9437	0	11.9437	1.954	1	1.954	8.1800	409.0022	30.681	13.33	K	127
6.4364	18.3801	11.9437	0	11.9437	0.349	1	0.349	1.4610	73.0511	30.681	2.38	Na	127
6.4364	18.3801	11.9437	0	11.9437	0.601	1	0.601	2.5160	125.7985	30.681	4.10	Ti	127
6.4676	18.5082	12.0406	0	12.0406	2.867	1	2.867	11.9056	595.2776	26.67	22.32	Al	128
6.4676	18.5082	12.0406	0	12.0406	0.492	1	0.492	2.0431	102.1544	26.67	3.83	Ca	128
6.4676	18.5082	12.0406	0	12.0406	0.543	1	0.543	2.2549	112.7436	26.67	4.23	K	128
6.4676	18.5082	12.0406	0	12.0406	0.588	1	0.588	2.4417	122.0869	26.67	4.58	Na	128
6.4676	18.5082	12.0406	0	12.0406	4.968	1	4.968	20.6302	1031.5101	26.67	38.68	Ti	128
6.4043	18.3491	11.9448	0	11.9448	2.213	1	2.213	9.2634	463.1723	26.985	17.16	Al	129
6.4043	18.3491	11.9448	0	11.9448	0.322	1	0.322	1.3479	67.3933	26.985	2.50	Ca	129
6.4043	18.3491	11.9448	0	11.9448	0.357	1	0.357	1.4944	74.7187	26.985	2.77	K	129
6.4043	18.3491	11.9448	0	11.9448	0.442	1	0.442	1.8502	92.5089	26.985	3.43	Na	129
6.4043	18.3491	11.9448	0	11.9448	0.784	1	0.784	3.2818	164.0881	26.985	6.08	Ti	129

6.4367	18.3924	11.9557	0	11.9557	2.259	1	2.259	9.4474	472.3688	1000	0.47	Al	130
6.4367	18.3924	11.9557	0	11.9557	0.072	1	0.072	0.3011	15.0556	1000	0.02	Ca	130
6.4367	18.3924	11.9557	0	11.9557	0	1	0	0.0000	0.0000	1000	0.00	K	130
6.4367	18.3924	11.9557	0	11.9557	0.005	1	0.005	0.0209	1.0455	1000	0.00	Na	130
6.4367	18.3924	11.9557	0	11.9557	0.003	1	0.003	0.0125	0.6273	1000	0.00	Ti	130
6.5218	18.4666	11.9448	0	11.9448	2.123	1	2.123	8.8867	444.3356	26.206	16.96	Al	131
6.5218	18.4666	11.9448	0	11.9448	0.463	1	0.463	1.9381	96.9041	26.206	3.70	Ca	131
6.5218	18.4666	11.9448	0	11.9448	0.358	1	0.358	1.4986	74.9280	26.206	2.86	K	131
6.5218	18.4666	11.9448	0	11.9448	0.359	1	0.359	1.5027	75.1373	26.206	2.87	Na	131
6.5218	18.4666	11.9448	0	11.9448	0.896	1	0.896	3.7506	187.5293	26.206	7.16	Ti	131
6.4748	18.438	11.9632	0	11.9632	1.075	1	1.075	4.4929	224.6473	28.654	7.84	Al	134
6.4748	18.438	11.9632	0	11.9632	0.694	1	0.694	2.9006	145.0281	28.654	5.06	Ca	134
6.4748	18.438	11.9632	0	11.9632	0.562	1	0.562	2.3489	117.4435	28.654	4.10	K	134
6.4748	18.438	11.9632	0	11.9632	0.24	1	0.24	1.0031	50.1538	28.654	1.75	Na	134
6.4748	18.438	11.9632	0	11.9632	0.166	1	0.166	0.6938	34.6897	28.654	1.21	Ti	134

Appendix Tables 12A-D: Blank calculations.

Sample ID	$^{10}Be/^{9}Be$	$^{10}Be/^{9}Be$ 1s	$^{10}Be/^{9}Be$ 1s (%)	avg. ^{9}Be current (A)	Blank type
EG13	1.73E-15	4.11E-16	23.76	1.26E-06	Be blank
EG17	2.02E-15	4.17E-16	20.63	1.40E-06	Be blank
EG24	3.23E-15	6.18E-16	19.14	1.41E-06	Be blank
EG30	1.90E-15	5.11E-16	26.9	1.20E-06	Be blank
EG36	1.05E-15	2.43E-16	23.14	2.39E-06	Be blank
EG45	3.24E-15	6.83E-16	21.07	9.39E-07	Be blank
EG66	6.96E-16	2.64E-16	37.92	1.82E-06	Be blank
EG76	5.33E-16	1.78E-16	33.47	2.86E-06	Be blank
EG86	9.79E-16	2.84E-16	29.03	2.22E-06	Be blank
EG106	1.37E-15	5.62E-16	40.95	1.49E-06	Be blank
EG96	1.33E-15	3.87E-16	29.05	3.06E-06	Be blank
EG115	1.17E-15	2.41E-16	20.64	3.64E-06	Be blank
EG125	0.00E+00	0.00E+00	100	2.34E-07	Be blank
EG50	1.88E-15	5.68E-16	30.3	8.19E-07	AlBe blank
EG70	2.36E-15	4.98E-16	21.07	1.76E-06	AlBe blank
EG80	2.10E-15	3.88E-16	18.51	2.59E-06	AlBe blank
EG110	4.27E-15	9.22E-16	21.56	1.75E-06	AlBe blank
EG100	3.54E-15	7.03E-16	19.87	2.49E-06	AlBe blank
EG120	2.68E-15	3.77E-16	14.07	3.46E-06	AlBe blank
EG130	1.24E-15	1.24E-15	100	2.20E-07	AlBe blank

372.5 mg/l	carrierconc=
1	carrierdensity=
9.01218	be atomic weight=
6.02E+23	avogadro=

sample	m(qtz) g	carrier m(9Be) g	m(9Be) mg	10Be/9Be	Error %	Error abs.	N(9Be) atoms	N(10Be) atoms
EG13	1	0.8735	0.3254	1.73E-15	23.76	4.11E-16	2.17E+19	3.76E+04
EG17	1	0.8730	0.3252	2.02E-15	20.63	4.17E-16	2.17E+19	4.39E+04
EG24	1	0.8768	0.3266	3.23E-15	19.14	6.18E-16	2.18E+19	7.05E+04
EG30	1	0.8721	0.3249	1.90E-15	26.9	5.11E-16	2.17E+19	4.12E+04
EG36	1	0.8887	0.3310	1.05E-15	23.14	2.43E-16	2.21E+19	2.33E+04
EG45	1	0.8755	0.3261	3.24E-15	21.07	6.83E-16	2.18E+19	7.07E+04
EG66	1	0.8869	0.3304	6.96E-16	37.92	2.64E-16	2.21E+19	1.54E+04
EG76	1	0.8862	0.3301	5.33E-16	33.47	1.78E-16	2.21E+19	1.17E+04
EG86	1	0.8892	0.3312	9.79E-16	29.03	2.84E-16	2.21E+19	2.17E+04
EG106	1	0.8830	0.3289	1.37E-15	40.95	5.62E-16	2.20E+19	3.01E+04
EG96	1	0.8792	0.3275	1.33E-15	29.05	3.87E-16	2.19E+19	2.91E+04
EG115	1	0.8818	0.3285	1.17E-15	20.64	2.41E-16	2.19E+19	2.57E+04
			3.28E-01	1.60E-15		average	2.19E+19	3.51E+04
			2.36E-03	8.84E-16		stddev	1.58E+17	1.92E+04
			0.72	54.66		%	0.72	54.66

Be blank in AlBe blanks

sample	m(qtz) g	carrier m(9Be) g	m(9Be) mg	10Be/9Be	Error %	Error abs.	N(9Be) atoms	N(10Be) atoms
EG50	1	0.8744	0.3257	1.88E-15	30.3	5.68E-16	2.18E+19	4.08E+04
EG70	1	0.8861	0.3301	2.36E-15	21.07	4.98E-16	2.21E+19	5.21E+04
EG80	1	0.8829	0.3289	2.10E-15	18.51	3.88E-16	2.20E+19	4.61E+04
EG110	1	0.8790	0.3274	4.27E-15	21.56	9.22E-16	2.19E+19	9.35E+04
EG100	1	0.8843	0.3294	3.54E-15	19.87	7.03E-16	2.20E+19	7.79E+04
EG120	1	0.8798	0.3277	2.68E-15	14.07	3.77E-16	2.19E+19	5.87E+04
EG130	1	0.8806	0.3280	1.24E-15	100	1.24E-15	2.19E+19	2.72E+04
			3.28E-01	2.58E-15		average	2.19E+19	5.66E+04
			1.44E-03	1.03E-15		stddev	9.62E+16	2.26E+04
			0.44	39.90		%	0.44	39.90

Al	Probe in g	Probe nach Leachen	Be carrier (0.8 ml)	Al blank
EG 50	93.551	19.0365	0.8744	5.0798
EG 70	92.5	15.3048	0.8861	5.1026
EG 80	94.299	10.1463	0.8829	5.0405
EG 100	93.869	12.227	0.879	5.1456
EG 110	93.53	10.0242	0.8843	5.1807
EG 120	92.488	9.9221	0.8798	5.1533
EG 130	91.685	12.7838	0.8806	5.1073

Appendix Table 13: $^{26}Al/^{10}Be$ ratio.

ID	Lab ID	m(qtz) g	$^{26}Al/^{27}Al$ (meas.)	Error %	Al in probe ppm	Al in probe g	^{27}Al in probe g	^{26}Al in probe	^{26}Al atome	^{26}Al conc corr	^{10}Be conc corr	$^{26}Al/^{10}Be$
6005	EG 12	54.686	5.8125E-14	1.27E-14	121.05	6.620E-03	6.620E-03	3.84772E-16	8.614E+06	157513	23011	6.85
7005	EG 15	34.963	2.81275E-14	8.76E-15	219.43	7.672E-03	7.672E-03	2.15792E-16	4.831E+06	138171	23119	5.98
7003	EG 32	43.31	3.483E-14	6.01E-15	137.35	5.949E-03	5.949E-03	2.07191E-16	4.638E+06	107095	16891	6.34
6001	EG 33	47.29	4.74367E-14	1.09E-14	116.1	5.490E-03	5.490E-03	2.60445E-16	5.830E+06	123292	16758	7.36
6002	EG 34	47.25	3.79325E-14	1.05E-14	147.32	6.961E-03	6.961E-03	2.64043E-16	5.911E+06	125101	19054	6.57
6004	EG 37	33.57	5.879E-14	8.48E-15	144.99	4.867E-03	4.867E-03	2.86149E-16	6.406E+06	190823	25146	7.59
5003	EG 38	46.35	1.82E-13	2.18E-14	118.3	5.483E-03	5.483E-03	9.97943E-16	2.234E+07	481997	70206	6.87
5004	EG 39	47.71	3.02033E-14	8.45E-15	151.97	7.250E-03	7.250E-03	2.18989E-16	4.902E+06	102755	15425	6.66
7006	EG 48	26.836	2.683E-14	4.30E-15	170.45	4.574E-03	4.574E-03	1.22726E-16	2.747E+06	102378	16759	6.11
5001	EG 49	40.746	1.138E-13	9.50E-15	79.19	3.227E-03	3.227E-03	3.67196E-16	8.220E+06	201744	38723	5.21
dbblank	EG 70	zero										
	Al STD		1.264E-15	8.95E-16								

Appendix Table 14: Moraine boulder sample ^{10}Be concentrations.

sample ID	m(qtz) g	carrier m(9Be) g	m(9Be) mg	10Be/9Be	Error %	Error abs.	N(9Be) atoms	N(10Be) atoms	N(10Be) abs err	N(10Be) atoms/g	N(10Be) atoms/g abs err
ER 001	20.014	0.893	0.3326	4.70E-13	3.38	1.59E-14	2.22E+19	10453623	353332	522316	17654
ER 002	23.931	0.8915	0.3321	3.68E-13	3.35	1.23E-14	2.22E+19	8170442	273710	341417	11437
ER 003	19.003	0.8895	0.3313	2.00E-13	3.92	7.85E-15	2.21E+19	4430303	173668	233137	9139
ER 004	19.089	0.8872	0.3305	6.42E-13	3.3	2.12E-14	2.21E+19	14175204	467782	742585	24505
ER 006	27.338	0.88	0.3278	2.87E-13	3.3	9.48E-15	2.19E+19	6286443	207453	229953	7588
ER 007	29.158	0.8826	0.3288	5.25E-14	4.55	2.39E-15	2.20E+19	1153357	52478	39555	1800
ER 008	23.778	0.8904	0.3317	3.64E-13	3.43	1.25E-14	2.22E+19	8056195	276327	338809	11621
ER 009	23.757	0.8971	0.3342	3.62E-13	3.4	1.23E-14	2.23E+19	8074389	274529	339874	11556
ER 010	20.046	0.8858	0.3300	3.17E-13	3.52	1.12E-14	2.20E+19	6995941	246257	348994	12285
ER 011	24.196	0.8895	0.3313	3.07E-13	3.35	1.03E-14	2.21E+19	6801545	227852	281102	9417
ER 013	23.634	0.8891	0.3312	3.67E-13	3.34	1.22E-14	2.21E+19	8117464	271123	343466	11472
ER 014	24.338	0.8864	0.3302	4.41E-13	3.25	1.43E-14	2.21E+19	9729908	316222	399783	12993
ER 015	17.542	0.8859	0.3300	2.81E-13	3.61	1.01E-14	2.21E+19	6185260	223288	352597	12729
ER 016	27.66	0.8802	0.3279	2.88E-13	3.29	9.46E-15	2.19E+19	6309781	207592	228119	7505
ER 017	20.228	0.8869	0.3304	5.40E-13	3.25	1.76E-14	2.21E+19	11920894	387429	589326	19153
ER 018	94.722	0.8832	0.3290	2.99E-13	3.82	1.14E-14	2.20E+19	6568710	250925	69347	2649
ER 018	94.722	0.8832	0.3290	4.27E-13	3.62	1.55E-14	2.20E+19	9391408	339969	99147	3589
ER 019	23.515	0.8906	0.3317	4.53E-13	3.57	1.61E-14	2.22E+19	10030941	358105	426576	15229
ER 020	16.205	0.8911	0.3319	1.81E-13	3.76	6.79E-15	2.22E+19	4007975	150700	247330	9300
LMA 002	31.816	0.8799	0.3278	4.14E-13	3.81	1.58E-14	2.19E+19	9062838	345294	284852	10853
LMA 003	23.729	0.8865	0.3302	3.50E-13	4.84	1.7E-14	2.21E+19	7727434	374008	325654	15762
LMA 004	24.155	0.8855	0.3298	2.22E-13	3.44	7.64E-15	2.20E+19	4897484	168473	202752	6975
LMA 005	24.862	0.8925	0.3325	3.80E-13	3.36	1.28E-14	2.22E+19	8439524	283568	339455	11406
LMA 008	28.236	0.8814	0.3283	2.96E-13	3.3	9.77E-15	2.19E+19	6493894	214298	229986	7590
LMA 009	27.508	0.8845	0.3295	3.02E-13	4.32	1.31E-14	2.20E+19	6657636	287610	242025	10455

LMA 010	27.662	0.8862	0.3301	2.62E-13	3.94	1.03E-14	2.21E+19	5785894	227964	209164	8241
LMB 001	19.961	0.8841	0.3293	4.27E-13	3.62	1.55E-14	2.20E+19	9400978	340315	470967	17049
LMB 001	19.961	0.8841	0.3293	2.99E-13	3.82	1.14E-14	2.20E+19	6575403	251180	329413	12584
LMB 002	26.67	0.8537	0.3180	2.33E-13	8.26	1.93E-14	2.12E+19	4959599	409663	185962	15360
LMB 004	33.754	0.8831	0.3290	4.30E-13	3.66	1.57E-14	2.20E+19	9458486	346181	280218	10256
LMB 005	23.603	0.8872	0.3305	3.30E-13	3.47	1.14E-14	2.21E+19	7283038	252721	308564	10707
LMB 006	28.922	0.8795	0.3276	5.04E-13	4.03	2.03E-14	2.19E+19	11039902	444908	381713	15383
LMB 007	28.788	0.8802	0.3279	3.88E-13	4.53	1.76E-14	2.19E+19	8500677	385081	295285	13376
LMB 008	23.398	0.8844	0.3294	2.79E-13	4.08	1.14E-14	2.20E+19	6141767	250584	262491	10710
LMC 001	30.052	0.8806	0.3280	4.66E-13	5.74	2.68E-14	2.19E+19	10214215	586296	339885	19509
LMC 002	30.681	0.8823	0.3287	4.97E-13	5.33	2.65E-14	2.20E+19	10908144	581404	355534	18950
LMC 003	32.05	0.8781	0.3271	5.10E-13	3.81	1.94E-14	2.19E+19	11140355	424448	347593	13243
LMC 004	28.654	0.8797	0.3277	5.21E-13	3.7	1.93E-14	2.19E+19	11412464	422261	398285	14737
LMC 005	30.387	0.8785	0.3272	3.65E-13	3.84	1.4E-14	2.19E+19	7985699	306651	262800	10092
LMC 006	27.869	0.8797	0.3277	4.94E-13	4.04	2E-14	2.19E+19	10819068	437090	388212	15684
LMC 008	29.394	0.7708	0.2871	2.57E-13	4.08	1.05E-14	1.92E+19	4932694	201254	167813	6847
LMC 009	32.035	0.8754	0.3261	4.09E-13	3.81	1.56E-14	2.18E+19	8911899	339543	278193	10599
LMC 010	24.061	0.8776	0.3269	3.24E-13	4.02	1.3E-14	2.18E+19	7077535	284517	294150	11825
LMD 001	25.665	0.8788	0.3274	3.82E-13	3.36	1.29E-14	2.19E+19	8358099	280832	325661	10942
LMD 002	28.353	0.8798	0.3277	5.35E-13	3.8	2.03E-14	2.19E+19	11711588	445040	413063	15696
LMD 003	26.153	0.8792	0.3275	4.13E-13	4.04	1.67E-14	2.19E+19	9033744	364963	345419	13955
LME 003	12.862	0.8856	0.3299	1.07E-13	4.08	4.36E-15	2.20E+19	2356436	96143	183209	7475
LME 005	27.96	0.8795	0.3276	4.48E-13	3.81	1.71E-14	2.19E+19	9798652	373329	350453	13352
LME 007	25.751	0.881	0.3282	2.33E-13	4.92	1.15E-14	2.19E+19	5118199	251815	198757	9779
LME 010	29.675	0.8816	0.3284	3.86E-13	3.22	1.24E-14	2.19E+19	8470310	272744	285436	9191
LME 012	26.126	0.8838	0.3292	3.78E-13	3.68	1.39E-14	2.20E+19	8324258	306333	318620	11725

Appendix Table 15: Moraine boulder exposure age CHRONOS input with maximum erosion.

Sample ID	Lat in °	Long. in °	alt(m)	hPa or m	thick in cm	density(g/cm^3)	shielding	eros rate(cm/yr)	^{10}Be conc	error(abs)	standardization	^{26}Al conc	^{26}Al error(abs)	^{26}Al std
ER001	39.28185	71.42316	2068	std	2.5	2.7	0.99	0.0003	520137	17689	07KNSTD	0	0	KNSTD
ER002	39.28128	71.42244	2072	std	2.5	2.7	0.99	0.0003	339598	11474	07KNSTD	0	0	KNSTD
ER003	39.28107	71.42232	2078	std	2.5	2.7	0.99	0.0003	230852	9212	07KNSTD	0	0	KNSTD
ER004	39.28098	71.42111	2068	std	2.5	2.7	0.99	0.0003	740316	24532	07KNSTD	0	0	KNSTD
ER006	39.28064	71.41969	2075	std	2.5	2.7	0.99	0.0003	228381	7631	07KNSTD	0	0	KNSTD
ER007	39.28092	71.41677	2048	std	2.5	2.7	0.99	0.0003	38078	1952	07KNSTD	0	0	KNSTD
ER008	39.28021	71.41484	2059	std	2.5	2.7	0.99	0.0003	336981	11658	07KNSTD	0	0	KNSTD
ER009	39.28021	71.41484	2059	std	2.5	2.7	0.99	0.0003	338031	11593	07KNSTD	0	0	KNSTD
ER010	39.28001	71.41446	2062	std	2.5	2.7	0.99	0.0003	346837	12334	07KNSTD	0	0	KNSTD
ER11	39.28207	71.42548	2078	std	2.5	2.7	0.99	0.0003	279307	9461	07KNSTD	0	0	KNSTD
ER013	39.28186	71.42601	2078	std	2.5	2.7	0.99	0.0003	341629	11510	07KNSTD	0	0	KNSTD
ER014	39.28164	71.42662	2082	std	2.5	2.7	0.99	0.0003	398004	13024	07KNSTD	0	0	KNSTD
ER015	39.28188	71.42793	2090	std	2.5	2.7	0.99	0.0003	350132	12791	07KNSTD	0	0	KNSTD
ER016	39.28175	71.42785	2090	std	2.5	2.6	0.99	0.0003	226566	7547	07KNSTD	0	0	KNSTD
ER017	39.28307	71.42754	2069	std	2.5	2.7	0.99	0.0003	587186	19184	07KNSTD	0	0	KNSTD
ER019	39.28304	71.42702	2077	std	2.5	2.7	0.99	0.0003	424727	15258	07KNSTD	0	0	KNSTD
ER020	39.28411	71.42448	2060	std	2.5	2.1	0.99	0.0003	244645	9398	07KNSTD	0	0	KNSTD
LMA002	39.23157	71.45891	2258	std	2.5	2.7	0.99	0.0003	283501	10875	07KNSTD	0	0	KNSTD
LMA003	39.23128	71.45942	2258	std	2.5	2.7	0.99	0.0003	323830	15789	07KNSTD	0	0	KNSTD
LMA004	39.23128	71.45942	2258	std	2.5	2.7	0.99	0.0003	200963	7034	07KNSTD	0	0	KNSTD
LMA005	39.23098	71.46027	2264	std	2.5	2.7	0.99	0.0003	337702	11440	07KNSTD	0	0	KNSTD
LMA008	39.23011	71.46222	2276	std	2.5	2.7	0.99	0.0003	228462	7630	07KNSTD	0	0	KNSTD
LMA009	39.22859	71.46568	2315	std	2.5	2.7	0.99	0.0003	240456	10486	07KNSTD	0	0	KNSTD
LMA010	39.22761	71.46804	2337	std	2.5	2.7	0.99	0.0003	207600	8279	07KNSTD	0	0	KNSTD
LMB001	39.23146	71.46003	2262	std	2.5	2.7	0.99	0.0003	468805	17085	07KNSTD	0	0	KNSTD
LMB001	39.23146	71.46003	2262	std	2.5	2.7	0.99	0.0003	327250	12632	07KNSTD	0	0	KNSTD
LMB002	39.22726	71.47054	2313	std	2.5	2.1	0.99	0.0003	184399	15383	07KNSTD	0	0	KNSTD
LMB004	39.22653	71.47211	2315	std	2.5	2.7	0.99	0.0003	278941	10277	07KNSTD	0	0	KNSTD
LMB005	39.23091	71.46139	2266	std	2.5	2.7	0.99	0.0003	306729	10748	07KNSTD	0	0	KNSTD
LMB006	39.22257	71.47916	2316	std	2.5	2.7	0.99	0.0003	380228	15402	07KNSTD	0	0	KNSTD

LMB007	39.22294	71.47839	2316	std	2.5	2.7	0.99	0.0003	293793	13398	07KNSTD	0	0	KNSTD
LMB008	39.22361	71.47729	2318	std	2.5	2.1	0.99	0.0003	260646	10751	07KNSTD	0	0	KNSTD
LMC001	39.22558	71.47550	2303	std	2.5	2.7	0.99	0.0003	338454	19523	07KNSTD	0	0	KNSTD
LMC002	39.22879	71.46790	2311	std	2.5	2.6	0.99	0.0003	354130	18964	07KNSTD	0	0	KNSTD
LMC003	39.23003	71.46506	2293	std	2.5	2.6	0.99	0.0003	346255	13261	07KNSTD	0	0	KNSTD
LMC004	39.23003	71.46506	2293	std	2.5	2.7	0.99	0.0003	396786	14757	07KNSTD	0	0	KNSTD
LMC005	39.23090	71.46325	2285	std	2.5	2.7	0.99	0.0003	261388	10117	07KNSTD	0	0	KNSTD
LMC006	39.23096	71.46301	2279	std	2.5	2.7	0.99	0.0003	386670	15704	07KNSTD	0	0	KNSTD
LMC008	39.23105	71.46276	2278	std	2.5	2.1	0.99	0.0003	166533	6888	07KNSTD	0	0	KNSTD
LMC009	39.23118	71.46252	2278	std	2.5	2.7	0.99	0.0003	276858	10621	07KNSTD	0	0	KNSTD
LMC010	39.23162	71.46124	2271	std	2.5	2.1	0.99	0.0003	292369	11860	07KNSTD	0	0	KNSTD
LMD001	39.23211	71.46103	2251	std	2.5	2.7	0.99	0.0003	323990	10976	07KNSTD	0	0	KNSTD
LMD002	39.23184	71.46165	2255	std	2.5	2.7	0.99	0.0003	411548	15716	07KNSTD	0	0	KNSTD
LMD003	39.23448	71.45472	2241	std	2.5	2.7	0.99	0.0003	343778	13980	07KNSTD	0	0	KNSTD
LME003	39.22499	71.47882	2281	std	2.5	2.1	0.99	0.0003	179848	7668	07KNSTD	0	0	KNSTD
LME005	39.22637	71.47633	2288	std	2.5	2.1	0.99	0.0003	348917	13375	07KNSTD	0	0	KNSTD
LME007	39.22820	71.47279	2305	std	2.5	2.1	0.99	0.0003	197087	9816	07KNSTD	0	0	KNSTD
LME010	39.23125	71.46468	2285	std	2.5	2.7	0.99	0.0003	283985	9221	07KNSTD	0	0	KNSTD
LME012	39.23259	71.46098	2255	std	2.5	2.7	0.99	0.0003	316968	11755	07KNSTD	0	0	KNSTD

Appendix Table 16: Moraine boulder exposure age CHRONOS input with minimum erosion.

ID	lat	long	alt(m)	hPa or m	s thick in cm	density	shielding	eros rate cm/yr	^{10}Be conc	abs err	standardization	^{26}Al conc	^{26}Al abs err	^{26}Al std
ER001	39.28185	71.42316	2068	std	2.5	2.7	0.99	0.0000001	520137	17689	07KNSTD	0	0	KNSTD
ER002	39.28128	71.42244	2072	std	2.5	2.7	0.99	0.0000001	339598	11474	07KNSTD	0	0	KNSTD
ER003	39.28107	71.42232	2078	std	2.5	2.7	0.99	0.0000001	230852	9212	07KNSTD	0	0	KNSTD
ER004	39.28098	71.42111	2068	std	2.5	2.7	0.99	0.0000001	740316	24532	07KNSTD	0	0	KNSTD
ER006	39.28064	71.41969	2075	std	2.5	2.7	0.99	0.0000001	228381	7631	07KNSTD	0	0	KNSTD
ER007	39.28092	71.41677	2048	std	2.5	2.7	0.99	0.0000001	38078	1952	07KNSTD	0	0	KNSTD
ER008	39.28021	71.41484	2059	std	2.5	2.7	0.99	0.0000001	336981	11658	07KNSTD	0	0	KNSTD
ER009	39.28021	71.41484	2059	std	2.5	2.7	0.99	0.0000001	338031	11593	07KNSTD	0	0	KNSTD
ER010	39.28001	71.41446	2062	std	2.5	2.7	0.99	0.0000001	346837	12334	07KNSTD	0	0	KNSTD
ER11	39.28207	71.42548	2078	std	2.5	2.7	0.99	0.0000001	279307	9461	07KNSTD	0	0	KNSTD
ER013	39.28186	71.42601	2078	std	2.5	2.7	0.99	0.0000001	341629	11510	07KNSTD	0	0	KNSTD
ER014	39.28164	71.42662	2082	std	2.5	2.7	0.99	0.0000001	398004	13024	07KNSTD	0	0	KNSTD
ER015	39.28188	71.42793	2090	std	2.5	2.7	0.99	0.0000001	350132	12791	07KNSTD	0	0	KNSTD
ER016	39.28175	71.42785	2090	std	2.5	2.6	0.99	0.0000001	226566	7547	07KNSTD	0	0	KNSTD
ER017	39.28307	71.42754	2069	std	2.5	2.7	0.99	0.0000001	587186	19184	07KNSTD	0	0	KNSTD
ER019	39.28304	71.42702	2077	std	2.5	2.7	0.99	0.0000001	424727	15258	07KNSTD	0	0	KNSTD
ER020	39.28411	71.42448	2060	std	2.5	2.1	0.99	0.0000001	244645	9398	07KNSTD	0	0	KNSTD
LMA002	39.23157	71.45891	2258	std	2.5	2.7	0.99	0.0000001	283501	10875	07KNSTD	0	0	KNSTD
LMA003	39.23128	71.45942	2258	std	2.5	2.7	0.99	0.0000001	323830	15789	07KNSTD	0	0	KNSTD
LMA004	39.23128	71.45942	2258	std	2.5	2.7	0.99	0.0000001	200963	7034	07KNSTD	0	0	KNSTD
LMA005	39.23098	71.46027	2264	std	2.5	2.7	0.99	0.0000001	337702	11440	07KNSTD	0	0	KNSTD
LMA008	39.23011	71.46222	2276	std	2.5	2.7	0.99	0.0000001	228462	7630	07KNSTD	0	0	KNSTD
LMA009	39.22859	71.46568	2315	std	2.5	2.7	0.99	0.0000001	240456	10486	07KNSTD	0	0	KNSTD
LMA010	39.22761	71.46804	2337	std	2.5	2.7	0.99	0.0000001	207600	8279	07KNSTD	0	0	KNSTD
LMB001	39.23146	71.46003	2262	std	2.5	2.7	0.99	0.0000001	468805	17085	07KNSTD	0	0	KNSTD
LMB001	39.23146	71.46003	2262	std	2.5	2.7	0.99	0.0000001	327250	12632	07KNSTD	0	0	KNSTD
LMB002	39.22726	71.47054	2313	std	2.5	2.1	0.99	0.0000001	184399	15383	07KNSTD	0	0	KNSTD
LMB004	39.22653	71.47211	2315	std	2.5	2.7	0.99	0.0000001	278941	10277	07KNSTD	0	0	KNSTD
LMB005	39.23091	71.46139	2266	std	2.5	2.7	0.99	0.0000001	306729	10748	07KNSTD	0	0	KNSTD
LMB006	39.22257	71.47916	2316	std	2.5	2.7	0.99	0.0000001	380228	15402	07KNSTD	0	0	KNSTD

LMB007	39.22294	71.47839	2316	std	2.5	2.7	0.99	0.0000001	293793	13398	07KNSTD	0	0	KNSTD
LMB008	39.22361	71.47729	2318	std	2.5	2.1	0.99	0.0000001	260646	10751	07KNSTD	0	0	KNSTD
LMC001	39.22558	71.47550	2303	std	2.5	2.7	0.99	0.0000001	338454	19523	07KNSTD	0	0	KNSTD
LMC002	39.22879	71.46790	2311	std	2.5	2.6	0.99	0.0000001	354130	18964	07KNSTD	0	0	KNSTD
LMC003	39.23003	71.46506	2293	std	2.5	2.6	0.99	0.0000001	346255	13261	07KNSTD	0	0	KNSTD
LMC004	39.23003	71.46506	2293	std	2.5	2.7	0.99	0.0000001	396786	14757	07KNSTD	0	0	KNSTD
LMC005	39.23090	71.46325	2285	std	2.5	2.7	0.99	0.0000001	261388	10117	07KNSTD	0	0	KNSTD
LMC006	39.23096	71.46301	2279	std	2.5	2.7	0.99	0.0000001	386670	15704	07KNSTD	0	0	KNSTD
LMC008	39.23105	71.46276	2278	std	2.5	2.1	0.99	0.0000001	166533	6888	07KNSTD	0	0	KNSTD
LMC009	39.23118	71.46252	2278	std	2.5	2.7	0.99	0.0000001	276858	10621	07KNSTD	0	0	KNSTD
LMC010	39.23162	71.46124	2271	std	2.5	2.1	0.99	0.0000001	292369	11860	07KNSTD	0	0	KNSTD
LMD001	39.23211	71.46103	2251	std	2.5	2.7	0.99	0.0000001	323990	10976	07KNSTD	0	0	KNSTD
LMD002	39.23184	71.46165	2255	std	2.5	2.7	0.99	0.0000001	411548	15716	07KNSTD	0	0	KNSTD
LMD003	39.23448	71.45472	2241	std	2.5	2.7	0.99	0.0000001	343778	13980	07KNSTD	0	0	KNSTD
LME003	39.22499	71.47882	2281	std	2.5	2.1	0.99	0.0000001	179848	7668	07KNSTD	0	0	KNSTD
LME005	39.22637	71.47633	2288	std	2.5	2.1	0.99	0.0000001	348917	13375	07KNSTD	0	0	KNSTD
LME007	39.22820	71.47279	2305	std	2.5	2.1	0.99	0.0000001	197087	9816	07KNSTD	0	0	KNSTD
LME010	39.23125	71.46468	2285	std	2.5	2.7	0.99	0.0000001	283985	9221	07KNSTD	0	0	KNSTD
LME012	39.23259	71.46098	2255	std	2.5	2.7	0.99	0.0000001	316968	11755	07KNSTD	0	0	KNSTD

Appendix Table 17: Modern river samples ^{10}Be concetrations.

ID	Lab ID	m(qtz)	carrier m(9Be)	m(9Be)	10Be/9Be	Error	10Be/9Be	N(9Be)	N(10Be) uncorr	err uncorr	N(10Be)corr	err corr	err corr	N(10Be)corr	err corr
		g	g	mg	(meas.)	%	corr atoms	atoms	atoms	abs	atoms	abs	rel	atoms/g(qtz)	abs
12 mod 7001	EG14	35.26	0.8742	0.3256	4.24E-14	5.55	4.04E-14	4.36E+19	1850387	102696	1807886	105031	5.81	51267	2978
12 mod 7002	EG 31	46.38	0.8948	0.3333	5.03E-14	4.93	4.83E-14	2.23E+19	1119409	55187	1076908	59418	5.52	23219	1281
12 mod 7003	EG 32	42.98	0.8913	0.3320	3.46E-14	6.61	3.27E-14	2.22E+19	768497	50798	725996	55365	7.63	16891	1288
12 mod 7005	EG15	34.96	0.8742	0.3256	3.91E-14	5.69	3.71E-14	2.18E+19	850801	48411	808300	53183	6.58	23119	1521
12 mod 7006	EG 48	26.84	0.8762	0.3264	2.26E-14	6.99	2.06E-14	2.18E+19	492238	34407	449737	40850	9.08	16759	1522
12 mod 7006	EG 129	26.99	0.8851	0.3297	2.88E-14	6.9	2.68E-14	2.20E+19	634711	43795	592210	49019	8.28	21946	1817
12 mod 7007	EG16	36.31	0.8766	0.3265	3.78E-14	6.7	3.58E-14	2.18E+19	824772	55260	782271	59485	7.60	21547	1638
13 mod 7001	EG 71	39.01	0.8935	0.3328	4.71E-14	5.13	4.52E-14	2.22E+19	1047949	53760	1005449	58095	5.78	25777	1489
12 mod 6001	EG 33	46.52	0.8883	0.3309	3.72E-14	4.96	3.52E-14	2.21E+19	822071	40775	779571	46341	5.94	16758	996
12 mod 6002	EG 34	46.42	0.8867	0.3303	4.20E-14	5	4.00E-14	2.21E+19	926972	46349	884471	51313	5.80	19054	1105
12 mod 6003	EG 35	35.77	0.8888	0.3311	5.09E-14	4.6	4.89E-14	2.21E+19	1126283	51809	1083782	56294	5.19	30299	1574
12 mod 6004	EG 37	33.30	0.8886	0.3310	3.98E-14	4.96	3.78E-14	2.21E+19	879856	43641	837355	48881	5.84	25146	1468
12 mod 6005	EG12	54.69	0.8769	0.3266	5.96E-14	7.19	5.76E-14	2.18E+19	1300879	93533	1258378	96090	7.64	23011	1757
12 mod 5001	EG 49	40.75	0.8726	0.3250	7.46E-14	4.53	7.26E-14	2.17E+19	1620296	73399	1577796	76631	4.86	38723	1881
12 mod 5003	EG 38	46.44	0.8864	0.3302	1.50E-13	3.64	1.48E-13	2.21E+19	3302874	120225	3260373	122224	3.75	70206	2632
12 mod 5004	EG 39	47.23	0.8873	0.3305	3.49E-14	6.08	3.29E-14	2.21E+19	771011	46877	728511	51792	7.11	15425	1097
13 mod 7003	EG141	38.0644	0.8915	0.3321	3.98E-14	5.27	3.78E-14	2.22E+19	883171	46543	840670	51489	6.12	22085	1353
13 mod 7007	EG142	40.1465	0.8911	0.3319	8.58E-14	4.20	8.38E-14	2.22E+19	1903067	79929	1860567	82906	4.46	46344	2065
13 mod 4001	EG143	39.6698	0.88	0.3278	1.56E-13	3.58	1.54E-13	2.19E+19	3412641	122173	3370140	124141	3.68	84955	3129
13 mod 4002	EG144	39.9474	0.846	0.3151	5.47E-14	4.59	5.28E-14	2.11E+19	1152277	52890	1109776	57290	5.16	27781	1434
13 mod 4003	EG146	38.0402	0.8813	0.3283	3.95E-14	4.94	3.75E-14	2.19E+19	865608	42761	823107	48098	5.84	21638	1264
13 mod 4004	EG147	40.0699	0.8832	0.3290	1.68E-15	23.76	-2.79E-16	2.20E+19	36976	8786	-5524	23708	-429.16	-138	592
13 mod 4011	EG148	37.42	0.8791	0.3275	5.49E-14	4.42	5.29E-14	2.19E+19	1200424	53059	1157923	57446	4.96	30944	1535
13 mod 4012	EG149	38.6635	0.881	0.3282	6.99E-14	4.27	6.80E-14	2.19E+19	1533705	65489	1491205	69092	4.63	38569	1787

Appendix Table 18: Terrace depth profile ^{10}Be concentrations.

Probe nach Leachen g	carrier m(9Be) g	m(9Be) mg	10Be/9Be	10Be/9Be corr	Error %	N(9Be) atoms	9 BeError abs.	N(10Be) uncorr atoms	N(10Be) uncorr abs err	N(10Be) uncorr atoms/g	N(10Be) uncorr atoms/g abs err	N(10Be) corr atoms	N(10Be) corr abs err	Error corr %	N(10Be) corr atoms/g	N(10Be) corr atoms/g abs err	DP ID	Terrassen ID
33.62	0.893	0.3326	3.75E-14	3.56E-14	13.35	2.22E+19	2.97E+18	8.34E+05	1.11E+05	2.48E+04	3.31E+03	7.90E+05	1.13E+05	14.36	2.35E+04	3.38E+03	12 S7 001 a	T1
26.21	0.8948	0.3333	3.28E-14	3.08E-14	6.57	2.23E+19	1.46E+18	7.30E+05	4.80E+04	2.79E+04	1.83E+03	6.87E+05	5.28E+04	7.69	2.62E+04	2.01E+03	12 S7 001 b	T1
24.68	0.8754	0.3261	2.71E-14	2.51E-14	5.63	2.18E+19	1.23E+18	5.89E+05	3.32E+04	2.39E+04	1.34E+03	5.47E+05	3.98E+04	7.29	2.21E+04	1.61E+03	12 S7 001 c	T1
28.00	0.874	0.3256	2.48E-14	2.28E-14	6.4	2.18E+19	1.39E+18	5.40E+05	3.45E+04	1.93E+04	1.23E+03	4.97E+05	4.10E+04	8.24	1.77E+04	1.46E+03	12 S7 001 d	T1
40.88	0.8773	0.3268	3.54E-14	3.34E-14	5.03	2.18E+19	1.10E+18	7.73E+05	3.89E+04	1.89E+04	9.51E+02	7.30E+05	4.47E+04	6.12	1.79E+04	1.09E+03	12 S7 001 e	T1
17.04	0.8753	0.3260	1.96E-14	1.76E-14	7.39	2.18E+19	1.61E+18	4.27E+05	3.15E+04	2.51E+04	1.85E+03	3.84E+05	3.85E+04	10.02	2.25E+04	2.26E+03	12 S7 002 a	T3
35.91	0.8781	0.3271	4.44E-14	4.24E-14	6.11	2.19E+19	1.34E+18	9.70E+05	5.93E+04	2.70E+04	1.65E+03	9.28E+05	6.33E+04	6.82	2.58E+04	1.76E+03	12 S7 002 b	T3
26.55	0.8763	0.3264	3.21E-14	3.01E-14	6.93	2.18E+19	1.51E+18	7.00E+05	4.85E+04	2.64E+04	1.83E+03	6.57E+05	5.33E+04	8.11	2.48E+04	2.01E+03	12 S7 002 c	T3
36.48	0.8763	0.3264	3.51E-14	3.31E-14	7.13	2.18E+19	1.56E+18	7.66E+05	5.46E+04	2.10E+04	1.50E+03	7.23E+05	5.89E+04	8.14	1.98E+04	1.61E+03	12 S7 002 d	T3
57.01	0.8831	0.3290	8.06E-14	7.87E-14	11.5	2.20E+19	2.53E+18	1.77E+06	2.04E+05	3.11E+04	3.58E+03	1.73E+06	2.05E+05	11.86	3.03E+04	3.60E+03	12 S7 002 e	T3
16.73	0.8757	0.3262	4.15E-14	3.95E-14	15.63	2.18E+19	3.41E+18	9.04E+05	1.41E+05	5.41E+04	8.45E+03	8.61E+05	1.43E+05	16.60	5.15E+04	8.55E+03	12 S7 003 a	AF
29.39	0.8821	0.3286	1.96E-14	1.76E-14	6.18	2.20E+19	1.36E+18	4.30E+05	2.66E+04	1.46E+04	9.05E+02	3.87E+05	3.45E+04	8.92	1.32E+04	1.17E+03	12 S7 003 b	AF
25.16	0.8747	0.3258	3.30E-14	3.10E-14	57.81	2.18E+19	1.26E+19	7.18E+05	4.15E+05	2.85E+04	1.65E+04	6.75E+05	4.15E+05	61.55	2.68E+04	1.65E+04	12 S7 003 c	AF
35.91	0.8867	0.3303	1.27E-14	1.07E-14	7.66	2.21E+19	1.69E+18	2.80E+05	2.14E+04	7.79E+03	5.97E+02	2.37E+05	3.07E+04	12.99	6.59E+03	8.56E+02	12 S7 003 d	AF
39.49	0.8831	0.3290	2.17E-15	2.09E-16	17.94	2.20E+19	3.94E+18	4.77E+04	8.56E+03	1.21E+03	2.17E+02	4.58E+03	2.36E+04	515.31	1.16E+02	5.98E+02	12 S7 003 e	AF
26.93	0.8743	0.3257	4.07E-14	3.87E-14	6.03	2.18E+19	1.31E+18	8.86E+05	5.34E+04	3.29E+04	1.98E+03	8.43E+05	5.78E+04	6.85	3.13E+04	2.15E+03	12 S7 004 a	T5
26.83	0.8737	0.3255	3.15E-14	2.95E-14	6.77	2.17E+19	1.47E+18	6.85E+05	4.64E+04	2.55E+04	1.73E+03	6.42E+05	5.13E+04	7.99	2.39E+04	1.91E+03	12 S7 004 b	T5
26.90	0.8737	0.3255	2.69E-14	2.49E-14	8.38	2.17E+19	1.82E+18	5.85E+05	4.90E+04	2.17E+04	1.82E+03	5.42E+05	5.37E+04	9.91	2.02E+04	2.00E+03	12 S7 004 c	T5
41.83	0.8761	0.3263	3.65E-14	3.45E-14	6.46	2.18E+19	1.41E+18	7.96E+05	5.14E+04	1.90E+04	1.23E+03	7.53E+05	5.59E+04	7.43	1.80E+04	1.34E+03	12 S7 004 d	T5
48.18	0.8736	0.3254	4.46E-14	4.26E-14	5.85	2.17E+19	1.27E+18	9.70E+05	5.67E+04	2.01E+04	1.18E+03	9.27E+05	6.09E+04	6.56	1.92E+04	1.26E+03	12 S7 004 e	T5

Appendix Table 19: Precipitation raw data and calculated mean annual precipitation from local weather stations in the Vakhsh catchment; time span: 1960 - 1990. I to XII represent months. Monthly precipitation is given in mm. Longitude and latitude are given in degrees.

Country	Code_WMO	Name	Long	Lat	Alt.(m)	Year	I	II	III	IV	V	VI	VII	VIII	IX	X	XI	XII	annual precipitation(mm/a)
227	38748	Altynmazar	72.22	39.18	2782	1960	8.0	19.0	25.0	24.0	22.0	22.0	0.0	0.0	4.0	0.0	37.0	4.0	165
227	38748	Altynmazar	72.22	39.18	2782	1961	22.0	9.0	15.0	6.0	33.0	2.0	0.0	8.0	2.0	0.0	14.0	3.0	114
227	38748	Altynmazar	72.22	39.18	2782	1962	8.0	11.0	0.0	49.0	8.0	2.0	11.0	3.0	2.0	3.0	13.0	11.0	121
227	38748	Altynmazar	72.22	39.18	2782	1963	2.0	10.0	18.0	14.0	6.0	44.0	8.0	0.0	0.0	2.0	10.0	19.0	133
227	38748	Altynmazar	72.22	39.18	2782	1964	16.0	35.0	18.0	53.0	19.0	7.0	4.0	1.0	2.0	0.0	3.0	29.0	187
227	38748	Altynmazar	72.22	39.18	2782	1965	16.0	14.0	16.0	10.0	21.0	7.0	20.0	22.0	1.0	4.0	22.0	3.0	156
227	38748	Altynmazar	72.22	39.18	2782	1966	11.0	40.0	42.0	10.0	53.0	1.0	6.0	3.0	10.0	14.0	2.0	22.0	214
227	38748	Altynmazar	72.22	39.18	2782	1967	15.0	21.0	6.0	10.0	11.0	8.0	5.0	6.0	2.0	10.0	10.0	17.0	121
227	38748	Altynmazar	72.22	39.18	2782	1968	13.0	7.0	20.0	16.0	5.0	17.0	5.0	10.0	0.0	1.0	6.0	62.0	162
227	38748	Altynmazar	72.22	39.18	2782	1969	52.0	27.0	45.0	24.0	18.0	8.0	17.0	2.0	3.0	19.0	9.0	17.0	241
227	38748	Altynmazar	72.22	39.18	2782	1970	13.0	3.0	11.0	32.0	16.0	22.0	24.0	3.0	0.0	2.0	8.0	16.0	150
227	38748	Altynmazar	72.22	39.18	2782	1971	2.0	17.0	12.0	8.0	25.0	6.0	3.0	6.0	0.0	0.0	1.0	7.0	87
227	38748	Altynmazar	72.22	39.18	2782	1972	30.0	27.0	35.0	6.0	21.0	11.0	5.0	4.0	1.0	5.0	2.0	20.0	167
227	38748	Altynmazar	72.22	39.18	2782	1973	9.0	16.0	67.0	15.0	47.0	12.0	0.0	2.0	0.0	1.0	1.0	8.0	178
227	38748	Altynmazar	72.22	39.18	2782	1974	21.0	29.0	18.0	13.0	8.0	30.0	12.0	4.0	2.0	0.0	3.0	24.0	164
227	38748	Altynmazar	72.22	39.18	2782	1975	11.0	7.0	14.0	18.0	23.0	18.0	4.0	0.0	0.0	0.0	6.0	9.0	110
227	38748	Altynmazar	72.22	39.18	2782	1976	18.0	30.0	30.0	11.0	24.0	12.0	5.0	22.0	1.0	16.0	3.0	5.0	177
227	38748	Altynmazar	72.22	39.18	2782	1977	34.0	3.0	15.0	9.0	38.0	6.0	1.0	1.0	0.0	24.0	21.0	21.0	173
227	38748	Altynmazar	72.22	39.18	2782	1978	16.0	4.0	9.0	14.0	30.0	7.0	0.0	0.0	0.0	9.0	25.0	28.0	142
227	38748	Altynmazar	72.22	39.18	2782	1979	19.0	4.0	16.0	46.0	11.0	9.0	0.0	19.0	1.0	5.0	6.0	16.0	152
227	38748	Altynmazar	72.22	39.18	2782	1980	17.0	47.0	12.0	11.0	28.0	6.0	4.0	0.0	4.0	8.0	19.0	2.0	158
227	38748	Altynmazar	72.22	39.18	2782	1981	22.0	36.0	10.0	34.0	30.0	5.0	8.0	0.0	3.0	11.0	12.0	17.0	188
227	38748	Altynmazar	72.22	39.18	2782	1982	8.0	15.0	46.0	4.0	24.0	21.0	0.0	0.0	0.0	7.0	35.0	8.0	168
227	38748	Altynmazar	72.22	39.18	2782	1983	16.0	1.0	15.0	7.0	15.0	11.0	45.0	2.0	5.0	0.0	0.0	4.0	121
227	38748	Altynmazar	72.22	39.18	2782	1984	6.0	17.0	38.0	35.0	6.0	6.0	8.0	2.0	1.0	1.0	11.0	11.0	142
227	38748	Altynmazar	72.22	39.18	2782	1985	13.0	6.0	52.0	5.0	5.0	29.0	7.0	0.0	7.0	11.0	8.0	20.0	163
227	38748	Altynmazar	72.22	39.18	2782	1986	5.0	18.0	24.0	28.0	17.0	16.0	17.0	2.0	4.0	0.0	21.0	43.0	195
227	38748	Altynmazar	72.22	39.18	2782	1987	3.0	14.0	26.0	54.0	14.0	48.0	11.0	12.0	2.0	46.0	2.0	25.0	257
227	38748	Altynmazar	72.22	39.18	2782	1988	29.0	15.0	34.0	23.0	48.0	3.0	24.0	2.0	4.0	8.0	3.0	30.0	223
227	38748	Altynmazar	72.22	39.18	2782	1989	7.0	12.0	13.0	11.0	5.0	37.0	17.0	8.0	1.0	1.0	12.0	22.0	146
227	38748	Altynmazar	72.22	39.18	2782	1990	17.0	20.0	18.0	10.0	23.0	7.0	21.0	17.0	0.0	2.0	1.0	17.0	153
							0.0	0.0	0.0	0.0	0.0	0.0	0.0	0.0	0.0	0.0	0.0	0.0	missing years
							100.0	100.0	100.0	100.0	100.0	100.0	100.0	100.0	100.0	100.0	100.0	100.0	completeness in %
						mean	15.5	17.2	23.2	19.7	21.1	14.2	9.4	5.2	2.0	6.8	10.5	17.4	162.2
						max	52.0	47.0	67.0	54.0	53.0	48.0	45.0	22.0	10.0	46.0	37.0	62.0	257.0
						min	2.0	1.0	0.0	4.0	5.0	1.0	0.0	0.0	0.0	0.0	0.0	2.0	87.0

Country	Code_WMO	Name	Long	Lat	Alt.(m)	Year	I	II	III	IV	V	VI	VII	VIII	IX	X	XI	XII	precipitation (mm)/a
227	38842	**Bustonabad**	**69.63**	**38.67**	**1983**	**1960**				93.7	232.2	9.1	27.5	0.0	2.5	11.0	126.2	16.4	
227	38842	**Bustonabad**	**69.63**	**38.67**	**1983**	**1961**	47.4	40.4	89.8	114.4	51.0	8.4	2.7	36.1	0.0		53.0	95.0	538.2
227	38842	**Bustonabad**	**69.63**	**38.67**	**1983**	**1962**	33.9	57.6	70.0	261.5	146.7	16.2	0.0	1.8	0.0	50.3	57.3	44.1	739.4
227	38842	**Bustonabad**	**69.63**	**38.67**	**1983**	**1963**	10.0	120.4	106.1	174.4	169.1	28.4	1.1	0.0	1.2	15.6	81.5	43.0	750.8
227	38842	**Bustonabad**	**69.63**	**38.67**	**1983**	**1964**	34.1	96.9	131.2	291.5	132.9	39.4	70.7	0.0	0.0	1.5	33.1	28.9	860.2
227	38842	**Bustonabad**	**69.63**	**38.67**	**1983**	**1965**	77.8	91.7	65.5	139.5	83.7	28.1	35.8	21.0	7.1	34.2	96.8	7.1	688.3
227	38842	**Bustonabad**	**69.63**	**38.67**	**1983**	**1966**	48.6	124.7	292.6	114.2	122.8	16.1	33.0	8.2	10.3	93.9	4.2	63.9	932.5
227	38842	**Bustonabad**	**69.63**	**38.67**	**1983**	**1967**	27.0	110.9	38.5	139.2	119.8	63.1	7.2	0.0	7.6	109.1	89.6	56.1	768.1
227	38842	**Bustonabad**	**69.63**	**38.67**	**1983**	**1968**	66.8	27.3	172.4	106.9	137.6	33.8	2.5	0.0	0.0	88.0	54.1	182.4	871.8
227	38842	**Bustonabad**	**69.63**	**38.67**	**1983**	**1969**	106.4	65.9	310.1	223.0	211.2	97.2	58.0	1.8	10.4	115.3	68.0	47.4	1314.7
227	38842	**Bustonabad**	**69.63**	**38.67**	**1983**	**1970**	97.6	42.9	89.0	149.6	71.2	18.4	54.2	0.0	1.7	10.3	20.9	57.4	613.2
227	38842	**Bustonabad**	**69.63**	**38.67**	**1983**	**1971**	27.1	69.8	83.4	195.2	29.4	2.8	2.8	0.0	0.0	23.3	66.7	34.9	535.4
227	38842	**Bustonabad**	**69.63**	**38.67**	**1983**	**1972**	61.9	34.3	153.6	139.1	171.2	56.2	10.6	1.9	0.8	30.3	39.2	55.5	754.6
227	38842	**Bustonabad**	**69.63**	**38.67**	**1983**	**1973**	46.2	136.7	238.5	132.1	173.4	1.1	4.4	0.0	10.5				
227	38842	**Bustonabad**	**69.63**	**38.67**	**1983**	**1974**	84.8	42.9	71.3	140.0	88.1	45.0	19.7	49.4	29.6	12.5	39.3	72.3	694.9
227	38842	**Bustonabad**	**69.63**	**38.67**	**1983**	**1975**	74.6	89.9	120.9	77.7	200.1	21.5	0.0	0.0	12.2		30.1	39.4	666.4
227	38842	**Bustonabad**	**69.63**	**38.67**	**1983**	**1976**	60.6	134.6	102.9	185.8	95.6	25.5	0.0	0.0	3.3	165.6	7.4	10.1	791.4
227	38842	**Bustonabad**	**69.63**	**38.67**	**1983**	**1977**	113.3	27.8	100.5	58.8	127.9	13.8	0.0	1.0	0.0	82.7	67.8	187.7	781.3
227	38842	**Bustonabad**	**69.63**	**38.67**	**1983**	**1978**	77.2	67.4	125.6	77.7	175.4	33.3	0.0	0.0	0.0	23.0	103.9	93.7	777.2
227	38842	**Bustonabad**	**69.63**	**38.67**	**1983**	**1979**	62.3	70.9	75.5	204.9	127.4	61.4	0.7	5.9	10.5	9.4	43.4	57.6	729.9
227	38842	**Bustonabad**	**69.63**	**38.67**	**1983**	**1980**	79.7	108.8	125.6	181.4	98.9	20.6	1.3	0.0	0.0	13.3	80.6	29.0	739.2
227	38842	**Bustonabad**	**69.63**	**38.67**	**1983**	**1981**	92.2	226.2	150.7	76.9	125.5	35.3	56.4	20.5	18.1	88.2	52.3	66.4	1008.7
227	38842	**Bustonabad**	**69.63**	**38.67**	**1983**	**1982**	53.6	74.4	148.4	24.9	57.5	42.5	5.1	6.1	20.9	131.9	67.7	22.8	655.8
227	38842	**Bustonabad**	**69.63**	**38.67**	**1983**	**1983**	50.7	30.0	91.4	145.6	74.8	94.1	16.1	0.3	16.3	5.0	24.1	38.1	586.5
227	38842	**Bustonabad**	**69.63**	**38.67**	**1983**	**1984**	51.7	99.9	237.9	158.5	92.2	1.1	2.3	0.0	9.5	38.0	116.1	61.3	868.5
227	38842	**Bustonabad**	**69.63**	**38.67**	**1983**	**1985**	98.2	69.3	131.5	117.0	151.6	64.0	0.0	13.6	0.3	54.8	14.6	58.3	773.2
227	38842	**Bustonabad**	**69.63**	**38.67**	**1983**	**1986**	36.8		65.9	76.6	121.0	27.3	2.2	2.8	16.8	72.7	44.0	152.9	619.0
227	38842	**Bustonabad**	**69.63**	**38.67**	**1983**	**1987**	55.1	48.9	274.1	217.5	89.3	28.3	85.3	2.6	3.7	174.9	38.2	44.8	1062.7
227	38842	**Bustonabad**	**69.63**	**38.67**	**1983**	**1988**	86.8	65.2	188.8	85.1	104.5	27.0	3.9	9.8	0.3	52.1	7.3	110.8	741.6
227	38842	**Bustonabad**	**69.63**	**38.67**	**1983**	**1989**	51.8	93.2	112.1	113.4	121.6	26.3	78.1	16.7	10.5	22.1	77.5	113.1	836.4
227	38842	**Bustonabad**	**69.63**	**38.67**	**1983**	**1990**	100.1	81.0	106.4	227.5	82.7	7.3	13.5	4.5	0.0	62.0	29.2	66.9	781.1
							30.0	29.0	30.0	31.0	31.0	31.0	31.0	31.0	31.0	28.0	30.0	30.0	years complete
							96.77	93.55	96.77	100.00	100.00	100.00	100.00	100.00	100.00	90.32	96.77	96.77	completeness in %

mean	63.8	81.0	135.7	143.3	122.1	32.0	19.2	6.6	6.6	56.8	54.5	65.2	775.2
max	113.3	226.2	310.1	291.5	232.2	97.2	85.3	49.4	29.6	174.9	126.2	187.7	1314.7
min	10.0	27.3	38.5	24.9	29.4	1.1	0.0	0.0	0.0	1.5	4.2	7.1	535.4

Country	Code_WMO	Name	Long	Lat	Alt.(m)	Year	I	II	III	IV	V	VI	VII	VIII	IX	X	XI	XII	precipitation (mm)/a
213	38745	**Daraut-Kurgan**	**72.18**	**39.55**	**2470**	**1960**	19.4	27.9	34.6	19.2	84.3	18.8	51.8	3.8	0.0	0.7	11.4	17.9	289.8
213	38745	**Daraut-Kurgan**	**72.18**	**39.55**	**2470**	**1961**	17.7	29.4	34.9	27.1	16.8	68.9	3.2	0.0	7.3	1.2	25.0	6.6	238.1
213	38745	**Daraut-Kurgan**	**72.18**	**39.55**	**2470**	**1962**	28.3	23.7	36.7	12.3	13.5	6.6	7.3	16.7	2.4	7.0	27.4	17.1	199.0
213	38745	**Daraut-Kurgan**	**72.18**	**39.55**	**2470**	**1963**	14.9	38.5	10.8	55.7	12.4	31.4	16.1	25.4	12.1	5.6	31.6	2.7	257.2
213	38745	**Daraut-Kurgan**	**72.18**	**39.55**	**2470**	**1964**	9.4	13.0	45.7	20.9	18.9	60.7	35.6	0.0	1.7	2.4	26.9	25.2	260.4
213	38745	**Daraut-Kurgan**	**72.18**	**39.55**	**2470**	**1965**	24.5	60.9	24.7	61.1	66.0	18.4	29.2	3.3	5.7	0.1	2.9	31.7	328.5
213	38745	**Daraut-Kurgan**	**72.18**	**39.55**	**2470**	**1966**	26.6	48.5	28.9	8.5	49.0	27.6	34.4	19.4	0.8	8.3	28.2	7.0	287.2
213	38745	**Daraut-Kurgan**	**72.18**	**39.55**	**2470**	**1967**	11.1	46.9	38.2	23.8	111.9	15.7	32.3	6.2	16.0	47.8	1.2	35.6	386.7
213	38745	**Daraut-Kurgan**	**72.18**	**39.55**	**2470**	**1968**	16.3	56.7	13.4	14.8	58.3	39.4	27.2	4.4	2.1	10.5	10.6	24.2	277.9
213	38745	**Daraut-Kurgan**	**72.18**	**39.55**	**2470**	**1969**	21.2	9.8	12.4	53.5	74.5	33.5	26.6	9.5	0.1	8.9	5.0	99.0	354.0
213	38745	**Daraut-Kurgan**	**72.18**	**39.55**	**2470**	**1970**	67.2	12.0	64.5	31.3	53.9	20.0	34.3	5.7	7.0	24.4	5.3	16.1	341.7
213	38745	**Daraut-Kurgan**	**72.18**	**39.55**	**2470**	**1971**	14.1	11.5	24.5	39.8	50.1	58.4	38.2	13.7	0.0	12.6	4.4	29.6	296.9
213	38745	**Daraut-Kurgan**	**72.18**	**39.55**	**2470**	**1972**	4.0	20.2	20.1	26.8	64.2	18.5	7.4	0.0	8.2	0.2	7.8	14.1	191.5
213	38745	**Daraut-Kurgan**	**72.18**	**39.55**	**2470**	**1973**	62.8	45.8	84.6	9.3	18.8	27.3	9.7	5.0	15.6	1.4	1.9	31.0	313.2
213	38745	**Daraut-Kurgan**	**72.18**	**39.55**	**2470**	**1974**	37.1	19.6	103.2	17.3	64.7	16.3	22.0	3.2	0.4	0.0	2.9	4.0	290.7
213	38745	**Daraut-Kurgan**	**72.18**	**39.55**	**2470**	**1975**	31.7	63.9	14.9	5.2	32.2	37.4	43.7	24.3	1.9	9.0	8.7	18.2	291.1
213	38745	**Daraut-Kurgan**	**72.18**	**39.55**	**2470**	**1976**	14.2	27.6	32.6	41.8	49.4	17.9	19.7	1.5	13.2	4.7	16.5	20.9	260.0
213	38745	**Daraut-Kurgan**	**72.18**	**39.55**	**2470**	**1977**	34.5	55.8	72.0	16.5	51.4	51.0	26.2	14.2	4.3	22.7	7.3	12.5	368.4
213	38745	**Daraut-Kurgan**	**72.18**	**39.55**	**2470**	**1978**	88.3	6.1	28.1	5.4	47.9	18.9	3.1	0.8	3.4	34.6	20.3	35.0	291.9
213	38745	**Daraut-Kurgan**	**72.18**	**39.55**	**2470**	**1979**	24.3	6.4	30.8	17.7	23.2	42.6	0.0	0.4	1.8	14.4	43.5	42.8	247.9
213	38745	**Daraut-Kurgan**	**72.18**	**39.55**	**2470**	**1980**	34.5	7.3	20.2	86.6	44.2	11.3	13.5	29.0	20.8	8.1	13.7	22.1	311.3
213	38745	**Daraut-Kurgan**	**72.18**	**39.55**	**2470**	**1981**	33.0	52.9	23.8	30.5	35.8	71.3	10.3	1.6	5.5	5.2	23.0	2.1	295.0
213	38745	**Daraut-Kurgan**	**72.18**	**39.55**	**2470**	**1982**	37.7	72.7	9.1	33.8	69.4	2.7	32.4	20.3	7.7	20.2	16.8	25.4	348.2
213	38745	**Daraut-Kurgan**	**72.18**	**39.55**	**2470**	**1983**	10.0	19.0	70.7	15.8	22.4	31.5	2.6	16.3	3.3	20.4	40.9	17.4	270.3
213	38745	**Daraut-Kurgan**	**72.18**	**39.55**	**2470**	**1984**	35.8	14.5	29.5	5.8	33.4	34.7	51.1	2.6	7.1	0.0	4.4	5.6	224.5
213	38745	**Daraut-Kurgan**	**72.18**	**39.55**	**2470**	**1985**	8.2	23.6	61.6	54.2	18.5	21.1	44.7	0.0	10.0	0.0	0.0	0.0	241.9
213	38745	**Daraut-Kurgan**	**72.18**	**39.55**	**2470**	**1986**	28.6	23.6	89.2	13.4	21.4	40.9	25.3	8.4	23.6	39.2	20.5	24.1	358.2
213	38745	**Daraut-Kurgan**	**72.18**	**39.55**	**2470**	**1987**	11.4	6.5	41.5	38.3	54.7	72.1	18.8	2.8	10.5	1.5	22.2	50.5	330.8
213	38745	**Daraut-Kurgan**	**72.18**	**39.55**	**2470**	**1988**	4.6	19.6	38.2	61.5	70.9	82.7	43.5	19.8	1.6	32.5	13.1	39.4	427.4
213	38745	**Daraut-Kurgan**	**72.18**	**39.55**	**2470**	**1989**	56.5	35.7	66.2	51.8	119.0	18.3	11.7	21.7	17.1	9	35	37	479.0
							30.0	30.0	30.0	30.0	30.0	30.0	30.0	30.0	30.0	30.0	30.0	30.0	years complete
							100.0	100.0	100.0	100.0	100.0	100.0	100.0	100.0	100.0	100.0	100.0	100.0	completeness in %

mean	27.6	30.0	40.2	30.0	48.4	33.9	24.1	9.3	7.0	11.8	15.9	23.8	302.0
max	88.3	72.7	103.2	86.6	119.0	82.7	51.8	29.0	23.6	47.8	43.5	99.0	479.0
min	4.0	6.1	9.1	5.2	12.4	2.7	0.0	0.0	0.0	0.0	0.0	0.0	191.5

Country	Code_WMO	Name	Long	Lat	Alt.(m)	Year	I	II	III	IV	V	VI	VII	VIII	IX	X	XI	XII	precipitation (mm)/a
227	38734	**Dehavz**	**70.20**	**39.45**	**2561**	**1960**	3.1	21.1	46.5	24.3	75.6	18.3	8.5	0.0	4.7	11.1	15.2	0.3	228.7
227	38734	**Dehavz**	**70.20**	**39.45**	**2561**	**1961**	14.0	9.0	32.0	25.4	31.1	18.8	7.9	32.6	2.7	1.5	13.0	1.7	189.7
227	38734	**Dehavz**	**70.20**	**39.45**	**2561**	**1962**	1.3	10.3	7.5	70.3	45.6	12.5	7.4	7.8	21.4	7.2	15.3	6.9	213.5
227	38734	**Dehavz**	**70.20**	**39.45**	**2561**	**1963**	0.0	28.5	31.0	81.7	70.2	47.9	11.8	0.7	0.1	5.4	8.6	12.0	297.9
227	38734	**Dehavz**	**70.20**	**39.45**	**2561**	**1964**	2.9	21.6	29.0	106.8	40.8	19.7	48.1	1.0	7.2	1.5	13.3	8.8	300.7
227	38734	**Dehavz**	**70.20**	**39.45**	**2561**	**1965**	10.6	7.4	34.1	43.2	34.8	42.0	33.1	17.5	13.1	61.7	15.2	1.7	314.4
227	38734	**Dehavz**	**70.20**	**39.45**	**2561**	**1966**	5.9	54.5	47.0	15.5	69.4	15.4	24.1	21.8	14.5	42.9	1.7	23.0	335.7
227	38734	**Dehavz**	**70.20**	**39.45**	**2561**	**1967**	13.2	21.4	8.4	28.2	54.8	28.7	12.0	5.2	8.0	25.6	16.8	20.5	242.8
227	38734	**Dehavz**	**70.20**	**39.45**	**2561**	**1968**	8.2	4.5	39.2	69.1	44.5	54.4	8.4	8.3	0.6	36.0	8.3	35.4	316.9
227	38734	**Dehavz**	**70.20**	**39.45**	**2561**	**1969**	9.5	5.9	73.2	86.4	41.7	53.3	49.4	4.5	11.8	61.8	30.3	5.1	432.9
227	38734	**Dehavz**	**70.20**	**39.45**	**2561**	**1970**	21.7	4.4	15.3	99.4	54.2	13.4	83.9	16.3	10.3	15.4	11.7	13.2	359.2
227	38734	**Dehavz**	**70.20**	**39.45**	**2561**	**1971**	2.4	12.2	23.1	92.6	32.5	9.4	26.1	1.2	13.6	8.7	25.1	11.5	258.4
227	38734	**Dehavz**	**70.20**	**39.45**	**2561**	**1972**	22.3	11.2	63.4	21.0	100.3	24.6	47.0	22.0	5.9	12.7	6.3	23.0	359.7
227	38734	**Dehavz**	**70.20**	**39.45**	**2561**	**1973**	3.8	36.0	124.8	60.4	69.8	3.0	5.5	1.8	2.3	7.0	4.0	4.0	322.4
227	38734	**Dehavz**	**70.20**	**39.45**	**2561**	**1974**	7.0	7.0	8.4	110.8	36.4	50.1	48.6	28.2	21.8	16.9	4.3	3.8	343.3
227	38734	**Dehavz**	**70.20**	**39.45**	**2561**	**1975**	4.1	14.9	22.7	13.5	72.6	38.3	39.6	2.8	12.6	12.4	10.2	9.7	253.4
227	38734	**Dehavz**	**70.20**	**39.45**	**2561**	**1976**	19.8	16.1	11.4	44.7	39.8	35.6	32.5	1.3	14.7	110.2	5.0	2.5	333.6
227	38734	**Dehavz**	**70.20**	**39.45**	**2561**	**1977**	22.6	3.3	18.7	31.8	67.0	22.8	14.7	6.4	0.0	58.3	10.6	18.7	274.9
227	38734	**Dehavz**	**70.20**	**39.45**	**2561**	**1978**	3.4	2.8	23.6	102.0	72.7	26.3	5.2	2.8	3.5	13.9	21.2	12.8	290.2
227	38734	**Dehavz**	**70.20**	**39.45**	**2561**	**1979**	17.3	1.6	13.8	151.0	70.3	18.3	8.3	31.5	13.3	7.0	4.7	8.1	345.2
227	38734	**Dehavz**	**70.20**	**39.45**	**2561**	**1980**	11.0	24.4	39.7	55.1	37.5	41.5	15.5	5.9	2.0	32.2	33.0	4.8	302.6
227	38734	**Dehavz**	**70.20**	**39.45**	**2561**	**1981**	9.4	20.8	36.9	66.2	74.8	68.4	59.4	33.1	9.0	5.9	11.5	3.9	399.3
227	38734	**Dehavz**	**70.20**	**39.45**	**2561**	**1982**	1.9	4.5	18.5	22.7	42.4	48.8	12.2	31.2	33.4	76.4	17.3	6.0	315.3
227	38734	**Dehavz**	**70.20**	**39.45**	**2561**	**1983**	11.6	3.3	15.2	27.0	40.5	45.5	26.1	4.9	25.9	11.3	14.2	7.2	232.7
227	38734	**Dehavz**	**70.20**	**39.45**	**2561**	**1984**	10.9	4.0	56.2	49.0	63.9	7.1	4.9	0.6	15.7	13.0	52.0	16.0	293.3
227	38734	**Dehavz**	**70.20**	**39.45**	**2561**	**1985**	10.0	12.0	37.0	25.0	83.0	14.0	7.0	15.0	3.0	16.0	2.0	12.0	236.0
227	38734	**Dehavz**	**70.20**	**39.45**	**2561**	**1986**	7.0	2.0	16.0	34.0	64.0	47.0	8.0	4.0	4.0	23.0	9.0	16.0	234.0
227	38734	**Dehavz**	**70.20**	**39.45**	**2561**	**1987**	6.0	6.0	36.0	78.0	41.0	55.0	73.0	9.0	27.0	30.0	29.0	13.0	403.0
227	38734	**Dehavz**	**70.20**	**39.45**	**2561**	**1988**	37.0	10.0	36.0	30.0	85.0	32.0	30.0	11.0	3.0	26.0	0.0	40.0	340.0
227	38734	**Dehavz**	**70.20**	**39.45**	**2561**	**1989**	6.0	9.0	24.0	12.0	28.0	59.0	24.0	14.0	12.0	38.0	27.0	19.0	272.0
227	38734	**Dehavz**	**70.20**	**39.45**	**2561**	**1990**	9.0	5.0	24.0	43.0	74.0	19.0	31.0	20.0	3.0	23.0	6.0	11.0	268.0
							30.0	30.0	30.0	30.0	30.0	30.0	30.0	30.0	30.0	30.0	30.0	30.0	years complete
							100.0	100.0	100.0	100.0	100.0	100.0	100.0	100.0	100.0	100.0	100.0	100.0	completeness in %

mean	10.1	12.7	32.7	55.5	56.7	31.9	26.2	11.7	10.3	26.2	14.3	12.0	300.3
max	37.0	54.5	124.8	151.0	100.3	68.4	83.9	33.1	33.4	110.2	52.0	40.0	432.9
min	0.0	1.6	7.5	12.0	28.0	3.0	4.9	0.0	0.0	1.5	0.0	0.3	189.7

Country	Code_WMO	Name	Long	Lat	Alt.(m)	Year	I	II	III	IV	V	VI	VII	VIII	IX	X	XI	XII	precipitation (mm)/a
227	38844	**Faizabad**	**69.32**	**38.55**	**1215**	**1960**	66.9	114.6	193.0	150.0	201.2	9.3	2.2	0.0	0.1	7.6	161.6	11.4	917.9
227	38844	**Faizabad**	**69.32**	**38.55**	**1215**	**1961**	61.6	49.1	156.5	197.0	78.5	2.9	0.0	18.0	0.0	16.4	99.9	95.5	775.4
227	38844	**Faizabad**	**69.32**	**38.55**	**1215**	**1962**	56.4	64.9	115.1	340.9	132.3	8.9	0.0	0.0	0.0	53.0	99.8	86.7	958.0
227	38844	**Faizabad**	**69.32**	**38.55**	**1215**	**1963**	8.8	130.7	154.9	215.3	250.9	23.1	3.2	0.0	0.0	2.6	93.1	63.4	946.0
227	38844	**Faizabad**	**69.32**	**38.55**	**1215**	**1964**	79.1	167.7	185.3	350.1	154.4	12.7	38.7	0.0	0.0	0.5	56.5	39.5	1084.5
227	38844	**Faizabad**	**69.32**	**38.55**	**1215**	**1965**	93.3	98.6	113.8	109.5	77.8	3.7	7.9	1.8	1.4	16.6	72.2	12.9	609.5
227	38844	**Faizabad**	**69.32**	**38.55**	**1215**	**1966**	23.5	148.2	266.9	179.4	63.0	0.0	22.2	2.3	2.5	83.4	13.6	83.8	888.8
227	38844	**Faizabad**	**69.32**	**38.55**	**1215**	**1967**	19.1	138.5	71.9	208.1	170.4	53.6	0.0	0.0	1.1	90.3	107.4	61.2	921.6
227	38844	**Faizabad**	**69.32**	**38.55**	**1215**	**1968**	94.0	31.7	181.5	145.3	137.5	15.3	4.4	0.0	0.0	54.9	37.6	199.4	901.6
227	38844	**Faizabad**	**69.32**	**38.55**	**1215**	**1969**	161.9	86.4	308.2	244.5	262.6	37.0	18.3	5.4	16.6	100.6	93.1	32.9	1367.5
227	38844	**Faizabad**	**69.32**	**38.55**	**1215**	**1970**	106.0	67.3	148.7	197.6	40.4	5.4	9.3	0.0	0.0	28.9	14.4	53.9	671.9
227	38844	**Faizabad**	**69.32**	**38.55**	**1215**	**1971**	22.2	76.2	72.2	172.2	8.1	0.8	0.0	0.0	0.0	8.1	28.3	38.8	426.9
227	38844	**Faizabad**	**69.32**	**38.55**	**1215**	**1972**	66.8	32.6	153.4	149.9	128.2	33.0	11.5	0.6	0.5	19.6	27.7	45.1	668.9
227	38844	**Faizabad**	**69.32**	**38.55**	**1215**	**1973**	40.3	99.1	155.1	93.5	124.7	8.7	0.0	0.0	17.3	0.1	19.5	17.4	575.7
227	38844	**Faizabad**	**69.32**	**38.55**	**1215**	**1974**	71.0	34.7	49.0	140.6	60.7	33.4	8.8	16.9	17.5	11.9	26.6	88.2	559.3
227	38844	**Faizabad**	**69.32**	**38.55**	**1215**	**1975**	97.1	102.7	132.6	105.2	208.1	7.9	0.0	0.0	5.8	29.1	59.7	74.4	822.6
227	38844	**Faizabad**	**69.32**	**38.55**	**1215**	**1976**	89.9	183.0	156.1	214.8	62.5	12.6	0.0	0.0	0.0	125.9	29.8	15.2	889.8
227	38844	**Faizabad**	**69.32**	**38.55**	**1215**	**1977**	131.5	54.4	109.9	44.3	87.2	14.1	0.0	0.0	0.0	61.6	38.9	144.3	686.2
227	38844	**Faizabad**	**69.32**	**38.55**	**1215**	**1978**	70.7	89.8	104.3	62.8	187.8	26.0	0.0	0.0	0.0	4.2	131.2	97.5	774.3
227	38844	**Faizabad**	**69.32**	**38.55**	**1215**	**1979**	103.6	87.6	102.0	182.4	154.9	36.4	0.0	3.4	0.7	0.6	73.6	66.5	811.7
227	38844	**Faizabad**	**69.32**	**38.55**	**1215**	**1980**	105.6	154.0	127.0	150.4	103.3	17.4	0.0	0.0	0.0	5.6	101.3	53.7	818.3
227	38844	**Faizabad**	**69.32**	**38.55**	**1215**	**1981**	99.8	226.7	141.2	119.8	223.1	38.3	0.0	0.4	23.0	61.7	45.9	54.8	1034.7
227	38844	**Faizabad**	**69.32**	**38.55**	**1215**	**1982**	88.4	108.2	192.1	120.6	47.3	26.6	0.4	0.0	6.1	110.3	100.6	48.4	849.0
227	38844	**Faizabad**	**69.32**	**38.55**	**1215**	**1983**	105.8	40.9	139.7	314.8	122.0	83.0	15.2	0.7	11.8	3.3	46.3	58.2	941.7
227	38844	**Faizabad**	**69.32**	**38.55**	**1215**	**1984**	50.0	132.7	252.5	167.3	128.9	0.0	0.3	0.0	0.3	89.4	115.8	107.3	1044.5
227	38844	**Faizabad**	**69.32**	**38.55**	**1215**	**1985**	113.6	120.5	171.3	129.9	181.4	13.3	0.0	4.6	0.0	42.0	32.9	65.8	875.3
227	38844	**Faizabad**	**69.32**	**38.55**	**1215**	**1986**	45.4	26.8	184.0	108.6	69.2	13.5	2.2	0.0	14.7	62.1	95.0	177.2	798.7
227	38844	**Faizabad**	**69.32**	**38.55**	**1215**	**1987**	82.5	108.9	326.5	242.4	65.4	2.5	20.6	0.0	6.1	207.2	30.1	41.0	1133.2
227	38844	**Faizabad**	**69.32**	**38.55**	**1215**	**1988**	123.6	66.5	219.8	112.7	67.6	3.6	0.0	3.0	0.6	41.0	8.1	115.4	761.9
227	38844	**Faizabad**	**69.32**	**38.55**	**1215**	**1989**	88.1	115.7	160.4	128.7	144.7	2.6	20.2	4.0	19.3	13.6	94.9	68.5	860.7
227	38844	**Faizabad**	**69.32**	**38.55**	**1215**	**1990**	122.0	80.6	120.4	193.1	38.2	24.5	4.2	0.0	0.0	76.0	38.3	75.7	773.0
							30.0	30.0	30.0	30.0	30.0	30.0	30.0	30.0	30.0	30.0	30.0	30.0	years complete
							100.0	100.0	100.0	100.0	100.0	100.0	100.0	100.0	100.0	100.0	100.0	100.0	completeness in %
						mean	80.3	98.0	160.2	170.7	122.0	18.4	6.1	2.0	4.7	46.1	64.3	70.8	843.5
						max	161.9	226.7	326.5	350.1	262.6	83.0	38.7	18.0	23.0	207.2	161.6	199.4	1367.5
						min	8.8	26.8	49.0	44.3	8.1	0.0	0.0	0.0	0.0	0.1	8.1	11.4	426.9

Country	Code_WMO	Name	Long	Lat	Alt.(m)	Year	I	II	III	IV	V	VI	VII	VIII	IX	X	XI	XII	precipitation (mm)/a
227	38862	**Fedchenko Glacier**	**72.22**	**38.83**	**4169**	**1960**	64.5	176.3	202.9	77.7	110.0	52.8	21.8	0.0	38.0	67.3	154.9	35.9	1002.1
227	38862	**Fedchenko Glacier**	**72.22**	**38.83**	**4169**	**1961**	79.6	72.7	124.3	87.2	72.1	40.8	15.5	36.9	2.0	123.1	144.4	103.2	901.8
227	38862	**Fedchenko Glacier**	**72.22**	**38.83**	**4169**	**1962**	155.6	153.5	40.9	193.7	89.9	46.2	40.7	41.1	22.8	99.8	190.1	140.5	1214.8
227	38862	**Fedchenko Glacier**	**72.22**	**38.83**	**4169**	**1963**	13.8	123.8	119.5	128.1	112.4	58.2	75.3	0.7	45.8	99.8	135.7	136.3	1049.4
227	38862	**Fedchenko Glacier**	**72.22**	**38.83**	**4169**	**1964**	110.7	188.5	147.2	250.8	146.7	49.9	37.8	43.2	13.6	5.3	72.3	103.2	1169.2
227	38862	**Fedchenko Glacier**	**72.22**	**38.83**	**4169**	**1965**	156.8	153.5	122.7	96.8	94.6	59.0	67.3	55.6	24.0	150.0	153.4	33.0	1166.7
227	38862	**Fedchenko Glacier**	**72.22**	**38.83**	**4169**	**1966**	94.8	104.2	157.2	79.6	126.4	17.8	47.9	12.0	34.0	149.4	29.2	113.6	966.1
227	38862	**Fedchenko Glacier**	**72.22**	**38.83**	**4169**	**1967**	57.6	127.9	36.1	40.9	81.6	55.9	43.7	8.2	18.3	83.5	98.8	76.0	728.5
227	38862	**Fedchenko Glacier**	**72.22**	**38.83**	**4169**	**1968**	59.9	44.7	173.1	108.2	88.8	66.6	23.0	35.4	2.2	46.8	98.3	246.1	993.1
227	38862	**Fedchenko Glacier**	**72.22**	**38.83**	**4169**	**1969**	231.2	228.5	265.8	57.9	90.7	31.4	75.6	13.4	29.4	176.3	55.4	86.3	1341.9
227	38862	**Fedchenko Glacier**	**72.22**	**38.83**	**4169**	**1970**	75.7	51.9	111.4	151.5	107.9	62.7	107.2	10.3	26.5	76.2	92.9	164.4	1038.6
227	38862	**Fedchenko Glacier**	**72.22**	**38.83**	**4169**	**1971**	42.7	107.7	75.3	119.2	132.2	30.1	22.2	1.8	33.3	20.2	86.4	111.8	782.9
227	38862	**Fedchenko Glacier**	**72.22**	**38.83**	**4169**	**1972**	214.8	97.0	231.3	72.2	110.6	124.1	55.5	14.1	32.5	99.3	110.0	149.9	1311.3
227	38862	**Fedchenko Glacier**	**72.22**	**38.83**	**4169**	**1973**	91.6	131.9	195.0	197.7	183.9	41.1	6.2	0.5	6.5	23.8	52.4	32.7	963.3
227	38862	**Fedchenko Glacier**	**72.22**	**38.83**	**4169**	**1974**	154.6	122.6	106.6	121.4	73.4	107.0	52.9	47.8	26.5	35.3	89.1	109.1	1046.3
227	38862	**Fedchenko Glacier**	**72.22**	**38.83**	**4169**	**1975**	69.7	110.2	115.0	126.8	167.2	65.2	26.5	13.2	24.8	41.3	119.6	80.9	960.4
227	38862	**Fedchenko Glacier**	**72.22**	**38.83**	**4169**	**1976**	63.4	176.5	132.2	74.4	87.3	84.4	33.1	15.5	37.0	286.5	79.2	97.5	1167.0
227	38862	**Fedchenko Glacier**	**72.22**	**38.83**	**4169**	**1977**	186.4	57.4	142.6	103.6	164.1	44.9	14.1	13.3	0.0	260.9	119.3	219.3	1325.9
227	38862	**Fedchenko Glacier**	**72.22**	**38.83**	**4169**	**1978**	136.1	127.7	117.5	139.3	143.2	45.0	7.4	1.7	2.3	72.3	181.0	219.6	1193.1
227	38862	**Fedchenko Glacier**	**72.22**	**38.83**	**4169**	**1979**	116.7	53.4	103.2	311.2	120.5	56.7	5.6	74.5	39.5	23.5	51.9	107.5	1064.2
227	38862	**Fedchenko Glacier**	**72.22**	**38.83**	**4169**	**1980**	111.3	148.5	151.5	106.3	133.6	32.1	1.3	4.4	6.4	87.0	112.5	42.5	937.4
227	38862	**Fedchenko Glacier**	**72.22**	**38.83**	**4169**	**1981**	107.0	204.5	86.6	241.4	183.2	57.1	99.9	25.8	29.2	131.9	135.3	114.2	1416.1
227	38862	**Fedchenko Glacier**	**72.22**	**38.83**	**4169**	**1982**	70.9	82.0	187.9	82.4	145.0	97.6	35.0	12.9	29.3	128.1	167.3	65.3	1103.7
227	38862	**Fedchenko Glacier**	**72.22**	**38.83**	**4169**	**1983**	124.6	47.9	155.2	102.7	143.1	83.8	96.7	14.8	104.8	21.3	92.0	89.0	1075.9
227	38862	**Fedchenko Glacier**	**72.22**	**38.83**	**4169**	**1984**	73.0	146.0	240.0	209.0	172.0	35.0	25.0	0.0	29.0	51.0	219.0	212.0	1411.0
227	38862	**Fedchenko Glacier**	**72.22**	**38.83**	**4169**	**1985**	115.6	127.9	272.8	68.9	113.9	75.8	25.4	15.0	9.8	161.2	111.0	104.1	1201.4
227	38862	**Fedchenko Glacier**	**72.22**	**38.83**	**4169**	**1986**	54.8	40.7	169.4	136.2	185.6	125.7	15.3	24.7	24.5	68.9	202.1	271.6	1319.5
227	38862	**Fedchenko Glacier**	**72.22**	**38.83**	**4169**	**1987**	136.6	153.5	297.3	400.3	274.4	106.2	66.8	26.7	22.0	298.0	172.9	203.7	2158.4
227	38862	**Fedchenko Glacier**	**72.22**	**38.83**	**4169**	**1988**	133.2	126.0	220.0	163.5	239.4	22.6	53.1	40.8	4.4	103.1	26.6	146.6	1279.3
227	38862	**Fedchenko Glacier**	**72.22**	**38.83**	**4169**	**1989**	88.0	102.0	66.0	90.0	84.0	136.0	94.0	35.0	53.0	59.0	113.0	118.0	1038.0
227	38862	**Fedchenko Glacier**	**72.22**	**38.83**	**4169**	**1990**	223.0	136.0	182.0	163.0	91.0	41.0	128.0	92.0	1.0	160.0	172.0	283.0	1672.0
							30.0	30.0	30.0	30.0	30.0	30.0	30.0	30.0	30.0	30.0	30.0	30.0	years complete
							100.0	100.0	100.0	100.0	100.0	100.0	100.0	100.0	100.0	100.0	100.0	100.0	completeness in %
						mean	110.1	120.2	153.2	138.8	131.2	63.0	45.8	23.6	24.9	103.6	117.4	129.6	1161.3
						max	231.2	228.5	297.3	400.3	274.4	136.0	128.0	92.0	104.8	298.0	219.0	283.0	2158.4
						min	13.8	40.7	36.1	40.9	72.1	17.8	1.3	0.0	0.0	5.3	26.6	32.7	728.5

Country	Code_WMO	Name	Long	Lat	Alt.(m)	Year	I	II	III	IV	V	VI	VII	VIII	IX	X	XI	XII	precipitation (mm)/a
227	38851	Garm	**69.95**	**39.00**	**1316**	**1960**	44.4	140.3	180.0	68.2	210.7	37.7	30.1	0.0	6.4	16.2	104.5	11.9	850.4
227	38851	Garm	**69.95**	**39.00**	**1316**	**1961**	70.2	69.1	100.5	52.8	44.1	0.7	0.2	51.5	0.0	8.4	38.1	80.8	516.4
227	38851	Garm	**69.95**	**39.00**	**1316**	**1962**	31.8	75.5	49.1	235.0	98.2	10.3	0.0	1.9	0.1	28.5	54.5	65.9	650.8
227	38851	Garm	**69.95**	**39.00**	**1316**	**1963**	3.9	110.8	148.1	125.2	135.7	49.1	3.9	0.0	6.7	15.1	52.7	66.5	717.7
227	38851	Garm	**69.95**	**39.00**	**1316**	**1964**	41.8	116.9	112.0	245.8	76.0	63.0	58.5	0.1	0.4	0.0	29.4	42.1	786.0
227	38851	Garm	**69.95**	**39.00**	**1316**	**1965**	88.5	96.6	93.7	111.1	64.7	37.0	7.1	12.9	15.8	43.7	94.2	5.7	671.0
227	38851	Garm	**69.95**	**39.00**	**1316**	**1966**	45.9	117.3	212.5	78.6	108.1	2.9	2.8	8.5	6.7	100.8	2.6	66.8	753.5
227	38851	Garm	**69.95**	**39.00**	**1316**	**1967**	32.1	97.4	34.0	100.5	71.2	32.9	6.4	1.2	4.1	71.3	90.9	68.5	610.5
227	38851	Garm	**69.95**	**39.00**	**1316**	**1968**	51.8	29.6	183.3	76.9	128.0	73.2	0.5	0.9	0.4	58.3	45.4	263.1	911.4
227	38851	Garm	**69.95**	**39.00**	**1316**	**1969**	175.0	74.8	304.9	204.7	197.9	88.5	74.0	9.8	1.3	99.6	56.5	46.4	1333.4
227	38851	Garm	**69.95**	**39.00**	**1316**	**1970**	117.7	28.3	91.6	152.4	99.1	35.7	67.4	0.3	0.8	14.1	17.7	83.0	708.1
227	38851	Garm	**69.95**	**39.00**	**1316**	**1971**	20.2	67.3	65.7	122.1	66.2	0.3	1.1	0.0	3.5	3.7	46.8	35.6	432.5
227	38851	Garm	**69.95**	**39.00**	**1316**	**1972**	97.5	43.2	210.1	131.0	134.9	67.8	6.8	0.8	0.8	40.1	37.6	62.4	833.0
227	38851	Garm	**69.95**	**39.00**	**1316**	**1973**	27.9	149.1	222.6	104.7	156.1	4.8	11.2	0.0	5.7	1.5	31.3	13.6	728.5
227	38851	Garm	**69.95**	**39.00**	**1316**	**1974**	98.3	74.4	67.8	179.2	113.5	38.9	20.4	23.6	35.1	7.3	34.6	93.7	786.8
227	38851	Garm	**69.95**	**39.00**	**1316**	**1975**	81.7	87.9	108.1	48.0	195.0	14.3	5.6	0.0	29.9	29.8	40.9	40.9	682.1
227	38851	Garm	**69.95**	**39.00**	**1316**	**1976**	47.0	130.5	102.2	135.5	48.2	15.3	1.4	0.0	2.2	200.2	3.7	10.0	696.2
227	38851	Garm	**69.95**	**39.00**	**1316**	**1977**	130.1	22.7	101.7	47.4	75.5	20.7	0.7	0.3	0.0	76.8	51.7	132.4	660.0
227	38851	Garm	**69.95**	**39.00**	**1316**	**1978**	65.3	61.9	111.6	108.7	129.3	44.4	0.0	0.0	0.0	29.0	94.0	90.7	734.9
227	38851	Garm	**69.95**	**39.00**	**1316**	**1979**	72.5	35.4	41.8	154.3	115.1	46.8	2.8	9.6	18.7	17.8	27.6	59.8	602.2
227	38851	Garm	**69.95**	**39.00**	**1316**	**1980**	69.3	174.3	128.4	175.6	109.8	30.7	9.7	0.0	0.0	17.0	69.9	11.4	796.1
227	38851	Garm	**69.95**	**39.00**	**1316**	**1981**	80.3	183.4	119.7	91.0	72.9	59.8	45.5	11.6	11.8	93.7	64.0	62.4	896.1
227	38851	Garm	**69.95**	**39.00**	**1316**	**1982**	33.4	55.4	124.6	37.1	114.2	30.9	21.9	9.9	27.3	148.1	69.0	36.1	707.9
227	38851	Garm	**69.95**	**39.00**	**1316**	**1983**	78.4	35.1	75.4	136.1	80.0	41.5	37.4	30.6	18.5	2.7	26.8	27.0	589.5
227	38851	Garm	**69.95**	**39.00**	**1316**	**1984**	31.8	76.4	226.6	121.0	178.6	4.9	2.2	0.0	15.6	27.2	116.9	71.8	873.0
227	38851	Garm	**69.95**	**39.00**	**1316**	**1985**	90.3	57.6	139.3	74.4	108.4	28.7	8.5	5.7	0.8	50.7	11.7	35.6	611.7
227	38851	Garm	**69.95**	**39.00**	**1316**	**1986**	27.4	20.9	56.8	52.3	119.4	26.1	2.3	0.8	11.1	80.5	45.9	180.1	623.6
227	38851	Garm	**69.95**	**39.00**	**1316**	**1987**	41.5	64.2	221.8	169.5	47.7	52.1	73.3	0.0	13.4	155.5	41.3	60.3	940.6
227	38851	Garm	**69.95**	**39.00**	**1316**	**1988**	99.2	57.8	185.0	69.4	164.3	27.1	7.9	7.7	0.0	34.0	0.0	148.0	800.4
227	38851	Garm	**69.95**	**39.00**	**1316**	**1989**	43.0	70.0	80.0	108.0	117.0	33.0	27.0	10.0	3.0	18.0	89.0	120.0	718.0
227	38851	Garm	**69.95**	**39.00**	**1316**	**1990**	124.0	69.0	114.0	190.0	80.0	33.0	43.0	9.0	0.0	38.0	32.0	86.0	818.0
							30.0	30.0	30.0	30.0	30.0	30.0	30.0	30.0	30.0	30.0	30.0	30.0	years complete
							100.0	100.0	100.0	100.0	100.0	100.0	100.0	100.0	100.0	100.0	100.0	100.0	completeness in %
						mean	66.5	80.4	129.4	119.6	111.6	33.9	18.7	6.7	7.7	49.3	49.1	70.3	743.2
						max	175.0	183.4	304.9	245.8	210.7	88.5	74.0	51.5	35.1	200.2	116.9	263.1	1333.4
						min	3.9	20.9	34.0	37.1	44.1	0.3	0.0	0.0	0.0	0.0	0.0	5.7	432.5

Country	Code_WMO	Name	Long	Lat	Alt.(m)	Year	I	II	III	IV	V	VI	VII	VIII	IX	X	XI	XII	precipitation (mm)/a
227	38853	Haburabad	**70.70**	**38.63**	**3347**	**1960**										6	94	21	
227	38853	Haburabad	**70.70**	**38.63**	**3347**	**1961**	138	132	126	116	56	8	0	31	0	27	66	85	785.0
227	38853	Haburabad	**70.70**	**38.63**	**3347**	**1962**	62	109	67	207	114	30	24	4	4	73	105	93	892.0
227	38853	Haburabad	**70.70**	**38.63**	**3347**	**1963**	9	93	130	129	150	89	28	0	12	14	60	48	762.0
227	38853	Haburabad	**70.70**	**38.63**	**3347**	**1964**	60	108	85	154	95	45	77	8	0	2	39	44	717.0
227	38853	Haburabad	**70.70**	**38.63**	**3347**	**1965**	95	67	84	84	45	44	54	12	22	51	65	25	648.0
227	38853	Haburabad	**70.70**	**38.63**	**3347**	**1966**	53	106	150	98	95	4	21	5	11	115	12	111	781.0
227	38853	Haburabad	**70.70**	**38.63**	**3347**	**1967**	35	117	40	72	180	65	16	5	5	59	56	84	734.0
227	38853	Haburabad	**70.70**	**38.63**	**3347**	**1968**	55	23	110	86	97	83	62	1	0	42	51	165	775.0
227	38853	Haburabad	**70.70**	**38.63**	**3347**	**1969**	125	93	141	104	103	104	81	2	14	105	70	41	983.0
227	38853	Haburabad	**70.70**	**38.63**	**3347**	**1970**	58	29	68	127	74	20	87	1	1	26	29	81	601.0
227	38853	Haburabad	**70.70**	**38.63**	**3347**	**1971**	21	71	56	91	73	4	3	0	9	9	45	37	419.0
227	38853	Haburabad	**70.70**	**38.63**	**3347**	**1972**	136	58	109	58	103	85	50	1	7	41	50	83	781.0
227	38853	Haburabad	**70.70**	**38.63**	**3347**	**1973**	61	102	144	60	133	21	6	0	6	7	17	19	576.0
227	38853	Haburabad	**70.70**	**38.63**	**3347**	**1974**	74	50	83	69	66	49	18	42	19	23	29	31	553.0
227	38853	Haburabad	**70.70**	**38.63**	**3347**	**1975**	19	36	52	58	43	20	17	0	26	20	63	56	410.0
227	38853	Haburabad	**70.70**	**38.63**	**3347**	**1976**	52	92	79	69	62	53	13	0	0	113	26	31	590.0
227	38853	Haburabad	**70.70**	**38.63**	**3347**	**1977**	86	19	46	51	105	41	13	0	0	46	34	89	530.0
227	38853	Haburabad	**70.70**	**38.63**	**3347**	**1978**	70	61	50	68	53	19	0	1	0	31	94	106	553.0
227	38853	Haburabad	**70.70**	**38.63**	**3347**	**1979**	48	33	66	89	114	26	12	37	12	14	45	70	566.0
227	38853	Haburabad	**70.70**	**38.63**	**3347**	**1980**	77	95	68	106	73	18	17	0	0	17	61	27	559.0
227	38853	Haburabad	**70.70**	**38.63**	**3347**	**1981**	66	118	62	53	82	63	67	25	5	61	53	48	703.0
227	38853	Haburabad	**70.70**	**38.63**	**3347**	**1982**	36	64	116	21	90	50	38	5	18	92	94	53	677.0
227	38853	Haburabad	**70.70**	**38.63**	**3347**	**1983**	81	29	83	93	111	88	72	0	13	9	25	54	658.0
227	38853	Haburabad	**70.70**	**38.63**	**3347**	**1984**	42	79	158	101	94	6	9	0	17	18	148	84	756.0
227	38853	Haburabad	**70.70**	**38.63**	**3347**	**1985**	70	54	134	55	117	44	20	8	0	54	61	48	665.0
227	38853	Haburabad	**70.70**	**38.63**	**3347**	**1986**	32	26	126	94	144	64	8	10	2	22	101	128	757.0
227	38853	Haburabad	**70.70**	**38.63**	**3347**	**1987**	39	65	152	133	105	54	59	12	12	140	35	38	844.0
227	38853	Haburabad	**70.70**	**38.63**	**3347**	**1988**	74	51	124	78	80	23	13	35	1	37	6	89	611.0
227	38853	Haburabad	**70.70**	**38.63**	**3347**	**1989**	52	77	69	85	83	53	41	17	14	27	85	97	700.0
227	38853	Haburabad	**70.70**	**38.63**	**3347**	**1990**	144	68	140	72	60	57	20	5					
							30	30	30	30	30	30	30	30	29	30	30	30	years complete
							96.77	96.77	96.77	96.77	96.77	96.77	96.77	96.77	93.55	96.77	96.77	96.77	completeness in %

mean	65.7	70.8	97.3	89.4	93.3	44.3	31.5	8.9	7.9	43.4	57.3	66.2	675.4
max	144.0	132.0	158.0	207.0	180.0	104.0	87.0	42.0	26.0	140.0	148.0	165.0	983.0
min	9.0	19.0	40.0	21.0	43.0	4.0	0.0	0.0	0.0	2.0	6.0	19.0	410.0

Country	Code_WMO	Name	Long	Lat	Alt.(m)	Year	I	II	III	IV	V	VI	VII	VIII	IX	X	XI	XII	precipitation (mm)/a
227	38846	**Hovaling**	**69.95**	**38.35**	**1468**	**1960**													
227	38846	**Hovaling**	**69.95**	**38.35**	**1468**	**1961**	75.9	100.7	167.5	205.3	86.5	13.5	0.0	3.0	0.0	40.5	104.7	84.0	881.6
227	38846	**Hovaling**	**69.95**	**38.35**	**1468**	**1962**													
227	38846	**Hovaling**	**69.95**	**38.35**	**1468**	**1963**	7.9	151.0	188.1	210.9	227.5	17.5	8.8	0.0	4.7	0.8	85.3	68.2	970.7
227	38846	**Hovaling**	**69.95**	**38.35**	**1468**	**1964**	74.6	157.6	208.8	301.9	104.8	34.9	40.8	0.0	0.0	5.3	56.3	33.0	1018.0
227	38846	**Hovaling**	**69.95**	**38.35**	**1468**	**1965**	106.3	153.3	136.0	160.4	110.5	2.3	12.1	0.6	7.6	55.7	51.7	12.2	808.7
227	38846	**Hovaling**	**69.95**	**38.35**	**1468**	**1966**	30.5	193.8	273.5	212.2	105.2	1.2	1.9	1.5	2.7	165.1	26.8	162.1	1176.5
227	38846	**Hovaling**	**69.95**	**38.35**	**1468**	**1967**	35.7	187.7	97.3	192.7	254.8	70.6	1.2	0.0	0.3	86.4	108.1	67.8	1102.6
227	38846	**Hovaling**	**69.95**	**38.35**	**1468**	**1968**	119.1	30.4	244.3	133.3	232.4	16.6	0.0	0.0	0.0	62.4	67.7	290.4	1196.6
227	38846	**Hovaling**	**69.95**	**38.35**	**1468**	**1969**	187.2	114.6	298.4	217.9	191.1	41.5	31.2	4.9	17.2	123.2	112.9	46.3	1386.4
227	38846	**Hovaling**	**69.95**	**38.35**	**1468**	**1970**	129.2	78.2	206.7	179.2	51.0	0.0	27.3	0.0	0.0	40.8	35.0	92.5	839.9
227	38846	**Hovaling**	**69.95**	**38.35**	**1468**	**1971**	45.1	126.6	104.3	216.8	44.1	0.0	0.0	0.0	0.5	30.7	51.8	43.6	663.5
227	38846	**Hovaling**	**69.95**	**38.35**	**1468**	**1972**	138.5	76.0	197.8	189.5	160.1	24.2	1.8	0.5	4.2	35.2	71.1	78.0	976.9
227	38846	**Hovaling**	**69.95**	**38.35**	**1468**	**1973**	90.6	212.4	213.0	163.5	184.5	0.6	0.0	0.0	17.8	1.3	26.9	26.5	937.1
227	38846	**Hovaling**	**69.95**	**38.35**	**1468**	**1974**	130.0	82.9	198.2	146.8	154.4	29.8	5.8	22.5	5.2	18.1	44.2	123.0	960.9
227	38846	**Hovaling**	**69.95**	**38.35**	**1468**	**1975**	129.3	123.5	170.2	195.8	312.6	19.4	0.3	0.0	4.8	58.6	85.1	99.0	1198.6
227	38846	**Hovaling**	**69.95**	**38.35**	**1468**	**1976**	108.8	210.5	165.3	285.0	78.6	27.8	0.0	0.0	0.9	132.2	24.4	35.3	1068.8
227	38846	**Hovaling**	**69.95**	**38.35**	**1468**	**1977**	194.1	59.2	159.1	119.4	140.1	36.1	0.0	0.0	0.0	45.6	67.1	144.0	964.7
227	38846	**Hovaling**	**69.95**	**38.35**	**1468**	**1978**	121.5	103.8	167.1	113.6	119.1	2.6	0.0	0.0	0.0	0.5	131.5	134.1	893.8
227	38846	**Hovaling**	**69.95**	**38.35**	**1468**	**1979**	104.8	116.5	137.8	189.1	193.6	19.3	0.0	0.8	10.8	0.0	47.1	87.9	907.7
227	38846	**Hovaling**	**69.95**	**38.35**	**1468**	**1980**	111.1	174.1	190.1	158.0	88.8	8.7	0.6	0.0	3.9	16.6	119.8	28.7	900.4
227	38846	**Hovaling**	**69.95**	**38.35**	**1468**	**1981**	161.0	211.8	199.2	199.8	121.6	24.1	34.4	11.2	16.7	72.4	42.6	64.3	1159.1
227	38846	**Hovaling**	**69.95**	**38.35**	**1468**	**1982**	99.8	158.9	244.3	86.5	64.3	16.9	14.9	0.0	18.7	133.1	130.3	55.3	1023.0
227	38846	**Hovaling**	**69.95**	**38.35**	**1468**	**1983**	102.3	34.3	192.1	202.6	106.1	37.7	16.8	0.0	14.4	0.0	43.5	51.5	801.3
227	38846	**Hovaling**	**69.95**	**38.35**	**1468**	**1984**	36.6	174.4	283.8	178.6	116.4	0.0	0.0	0.0	2.3	60.3	131.3	117.0	1100.7
227	38846	**Hovaling**	**69.95**	**38.35**	**1468**	**1985**	161.1	124.2	165.9	188.9	177.0	2.3	0.4	0.4	0.0	34.1	40.4	87.4	982.1
227	38846	**Hovaling**	**69.95**	**38.35**	**1468**	**1986**	70.4	51.8	144.4	114.3	116.8	29.4	4.8	4.4	3.1	33.1	101.5	218.7	892.7
227	38846	**Hovaling**	**69.95**	**38.35**	**1468**	**1987**	67.5	146.3	465.6	247.8	65.5	59.5	27.1	1.4	7.5	219.8	14.3	36.9	1359.2
227	38846	**Hovaling**	**69.95**	**38.35**	**1468**	**1988**	118.3	118.5	287.5	149.7	78.4	5.7	1.0	10.8	2.7	33.3	6.5	138.0	950.4
227	38846	**Hovaling**	**69.95**	**38.35**	**1468**	**1989**	95.4	164.7	168.1	126.7	89.2	1.6	21.8	5.8	32.7	8.0	96.2	90.1	900.3
227	38846	**Hovaling**	**69.95**	**38.35**	**1468**	**1990**	150.3	117.5	165.3	204.8	41.7	15.8	0.5	8.0	0.0	54.0	43.0	137.0	937.9
							29.0	29.0	29.0	29.0	29.0	29.0	29.0	29.0	29.0	29.0	29.0	29.0	years complete
							93.55	93.55	93.55	93.55	93.55	93.55	93.55	93.55	93.55	93.55	93.55	93.55	completeness in %

mean	103.5	129.5	201.4	182.4	131.6	19.3	8.7	2.6	6.2	54.0	67.8	91.5	998.6
max	194.1	212.4	465.6	301.9	312.6	70.6	40.8	22.5	32.7	219.8	131.5	290.4	1386.4
min	7.9	30.4	97.3	86.5	41.7	0.0	0.0	0.0	0.0	0.0	6.5	12.2	663.5

Country	Code_WMO	Name	Long	Lat	Alt.(m)	Year	I	II	III	IV	V	VI	VII	VIII	IX	X	XI	XII	precipitation (mm)/a
227	38871	**Karakul**	**73.56**	**39.01**	**3935**	**1960**	3.3	11.0	13.8	5.5	4.9	6.6	0.0	0.4	17.2	6.9	4.9	2.1	76.6
227	38871	**Karakul**	**73.56**	**39.01**	**3935**	**1961**	1.5	2.9	9.4	12.8	24.8	1.2	0.0	3.6	0.1	7.9	1.9	1.0	67.1
227	38871	**Karakul**	**73.56**	**39.01**	**3935**	**1962**	0.9	2.3	5.9	16.7	10.2	4.8	21.7	22.0	11.0	21.2	2.2	0.5	119.4
227	38871	**Karakul**	**73.56**	**39.01**	**3935**	**1963**	0.1	0.6	4.0	1.8	10.9	3.9	1.5	0.0	0.0	0.0	2.1	1.7	26.6
227	38871	**Karakul**	**73.56**	**39.01**	**3935**	**1964**	5.2	7.7	3.1	22.3	3.0	1.7	4.6	0.0	24.0	0.6	2.0	4.8	79.0
227	38871	**Karakul**	**73.56**	**39.01**	**3935**	**1965**	10.4	4.0	16.0	5.1	21.6	0.4	13.8	32.4	10.3	0.7	4.6	0.8	120.1
227	38871	**Karakul**	**73.56**	**39.01**	**3935**	**1966**	0.0	15.6	18.8	14.6	3.1	0.0	5.0	9.0	26.7	9.3	0.8	1.5	104.4
227	38871	**Karakul**	**73.56**	**39.01**	**3935**	**1967**	1.9	4.8	2.7	2.8	17.5	13.3	13.0	0.0	0.0	0.0	9.5	3.6	69.1
227	38871	**Karakul**	**73.56**	**39.01**	**3935**	**1968**	8.6	3.6	9.2	15.7	33.6	9.3	6.1	8.6	2.8	7.2	0.0	8.5	113.2
227	38871	**Karakul**	**73.56**	**39.01**	**3935**	**1969**	6.4	7.9	14.5	29.5	6.8	22.5	5.1	2.5	3.1	1.8	3.4	2.6	106.1
227	38871	**Karakul**	**73.56**	**39.01**	**3935**	**1970**	3.9	1.0	5.8	10.2	1.3	6.8	18.7	0.0	8.6	1.0	1.7	6.7	65.7
227	38871	**Karakul**	**73.56**	**39.01**	**3935**	**1971**	0.3	11.7	1.4	20.2	9.8	16.5	2.0	0.0	7.0	1.1	2.5	1.3	73.8
227	38871	**Karakul**	**73.56**	**39.01**	**3935**	**1972**	6.3	16.7	7.7	21.0	17.8	10.4	10.2	11.3	11.9	0.3	3.3	2.4	119.3
227	38871	**Karakul**	**73.56**	**39.01**	**3935**	**1973**	10.8	1.5	22.8	9.9	17.6	2.4	0.5	0.0	0.0	0.0	2.1	1.7	69.3
227	38871	**Karakul**	**73.56**	**39.01**	**3935**	**1974**	10.7	7.7	9.6	7.0	24.5	7.3	16.4	0.7	1.8	33.7	2.0	9.5	130.9
227	38871	**Karakul**	**73.56**	**39.01**	**3935**	**1975**	4.1	7.6	7.8	11.5	23.3	11.0	3.1	8.5	0.0	0.3	1.6	5.8	84.6
227	38871	**Karakul**	**73.56**	**39.01**	**3935**	**1976**	8.8	9.5	7.0	6.6	25.5	17.6	1.9	4.6	0.0	0.4	0.5	4.7	87.1
227	38871	**Karakul**	**73.56**	**39.01**	**3935**	**1977**	4.2	0.4	6.5	10.9	25.7	9.5	1.4	9.0	0.6	10.5	2.6	0.0	81.3
227	38871	**Karakul**	**73.56**	**39.01**	**3935**	**1978**	6.3	0.6	14.1	8.9	9.7	2.2	0.0	0.0	0.3	3.7	4.8	1.8	52.4
227	38871	**Karakul**	**73.56**	**39.01**	**3935**	**1979**	0.6	1.4	5.9	13.3	25.2	0.6	0.2	14.6	6.6	1.5	4.3	5.6	79.8
227	38871	**Karakul**	**73.56**	**39.01**	**3935**	**1980**	2.4	4.8	8.4	1.8	27.9	2.4	18.8	0.5	0.9	4.6	12.5	0.5	85.5
227	38871	**Karakul**	**73.56**	**39.01**	**3935**	**1981**	0.8	7.3	7.8	13.9	9.1	10.3	4.2	15.7	5.7	1.2	0.2	1.4	77.6
227	38871	**Karakul**	**73.56**	**39.01**	**3935**	**1982**	2.3	2.4	5.5	3.7	6.9	20.0	4.3	0.0	2.9	4.4	17.0	1.2	70.6
227	38871	**Karakul**	**73.56**	**39.01**	**3935**	**1983**	0.8	1.7	11.1	20.4	1.1	1.3	9.6	1.9	1.6	0.7	0.0	1.8	52.0
227	38871	**Karakul**	**73.56**	**39.01**	**3935**	**1984**	1.5	5.2	1.9	5.2	1.9	0.0	1.4	8.7	0.6	10.6	2.0	1.6	40.6
227	38871	**Karakul**	**73.56**	**39.01**	**3935**	**1985**	3.3	3.7	7.7	2.5	11.9	13.2	9.2	7.9	6.7	6.7	1.7	2.9	77.4
227	38871	**Karakul**	**73.56**	**39.01**	**3935**	**1986**	1.2	3.4	15.1	10.1	3.7	6.4	16.5	5.4	22.7	0.0	1.2	6.5	92.2
227	38871	**Karakul**	**73.56**	**39.01**	**3935**	**1987**	0.1	3.2	3.2	17.5	0.6	15.7	14.4	8.9	0.0	13.5	0.0	4.9	82.0
227	38871	**Karakul**	**73.56**	**39.01**	**3935**	**1988**	2.1	8.8	6.0	9.4	8.4	2.9	3.9	2.6	0.3	3.4	0.8	7.0	55.6
227	38871	**Karakul**	**73.56**	**39.01**	**3935**	**1989**	2.1	3.2	11.0	2.8	13.4	0.5	9.0	15.8	0.0	6.9	1.2	7.0	72.9
227	38871	**Karakul**	**73.56**	**39.01**	**3935**	**1990**	1.6	4.2	3.6	5.8	5.9	10.1	1.4	4.4	0.4	23.3	0.3	6.8	67.8
							30.0	30.0	30.0	30.0	30.0	30.0	30.0	30.0	30.0	30.0	30.0	30.0	years complete
							100.0	100.0	100.0	100.0	100.0	100.0	100.0	100.0	100.0	100.0	100.0	100.0	completeness in %

mean	3.6	5.4	8.6	10.9	13.1	7.4	7.0	6.4	5.6	5.9	3.0	3.5	80.6
max	10.8	16.7	22.8	29.5	33.6	22.5	21.7	32.4	26.7	33.7	17.0	9.5	130.9
min	0.0	0.4	1.4	1.8	0.6	0.0	0.0	0.0	0.0	0.0	0.0	0.0	26.6

Country	Code_WMO	Name	Long	Lat	Alt.(m)	Year	I	II	III	IV	V	VI	VII	VIII	IX	X	XI	XII	precipitation (mm)/a
227	38840	Komsomolabad	69.98	38.87	1259	1960				79.8	210.3	40.2	15.4	0.0	0.8	18.0	125.9	21.7	
227	38840	Komsomolabad	69.98	38.87	1259	1961	66.3	51.8	161.9	83.3	98.5	3.2	0.6	30.7	0.0	15.0	68.1	144.1	723.5
227	38840	Komsomolabad	69.98	38.87	1259	1962	49.0	99.8	61.2	292.7	125.6	11.5	0.0	3.7	0.1	42.6	76.8	92.3	855.3
227	38840	Komsomolabad	69.98	38.87	1259	1963	9.9	163.0	157.4	150.3	162.2	33.0	1.6	0.1	6.4	16.6	72.6	75.5	848.6
227	38840	Komsomolabad	69.98	38.87	1259	1964	68.4	171.5	160.3	301.2	78.8	40.8	68.8	0.0	2.0	0.6	52.7	49.5	994.6
227	38840	Komsomolabad	69.98	38.87	1259	1965	127.4	155.5	101.2	152.0	48.5	18.2	29.7	17.6	14.5	51.1	103.7	5.8	825.2
227	38840	Komsomolabad	69.98	38.87	1259	1966	65.7	156.4	299.4	99.4	103.8	2.1	28.7	3.9	11.8	108.5	1.6	82.8	964.1
227	38840	Komsomolabad	69.98	38.87	1259	1967	59.5	171.4	55.0	132.1	82.7	38.7	3.0	1.1	5.7	91.6	96.0	74.5	811.3
227	38840	Komsomolabad	69.98	38.87	1259	1968	96.5	37.3	212.5	86.3	112.5	50.4	0.8	0.6	0.0	69.6	44.5	327.0	1038.0
227	38840	Komsomolabad	69.98	38.87	1259	1969	184.5	111.7	396.7	211.7	237.3	81.1	44.2	6.7	4.0	120.6	76.5	63.5	1538.5
227	38840	Komsomolabad	69.98	38.87	1259	1970	160.7	65.0	130.8	153.6	82.2	27.3	81.2	1.2	2.9	15.8	22.3	95.0	838.0
227	38840	Komsomolabad	69.98	38.87	1259	1971	28.4	120.8	77.4	182.4	51.2	0.7	0.7	0.0	2.1	7.9	65.4	53.2	590.2
227	38840	Komsomolabad	69.98	38.87	1259	1972	124.6	51.3	261.2	145.1	156.3	63.7	7.3	2.2	2.4	36.8	40.3	81.7	972.9
227	38840	Komsomolabad	69.98	38.87	1259	1973	54.0	202.5	278.9	110.6	149.5	5.5	9.1	0.0	9.2				
227	38840	Komsomolabad	69.98	38.87	1259	1974	101.1	82.2	71.4	183.8	98.8	56.3	13.7	14.4	30.0	15.5	52.5	94.2	813.9
227	38840	Komsomolabad	69.98	38.87	1259	1975	116.5	100.3	137.1	58.8	182.7	3.1	4.7	0.0	28.7	29.1	35.8	53.9	750.7
227	38840	Komsomolabad	69.98	38.87	1259	1976	68.0	183.0	125.1	171.4	67.5		0.0	0.0	2.4		13.2	10.1	
227	38840	Komsomolabad	69.98	38.87	1259	1977	166.8	54.8	108.5	39.4	105.2	11.3	0.0	3.8	0.0	93.4	52.2	164.1	799.5
227	38840	Komsomolabad	69.98	38.87	1259	1978	91.9	74.5	153.7	94.3	151.5	57.2	0.0	0.0	0.0	23.1	128.0	117.1	891.3
227	38840	Komsomolabad	69.98	38.87	1259	1979	109.0	76.2	67.8	195.2	137.6		1.1		14.1	14.3	37.3	73.9	
227	38840	Komsomolabad	69.98	38.87	1259	1980	114.1	209.8	178.5	161.1	95.9	32.1	0.4		0.6	10.6	91.1	35.4	
227	38840	Komsomolabad	69.98	38.87	1259	1981	124.6	255.0		89.3	85.7	51.2	59.6	13.8	21.5	92.8		83.1	
227	38840	Komsomolabad	69.98	38.87	1259	1982	59.8	102.5	198.4	53.5	67.8	46.4	18.6	15.4	16.3	141.8	105.3	44.2	870.0
227	38840	Komsomolabad	69.98	38.87	1259	1983	90.2	43.1	73.8	141.5	91.9	62.1	18.2	1.6	13.8	7.3	27.4	51.4	622.3
227	38840	Komsomolabad	69.98	38.87	1259	1984	53.2	134.8	285.5	155.5	91.7	3.3	0.3	0.0	3.5	43.3	141.3	86.3	998.7
227	38840	Komsomolabad	69.98	38.87	1259	1985	121.0	79.5	183.9	105.5	136.8	11.7	3.0	7.7	0.0	61.8	23.1		
227	38840	Komsomolabad	69.98	38.87	1259	1986	62.5	24.1	62.5	76.7	119.6	36.5		2.6	17.0	91.1	49.7	226.5	
227	38840	Komsomolabad	69.98	38.87	1259	1987	55.1	67.8	295.9	184.8	66.2	50.1		0.4	9.9	184.6	51.0	63.4	
227	38840	Komsomolabad	69.98	38.87	1259	1988	115.3	75.5	204.0	71.0	171.1	20.0	8.4	4.2	1.2	41.1	3.6	154.7	870.1
227	38840	Komsomolabad	69.98	38.87	1259	1989	65.1	99.0	100.8			33.6		13.6	4.0	23.8	98.5	143.2	
							30.0	30.0	29.0	30.0	30.0	29.0	28.0	29.0	31.0	29.0	29.0	29.0	years complete
							96.77	96.77	93.55	96.77	96.77	93.55	90.32	93.55	100.00	93.55	93.55	93.55	completeness in %

mean	90.0	111.0	164.3	136.6	116.2	31.8	15.5	5.2	7.5	52.4	62.7	91.7	880.8
max	184.5	255.0	396.7	301.2	237.3	81.1	81.2	30.7	30.0	184.6	141.3	327.0	1538.5
min	9.9	24.1	55.0	39.4	48.5	0.7	0.0	0.0	0.0	0.6	1.6	5.8	590.2

Country	Code_WMO	Name	Long	Lat	Alt.(m)	Year	I	II	III	IV	V	VI	VII	VIII	IX	X	XI	XII	precipitation (mm)/a
227	38854	Lyairun	**70.90**	**38.90**	**2008**	**1960**										11	162	43	
227	38854	Lyairun	**70.90**	**38.90**	**2008**	**1961**	76	74	171	72	44	8	0	0	0	17	62	132	656.0
227	38854	Lyairun	**70.90**	**38.90**	**2008**	**1962**	52	25	152	308	166	20	0	0	0	72	92	68	955.0
227	38854	Lyairun	**70.90**	**38.90**	**2008**	**1963**	12	75	95	139	143	59	7	0	33	33	86	71	753.0
227	38854	Lyairun	**70.90**	**38.90**	**2008**	**1964**	63	163	95	237	181	73	78	7	0	1	33	61	992.0
227	38854	Lyairun	**70.90**	**38.90**	**2008**	**1965**	120	115	126	135	65	83	64	12	19	66	117	24	946.0
227	38854	Lyairun	**70.90**	**38.90**	**2008**	**1966**	55	126	172	90	124	6	11	0	5	185	9	124	907.0
227	38854	Lyairun	**70.90**	**38.90**	**2008**	**1967**	65	137	33	89	145	46	15	7	5	79	78	83	782.0
227	38854	Lyairun	**70.90**	**38.90**	**2008**	**1968**	55	29	217	119	110	69	39	0	0	60	78	277	1053.0
227	38854	Lyairun	**70.90**	**38.90**	**2008**	**1969**	212	129	289	166	182.2	91	75	5	19	164	93	70	1495.2
227	38854	Lyairun	**70.90**	**38.90**	**2008**	**1970**	101	42	107	164	132	32	84	2	5	45	43	129	886.0
227	38854	Lyairun	**70.90**	**38.90**	**2008**	**1971**	28	88	64	131	88	6	4	0	0	11	72	35	527.0
227	38854	Lyairun	**70.90**	**38.90**	**2008**	**1972**	149	76	206	68	160	105	42	1	15	28	47	85	982.0
227	38854	Lyairun	**70.90**	**38.90**	**2008**	**1973**	60	139	251	117	238	20	5	0	0	3	15	9	857.0
227	38854	Lyairun	**70.90**	**38.90**	**2008**	**1974**	105	109	111	128	91	30	13	42	26	13	54	63	785.0
227	38854	Lyairun	**70.90**	**38.90**	**2008**	**1975**	57	75	100	112	154	39	36	0	26	32	51	53	735.0
227	38854	Lyairun	**70.90**	**38.90**	**2008**	**1976**	101	129	106	105	89	34	15	0	6	146	12	39	782.0
227	38854	Lyairun	**70.90**	**38.90**	**2008**	**1977**	209	23	83	62	155	40	3	0	0	130	66	126	897.0
227	38854	Lyairun	**70.90**	**38.90**	**2008**	**1978**	84	83	106	122	155	36	4	0	0	57	134	176	957.0
227	38854	Lyairun	**70.90**	**38.90**	**2008**	**1979**	56	46	90	214	151	66	3	34	38	13	46	89	846.0
227	38854	Lyairun	**70.90**	**38.90**	**2008**	**1980**	113	178	122	195	125	46	23	1	0	21	53	19	896.0
227	38854	Lyairun	**70.90**	**38.90**	**2008**	**1981**	107	180	103	119	115	45	72	43	9	100	79	79	1051.0
227	38854	Lyairun	**70.90**	**38.90**	**2008**	**1982**	42	79	119	30	103	64	45	8	25	167	159	55	896.0
227	38854	Lyairun	**70.90**	**38.90**	**2008**	**1983**	99	35	90	115	164	148	76	1	24	5	18	50	825.0
227	38854	Lyairun	**70.90**	**38.90**	**2008**	**1984**	41	129	233	172	138	9	6	0	7	25	117	109	986.0
227	38854	Lyairun	**70.90**	**38.90**	**2008**	**1985**	117	60	233	84	193	54	37	15	0	71	61	77	1002.0
227	38854	Lyairun	**70.90**	**38.90**	**2008**	**1986**	46	30	113	90	188	73	13	18	3	49	90	193	906.0
227	38854	Lyairun	**70.90**	**38.90**	**2008**	**1987**	29	80	262	275	168	65	55	27	23	263	49	69	1365.0
227	38854	Lyairun	**70.90**	**38.90**	**2008**	**1988**	121	66	248	115	158	47	5	25	0	59	6	123	973.0
227	38854	Lyairun	**70.90**	**38.90**	**2008**	**1989**	67	89	80	163	118	84	33	8	8	23	105	142	920.0
227	38854	Lyairun	**70.90**	**38.90**	**2008**	**1990**	177	84	137	113	108	27	33	14	0				
							30	30	30	30	30	30	30	30	30	30	30	30	years complete
							96.77	96.77	96.77	96.77	96.77	96.77	96.77	96.77	96.77	96.77	96.77	96.77	completeness in %

mean	87.3	89.8	143.8	135.0	138.4	50.8	29.9	9.0	9.9	65.0	69.6	89.1	917.7
max	212.0	180.0	289.0	308.0	238.0	148.0	84.0	43.0	38.0	263.0	162.0	277.0	1495.2
min	12.0	23.0	33.0	30.0	44.0	6.0	0.0	0.0	0.0	1.0	6.0	9.0	527.0

Country	Code_WMO	Name	Long	Lat	Alt.(m)	Year	I	II	III	IV	V	VI	VII	VIII	IX	X	XI	XII	precipitation (mm)/a
213	38745	**Sarytash**	**73.25**	**39.73**	**3153**	**1960**	9.0	27.0	37.0	33.0	55.0	56.0	39.0	0.0	18.0	16.0	42.0	6.0	338.0
213	38745	**Sarytash**	**73.25**	**39.73**	**3153**	**1961**	15.0	20.0	32.0	34.0	31.0	15.0	19.0	32.0	5.0	21.0	22.0	17.0	263.0
213	38745	**Sarytash**	**73.25**	**39.73**	**3153**	**1962**	16.0	21.0	3.0	50.0	38.0	63.0	25.0	50.0	25.0	25.0	43.0	24.0	383.0
213	38745	**Sarytash**	**73.25**	**39.73**	**3153**	**1963**	1.0	28.0	28.0	73.0	63.0	38.0	45.0	0.0	17.0	12.0	38.0	32.0	375.0
213	38745	**Sarytash**	**73.25**	**39.73**	**3153**	**1964**	23.0	46.0	52.0	52.0	76.0	39.0	57.0	20.0	16.0	3.0	6.0	15.0	405.0
213	38745	**Sarytash**	**73.25**	**39.73**	**3153**	**1965**	16.0	20.0	24.0	20.0	73.0	61.0	53.0	61.0	8.0	29.0	46.0	10.0	421.0
213	38745	**Sarytash**	**73.25**	**39.73**	**3153**	**1966**	14.0	30.0	46.0	49.0	120.0	12.0	41.0	32.0	44.0	29.0	12.0	26.0	455.0
213	38745	**Sarytash**	**73.25**	**39.73**	**3153**	**1967**	24.0	36.0	15.0	18.0	63.0	52.0	42.0	5.0	7.0	16.0	22.0	9.0	309.0
213	38745	**Sarytash**	**73.25**	**39.73**	**3153**	**1968**	13.0	6.0	35.0	50.0	114.0	56.0	44.0	18.0	0.0	27.0	16.0	57.0	436.0
213	38745	**Sarytash**	**73.25**	**39.73**	**3153**	**1969**	50.0	31.0	44.0	60.0	64.0	49.0	33.0	8.0	20.0	35.0	19.0	14.0	427.0
213	38745	**Sarytash**	**73.25**	**39.73**	**3153**	**1970**	14.0	13.0	54.0	63.0	44.0	40.0	111.0	29.0	15.0	17.0	18.0	28.0	446.0
213	38745	**Sarytash**	**73.25**	**39.73**	**3153**	**1971**	5.0	22.0	12.0	68.0	81.0	36.0	37.0	2.0	16.0	5.0	16.0	8.0	308.0
213	38745	**Sarytash**	**73.25**	**39.73**	**3153**	**1972**	41.0	19.0	29.0	25.0	46.0	54.0	41.0	24.0	7.0	39.0	16.0	22.0	363.0
213	38745	**Sarytash**	**73.25**	**39.73**	**3153**	**1973**	21.0	22.0	43.0	13.0	41.0	24.0	24.0	1.0	1.0	10.0	8.0	2.0	210.0
213	38745	**Sarytash**	**73.25**	**39.73**	**3153**	**1974**	40.0	30.0	36.0	20.0	36.0	39.0	60.0	31.0	19.0	27.0	22.0	18.0	378.0
213	38745	**Sarytash**	**73.25**	**39.73**	**3153**	**1975**	19.0	26.0	32.0	46.0	105.0	55.0	42.0	10.0	16.0	45.0	30.0	31.0	457.0
213	38745	**Sarytash**	**73.25**	**39.73**	**3153**	**1976**	21.0	37.0	30.0	50.0	68.0	75.0	44.0	8.0	12.0	28.0	6.0	16.0	395.0
213	38745	**Sarytash**	**73.25**	**39.73**	**3153**	**1977**	25.0	9.0	44.0	42.0	61.0	70.0	18.0	23.0	2.0	42.0	28.0	30.0	394.0
213	38745	**Sarytash**	**73.25**	**39.73**	**3153**	**1978**	30.0	15.0	27.0	25.0	31.0	20.0	5.0	7.0	1.0	26.0	27.0	22.0	236.0
213	38745	**Sarytash**	**73.25**	**39.73**	**3153**	**1979**	24.0	7.0	20.0	78.0	35.0	24.0	21.0	51.0	6.0	12.0	10.0	29.0	317.0
213	38745	**Sarytash**	**73.25**	**39.73**	**3153**	**1980**	27.0	42.0	36.0	29.0	36.0	80.0	31.0	20.0	7.0	10.0	27.0	5.0	350.0
213	38745	**Sarytash**	**73.25**	**39.73**	**3153**	**1981**	20.0	55.0	15.0	52.0	102.0	42.0	56.0	32.0	10.0	25.0	47.0	17.0	473.0
213	38745	**Sarytash**	**73.25**	**39.73**	**3153**	**1982**	9.0	18.0	35.0	8.0	20.0	69.0	17.0	32.0	4.0	25.0	26.0	15.0	278.0
213	38745	**Sarytash**	**73.25**	**39.73**	**3153**	**1983**	10.0	4.0	17.0	53.0	53.0	62.0	45.0	16.0	25.0	3.0	8.0	5.0	301.0
213	38745	**Sarytash**	**73.25**	**39.73**	**3153**	**1984**	10.0	16.0	52.0	38.0	37.0	16.0	25.0	0.0	10.0	7.0	32.0	38.0	281.0
213	38745	**Sarytash**	**73.25**	**39.73**	**3153**	**1985**	34.0	22.0	43.0	21.0	54.0	44.0	28.0	16.0	25.0	18.0	33.0	16.0	354.0
213	38745	**Sarytash**	**73.25**	**39.73**	**3153**	**1986**	9.0	20.0	31.0	39.0	53.0	65.0	9.0	8.0	12.0	9.0	46.0	36.0	337.0
213	38745	**Sarytash**	**73.25**	**39.73**	**3153**	**1987**	8.0	19.0	48.0	87.0	68.0	97.0	80.0	28.0	8.0	95.0	13.0	28.0	579.0
213	38745	**Sarytash**	**73.25**	**39.73**	**3153**	**1988**	25.0	26.0	55.0	20.0	108.0	37.0	45.0	17.0	8.0	30.0	3.0	12.0	386.0
213	38745	**Sarytash**	**73.25**	**39.73**	**3153**	**1989**	21.0	38.0	20.0	41.0	49.0	59.0	39.0	36.0	18.0	19.0	25.0	28.0	393.0
213	38745	**Sarytash**	**73.25**	**39.73**	**3153**	**1990**	46.0	29.0	27.0	23.0	57.0	56.0	97.0	51.0	3.0	11.0	5.0	30.0	435.0
							30.0	30.0	30.0	30.0	30.0	30.0	30.0	30.0	30.0	30.0	30.0	30.0	years complete
							100.0	100.0	100.0	100.0	100.0	100.0	100.0	100.0	100.0	100.0	100.0	100.0	completeness in %

mean	20.6	24.3	33.0	41.3	60.7	48.5	41.1	21.5	12.4	23.1	23.0	20.8	370.4
max	50.0	55.0	55.0	87.0	120.0	97.0	111.0	61.0	44.0	95.0	47.0	57.0	579.0
min	1.0	4.0	3.0	8.0	20.0	12.0	5.0	0.0	0.0	3.0	3.0	2.0	210.0

Country	Code_WMO	Name	Long	Lat	Alt.(m)	Year	I	II	III	IV	V	VI	VII	VIII	IX	X	XI	XII	precipitation (mm)/a
227	38852	Tavildara	**70.48**	**38.70**	**1616**	**1960**	29.7				239.8	19.6	5.4	0.0	4.2	5.8	160.0	21.0	
227	38852	Tavildara	**70.48**	**38.70**	**1616**	**1961**	82.6	77.7	158.2	66.0	45.2	7.8	0.0	30.8	0.0	12.8	63.0	141.1	685.2
227	38852	Tavildara	**70.48**	**38.70**	**1616**	**1962**	65.4	70.6		308.8	166.8	16.4	5.3	0.9	0.0	73.1	90.4	61.7	859.4
227	38852	Tavildara	**70.48**	**38.70**	**1616**	**1963**	3.8	104.3	154.6	143.6	154.4	55.8	14.3	0.0	10.4	12.3	57.8	40.1	751.4
227	38852	Tavildara	**70.48**	**38.70**	**1616**	**1964**	38.3	160.0	135.6	215.4	133.7	72.9	55.5	0.0	0.0	0.1	24.3	26.0	861.8
227	38852	Tavildara	**70.48**	**38.70**	**1616**	**1965**	106.0	153.0	123.0	121.0	64.0	31.0	12.0	16.0	9.0	64.0	99.0	30.0	828.0
227	38852	Tavildara	**70.48**	**38.70**	**1616**	**1966**	75.0	162.0	243.0	131.0	141.0	3.0	7.0	0.0	4.0	186.0	3.0	120.0	1075.0
227	38852	Tavildara	**70.48**	**38.70**	**1616**	**1967**	23.0	161.0	27.0	129.0	146.0	43.0	2.0	0.0	2.0	106.0	99.0	112.0	850.0
227	38852	Tavildara	**70.48**	**38.70**	**1616**	**1968**	61.0	19.0	161.0	83.0	110.0	37.0	3.0	1.0	0.0	81.0	79.0	302.0	937.0
227	38852	Tavildara	**70.48**	**38.70**	**1616**	**1969**	225.0	122.0	329.0	180.0	216.0	94.0	90.0	11.0	3.0	150.0	57.0	42.0	1519.0
227	38852	Tavildara	**70.48**	**38.70**	**1616**	**1970**	104.0	28.0	103.0	163.0	113.0	7.0	52.0	0.0	1.0	36.0	36.0	127.0	770.0
227	38852	Tavildara	**70.48**	**38.70**	**1616**	**1971**	35.0	112.0	70.0	123.0	79.0	15.0	1.0	0.0	2.0	17.0	99.0	26.0	579.0
227	38852	Tavildara	**70.48**	**38.70**	**1616**	**1972**	124.0	64.0	202.0	138.0	167.0	90.0	22.0	0.0	2.0	3.0	59.0	62.0	933.0
227	38852	Tavildara	**70.48**	**38.70**	**1616**	**1973**	62.0	183.0	241.0	125.0	221.0	20.0	3.0	0.0	8.0	3.0	7.0	7.0	880.0
227	38852	Tavildara	**70.48**	**38.70**	**1616**	**1974**	106.0	72.0	100.0	113.0	127.0	69.0	41.0	24.0	14.0	8.0	63.0	86.0	823.0
227	38852	Tavildara	**70.48**	**38.70**	**1616**	**1975**	96.0	98.0	109.0	93.0	189.0	35.0	3.0	0.0	22.0	37.0	67.0	45.0	794.0
227	38852	Tavildara	**70.48**	**38.70**	**1616**	**1976**	115.0	168.0	107.0	132.0	105.0	40.0	4.0	0.0	1.0	151.0	8.0	14.0	845.0
227	38852	Tavildara	**70.48**	**38.70**	**1616**	**1977**	177.0	33.0	85.0	80.0	135.0	28.0	5.0	4.0	0.0	101.0	78.0	188.0	914.0
227	38852	Tavildara	**70.48**	**38.70**	**1616**	**1978**	98.0	81.0	111.0	107.0	106.0	46.0	0.0	0.0	2.0	19.0	95.0	160.0	825.0
227	38852	Tavildara	**70.48**	**38.70**	**1616**	**1979**	53.0	42.0	76.0	159.0	163.0	58.0	4.0	9.0	33.0	11.0	46.0	58.0	712.0
227	38852	Tavildara	**70.48**	**38.70**	**1616**	**1980**	115.0	178.0	142.0	238.0	126.0	13.0	14.0	0.0	4.0	17.0	112.0	26.0	985.0
227	38852	Tavildara	**70.48**	**38.70**	**1616**	**1981**	110.0	251.0	118.0	112.0	90.0	53.0	72.0	35.0	6.0	91.0	90.0	86.0	1114.0
227	38852	Tavildara	**70.48**	**38.70**	**1616**	**1982**	56.0	76.0	170.0	46.0	106.0	51.0	27.0	0.0	27.0	159.0	96.0	27.0	841.0
227	38852	Tavildara	**70.48**	**38.70**	**1616**	**1983**	102.0	46.0	62.0	121.0	156.0	181.0		0.0	15.0	2.0	32.0	20.0	
227	38852	Tavildara	**70.48**	**38.70**	**1616**	**1984**	41.0	138.0	310.0	182.0	124.0	7.0	9.0	0.0	8.0	15.0	165.0	106.0	1105.0
227	38852	Tavildara	**70.48**	**38.70**	**1616**	**1985**	111.0	96.0	19.0	90.0	206.0	37.0	5.0	10.0	0.0	50.0	44.0	55.0	723.0
227	38852	Tavildara	**70.48**	**38.70**	**1616**	**1986**	53.0	20.0	66.0	106.0	158.0	49.0	12.0	2.0	6.0	51.0	81.0	217.0	821.0
227	38852	Tavildara	**70.48**	**38.70**	**1616**	**1987**	50.0	77.0	295.0	277.0	170.0	47.0	99.0	4.0	20.0	211.0	22.0	84.0	1356.0
227	38852	Tavildara	**70.48**	**38.70**	**1616**	**1988**	127.0	64.0	286.0	117.0	150.0	37.0	15.0	16.0	0.0	61.0	4.0	152.0	1029.0
227	38852	Tavildara	**70.48**	**38.70**	**1616**	**1989**	65.0	93.0	71.0	143.0	149.0	42.0	62.0	29.0	3.0	21.0	160.0	139.0	977.0
227	38852	Tavildara	**70.48**	**38.70**	**1616**	**1990**	175.0	90.0	119.0	162.0	107.0	32.0	16.0	7.0	0.0	54.0	43.0	137.0	942.0
							31.0	30.0	30.0	30.0	31.0	31.0	31.0	31.0	31.0	31.0	31.0	31.0	years complete
							100.00	96.77	96.77	96.77	100.00	100.00	100.00	100.00	100.00	100.00	100.00	100.00	completeness in %

mean	86.6	101.3	144.6	140.2	140.8	43.1	22.0	6.4	6.7	58.4	69.0	87.7	908.1
max	225.0	251.0	329.0	308.8	239.8	181.0	99.0	35.0	33.0	211.0	165.0	302.0	1519.0
min	3.8	19.0	19.0	46.0	45.2	3.0	0.0	0.0	0.0	0.1	3.0	7.0	579.0

Appendix Table 20: Temperature raw data and calculated mean annual temperature from local weather stations in Vakhsh catchment; time span 1960 - 1990.
I to XII represent months. Monthly temperature is given in ˚C. Longitude and Latitude are given in degrees.

Country	Code_WMO	Name	Long	Lat	Alt.(m)	Year	I	II	III	IV	V	VI	VII	VIII	IX	X	XI	XII	mean annual T (˚C)
227	38842	Bustonabad	69.63	38.67	1983	1960	-3.4	0.1	-1.9	5.1	10.1	17.2	19.8	20.6	15.5	10.4	1.4	-1.5	7.8
227	38842	Bustonabad	69.63	38.67	1983	1961	-3.6	-6.3	0.2	7.6	15.1	17.5	22.0	19.7	17.3	8.4	2.5	-2.9	8.1
227	38842	Bustonabad	69.63	38.67	1983	1962	-5.0	-1.7	3.9	6.5	10.8	15.9	20.6	19.3	13.9	9.1	-1.1	-2.5	7.5
227	38842	Bustonabad	69.63	38.67	1983	1963	-2.1	-0.6	1.4	8.8	12.2	17.4	19.5	19.1	15.3	11.4	3.1	-1.6	8.7
227	38842	Bustonabad	69.63	38.67	1983	1964	-9.7	-4.2	1.8	4.8	11.1	16.1	18.8	19.5	15.1	8.3	3.7	-3.9	6.8
227	38842	Bustonabad	69.63	38.67	1983	1965	-2.4	-5.3	-1.0	5.9	13.0	16.3	19.7	18.7	14.4	10.9	4.6	-1.1	7.8
227	38842	Bustonabad	69.63	38.67	1983	1966	1.0	0.3	0.2	6.5	11.4	19.4	19.6	20.1	15.1	7.3	2.5	-1.4	8.5
227	38842	Bustonabad	69.63	38.67	1983	1967	-5.5	-4.1	0.3	6.1	10.4	16.2	19.9	20.1	16.2	7.8	2.4	-1.4	7.4
227	38842	Bustonabad	69.63	38.67	1983	1968	-4.5	-4.8	1.6	8.0	9.9	16.4	20.0	20.1	16.2	9.1	3.0	-3.5	7.6
227	38842	Bustonabad	69.63	38.67	1983	1969	-7.1	-6.5	2.3	5.5	11.3	15.9	18.5	19.2	14.4	9.4	2.3	0.4	7.1
227	38842	Bustonabad	69.63	38.67	1983	1970	-4.0	-1.4	0.0	9.0	13.9	17.6	18.4	21.9	15.8	10.8	5.2	-1.9	8.8
227	38842	Bustonabad	69.63	38.67	1983	1971	-5.1	-2.7	3.3	9.1	14.5	19.8	22.4	19.9	15.0	10.6	4.7	2.1	9.4
227	38842	Bustonabad	69.63	38.67	1983	1972	-5.5	-10.2	-0.6	5.9	11.2	15.8	17.1	17.4	15.4	10.2	5.4	-3.7	6.5
227	38842	Bustonabad	69.63	38.67	1983	1973	-7.3	-1.9	-0.9	7.5	12.5	19.2	22.0	21.2	15.4	11.1	6.2	-0.6	8.7
227	38842	Bustonabad	69.63	38.67	1983	1974	-6.2	-5.7	1.2	9.3	12.8	16.8	20.2	17.8	15.4	9.3	3.4	-4.4	7.5
227	38842	Bustonabad	69.63	38.67	1983	1975	-5.5	-4.6	-0.2	7.8	10.7	16.8	21.2	21.0	16.1		-0.3	-2.9	
227	38842	Bustonabad	69.63	38.67	1983	1976	-2.6	-5.2	-1.9	5.9	13.3	16.5	22.0	21.3	16.6	8.7	1.6	-2.2	7.8
227	38842	Bustonabad	69.63	38.67	1983	1977	-6.8	-4.2	4.2	10.3	11.8	18.9	21.7	20.7	16.2	10.1	5.4	-1.7	8.9
227	38842	Bustonabad	69.63	38.67	1983	1978	-5.8	-3.8	-1.4	9.9	13.4	18.0	21.8	20.5	17.6	10.9	0.3	1.1	8.5
227	38842	Bustonabad	69.63	38.67	1983	1979	-2.8	-1.6	-0.2	9.5	9.7	16.7	22.1	19.9	16.5	13.6	4.2	-0.5	8.9
227	38842	Bustonabad	69.63	38.67	1983	1980	-4.6	-4.5	-0.2	8.9	14.0	18.1	22.2	20.7	16.5	11.0	5.9	0.9	9.1
227	38842	Bustonabad	69.63	38.67	1983	1981	-2.9	-2.7	1.2	8.5	13.9	15.4	19.0	17.9	15.9	7.8	4.6	-1.2	8.1
227	38842	Bustonabad	69.63	38.67	1983	1982	-3.2	-5.6	-0.3	9.2	13.6	16.7	19.7	19.6	14.0	8.5	0.4	-2.7	7.5
227	38842	Bustonabad	69.63	38.67	1983	1983	-3.9	-2.9	-1.5	7.9	13.2	15.6	20.1	22.0	16.7	9.7	6.1		
227	38842	Bustonabad	69.63	38.67	1983	1984	-5.3	-8.7	1.6	8.0	12.7	18.9	22.5	23.5	15.1	8.7	3.5	-6.3	7.8
227	38842	Bustonabad	69.63	38.67	1983	1985	-4.3	-1.6	-0.5	9.8	11.9	18.0	21.9	19.1	16.8	9.1	3.4	-1.3	8.5
227	38842	Bustonabad	69.63	38.67	1983	1986	-3.7	-1.9	-1.1	7.2	12.0	16.7	21.6	20.3	16.9	11.3	3.2	-3.7	8.2
227	38842	Bustonabad	69.63	38.67	1983	1987	-1.9	-1.6	2.8	6.1		15.6	17.7	21.6	16.5	6.2	4.7	1.8	
227	38842	Bustonabad	69.63	38.67	1983	1988	-3.1	-2.7	0.1	9.1	12.5	17.7	21.9	19.6	16.8	8.5	7.3	0.7	9.0
227	38842	Bustonabad	69.63	38.67	1983	1989	-6.3	-6.7	0.9	5.3	10.2	16.1	18.7	19.3	15.8			0.3	6.1
227	38842	Bustonabad	69.63	38.67	1983	1990	-3.0					19.2	20.6	21.7	18.6	9.9	6.2	-1.7	
							31	30	30	30	29	31	31	31	31	29	30	30	complete years
							100	96.8	96.8	96.8	93.5	100	100	100	100	93.5	96.8	96.8	in %
						mean	-4.4	-3.7	0.5	7.6	12.2	17.2	20.4	20.1	15.9	9.6	3.5	-1.6	8.0
						max	1.0	0.3	4.2	10.3	15.1	19.8	22.5	23.5	18.6	13.6	7.3	2.1	9.4
						min	-9.7	-10.2	-1.9	4.8	9.7	15.4	17.1	17.4	13.9	6.2	-1.1	-6.3	6.1

Country	Code_WMO	Name	Long	Lat	Alt.(m)	Year	I	II	III	IV	V	VI	VII	VIII	IX	X	XI	XII	mean annual T (˚C)
213	38745	Daraut-Kurga	**72.18**	**39.55**	**2470**	**1961**	-13.9	-13.5	-5.6	5.3	11.9	13.0	17.0	15.2	12.6	4.3	-5.6	-13.0	2.3
213	38745	Daraut-Kurga	**72.18**	**39.55**	**2470**	**1962**	-13.4	-9.4	-1.8	5.1	8.9	12.4	15.6	15.7	10.7	5.1	-6.1	-9.1	2.8
213	38745	Daraut-Kurga	**72.18**	**39.55**	**2470**	**1963**	-12.4	-6.6	-4.1			14.4	15.8	15.4	10.9	7.4	-5.4	-11.2	
213	38745	Daraut-Kurga	**72.18**	**39.55**	**2470**	**1964**	-17.2	-10.4	-2.5	4.0	8.1	12.3	14.7	15.2	11.5	4.0	-2.6	-10.8	2.2
213	38745	Daraut-Kurga	**72.18**	**39.55**	**2470**	**1965**	-11.5	-13.6	-7.0	5.3	10.1	12.3	16.1	14.2	10.5	7.0	-1.9	-10.7	2.6
213	38745	Daraut-Kurga	**72.18**	**39.55**	**2470**	**1966**	-7.5	-7.7	-2.8	4.1	8.1	14.1	14.6	15.3	11.1	3.7	-3.5	-8.4	3.4
213	38745	Daraut-Kurga	**72.18**	**39.55**	**2470**	**1967**	-16.1	-10.1	-6.7	4.2	8.5	13.1	15.5	15.2	11.5	4.1	-1.4	-9.1	2.4
213	38745	Daraut-Kurga	**72.18**	**39.55**	**2470**	**1968**	-14.5	-12.5	-0.4	5.6	8.4	12.9	16.1	15.9	11.4	4.9	-1.4	-10.8	3.0
213	38745	Daraut-Kurga	**72.18**	**39.55**	**2470**	**1969**	-10.5		1.5	4.6	9.5	12.7	14.6	15.7	10.3	6.2	-2.5	-6.5	
213	38745	Daraut-Kurga	**72.18**	**39.55**	**2470**	**1970**	-11.3	-6.8	-3.4	7.1	10.0	12.8	14.2	16.9	12.0	5.6	-2.0	-7.4	4.0
213	38745	Daraut-Kurga	**72.18**	**39.55**	**2470**	**1971**	-14.3	-8.4	-0.2	7.3	10.7	15.6	16.6	15.9	10.3	5.5	-0.8	-5.2	4.4
213	38745	Daraut-Kurga	**72.18**	**39.55**	**2470**	**1972**	-8.9	-15.2	-4.5	2.5	10.8	12.4	13.2	14.6	11.1	5.3	-0.3		
213	38745	Daraut-Kurga	**72.18**	**39.55**	**2470**	**1973**	-12.1					15.0	18.4	17.2	13.8			-8.4	
213	38745	Daraut-Kurga	**72.18**	**39.55**	**2470**	**1974**	-11.1				10.5	13.2	16.2	14.4	11.2	4.9	-3.3	-11.6	4.9
213	38745	Daraut-Kurga	**72.18**	**39.55**	**2470**	**1975**	-15.0	-10.7	-3.8						11.5	5.1	-7.8	-13.3	
213	38745	Daraut-Kurga	**72.18**	**39.55**	**2470**	**1976**	-14.2	-12.3	-7.9	3.3	10.3	12.1	17.0	16.4	11.7	4.6	-4.4	-7.8	2.4
213	38745	Daraut-Kurga	**72.18**	**39.55**	**2470**	**1977**	-11.2	-13.9	-0.8	7.5	9.8	14.7	17.1	16.1	12.4	6.4	-0.6	-7.6	4.2
213	38745	Daraut-Kurga	**72.18**	**39.55**	**2470**	**1978**	-12.7	-7.0	-3.8	6.7	11.0	13.9	18.3	16.6	12.1	5.9	-6.4	-7.6	3.9
213	38745	Daraut-Kurga	**72.18**	**39.55**	**2470**	**1979**	-12.1	-10.9	-5.3	7.1	7.9	12.7	17.2	15.4	11.2	7.5	-4.5	-9.2	3.1
213	38745	Daraut-Kurga	**72.18**	**39.55**	**2470**	**1980**	-13.4	-8.6	-4.4	6.4	10.8	13.4	17.1	16.1	11.9	6.4	0.2	-7.7	4.0
213	38745	Daraut-Kurga	**72.18**	**39.55**	**2470**	**1981**	-10.2	-8.7	-4.8	5.8	11.6	12.2	15.6	14.3	10.9	4.2	-1.5	-9.8	3.3
213	38745	Daraut-Kurga	**72.18**	**39.55**	**2470**	**1982**	-12.8	-12.3	-4.7	4.6	10.8	13.1	15.2	15.4	9.8	4.1	-5.2	-12.6	2.1
213	38745	Daraut-Kurga	**72.18**	**39.55**	**2470**	**1983**	-13.3	-14.2	-9.0	4.6	10.8	12.0	15.2	18.0	12.1	5.3	-0.3	-7.4	2.8
213	38745	Daraut-Kurga	**72.18**	**39.55**	**2470**	**1984**	-13.4	-11.9	-1.5	5.0	9.7	15.3	17.8	19.2	10.4	4.5	-0.2	-10.8	3.7
213	38745	Daraut-Kurga	**72.18**	**39.55**	**2470**	**1985**	-11.8	-8.2	-2.8	6.5	9.7	13.5	17.5	15.8	11.8	6.1	-4.4	-10.5	3.6
213	38745	Daraut-Kurga	**72.18**	**39.55**	**2470**	**1986**	-16.0	-11.3	-5.8	2.5	9.0	12.5	16.7	15.9	12.2	6.6	-1.8	-10.5	2.5
213	38745	Daraut-Kurga	**72.18**	**39.55**	**2470**	**1987**	-9.1	-6.7	1.4	4.2	7.7	11.2	14.3	16.0	12.1	3.9	0.6	-6.3	4.1
213	38745	Daraut-Kurga	**72.18**	**39.55**	**2470**	**1988**	-11.5	-10.9	-5.0	3.2	8.7	13.9	17.1	15.0	11.9	4.4	1.2	-6.0	3.5
213	38745	Daraut-Kurga	**72.18**	**39.55**	**2470**	**1989**	-14.2	-12.3	-2.2	3.4	8.4	11.9	15.2	15.2	12.0	6.8	-6.2	-10.1	2.3
213	38745	Daraut-Kurga	**72.18**	**39.55**	**2470**	**1990**	-9.7	-11.4	-7.5	2.4	11.2	14.7	15.5	15.9	13.0	5.5			
							30	27	28	26	27	29	29	29	30	29	28	28	complete years
							96.8	87.1	90.3	83.9	87.1	93.5	93.5	93.5	96.8	93.5	90.3	90.3	in %
						mean	-12.6	-10.5	-3.6	5.0	9.7	13.1	16.0	15.8	11.5	5.3	-2.8	-9.2	3.2
						max	-7.5	-6.6	1.5	7.5	11.9	15.6	18.4	19.2	13.8	7.5	1.2	-5.2	4.9
						min	-17.2	-15.2	-9.0	2.5	7.7	11.2	13.2	14.2	9.8	3.7	-7.8	-13.3	2.1

Country	Code_WMO	Name	Long	Lat	Alt.(m)	Year	I	II	III	IV	V	VI	VII	VIII	IX	X	XI	XII	mean annual T (°C)
227	38734	Dehavz	**70.20**	**39.45**	**2561**	**1960**	-6.1	-2.1	-3.7	2.0	6.6	12.4	14.8	16.1	10.8	5.9	-1.4	-3.9	4.3
227	38734	Dehavz	**70.20**	**39.45**	**2561**	**1961**	-6.1	-8.8	-1.8	5.0	11.9	12.7	16.2	14.5	12.7	5.0	-0.8	-5.9	4.6
227	38734	Dehavz	**70.20**	**39.45**	**2561**	**1962**	-6.6	-4.2	2.5	4.4	7.7	12.1	15.3	14.9	10.2	5.3	-3.7	-5.5	4.4
227	38734	Dehavz	**70.20**	**39.45**	**2561**	**1963**	-4.6	-3.1	-0.9	5.5	8.9	12.7	14.1	14.5	11.2	7.5	0.8	-3.7	5.2
227	38734	Dehavz	**70.20**	**39.45**	**2561**	**1964**	-10.8	-6.4	0.6	2.5	7.6	11.7	13.6	14.7	11.1	5.0	-0.2	-6.8	3.6
227	38734	Dehavz	**70.20**	**39.45**	**2561**	**1965**	-4.8	-7.6	-1.7	3.6	9.7	11.5	14.9	13.6	10.1	6.4	0.2	-4.2	4.3
227	38734	Dehavz	**70.20**	**39.45**	**2561**	**1966**	-3.3	-3.3	-1.8	3.9	7.6	13.7	14.3	14.3	11.0	4.0	-1.1	-5.3	4.5
227	38734	Dehavz	**70.20**	**39.45**	**2561**	**1967**	-8.6	-5.8	-1.2	4.3	8.0	12.6	15.1	15.5	11.8	4.1	-0.8	-3.6	4.3
227	38734	Dehavz	**70.20**	**39.45**	**2561**	**1968**	-6.7	-6.5	-0.1	5.4	7.7	11.8	15.4	15.4	11.5	5.1	-0.2	-6.9	4.3
227	38734	Dehavz	**70.20**	**39.45**	**2561**	**1969**	-8.6	-7.8	1.5	3.6	8.8	12.2	13.9	14.8	9.9	5.6	-1.1	-2.8	4.2
227	38734	Dehavz	**70.20**	**39.45**	**2561**	**1970**	-6.6	-3.6	-1.9	6.1	9.4	12.7	13.2	15.5	11.7	6.9	0.4	-4.3	5.0
227	38734	Dehavz	**70.20**	**39.45**	**2561**	**1971**	-7.6	-5.0	1.4	6.1	9.2	14.9	14.9	15.1	10.2	6.7	1.1	-1.4	5.5
227	38734	Dehavz	**70.20**	**39.45**	**2561**	**1972**	-6.8	-10.4	-1.9	3.2	7.6	11.7	12.0	12.9	10.7	5.9	1.1	-5.6	3.4
227	38734	Dehavz	**70.20**	**39.45**	**2561**	**1973**	-9.2	-4.3	-3.3	4.4	9.0	14.2	16.3	15.9	11.2	5.9	2.7	-4.6	4.8
227	38734	Dehavz	**70.20**	**39.45**	**2561**	**1974**	-8.4	-7.7	0.3	5.4	9.0	11.5	14.3	12.4	9.8	6.3	-0.1	-7.1	3.8
227	38734	Dehavz	**70.20**	**39.45**	**2561**	**1975**	-7.2	-6.7	-2.2	5.8	7.0	12.0	15.5	16.3	11.0	6.3	-2.8	-4.8	4.2
227	38734	Dehavz	**70.20**	**39.45**	**2561**	**1976**	-4.7	-6.6	-2.4	4.3	9.7	12.2	16.2	17.0	11.5	4.8	-2.1	-5.4	4.5
227	38734	Dehavz	**70.20**	**39.45**	**2561**	**1977**	-8.4	-6.5	1.7	7.0	8.9	14.3	16.5	15.9	12.3	6.4	2.6	-4.7	5.5
227	38734	Dehavz	**70.20**	**39.45**	**2561**	**1978**	-8.2	-5.4	-3.3	5.2	9.9	13.6	16.9	16.4	13.5	6.5	-2.1	-1.8	5.1
227	38734	Dehavz	**70.20**	**39.45**	**2561**	**1979**	-5.7	-4.3	-1.9	5.7	7.0	12.3	16.5	14.6	11.7	9.0	1.0	-2.9	5.2
227	38734	Dehavz	**70.20**	**39.45**	**2561**	**1980**	-6.3	-5.9	-2.7	6.4	10.4	13.1	16.8	15.7	12.0	6.6	2.2	-2.8	5.4
227	38734	Dehavz	**70.20**	**39.45**	**2561**	**1981**	-5.6	-4.1	-0.1	5.2	10.4	10.7	14.3	12.7	10.8	4.7	0.1	-3.9	4.6
227	38734	Dehavz	**70.20**	**39.45**	**2561**	**1982**	-4.7	-6.2	-1.2	6.4	10.5	12.4	14.4	14.6	9.4	4.3	-1.8	-5.4	4.4
227	38734	Dehavz	**70.20**	**39.45**	**2561**	**1983**	-5.6	-5.8	-2.8	5.8	10.2	12.1	15.7	17.4	12.0	5.9	1.9	-5.1	5.1
227	38734	Dehavz	**70.20**	**39.45**	**2561**	**1984**	-8.6	-9.0	-0.4	4.6	8.7	14.7	17.3	18.8	10.6	5.6	0.0	-9.2	4.4
227	38734	Dehavz	**70.20**	**39.45**	**2561**	**1985**	-6.5	-3.9	-1.7	6.9	8.4	13.5	17.2	14.5	12.5	5.5	0.0	-3.6	5.2
227	38734	Dehavz	**70.20**	**39.45**	**2561**	**1986**	-5.7	-3.0	-3.1	4.6	8.7	12.5	16.2	15.6	13.0	6.9	0.1	-5.5	5.0
227	38734	Dehavz	**70.20**	**39.45**	**2561**	**1987**	-4.4	-3.3		3.5	8.4	10.7	12.9	15.8	12.0	4.1	2.1	-1.2	
227	38734	Dehavz	**70.20**	**39.45**	**2561**	**1988**	-5.5	-4.8	-1.1	6.4	8.5	13.4	16.4	14.6	12.3	4.5	3.6	-2.3	5.5
227	38734	Dehavz	**70.20**	**39.45**	**2561**	**1989**	-8.4	-8.7	-0.6	2.4	7.6	11.3	14.2	14.5	11.6	6.9	-1.7	-2.9	3.8
227	38734	Dehavz	**70.20**	**39.45**	**2561**	**1990**	-4.8	-5.1	-1.6	3.3	10.2	14.9	15.2	16.4	14.1	6.3			
							31.0	31.0	30.0	31.0	31.0	31.0	31.0	31.0	31.0	31.0	30.0	30.0	complete years
							100.0	100.0	96.8	100.0	100.0	100.0	100.0	100.0	100.0	100.0	96.8	96.8	in %
						mean	-6.6	-5.6	-1.2	4.8	8.8	12.6	15.1	15.2	11.4	5.8	0.0	-4.4	4.6
						max	-3.3	-2.1	2.5	7.0	11.9	14.9	17.3	18.8	14.1	9.0	3.6	-1.2	5.5
						min	-10.8	-10.4	-3.7	2.0	6.6	10.7	12.0	12.4	9.4	4.0	-3.7	-9.2	3.4

Country	Code_WMO	Name	Long	Lat	Alt.(m)	Year	I	II	III	IV	V	VI	VII	VIII	IX	X	XI	XII	mean annual T (°C)
227	38862	Fedchenko Glacier	**72.22**	**38.83**	**4169**	**1960**	-16.5	-12.7	-13.9	-9.2	-5.4	-0.6	4.1	5.3	-0.6	-6.1	-12.8	-14.1	-6.9
227	38862	Fedchenko Glacier	**72.22**	**38.83**	**4169**	**1961**	-15.9	-19.0	-13.3	-7.5	-1.5	0.8	5.6	4.3	2.1	-7.3	-12.0	-16.5	-6.7
227	38862	Fedchenko Glacier	**72.22**	**38.83**	**4169**	**1962**	-17.3	-15.1	-10.4	-7.5	-4.9	-0.5	3.5	3.9	-0.8	-7.0	-13.8	-15.2	-7.1
227	38862	Fedchenko Glacier	**72.22**	**38.83**	**4169**	**1963**	-14.9	-13.7	-12.0	-6.3	-2.9	0.9	3.3	4.1	-0.2	-5.0	-11.2	-13.3	-5.9
227	38862	Fedchenko Glacier	**72.22**	**38.83**	**4169**	**1964**	-20.4	-16.5	-10.7	-8.5	-5.9	-1.2	2.2	3.6	0.0	-6.0	-11.6	-14.5	-7.4
227	38862	Fedchenko Glacier	**72.22**	**38.83**	**4169**	**1965**	-15.2	-18.1	-12.9	-8.3	-3.8	-0.7	3.7	2.2	-0.7	-5.8	-10.7	-14.8	-7.1
227	38862	Fedchenko Glacier	**72.22**	**38.83**	**4169**	**1966**	-14.4	-12.9	-12.7	-8.8	-5.4	1.0	2.2	3.8	-0.7	-8.2	-13.4	-15.7	-7.1
227	38862	Fedchenko Glacier	**72.22**	**38.83**	**4169**	**1967**	-18.3	-15.8	-13.1	-8.1	-5.0	-0.1	3.1	3.8	0.3	-7.7	-12.9	-14.3	-7.3
227	38862	Fedchenko Glacier	**72.22**	**38.83**	**4169**	**1968**	-17.4	-17.3	-11.6	-7.1	-4.8	-0.2	4.1	4.0	0.7	-7.1	-11.3	-15.8	-7.0
227	38862	Fedchenko Glacier	**72.22**	**38.83**	**4169**	**1969**	-18.4	-17.7	-9.4	-7.8	-3.5	-0.2	2.5	4.4	-0.9	-5.4	-11.0	-13.6	-6.7
227	38862	Fedchenko Glacier	**72.22**	**38.83**	**4169**	**1970**	-16.7	-15.6	-13.7	-6.0	-3.2	0.2	2.0	5.2	0.5	-5.3	-11.6	-15.4	-6.6
227	38862	Fedchenko Glacier	**72.22**	**38.83**	**4169**	**1971**	-17.8	-16.2	-10.7	-6.2	-3.2	2.8	4.3	4.4	-1.7	-5.1	-10.5	-12.4	-6.0
227	38862	Fedchenko Glacier	**72.22**	**38.83**	**4169**	**1972**	-16.8	-20.0	-12.2	-9.1	-4.6	-1.4	0.2	2.6	-0.6	-6.3	-10.8	-14.7	-7.8
227	38862	Fedchenko Glacier	**72.22**	**38.83**	**4169**	**1973**	-18.8	-15.2	-13.3	-6.7	-3.8	1.8	6.4	6.0	1.6	-5.6	-9.1	-15.2	-6.0
227	38862	Fedchenko Glacier	**72.22**	**38.83**	**4169**	**1974**	-18.4	-17.8	-11.5	-5.8	-3.5	-0.5	3.7	2.1	-0.9	-6.3	-12.4	-17.4	-7.4
227	38862	Fedchenko Glacier	**72.22**	**38.83**	**4169**	**1975**	-17.7	-16.9	-12.6	-6.4	-4.8	-0.5	3.8	5.2	0.2	-5.9	-13.2	-15.2	-7.0
227	38862	Fedchenko Glacier	**72.22**	**38.83**	**4169**	**1976**	-15.5	-17.1	-13.6	-7.5	-3.5	-0.5	5.6	5.6	-0.2				
227	38862	Fedchenko Glacier	**72.22**	**38.83**	**4169**	**1977**	-17.9	-16.9	-10.3	-5.9	-3.9	1.4	5.4	5.3	1.8	-5.1	-9.8	-15.2	-5.9
227	38862	Fedchenko Glacier	**72.22**	**38.83**	**4169**	**1978**	-18.5	-16.5	-14.5	-6.4	-2.3	2.1	6.8	5.8	1.8	-5.3	-13.0	-12.4	-6.0
227	38862	Fedchenko Glacier	**72.22**	**38.83**	**4169**	**1979**	-15.4	-15.1	-13.4	-5.3	-5.2	-0.3	4.9	3.4	-0.4		-10.8	-13.9	-6.5
227	38862	Fedchenko Glacier	**72.22**	**38.83**	**4169**	**1980**	-17.0	-15.7	-13.6	-6.1	-2.3	1.5	5.5	4.8	1.1	-5.0	-9.0	-12.7	-5.7
227	38862	Fedchenko Glacier	**72.22**	**38.83**	**4169**	**1981**	-16.2	-15.1	-11.5	-6.8	-1.6	-1.0	3.8	2.8	-0.4	-7.5	-11.8	-14.8	-6.7
227	38862	Fedchenko Glacier	**72.22**	**38.83**	**4169**	**1982**	-15.7	-17.9	-13.1	-6.7	-3.0	0.0	3.6	4.3	-1.7	-6.4	-12.3	-15.8	-7.0
227	38862	Fedchenko Glacier	**72.22**	**38.83**	**4169**	**1983**	-15.8	-16.4	-14.5	-7.4	-3.4	-1.4	2.9	6.7	0.4	-5.7	-9.9	-15.0	-6.6
227	38862	Fedchenko Glacier	**72.22**	**38.83**	**4169**	**1984**	-18.7	-19.5	-11.0	-7.8	-3.9	2.2	5.8	8.6	-0.3	-6.0	-11.3	-17.7	-6.6
227	38862	Fedchenko Glacier	**72.22**	**38.83**	**4169**	**1985**	-17.1	-14.9	-12.6	-6.1	-4.1	0.4	5.8	4.4	0.9	-6.4		-14.0	
227	38862	Fedchenko Glacier	**72.22**	**38.83**	**4169**	**1986**	-17.0	-15.3	-14.6	-8.1	-4.9	-0.7	4.9	4.2	0.9	-5.4	-11.0	-14.8	-6.8
227	38862	Fedchenko Glacier	**72.22**	**38.83**	**4169**	**1987**		-14.1	-10.4	-8.3	-5.4	-1.9	1.4	4.3	0.7	-7.6	-10.2	-11.7	
227	38862	Fedchenko Glacier	**72.22**	**38.83**	**4169**	**1988**	-15.2	-15.1	-12.7	-6.3	-4.0	1.0	5.6	4.0	1.0	-7.5	-8.7	-12.6	-5.9
227	38862	Fedchenko Glacier	**72.22**	**38.83**	**4169**	**1989**	-18.6	-19.2	-12.1	-10.8	-5.0	-1.7	2.6	3.1	-0.1	-5.3	-12.4	-13.2	-7.7
227	38862	Fedchenko Glacier	**72.22**	**38.83**	**4169**	**1990**	-15.3	-15.9	-13.5	-9.3	-1.5	2.5	3.8	5.2	3.2				
								30	31	31	31	31	31	31	31	31	28	28	29	complete years
								97	100	100	100	100	100	100	100	100	90	90	94	in %
						mean	-16.9	-16.3	-12.4	-7.3	-3.9	0.2	3.9	4.4	0.2	-6.2	-11.3	-14.5	-6.7
						max	-14.4	-12.7	-9.4	-5.3	-1.5	2.8	6.8	8.6	3.2	-5.0	-8.7	-11.7	-5.7
						min	-20.4	-20.0	-14.6	-10.8	-5.9	-1.9	0.2	2.1	-1.7	-8.2	-13.8	-17.7	-7.8

Country	Code_WMO	Name	Long	Lat	Alt.(m)	Year	I	II	III	IV	V	VI	VII	VIII	IX	X	XI	XII	mean annual T (°C)
227	38851	Garm	**69.95**	**39.00**	**1316**	**1960**	-1.4	2.7	3.5	10.4	14.0	19.9	23.1	24.3	19.1	13.3	5.3	0.9	11.2
227	38851	Garm	**69.95**	**39.00**	**1316**	**1961**	-0.8	-3.8	4.2	12.6	19.0	21.6	25.8	23.1	20.9	12.2	6.0	-1.0	11.6
227	38851	Garm	**69.95**	**39.00**	**1316**	**1962**	-6.2	0.4	8.7	10.9	14.9	19.5	24.4	24.0	18.5	13.1	3.6	-0.5	10.9
227	38851	Garm	**69.95**	**39.00**	**1316**	**1963**	-1.9	2.6	5.4	13.1	16.2	21.0	22.9	22.6	19.0	15.0		0.8	
227	38851	Garm	**69.95**	**39.00**	**1316**	**1964**			5.1	10.1	15.4	19.5	22.3	23.3	19.2	11.8	7.0	-0.6	
227	38851	Garm	**69.95**	**39.00**	**1316**	**1965**	-0.1	-3.7	2.5	10.9	17.2	19.9	23.7	22.9	18.2	14.2	7.9	2.5	11.3
227	38851	Garm	**69.95**	**39.00**	**1316**	**1966**	3.1	3.4	4.9	11.2	15.3	22.4	23.9	23.6	18.8	11.0	5.9	0.5	12.0
227	38851	Garm	**69.95**	**39.00**	**1316**	**1967**	-3.5	-1.6	3.8	11.2	14.8	20.1	23.6	23.9	19.4	11.4	6.3	1.8	10.9
227	38851	Garm	**69.95**	**39.00**	**1316**	**1968**	-2.2	-3.7	6.2	12.8	14.5	19.8	23.8	23.8	19.0	12.1	6.8	-2.7	10.8
227	38851	Garm	**69.95**	**39.00**	**1316**	**1969**	-6.6	-5.3	3.5	9.8	15.5	19.7	22.1	22.8	17.9	13.3	6.6	3.4	10.2
227	38851	Garm	**69.95**	**39.00**	**1316**	**1970**	-3.9	0.0	5.2	13.4	16.8	20.9	22.0	24.8	19.5	14.1	8.0	1.4	11.8
227	38851	Garm	**69.95**	**39.00**	**1316**	**1971**	-6.1	0.0	8.8	13.6	17.7	22.9	24.9	23.7	18.9	13.7	8.0		
227	38851	Garm	**69.95**	**39.00**	**1316**	**1972**				10.3	15.7	18.8	20.9	21.8	19.1	13.2	8.8	-0.1	
227	38851	Garm	**69.95**	**39.00**	**1316**	**1973**	-5.0	-1.0	2.1	12.5	16.3	22.4	25.8	25.5	19.7	13.6	8.5	3.1	11.9
227	38851	Garm	**69.95**	**39.00**	**1316**	**1974**	-4.3	-5.3	4.4	13.9	16.2	20.0	23.3	20.9	18.3	12.6	6.9	-2.6	10.4
227	38851	Garm	**69.95**	**39.00**	**1316**	**1975**	-6.8	-3.2	3.3	12.6	14.9	20.4	24.3	24.6	19.4	12.7	4.3	-0.1	10.5
227	38851	Garm	**69.95**	**39.00**	**1316**	**1976**	-1.3	-2.8	1.5	10.8	17.2	20.2	25.6	25.1	19.5	11.8	5.6	1.6	11.2
227	38851	Garm	**69.95**	**39.00**	**1316**	**1977**	-4.9	-4.7	7.8	14.2	15.8	22.2	25.0	24.1	19.6	13.5	8.9	-0.2	11.8
227	38851	Garm	**69.95**	**39.00**	**1316**	**1978**	-5.9	-3.5	2.8	13.0	17.0	20.9	24.7	24.2	20.2	13.6	4.6	2.7	11.2
227	38851	Garm	**69.95**	**39.00**	**1316**	**1979**	-0.4	2.1	5.2	13.5	14.0	19.6	24.4	23.4	19.3	14.8	7.5	2.7	12.2
227	38851	Garm	**69.95**	**39.00**	**1316**	**1980**	-2.9	-1.9	2.5	12.8	17.0	20.6	24.6	23.8	19.7	14.3	9.0	4.1	12.0
227	38851	Garm	**69.95**	**39.00**	**1316**	**1981**	-0.5	-1.5	4.7	13.0	17.6	18.7	22.5	20.8	18.4	11.2	6.6	2.0	11.1
227	38851	Garm	**69.95**	**39.00**	**1316**	**1982**	-1.2	-3.3	4.0	13.6	16.7	19.8	22.4	23.0	17.0	11.7	4.6	-0.4	10.6
227	38851	Garm	**69.95**	**39.00**	**1316**	**1983**	-2.2	-0.2	3.0	12.5	16.6	19.1	23.2	25.0	19.5	13.0	9.1		
227	38851	Garm	**69.95**	**39.00**	**1316**	**1984**	-4.1	-6.0	3.9	12.1	16.0	22.4	25.5	26.8	18.4	12.3	7.2	-6.2	10.7
227	38851	Garm	**69.95**	**39.00**	**1316**	**1985**	-3.4	0.2	4.8	14.4	15.6	20.9	24.9	23.1	19.6	13.3	7.4	2.3	11.9
227	38851	Garm	**69.95**	**39.00**	**1316**	**1986**	-1.0	2.5	4.6	12.3	15.8	19.9	24.9	23.7	20.0	13.6	6.4	-2.3	11.7
227	38851	Garm	**69.95**	**39.00**	**1316**	**1987**	-2.4	1.6	7.1	10.8		18.9	21.1	23.4	19.3	10.3	7.4	4.1	
227	38851	Garm	**69.95**	**39.00**	**1316**	**1988**	-1.4	-0.1	4.7	13.5	15.8	20.5	24.5	22.4	19.9	11.9	9.8	3.4	12.1
227	38851	Garm	**69.95**	**39.00**	**1316**	**1989**	-5.2	-4.9	4.5	10.4	14.2	19.3	21.5	22.4	18.5	13.8	5.4	2.7	10.2
227	38851	Garm	**69.95**	**39.00**	**1316**	**1990**	-1.3	-0.8	3.9	10.6	17.6	21.9	23.2	24.4	20.8	13.2	8.9	1.4	12.0
							29	29	30	31	30	31	31	31	31	31	30	29	complete years
							93.5	93.5	96.8	100.0	96.8	100.0	100.0	100.0	100.0	100.0	96.8	93.5	in %
						mean	-2.9	-1.5	4.6	12.2	16.0	20.4	23.7	23.5	19.1	12.9	6.8	0.8	11.3
						max	3.1	3.4	8.8	14.4	19.0	22.9	25.8	26.8	20.9	15.0	9.8	4.1	12.2
						min	-6.8	-6.0	1.5	9.8	14.0	18.7	20.9	20.8	17.0	10.3	3.6	-6.2	10.2

Country	Code_WMO	Name	Long	Lat	Alt.(m)	Year	I	II	III	IV	V	VI	VII	VIII	IX	X	XI	XII	mean annual T (°C)
227	38853	**Haburaba**	**70.70**	**38.63**	**3347**	**1960**	-11.8	-7.7	-9.3	-3.6	0.6	7.0	10.3	12.1	6.1	1.2	-7.6	-9.7	-1.0
227	38853	**Haburaba**	**70.70**	**38.63**	**3347**	**1961**	-11.6	-14.1	-8.4	-1.7	5.2	8.0	12.7	10.3	8.5	-0.9	-6.3	-7.0	-0.4
227	38853	**Haburaba**	**70.70**	**38.63**	**3347**	**1962**	-12.4	-9.8	-4.5	-1.9	1.1	6.2	10.9	10.3	5.2	-0.2	-8.8	-10.5	-1.2
227	38853	**Haburaba**	**70.70**	**38.63**	**3347**	**1963**	-10.3	-8.6	-6.5	-0.4	2.9	7.4	9.7	10.0	6.7	2.7	-5.9	-8.5	-0.1
227	38853	**Haburaba**	**70.70**	**38.63**	**3347**	**1964**	-16.0	-11.6	-5.5	-3.1	0.7	6.0	8.8	9.9	5.9	-0.1	-5.2	-10.6	-1.7
227	38853	**Haburaba**	**70.70**	**38.63**	**3347**	**1965**	-9.8	-13.0	-7.9	-2.7	3.0	5.9	9.6	8.7	5.0	1.1	-5.6	-10.3	-1.3
227	38853	**Haburaba**	**70.70**	**38.63**	**3347**	**1966**	-8.8	-7.7	-7.8	-3.5	1.0	8.9	9.4	10.3	5.8	-2.2	-6.4	-10.1	-0.9
227	38853	**Haburaba**	**70.70**	**38.63**	**3347**	**1967**	-13.4	-10.8	-7.7	-2.7	0.9	6.2	10.0	10.3	6.9	-1.6	-6.6	-8.1	-1.4
227	38853	**Haburaba**	**70.70**	**38.63**	**3347**	**1968**	-11.6	-11.0	-5.8	-1.4	0.2	6.3	9.8	11.8	7.1	-0.5	-6.3	-9.9	-0.9
227	38853	**Haburaba**	**70.70**	**38.63**	**3347**	**1969**	-13.1	-11.9	-4.4	-2.2	2.7	6.1	8.6	9.5	4.6	0.5	-5.0	-7.4	-1.0
227	38853	**Haburaba**	**70.70**	**38.63**	**3347**	**1970**	-10.5	-8.7	-7.3	-0.4	3.6	7.7	8.3	12.4	6.6	1.7	-4.7	-10.3	-0.1
227	38853	**Haburaba**	**70.70**	**38.63**	**3347**	**1971**	-12.7	-10.9	-5.5	-0.3	4.2	9.8	10.7	10.4	5.1	1.5	-4.9	-6.6	0.1
227	38853	**Haburaba**	**70.70**	**38.63**	**3347**	**1972**	-11.7	-15.5	-7.3	-3.2	1.6	5.8	6.8	8.0	6.2	0.9	-4.2	-9.7	-1.8
227	38853	**Haburaba**	**70.70**	**38.63**	**3347**	**1973**	-14.3	-9.9	-8.3	-1.5	2.7	9.3	12.6	12.0	6.6	1.6	-2.5	-8.8	0.0
227	38853	**Haburaba**	**70.70**	**38.63**	**3347**	**1974**	-13.2	-12.4	-6.1	0.2	3.0	6.6	9.7	8.0	5.5	0.3	-6.1	-12.3	-1.4
227	38853	**Haburaba**	**70.70**	**38.63**	**3347**	**1975**	-13.0	-12.5	-8.0	-1.5	1.0	6.3	11.0	11.4	6.5	0.7	-8.2	-10.4	-1.4
227	38853	**Haburaba**	**70.70**	**38.63**	**3347**	**1976**	-10.6	-12.0	-8.5	-2.3	3.3	5.9	11.7	11.7	6.5	-0.7	-7.0	-10.3	-1.0
227	38853	**Haburaba**	**70.70**	**38.63**	**3347**	**1977**	-13.4	-11.9	-4.9	0.7	2.0	8.2	11.5	10.9	7.0	1.3	-4.3	-10.1	-0.3
227	38853	**Haburaba**	**70.70**	**38.63**	**3347**	**1978**	-13.7	-10.9	-9.1	-0.6	4.4	8.8	12.2	11.4	8.2	1.0	-7.7	-7.4	-0.3
227	38853	**Haburaba**	**70.70**	**38.63**	**3347**	**1979**	-10.2	-9.8	-8.5	0.2	0.4	7.0	11.8	12.8	6.1	4.0	-4.1	-8.7	0.1
227	38853	**Haburaba**	**70.70**	**38.63**	**3347**	**1980**	-11.7	-11.4	-8.1	0.0	3.9	8.3	11.9	10.7	7.1	2.2	-3.3	-7.6	0.2
227	38853	**Haburaba**	**70.70**	**38.63**	**3347**	**1981**	-11.4	-9.9	-6.3	-1.1	4.7	5.6	9.4	8.3	6.4	-1.5	-5.0	-9.5	-0.9
227	38853	**Haburaba**	**70.70**	**38.63**	**3347**	**1982**	-10.9	-13.1	-7.8	-0.7	3.4	6.5	9.8	10.1	4.2	-0.8	-7.4	-10.5	-1.4
227	38853	**Haburaba**	**70.70**	**38.63**	**3347**	**1983**	-11.5	-11.2	-9.4	-1.7	2.8	5.3	9.7	12.7	7.3	1.0	-3.5	-9.6	-0.7
227	38853	**Haburaba**	**70.70**	**38.63**	**3347**	**1984**	-13.7	-15.3	-5.7	-2.2	2.5	9.2	12.3	14.5	5.4	0.5	-5.0	-12.8	-0.9
227	38853	**Haburaba**	**70.70**	**38.63**	**3347**	**1985**	-12.2	-9.7	-7.9	0.2	2.5		12.0	9.3	7.2	-0.1	-6.1	-9.4	
227	38853	**Haburaba**	**70.70**	**38.63**	**3347**	**1986**	-12.5	-9.9	-9.2	-2.6	1.6	6.3	11.1	10.0	7.0	1.3	-5.4	-10.9	-1.1
227	38853	**Haburaba**	**70.70**	**38.63**	**3347**	**1987**	-10.7	-9.4	-5.4	-3.1		5.1			6.7	-1.9	-4.3	-6.4	
227	38853	**Haburaba**	**70.70**	**38.63**	**3347**	**1988**	-10.0	-10.0	-7.3	-0.8	2.8	7.7	11.8	9.2	7.2	-1.0	-1.1	-7.4	0.1
227	38853	**Haburaba**	**70.70**	**38.63**	**3347**	**1989**	-13.5	-13.6	-6.1	-4.3	1.5	5.7	8.4	9.0	6.7	2.2	-6.7	-8.4	-1.6
227	38853	**Haburaba**	**70.70**	**38.63**	**3347**	**1990**	-9.9	-10.5	-8.1	-3.1	4.5	8.7	10.5	11.8					
							31	31	31	31	30	30	30	30	30	30	30	30	complete years
							100.0	100.0	100.0	100.0	96.8	96.8	96.8	96.8	96.8	96.8	96.8	96.8	in %
						mean	-12.0	-11.1	-7.1	-1.6	2.4	7.0	10.4	10.5	6.4	0.5	-5.5	-9.3	-0.8
						max	-8.8	-7.7	-4.4	0.7	5.2	9.8	12.7	14.5	8.5	4.0	-1.1	-6.4	0.2
						min	-16.0	-15.5	-9.4	-4.3	0.2	5.1	6.8	8.0	4.2	-2.2	-8.8	-12.8	-1.8

Country	Code_WMO	Name	Long	Lat	Alt.(m)	Year	I	II	III	IV	V	VI	VII	VIII	IX	X	XI	XII	mean annual T (°C)
227	38846	Hovaling	**69.95**	**38.35**	**1468**	**1960**	-0.9	5.3	3.1	9.8	14.2	21.9	24.1	24.5	19.2	14.0	5.8	3.9	12.1
227	38846	Hovaling	**69.95**	**38.35**	**1468**	**1961**	1.7	-2.1	5.1	11.6	18.2	21.4	25.4	23.5	20.6	11.5	6.4	1.5	12.0
227	38846	Hovaling	**69.95**	**38.35**	**1468**	**1962**	-2.8	2.4	8.8	11.3	14.9	19.6	24.2	22.6	17.1	12.2	2.6	1.7	11.2
227	38846	Hovaling	**69.95**	**38.35**	**1468**	**1963**	3.3	4.9	7.0	11.6	16.1	21.8	23.2	22.4	18.8	15.4	7.7	4.9	13.1
227	38846	Hovaling	**69.95**	**38.35**	**1468**	**1964**	-6.4	0.0	6.5	10.4	14.9	20.2	22.7	23.0	18.2	10.4	7.5	-2.4	10.4
227	38846	Hovaling	**69.95**	**38.35**	**1468**	**1965**	1.2	-2.1	3.1	11.0	16.0	20.4	23.8	22.5	17.8	14.7	9.4	4.6	11.8
227	38846	Hovaling	**69.95**	**38.35**	**1468**	**1966**	6.7	6.2	5.2	10.6	15.3	22.8	24.0	23.7	18.6	11.2	5.7	2.2	12.7
227	38846	Hovaling	**69.95**	**38.35**	**1468**	**1967**	-2.5	0.5	4.6	10.2	14.0	19.9	23.9	23.5	19.2	11.7	7.6	3.2	11.3
227	38846	Hovaling	**69.95**	**38.35**	**1468**	**1968**	-0.3	-0.8	6.5	11.7	13.5	20.8	24.0	23.5	19.2	12.8	8.2	0.5	11.6
227	38846	Hovaling	**69.95**	**38.35**	**1468**	**1969**	-3.6	-3.4	6.8	10.7	15.3	20.3	23.4	23.0	18.2	13.9	6.8	6.0	11.4
227	38846	Hovaling	**69.95**	**38.35**	**1468**	**1970**	0.3	2.9	4.7	13.4	17.9	21.9	23.4	25.5	19.0	14.5	9.9	2.3	13.0
227	38846	Hovaling	**69.95**	**38.35**	**1468**	**1971**	-2.9	0.3	7.2	13.4	18.3	23.2	24.4	23.1	18.2	13.7	9.9	6.9	13.0
227	38846	Hovaling	**69.95**	**38.35**	**1468**	**1972**	-2.5	-7.2	3.7	11.5	15.4	20.0	21.9	21.1	18.9	14.0	10.3	0.0	10.6
227	38846	Hovaling	**69.95**	**38.35**	**1468**	**1973**	-4.4	1.2	4.5	13.1	16.5	23.6	25.8	24.5	18.5	14.2	10.9	3.8	12.7
227	38846	Hovaling	**69.95**	**38.35**	**1468**	**1974**	-3.3	-3.4	5.1	14.2	16.6	20.9	24.4	21.9	18.6	12.3	8.0	-0.2	11.2
227	38846	Hovaling	**69.95**	**38.35**	**1468**	**1975**	-3.0	-1.5	3.5	11.0	15.2	21.0	25.1	24.3	19.6	13.1	4.5	1.4	11.2
227	38846	Hovaling	**69.95**	**38.35**	**1468**	**1976**	1.9	-1.6	2.1	11.0	16.7	20.8	26.0	24.9	19.9	13.1	5.1	1.8	11.8
227	38846	Hovaling	**69.95**	**38.35**	**1468**	**1977**	-4.3	-1.0	9.0	13.6	15.9	22.8	25.4	23.9	19.7	13.0	10.0	2.6	12.5
227	38846	Hovaling	**69.95**	**38.35**	**1468**	**1978**	-2.1	-1.3	3.3	14.1	17.8	22.6	25.7	24.1	20.7	15.1	4.8	5.8	12.5
227	38846	Hovaling	**69.95**	**38.35**	**1468**	**1979**	0.8	2.9	4.2	14.2	13.5	21.2	26.0	23.6	19.8	16.6	7.8	4.8	12.9
227	38846	Hovaling	**69.95**	**38.35**	**1468**	**1980**	-0.8	-1.2	4.3	14.8	18.2	22.7	26.0	24.0	19.8	15.0	10.6	6.3	13.3
227	38846	Hovaling	**69.95**	**38.35**	**1468**	**1981**	1.2	1.1	7.3	13.4	17.7	20.3	24.1	22.5	19.2	11.7	8.7	5.1	12.7
227	38846	Hovaling	**69.95**	**38.35**	**1468**	**1982**	1.9	-1.9	3.9	13.5	17.5	21.7	24.1	23.5	17.7	13.4	5.3	1.8	11.9
227	38846	Hovaling	**69.95**	**38.35**	**1468**	**1983**	0.5	4.3	4.1	11.9	17.5	21.0	25.3	25.9	20.3	13.3	11.0		
227	38846	Hovaling	**69.95**	**38.35**	**1468**	**1984**	0.0	-6.0	6.3	12.8	17.1	23.1	26.6	27.1	18.8	12.5	8.9	-3.8	11.9
227	38846	Hovaling	**69.95**	**38.35**	**1468**	**1985**	-0.9	2.5	4.4	14.1	16.5	22.7		22.8	20.1	12.9	8.3	3.8	
227	38846	Hovaling	**69.95**	**38.35**	**1468**	**1986**	1.9	3.3	3.4	11.5	16.5	21.5	25.4	23.4	20.1	15.1	7.5	0.3	12.5
227	38846	Hovaling	**69.95**	**38.35**	**1468**	**1987**	1.8	2.6	8.4	11.2		20.2	22.8	25.2	19.7	9.8	9.3	7.3	
227	38846	Hovaling	**69.95**	**38.35**	**1468**	**1988**	1.4	1.3	5.6	14.3	16.9	22.7	26.4	23.1	19.9	12.8	12.3	6.2	13.6
227	38846	Hovaling	**69.95**	**38.35**	**1468**	**1989**	-2.8	-4.1	4.8	10.0	13.7	21.1	23.6	23.3	19.0	15.1	7.5	6.0	11.4
227	38846	Hovaling	**69.95**	**38.35**	**1468**	**1990**	-0.3	0.5	4.8	11.2	18.9	23.1	24.5	25.0	21.5	13.9	11.2	2.1	13.0
							31.0	31.0	31.0	31.0	30.0	31.0	30.0	31.0	31.0	31.0	31.0	30.0	complete years
							100.0	100.0	100.0	100.0	96.8	100.0	96.8	100.0	100.0	100.0	100.0	96.8	in %
						mean	-0.6	0.1	5.2	12.2	16.1	21.4	24.5	23.6	19.1	13.3	7.9	3.0	12.1
						max	6.7	6.2	9.0	14.8	18.3	23.6	26.6	27.1	20.7	16.6	12.3	7.3	13.6
						min	-6.4	-7.2	2.1	9.8	13.5	19.6	21.9	21.1	17.1	9.8	2.6	-3.8	10.4

Country	Code_WMO	Name	Long	Lat	Alt.(m)	Year	I	I	III	IV	V	VI	VII	VIII	IX	X	XI	XII	mean annual T (°C)
227	38871	**Karakul**	**73.55**	**39.02**	**3930**	**1960**	-18.4	-14.5	-10.6	-5.0	0.3	4.0	8.3	9.1	3.2	-3.0	-10.0	-16.3	-4.4
227	38871	**Karakul**	**73.55**	**39.02**	**3930**	**1961**	-17.1	-16.5	-10.2	-3.8	2.1	5.0	10.1	8.3	5.4	-3.9	-10.6	-15.9	-3.9
227	38871	**Karakul**	**73.55**	**39.02**	**3930**	**1962**	-15.9	-12.9	-7.8	-2.4	0.3	4.6	7.7	7.8	3.1	-4.1	-10.0	-14.7	-3.7
227	38871	**Karakul**	**73.55**	**39.02**	**3930**	**1963**	-15.9	-11.2	-7.7	-1.3	2.4	6.0	8.1	8.1	3.3	-1.4	-8.8	-12.5	-2.6
227	38871	**Karakul**	**73.55**	**39.02**	**3930**	**1964**	-19.4	-13.6	-6.7	-3.6	-0.6	4.5	7.7	8.6	3.4	-2.1	-8.9	-18.0	-4.0
227	38871	**Karakul**	**73.55**	**39.02**	**3930**	**1965**	-20.8	-20.4	-15.6	-6.6	0.3	3.7	8.3	6.3	2.9	-0.9	-7.9	-16.2	-5.6
227	38871	**Karakul**	**73.55**	**39.02**	**3930**	**1966**	-14.4	-14.9	-9.5	-3.9	-0.3	5.9	7.1	8.2	3.1	-3.6	-10.9	-13.3	-3.9
227	38871	**Karakul**	**73.55**	**39.02**	**3930**	**1967**	-17.8	-11.9	-9.4	-2.9	-0.5	5.4	8.6	7.9	4.2	-3.0	-9.5	-12.7	-3.5
227	38871	**Karakul**	**73.55**	**39.02**	**3930**	**1968**	-17.2	-14.4	-6.9	-6.2	-0.4	5.3	9.1	8.5	3.8	-3.2	-8.3	-16.1	-3.8
227	38871	**Karakul**	**73.55**	**39.02**	**3930**	**1969**	-14.4	-13.7	-4.7	-4.3	1.3	5.0	8.4	8.9	3.1	-0.7	-9.1	-16.4	-3.0
227	38871	**Karakul**	**73.55**	**39.02**	**3930**	**1970**	-17.4	-15.4	-10.2	-1.6	1.6	5.1	7.6	10.0	4.7	-1.0	-7.8	-11.9	-3.0
227	38871	**Karakul**	**73.55**	**39.02**	**3930**	**1971**	-16.3	-13.2	-6.2	-1.0	2.2	7.7	9.3	6.9	1.8	-2.3	-7.7	-10.3	-2.4
227	38871	**Karakul**	**73.55**	**39.02**	**3930**	**1972**	-12.4	-16.9	-10.5	-4.6	0.8	5.1	6.3	8.0	3.3	-2.4	-8.7	-14.0	-3.8
227	38871	**Karakul**	**73.55**	**39.02**	**3930**	**1973**		-12.5	-10.1	-2.5	1.1	6.8	11.1	9.9		-2.2	-8.1	-16.7	
227	38871	**Karakul**	**73.55**	**39.02**	**3930**	**1974**	-16.7	-17.3	-9.7	-1.0	1.3	5.1	8.3	6.9	2.6	-5.1	-11.1	-17.6	-4.5
227	38871	**Karakul**	**73.55**	**39.02**	**3930**	**1975**	-21.7	-15.8	-9.0	-3.1	-0.2			8.9	3.6	-1.7	-10.2		
227	38871	**Karakul**	**73.55**	**39.02**	**3930**	**1976**	-22.9	-16.9	-11.4	-2.9	0.9	4.2		8.8	4.1	-1.5	-9.2		
227	38871	**Karakul**	**73.55**	**39.02**	**3930**	**1977**	-14.9	-14.6	-8.6	-1.9	0.9	6.7	9.7	8.7	4.6	-0.5	-7.2	-13.3	-2.5
227	38871	**Karakul**	**73.55**	**39.02**	**3930**	**1978**	-19.5	-13.1	-10.8	-1.4	3.0	7.7	11.8	10.0	4.6	-1.3	-9.4	-9.8	-2.4
227	38871	**Karakul**	**73.55**	**39.02**	**3930**	**1979**	-13.3	-11.8	-9.9	-0.6	-0.4	5.4	9.2	8.1	3.3	-0.7	-8.3	-14.7	-2.8
227	38871	**Karakul**	**73.55**	**39.02**	**3930**	**1980**	-18.6	-12.6	-9.5	-0.8	2.8	6.5	9.8	8.4	3.8	-1.4	-8.5	-17.8	-3.2
227	38871	**Karakul**	**73.55**	**39.02**	**3930**	**1981**	-18.7	-14.0	-9.0	-2.3	3.8	5.3	9.4	7.5		-2.8	-8.3	-13.8	
227	38871	**Karakul**	**73.55**	**39.02**	**3930**	**1982**	-13.7	-14.7	-8.3	-2.7	1.6	4.9	8.3	8.7	2.1	-1.8	-9.6	-17.7	-3.6
227	38871	**Karakul**	**73.55**	**39.02**	**3930**	**1983**	-16.6	-15.4	-13.4	-4.5	2.0	4.1	7.7	10.9	5.0	-2.0	-6.5	-12.5	-3.4
227	38871	**Karakul**	**73.55**	**39.02**	**3930**	**1984**	-17.4	-15.9	-6.9	-3.0	1.8	7.0	9.8	12.0	3.1	-3.0	-7.4	-13.8	-2.8
227	38871	**Karakul**	**73.55**	**39.02**	**3930**	**1985**	-16.4	-12.7	-7.2	-1.7	1.2	5.3	10.2	9.2	3.9	-1.6	-8.5	-18.8	-3.1
227	38871	**Karakul**	**73.55**	**39.02**	**3930**	**1986**	-27.7	-21.8	-14.2	-6.0	-1.7	4.3	9.4	8.8	3.8	-0.9	-7.0	-15.0	-5.6
227	38871	**Karakul**	**73.55**	**39.02**	**3930**	**1987**	-18.0	-12.6	-6.0		0.0	3.7	6.9	8.9	4.7	-2.7	-6.6	-13.7	
227	38871	**Karakul**	**73.55**	**39.02**	**3930**	**1988**	-15.6	-16.0	-9.5	-1.1	1.1	6.4	10.3	8.4	4.7	-2.8	-6.4	-11.1	-2.6
227	38871	**Karakul**	**73.55**	**39.02**	**3930**	**1989**	-16.9	-15.0	-8.4	-6.3	-0.3	4.2	8.3	7.3	4.4	-1.7	-8.8	-14.8	-4.0
227	38871	**Karakul**	**73.55**	**39.02**	**3930**	**1990**	-12.6	-12.4	-9.5	-4.1	2.9	7.5	9.2	9.2	5.9	-2.2	-6.3	-12.5	-2.1
							30	31	31	30	31	30	29	31	29	31	31	29	complete years
							96.8	100.0	100.0	96.8	100.0	96.8	93.5	100.0	93.5	100.0	100.0	93.5	in %
mean							-17.4	-14.7	-9.2	-3.0	0.9	5.3	8.8	8.6	3.7	-2.2	-8.6	-14.6	-3.5
max							-12.4	-11.2	-4.7	-0.6	3.8	7.7	11.8	12.0	5.4	-0.5	-6.4	-9.8	-2.4
min							-27.7	-21.8	-15.6	-6.6	-1.7	3.7	6.3	6.3	1.8	-5.1	-11.1	-18.8	-5.6

Country	Code_WMO	Name	Long	Lat	Alt.(m)	Year	I	II	III	IV	V	VI	VII	VIII	IX	X	XI	XII	mean annual T (°C)
227	38854	Lyairun	70.90	38.90	2008	1963	-2.6	0.0	2.7	9.3	12.0	15.7	17.7	18.7	15.2	11.7	2.7	-1.2	8.5
227	38854	Lyairun	70.90	38.90	2008	1964	-9.2	-3.6	2.4	6.2	10.3	14.6	17.4	18.7	15.1	8.8	3.7	-3.5	6.7
227	38854	Lyairun	70.90	38.90	2008	1965	-2.5	-5.2	0.7	6.0	12.5	14.5	18.5	18.2	14.2	10.4	4.1	-1.0	7.5
227	38854	Lyairun	70.90	38.90	2008	1966	0.0	0.3	0.8	5.7	10.9	17.4	18.5	19.6	15.0	7.2	3.1	-2.9	7.9
227	38854	Lyairun	70.90	38.90	2008	1967	-6.8	-3.3	0.7	6.7	10.2	15.2	18.6	19.3	15.7	7.9	2.7	-1.3	7.1
227	38854	Lyairun	70.90	38.90	2008	1968	-5.1	-4.2	2.6	8.3	10.1	15.1	19.0	19.4	15.7	8.6	2.8		
227	38854	Lyairun	70.90	38.90	2008	1969	-7.7	-6.6	2.4	5.0	10.9	14.7	16.9	18.2	13.8	9.4	2.8	0.0	6.6
227	38854	Lyairun	70.90	38.90	2008	1970	-3.9	-0.9	0.7	8.8	12.5	15.9	16.9	20.7	15.8	10.8	4.8	-2.2	8.3
227	38854	Lyairun	70.90	38.90	2008	1971	-5.3	-1.6	3.8	9.5	12.9	17.9	19.7	19.5	14.4	10.4	4.6	2.1	9.0
227	38854	Lyairun	70.90	38.90	2008	1972	-4.8	-9.4	0.8	5.8	11.3	13.9	15.7	17.2	15.0	9.5	5.8	-1.8	6.6
227	38854	Lyairun	70.90	38.90	2008	1973	-7.3	-1.9	-0.4	7.7	11.9	17.5	21.2	21.0	15.7	10.4	6.4	0.2	8.5
227	38854	Lyairun	70.90	38.90	2008	1974	-6.4	-5.7	1.7	9.7	11.8	15.1	18.6	16.9	14.8	9.4	3.2	-3.9	7.1
227	38854	Lyairun	70.90	38.90	2008	1975	-5.7	-4.2	1.1	8.2	10.2	15.2	19.7	21.0	15.2	9.9	0.8	-2.7	7.4
227	38854	Lyairun	70.90	38.90	2008	1976	-2.6	-4.6	-0.4		12.6	14.6	20.5	21.1	15.8	8.5	2.7	-1.6	
227	38854	Lyairun	70.90	38.90	2008	1977	-6.4	-4.3	4.0	10.1	11.5	17.1	20.1	19.9	16.0	10.2	5.7	-2.3	8.5
227	38854	Lyairun	70.90	38.90	2008	1978	-6.3	-3.6	-0.4	8.3	13.5	17.0	20.6	20.4	17.0	10.2	0.2	-0.2	8.1
227	38854	Lyairun	70.90	38.90	2008	1979	-3.5	-1.6	0.0	9.4	9.9	15.9	20.1	19.1	15.4	12.4	4.5	-0.4	8.4
227	38854	Lyairun	70.90	38.90	2008	1980	-4.7	-4.0	0.3	7.9	12.9	16.5	20.5	20.1	16.3	11.0	5.4	0.8	8.6
227	38854	Lyairun	70.90	38.90	2008	1981	-3.6	-3.0	1.6	8.6	13.7	14.2	18.2	17.2	15.2	7.5	3.7	-1.9	7.6
227	38854	Lyairun	70.90	38.90	2008	1982	-3.6	-5.0	0.5	8.9	12.7	15.1	18.0	19.3	13.2	8.6	-0.1	-3.4	7.0
227	38854	Lyairun	70.90	38.90	2008	1983	-3.9	-2.3	-0.1	8.2	12.2	14.0	18.1	21.2	16.1	10.2	6.3	-1.3	8.2
227	38854	Lyairun	70.90	38.90	2008	1984	-5.2	-8.0	1.8	7.4	11.8	17.7	20.9	23.2	14.9	9.5	3.0	-7.4	7.5
227	38854	Lyairun	70.90	38.90	2008	1985	-4.9	-1.8	0.2	9.1	11.3	16.1	20.7	19.1	15.9	9.7	3.4	-0.9	8.1
227	38854	Lyairun	70.90	38.90	2008	1986	-4.0	-0.7	-0.2	7.1	11.2	15.0	19.5	19.0	15.9	10.8	2.5	-4.4	7.6
227	38854	Lyairun	70.90	38.90	2008	1987	-3.2	-1.5			10.4	13.9	16.1	18.8	15.3	6.3	4.2	1.7	
227	38854	Lyairun	70.90	38.90	2008	1988	-3.2	-2.0	1.1	7.5	11.6	16.4	20.3	18.3	16.3	8.5	7.6	0.7	8.6
227	38854	Lyairun	70.90	38.90	2008	1989	-6.5	-6.6	1.8	5.3	10.3	14.2	17.2	17.7	15.0	11.2	4.6	-0.7	7.0
227	38854	Lyairun	70.90	38.90	2008	1990	-3.1	-3.1	-0.2	6.2	13.5	17.3	19.1	20.5	17.6	10.1	6.2		
							29	29	28	27	29	29	29	29	29	29	29	27	complete years
							93.5	93.5	90.3	87.1	93.5	93.5	93.5	93.5	93.5	93.5	93.5	87.1	in %
						mean	-4.8	-3.5	1.1	7.8	11.6	15.5	18.8	19.3	15.3	9.6	3.7	-1.5	7.8
						max	0.0	0.3	4.0	10.1	13.7	17.9	21.2	23.2	17.0	12.4	7.6	2.1	9.0
						min	-9.2	-9.4	-0.4	5.0	9.9	13.9	15.7	16.9	13.2	6.3	-0.1	-7.4	6.6

Country	Code_WMO	Name	Long	Lat	Alt.(m)	Year	I	II	III	IV	V	VI	VII	VIII	IX	X	XI	XII	mean annual T (°C)
213	38745	**Sarytash**	**73.25**	**39.73**	**3153**	**1961**	-16.5	-17.1	-10.5	-1.5	5.7	6.7	11.0	9.9	6.8	-2.3	-11.3	-16.9	-3.0
213	38745	**Sarytash**	**73.25**	**39.73**	**3153**	**1962**	-17.4	-13.1	-5.9	-0.1	3.6	6.6	9.6	9.8	4.5	-1.0	-11.6	-14.7	-2.5
213	38745	**Sarytash**	**73.25**	**39.73**	**3153**	**1963**	-15.0	-11.3	-8.4		5.2	7.6	9.2	9.6	5.3	1.3	-10.7	-14.1	
213	38745	**Sarytash**	**73.25**	**39.73**	**3153**	**1964**	-20.1	-14.6	-7.5	-2.9	2.0	6.4	8.9	9.8	5.9	-2.2	-8.5	-13.7	-3.0
213	38745	**Sarytash**	**73.25**	**39.73**	**3153**	**1965**	-13.1	-15.9	-10.0	-1.9	4.5	6.5	9.9	8.3	5.4	1.5	-8.5	-16.0	-2.4
213	38745	**Sarytash**	**73.25**	**39.73**	**3153**	**1966**	-14.1	-11.4	-4.8	-3.8	1.8	8.1	8.7	9.7	5.5	-1.9	-9.8	-12.7	-2.1
213	38745	**Sarytash**	**73.25**	**39.73**	**3153**	**1967**	-17.5	-14.1	-10.8	-3.0	2.7	7.1	9.4	9.2	5.9	-1.2	-8.9	-12.2	-2.8
213	38745	**Sarytash**	**73.25**	**39.73**	**3153**	**1968**	-16.4	-15.5	-7.0	-1.2	3.0	7.0	9.7	10.0	5.4	-1.0	-9.5	-14.3	-2.5
213	38745	**Sarytash**	**73.25**	**39.73**	**3153**	**1969**	-16.1		-4.6	-3.1	3.4	7.0	9.1	10.0	4.8	-1.1	-8.5	-12.6	
213	38745	**Sarytash**	**73.25**	**39.73**	**3153**	**1970**	-16.4	-13.4	-10.9	-0.5	4.8	7.1	8.7	11.1	6.1	-0.4	-7.4	-13.8	-2.1
213	38745	**Sarytash**	**73.25**	**39.73**	**3153**	**1971**	-17.7	-13.0	-7.1	1.4	4.6	9.2	10.2	10.0	5.0	0.0	-7.5	-9.8	-1.2
213	38745	**Sarytash**	**73.25**	**39.73**	**3153**	**1972**	-14.6	-17.9		-3.1	6.3	7.1	8.0	9.1	6.0	-1.6	-3.7	-14.1	
213	38745	**Sarytash**	**73.25**	**39.73**	**3153**	**1973**	-17.4	-12.2	-10.0	-0.7	4.5	9.0	12.4	11.2	6.3	-0.5	-5.4	-13.3	-1.3
213	38745	**Sarytash**	**73.25**	**39.73**	**3153**	**1974**	-17.5	-15.9	-9.4	2.2	5.2	6.9	9.7	8.4	5.7	-1.4	-9.5	-16.6	-2.7
213	38745	**Sarytash**	**73.25**	**39.73**	**3153**	**1975**	-17.3	-15.4	-9.1	0.3	2.8	6.7	9.7	10.9		-1.3	-12.7	-15.7	
213	38745	**Sarytash**	**73.25**	**39.73**	**3153**	**1976**	-15.5	-15.0	-11.3	-2.2	5.0	6.3	10.6	10.5	5.9	-1.0	-10.3	-13.9	-2.6
213	38745	**Sarytash**	**73.25**	**39.73**	**3153**	**1977**	-15.9	-15.8	-7.0	1.8	4.4	8.5	10.9	11.0	7.1	1.0	-8.2	-14.1	-1.4
213	38745	**Sarytash**	**73.25**	**39.73**	**3153**	**1978**	-17.7	-14.4	-10.4	1.0	6.2	9.3	13.2	11.7	7.4	0.3	-11.0	-10.8	-1.3
213	38745	**Sarytash**	**73.25**	**39.73**	**3153**	**1979**	-14.9	-13.0	-10.3	1.2	2.4	7.5	11.1	10.0	5.6	2.4	-7.4	-13.4	-1.6
213	38745	**Sarytash**	**73.25**	**39.73**	**3153**	**1980**	-17.2	-13.4	-10.2	-0.4	5.8	7.7	11.0	10.1	6.3	1.3	-5.5	-11.8	-1.4
213	38745	**Sarytash**	**73.25**	**39.73**	**3153**	**1981**	-14.7	-13.0	-8.1	-0.8	0.6	6.9	9.9	8.4	5.0	-0.9	-7.7	-14.1	-2.4
213	38745	**Sarytash**	**73.25**	**39.73**	**3153**	**1982**	-15.2	-16.0	-9.6	-1.3	5.2	7.3	9.6	9.3	4.6	-0.5	-10.0	-14.0	-2.6
213	38745	**Sarytash**	**73.25**	**39.73**	**3153**	**1983**	-15.1	-14.6	-11.4	-0.1	5.2	6.0	9.5	12.5	6.6	-0.3	-5.2	-12.4	-1.6
213	38745	**Sarytash**	**73.25**	**39.73**	**3153**	**1984**	-16.9	-15.9	-6.9	-1.4	4.6	9.4	11.7	14.1	5.1	-1.0	-7.1	-17.0	-1.8
213	38745	**Sarytash**	**73.25**	**39.73**	**3153**	**1985**	-16.0	-12.1		-0.7	4.3	7.5	11.2		6.9		-9.9	-12.5	
213	38745	**Sarytash**	**73.25**	**39.73**	**3153**	**1986**	-16.1	-13.5	-10.4	-2.4	3.7	7.0	11.0	10.4	7.1	1.4	-7.2	-11.7	-1.7
213	38745	**Sarytash**	**73.25**	**39.73**	**3153**	**1987**	-13.9	-11.9	-6.0	-3.2	0.7	5.4	8.4	10.6	7.1	-3.5	-7.8	-10.6	-2.1
213	38745	**Sarytash**	**73.25**	**39.73**	**3153**	**1988**	-14.9	-13.7	-9.5	-2.2	2.5	7.9	11.5	9.7	6.7	-1.8	-5.2	-9.9	-1.6
213	38745	**Sarytash**	**73.25**	**39.73**	**3153**	**1989**	-16.9	-17.1	-8.4	-4.2	3.2	6.3	9.3	9.3	6.1	1.3	-11.1	-11.7	-2.8
213	38745	**Sarytash**	**73.25**	**39.73**	**3153**	**1990**	-14.0	-14.0	-10.2	-3.1	6.1	9.4	9.6	10.5	8.6	0.3	-5.1		
							30	29	28	29	30	30	30	29	29	29	30	29	complete years
							96.8	93.5	90.3	93.5	96.8	96.8	96.8	93.5	93.5	93.5	96.8	93.5	in %
						mean	-16.1	-14.3	-8.7	-1.2	3.9	7.3	10.1	10.1	5.9	-0.5	-8.5	-13.4	-2.1
						max	-13.1	-11.3	-4.6	2.2	6.3	9.4	13.2	14.1	7.4	2.4	-3.7	-9.8	-1.2
						min	-20.1	-17.9	-11.4	-4.2	0.6	5.4	8.0	8.3	4.5	-3.5	-12.7	-17.0	-3.0

Country	Code_WMO	Name	Long	Lat	Alt.(m)	Year	I	II	III	IV	V	VI	VII	VIII	IX	X	XI	XII	mean annual T (˚C)
227	38852	**Tavildara**	**70.48**	**38.70**	**1616**	**1960**	-4.1	1.9	2.4	8.1	11.9	18.6	21.3	22.4	17.2	11.3	3.3	-2.7	9.3
227	38852	**Tavildara**	**70.48**	**38.70**	**1616**	**1961**	-3.1	-4.7	1.7	10.0	16.5	18.9	23.5	21.5	18.9	10.7	3.9	-3.8	9.5
227	38852	**Tavildara**	**70.48**	**38.70**	**1616**	**1962**	-7.3	-1.5		9.2	12.8	17.7	22.0	21.5	16.3	10.7	1.6	-2.2	
227	38852	**Tavildara**	**70.48**	**38.70**	**1616**	**1963**	-3.3	1.8	4.2	11.3	14.1	18.7	20.6	20.8	17.4	13.5	5.2	-0.5	10.3
227	38852	**Tavildara**	**70.48**	**38.70**	**1616**	**1964**	-10.3	-3.2	3.7	8.6	12.9	17.1	20.0	20.9	16.8	9.9	4.7	-2.2	8.2
227	38852	**Tavildara**	**70.48**	**38.70**	**1616**	**1965**	-1.5	-4.6	2.0	8.3	14.8	18.0	21.5	20.4	16.0	12.5	6.1	-0.7	9.4
227	38852	**Tavildara**	**70.48**	**38.70**	**1616**	**1966**	1.1	3.1	3.8	8.9	13.2	19.8	21.2	21.4	17.0	9.2	3.5	-1.3	10.1
227	38852	**Tavildara**	**70.48**	**38.70**	**1616**	**1967**	-5.7	-1.6	2.9	9.1	12.3	18.0	21.5	21.4	17.4	9.3	4.4	0.3	9.1
227	38852	**Tavildara**	**70.48**	**38.70**	**1616**	**1968**	-4.1	-3.3	4.8	10.9	12.1	18.0	21.1	21.6	17.1	10.3	5.3	-3.8	9.1
227	38852	**Tavildara**	**70.48**	**38.70**	**1616**	**1969**	-6.9	-6.1	3.5	7.6	13.5	17.3	19.7	20.2	15.9	11.4	4.4	1.9	8.5
227	38852	**Tavildara**	**70.48**	**38.70**	**1616**	**1970**	-3.8	-0.1	3.3	11.8	15.2	19.0	20.1	22.8	17.5	12.1	6.6	-1.0	10.3
227	38852	**Tavildara**	**70.48**	**38.70**	**1616**	**1971**	-7.4	-1.3	5.5	11.7	15.8	20.8	22.3	21.1	16.4	11.3	5.7	2.7	10.4
227	38852	**Tavildara**	**70.48**	**38.70**	**1616**	**1972**	-3.6	-9.9	1.8	8.4	13.5	16.3	18.4	19.2	16.7	11.3	6.8	-1.4	8.1
227	38852	**Tavildara**	**70.48**	**38.70**	**1616**	**1973**	-6.6	-1.4	1.7		14.3	20.4	23.5	22.8	17.5	11.5	6.8	0.2	
227	38852	**Tavildara**	**70.48**	**38.70**	**1616**	**1974**	-5.6	-5.4	3.2	12.3	14.3	18.1	21.5	19.4	16.7	10.5	4.9	-3.5	8.9
227	38852	**Tavildara**	**70.48**	**38.70**	**1616**	**1975**	-8.0	-4.2	2.4	10.4	12.8	18.4	22.2	22.8	17.8	11.3	1.9	-2.2	8.8
227	38852	**Tavildara**	**70.48**	**38.70**	**1616**	**1976**	-3.1	-3.6	0.9	8.8	15.3	18.0	23.1	23.4	17.9	10.7	3.7	0.1	9.6
227	38852	**Tavildara**	**70.48**	**38.70**	**1616**	**1977**	-6.2	-5.0	5.9	12.3			22.6	21.7	17.3	11.7	6.8	-1.9	8.5
227	38852	**Tavildara**	**70.48**	**38.70**	**1616**	**1978**		-3.7	1.5	11.2	15.5	19.4	22.9	22.0	18.3	11.9	2.6	1.5	
227	38852	**Tavildara**	**70.48**	**38.70**	**1616**	**1979**	-1.4	1.0	3.3	12.0	12.1	17.8	22.4	21.3	17.5	13.5	5.0	0.7	10.4
227	38852	**Tavildara**	**70.48**	**38.70**	**1616**	**1980**	-4.4	-2.5	2.0	11.1	15.5	19.5	23.0	21.9	17.8	12.6	7.3		11.2
227	38852	**Tavildara**	**70.48**	**38.70**	**1616**	**1981**	-2.4	-2.0	3.9	11.5	16.2	16.8	20.6	19.5	16.7	9.4	5.3	0.7	9.7
227	38852	**Tavildara**	**70.48**	**38.70**	**1616**	**1982**	-2.8	-5.2	2.5	11.6	15.1	17.9	20.7	21.0	15.1	9.9	2.3	-3.3	8.7
227	38852	**Tavildara**	**70.48**	**38.70**	**1616**	**1983**	-3.4	-1.6	1.8	10.5	14.6	16.7			17.6	11.0	6.9		
227	38852	**Tavildara**	**70.48**	**38.70**	**1616**	**1984**	-4.9	-6.9	3.3	10.1	14.2	20.2	23.4	24.7		10.3	5.6		
227	38852	**Tavildara**	**70.48**	**38.70**	**1616**	**1985**	-4.9	-1.1	2.3	11.9	13.6	18.9	22.8	20.7	17.5	11.1	5.0	-0.1	9.8
227	38852	**Tavildara**	**70.48**	**38.70**	**1616**	**1986**	-3.5	-0.3	2.5	9.7	13.4	17.8	22.2	21.2	17.5	12.0	4.5	-3.5	9.4
227	38852	**Tavildara**	**70.48**	**38.70**	**1616**	**1987**	-4.0	0.4	5.4	9.0		16.8	19.2	21.6	17.8	8.8	6.3	2.6	
227	38852	**Tavildara**	**70.48**	**38.70**	**1616**	**1988**	-2.2	-0.8	3.0	11.0	14.2	18.9	23.1	20.8	18.3	10.0	7.5	1.6	10.4
227	38852	**Tavildara**	**70.48**	**38.70**	**1616**	**1989**	-6.8	-6.3	3.3	8.3	12.7	17.6	20.1	20.3	16.9	12.1	3.8	1.9	8.7
227	38852	**Tavildara**	**70.48**	**38.70**	**1616**	**1990**	-2.6	-2.1	2.2	9.0	15.7	19.8	21.9	23.1	19.7	11.7	6.9	-0.4	10.4
							30	31	30	30	29	30	30	30	30	31	31	28	complete years
							96.8	100.0	96.8	96.8	93.5	96.8	96.8	96.8	96.8	100.0	100.0	90.3	in %

mean	-4.5	-2.6	3.0	10.2	14.0	18.3	21.6	21.4	17.2	11.0	4.9	-0.7	9.4
max	1.1	3.1	5.9	12.3	16.5	20.8	23.5	24.7	18.9	13.5	7.5	2.7	11.2
min	-10.3	-9.9	0.9	7.6	11.9	16.3	18.4	19.2	15.1	8.8	1.6	-3.8	8.1